BEILSTEIN JOURNAL OF ORGANIC CHEMISTRY

Synthetic electrochemistry

Edited by Kevin Lam and Shinsuke Inagi

Imprint

Beilstein Journal of Organic Chemistry
www.bjoc.org
ISSN 1860-5397
Email: journals-support@beilstein-institut.de

The *Beilstein Journal of Organic Chemistry* is published by the Beilstein-Institut zur Förderung der Chemischen Wissenschaften.

Beilstein-Institut zur Förderung der Chemischen Wissenschaften
Trakehner Straße 7–9
60487 Frankfurt am Main
Germany
www.beilstein-institut.de

BEILSTEIN JOURNAL OF ORGANIC CHEMISTRY

1-Butyl-3-methylimidazolium tetrafluoroborate as suitable solvent for BF_3: the case of alkyne hydration. Chemistry vs electrochemistry

Marta David[1], Elisa Galli[1], Richard C. D. Brown[2], Marta Feroci[1], Fabrizio Vetica[3] and Martina Bortolami[*1]

Full Research Paper

Open Access

Address:
[1]Department of Basic and Applied Sciences for Engineering (SBAI), Sapienza University of Rome, via Castro Laurenziano, 7, 00161 Rome, Italy, [2]School of Chemistry, University of Southampton, Southampton SO17 1BJ, UK and [3]Department of Chemistry, Sapienza University of Rome, piazzale Aldo Moro, 5, 00185 Rome, Italy

Email:
Martina Bortolami[*] - martina.bortolami@uniroma1.it

* Corresponding author

Keywords:
alkyne hydration; boron trifluoride; electrochemical synthesis; ionic liquids

Beilstein J. Org. Chem. **2023,** *19,* 1966–1981.
https://doi.org/10.3762/bjoc.19.147

Received: 28 August 2023
Accepted: 12 December 2023
Published: 28 December 2023

This article is part of the thematic issue "Synthetic electrochemistry".

Associate Editor: L. Vaccaro

Abstract

In order to replace the expensive metal/ligand catalysts and classic toxic and volatile solvents, commonly used for the hydration of alkynes, the hydration reaction of alkynes was studied in the ionic liquid 1-butyl-3-methylimidazolium tetrafluoroborate (BMIm-BF_4) adding boron trifluoride diethyl etherate ($BF_3{\cdot}Et_2O$) as catalyst. Different ionic liquids were used, varying the cation or the anion, in order to identify the best one, in terms of both efficiency and reduced costs. The developed method was efficaciously applied to different alkynes, achieving the desired hydration products with good yields. The results obtained using a conventional approach (i.e., adding $BF_3{\cdot}Et_2O$) were compared with those achieved using BF_3 electrogenerated in BMIm-BF_4, demonstrating the possibility of obtaining the products of alkyne hydration with analogous or improved yields, using less hazardous precursors to generate the reactive species in situ. In particular, for terminal arylalkynes, the electrochemical route proved to be advantageous, yielding preferentially the hydration products vs the aldol condensation products. Importantly, the ability to recycle the ionic liquid in subsequent reactions was successfully demonstrated.

Introduction

Alkynes are fundamental starting materials towards more complex organic compounds, widely used both in organic chemistry and in electrochemistry as raw materials for the preparation of different molecules of pharmaceutical and industrial interest [1-9]. Among the different organic transformations involving alkynes, their hydration is a well-known and useful

reaction in organic chemistry, affording carbonyl compounds based on an atom-economical approach. Indeed, the addition of water to the triple bond of a terminal alkyne leads to the formation of the corresponding methyl ketone or aldehyde, in the case of Markovnikov or *anti*-Markovnikov addition, respectively. On the other hand, the hydration of an internal unsymmetrical alkyne can lead to the formation of the two possible regioisomeric ketones.

The hydration reaction requires a catalytic species, able to polarize the alkyne triple bond to facilitate water attack. Initially, in 1881, Kucherov identified mercury(II) salts in sulfuric acid as efficient promoters of the hydration of alkynes and this catalyst system has found applications in industrial scale synthesis [10]. However, the toxicity and the environmental issues associated with the use of mercury-based compounds have stimulated the search for alternative catalysts and conditions for the hydration of alkynes, in order to identify safer and more sustainable methods [11-13]. In particular, transition-metal catalysts containing Au(I) or (III) [14-24], Ru(II) [25-30], Pd(II) [31-33], Pt(II) [34,35], Fe(III) [36,37], Cu(I) [38-41], Co(III) [42-44], as well as other metals, have been widely studied. In addition, methods involving Brønsted acids, alone or in presence of Lewis acids as co-catalysts, have been developed [45-54]. However, some of these procedures suffer from major drawbacks, such as the toxicity and/or high cost of the metal catalysts, the need to use concentrated Brønsted acids in high excess, long reaction times, and high temperatures. In addition, these reactions have been studied mainly in classical volatile and, in some cases, toxic organic solvents, such as dioxane, tetrahydrofuran, methanol, dichloromethane or 1,2-dichloroethane.

The efficiency of the reported catalysts and of the examined reaction conditions are variable according to the alkynes considered and, nowadays, the identification of new catalysts as well as increasingly mild, economic and sustainable reaction conditions remain fundamental objectives for research in the field of organic chemistry. In recent years, alternative methods have been developed, including the use of different heterogeneous catalysts, to ensure their recovery and reusability after several reaction cycles [55-68], or the use of eco-friendly reaction media [69-72]. Recently, Zhang and co-workers reported an electrochemical procedure for the hydration of arylacetylenes, under mild reaction conditions, without transition metal catalysts, added oxidants, or strong acids involved, using Selectfluor (1-(chloromethyl)-4-fluoro-1,4-diazabicyclo[2.2.2]octane-1,4-diium ditetrafluoroborate) as essential additive [73].

With regard to the reaction medium, the idea of replacing classic organic solvents with alternative solvents could represent an important innovation for alkyne hydration. In particular, ionic liquids (ILs) could represent a valid alternative to conventional organic solvents. ILs are generally liquid salts at or near room temperature, formed by large unsymmetrical organic cations and weakly coordinating or not-coordinating organic or inorganic anions. They have interesting physicochemical properties that differentiate them from the organic solvents commonly used in synthesis [74-77]. Importantly, they have a very low vapour pressure, and therefore do not behave as air pollutants. This also facilitates their recovery and recycling. Furthermore, they generally exhibit low flammability, high thermal and chemical stability, good thermal and electrical conductivity, together with the ability to solubilize organic and inorganic compounds of different polarity [78-81]. Considering the intrinsic ionic nature of ILs, they act as very different chemical medium compared to molecular solvents, having the possibility of stabilizing charged or dipolar intermediates. Therefore, ILs can be used to modulate outcomes for some chemical reactions [82,83].

There are only a few reported examples of the hydration reaction of alkynes carried out in ILs. In one case, a dicationic IL, containing sulfuric acid as catalyst, was used as reaction medium to carry out the hydration of different alkynes under mild conditions (40–60 °C, 0.5–1 h) [84]. In a second case, different Brønsted acid ionic liquids (BAILs) have been used both as medium and as catalysts for the hydration of various alkynes (60 °C, 10–24 h) [85,86]. In these works, the ILs were efficiently reused for subsequent reaction cycles. Another research group reported the use of commercially available 1-butyl-3-methylimidazolium hexafluorophosphate (BMIm-PF_6) as co-solvent with methanol and water to allow recycling of a phosphine-based Au(I) complex, as an efficient catalytic system for the hydration of terminal alkynes [87]. Moreover, the interesting properties of ILs have also been exploited to synthesize new solid polymeric catalysts for the hydration of alkynes, named poly(ionic liquid)s (PILs), using trifluoroethanol as solvent [88,89].

One of the most studied classes of ILs in organic chemistry are 1,3-disubstitued imidazolium cations, which are cheap, liquid over a wide range of temperatures, and possess good solvating properties [90,91]. Due to their wide electrochemical window, imidazolium ILs are commonly used in organic electrochemistry, simultaneously as solvents and supporting electrolytes [92-94]. In addition, the cathodic reduction (both in batch [95] and in flow [96]) can be exploited for the generation of N-heterocyclic carbenes (NHCs), extensively studied as organocatalysts as well as ligands for transition-metal-promoted synthetic methodologies [97-99]. Under anodic oxidation, the electrogeneration of boron trifluoride (BF_3) from tetrafluoroborate

ILs occurs [100,101]. Moreover, we have recently demonstrated the possibility to efficiently apply the electrogenerated BF_3 in IL for different classical acid-catalysed reactions [102,103]. Specifically, electrogenerated BF_3 in 1-butyl-3-methylimidazolium tetrafluoroborate (BMIm-BF_4) appears as an alternative and less dangerous source of BF_3 compared to commercially available BF_3 diethyl etherate ($BF_3{\cdot}Et_2O$), commonly used in organic synthesis. Indeed, the main advantages of the developed system are: 1) in situ generation of BF_3, which avoids its storage and handling, 2) the possibility to control the amount of electrogenerated BF_3 using current by simply starting or stopping the electrolysis, 3) the absence of fuming, most probably due to the ability of the IL to stabilize the Lewis acid, 4) reduced sensitivity to moisture, due to the protective action of the IL, and 5) the possibility of recycling the same sample of IL for subsequent reaction cycles. In addition, with computational studies we demonstrated the greater stability of BF_3 in BMIm-BF_4 compared to $BF_3{\cdot}Et_2O$ [103].

Based on the ever increasing need to identify new eco-friendly catalysts and/or reaction media for the hydration of alkynes, and considering our previous works on ILs and electrogeneration of BF_3, the aim of this work was to explore the hydration of alkynes using ILs as reaction medium and BF_3 as catalyst. First of all, we investigated the behaviour of diphenylacetylene in BMIm-BF_4 containing $BF_3{\cdot}Et_2O$. Then we evaluated the same reaction in different ILs, modifying the cation or the anion. Subsequently, we extended the method to different internal and terminal alkynes. Finally, we studied the reaction in the electrogenerated BF_3/BMIm-BF_4 system, comparing the results with those obtained with the chemical route ($BF_3{\cdot}Et_2O$).

Results and Discussion

Optimization of the reaction conditions for hydration of diphenylacetylene in BMIm-BF_4 with $BF_3{\cdot}Et_2O$

In the initial investigation, the internal alkyne diphenylacetylene (**1a**) was selected as a model substrate to evaluate alkyne reactivity in the ionic liquid 1-butyl-3-methylimidazolium tetrafluoroborate (BMIm-BF_4) catalysed by $BF_3{\cdot}Et_2O$ and to optimize the reaction conditions for hydration. All reactions were carried out in sealed vials, in 1 mL BMIm-BF_4 at 80 °C for the time indicated in Table 1. At the end of the reaction the mixture was extracted with diethyl ether and the extracts were washed with water to obtain the crude, which was analysed using NMR spectroscopy.

Initially the reaction was carried out without added water, in the presence of a large excess of $BF_3{\cdot}Et_2O$ (5 equiv) (as often re-

Table 1: Optimization of the reaction conditions for hydration of diphenylacetylene (**1a**)[a].

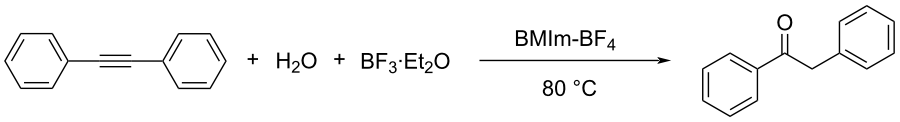

1a **2a**

Entry	$BF_3{\cdot}Et_2O$[b]	H_2O[b]	BMIm-BF_4[c]	Time	Yield **2a** [%][d]	Recovered **1a** [%][d]
1[e]	5	–	dried	5 h	53	46
2[f]	5	–	not dried	5 h	73	24
3[e]	5	–	dried	18 h	87	10
4[f]	5	1	dried	5 h	72	24
5[f]	5	1	dried	18 h	95	4
6[f]	5	2	dried	5 h	73	26
7[g]	5	2	dried	18 h	96 (90)[h]	1
8[f]	4	1	dried	18 h	83	13
9[g]	3	1	dried	18 h	81	11
10	3	–	not dried	65 h	92	3
11	2	–	not dried	65 h	66	28

[a]All the reactions were carried out at 80 °C in BMIm-BF_4, with 0.3 mmol of diphenylacetylene (**1a**); [b]equivalents with respect to **1a**; [c]BMIm-BF_4 was kept under vacuum (7 mbar) for 16 h before each use (dried) or used as such (not dried); [d]yields calculated from ^{1}H NMR spectra of the crude extracts; [e]the same recycled IL was used for the experiments in entry 1 and 3; [f]the same recycled IL was used for the experiments in entries 2, 4–6 and 8; [g]the same recycled IL was used for the experiments in entries 7 and 9; [h]yield of the product **2a** isolated after column chromatography.

ported in literature, see as an example [104]). The reaction was conducted for 5 h at 80 °C using either "stock" (undried) BMIm-BF_4 (Table 1, entry 2) or "dry" BMIm-BF_4 (kept under vacuum for 16 h before use, entry 1). Due to the hygroscopic nature of the ILs, the water present within the "stock" BMIm-BF_4 was evidently enough to give the hydration product **2a** with 73% yield (Table 1, entry 2). However, even in the dried IL, without external addition of water, the product was obtained with 53% yield (Table 1, entry 1), demonstrating that the applied drying process was not sufficient to eliminate all the water present.

By increasing the reaction time, from 5 h to 18 h (Table 1, entry 3), recycling the IL used in the experiment in entry 1 (after drying the IL under vacuum for 16 h), there was a significant increase in product yield from 53% to 87%.

Then, we investigated addition of water to BMIm-BF_4, as the literature reports that the hydrolysis of the anion of this IL is quite slow in the presence of excess water (less than 5% BF_4^- hydrolysis in a 1:1 in volume IL/water solution kept at 45 °C for 24 h) [105]. It should be noted that the same treatment carried out on 1-methyl-3-octylimidazolium tetrafluoroborate (OMIm-BF_4) evidenced a much higher extent of BF_4^- hydrolysis. This is probably due to the weaker interaction between cation and anion of the IL as the length of the side alkyl chain increases, which makes the BF_4^-/water interaction more effective. Although Saihara and co-workers demonstrated that BF_4^- hydrolysis generates HF, which reacts with the surrounding glass container yielding SiF_6^{2-} (signal at −130 ppm in ^{19}F NMR spectrum) [106], we never detected such a peak in ^{19}F NMR spectra of the neat IL, analysed after reaction work-up, keeping it under vacuum to completely eliminate diethyl ether traces before NMR analysis. It should be mentioned that the solution was kept in the NMR tubes only for the time necessary to record the NMR spectra. We cannot exclude that a much longer contact time between glass and solution could evidence such a signal.

Using dried IL and adding 1 equiv of water with respect to alkyne (Table 1, entries 4 and 5), the yield of **2a** improved from 53% to 72% after 5 h (Table 1, entry 1 vs 4), and from 87% to 95% after 18 h (Table 1, entry 3 vs 5). Therefore, comparable yields of **2a** can be obtained using the "stock" IL (Table 1, entry 2) or the dried IL by adding 1 equiv of water (Table 1, entry 4). Clearly, the amount of water contained in the IL can be affected by various factors, in particular how long the bottle has been opened and to how much moisture it has been exposed, so from the point of view of reproducibility it was preferred to dry the IL and add a defined amount of water. By increasing the amount of water to 2 equiv, the yields of the desired product did not change (compare Table 1, entries 4 vs 6, and 5 vs 7).

A modest decrease in the yield of **2a** was observed when the amount of $BF_3{\cdot}Et_2O$ was reduced (4 and 3 equiv) in the presence of 1 equiv of water for 18 h, although the yields of the reaction product still remained high (>80%, Table 1, entries 8 and 9). Further investigation using lower amounts of $BF_3{\cdot}Et_2O$ revealed that a 92% yield of **2a** could be realized using 3 equiv of the Lewis acid by extending the reaction time to 65 h (Table 1, entry 10). A further reduction in the amount of $BF_3{\cdot}Et_2O$ to 2 equiv resulted in a lower yield of 66% after the same reaction time (65 h, Table 1, entry 11). The experiments reported in Table 1 suggest that the best conditions for the hydration of diphenylacetylene (**1a**) are 5 equiv of $BF_3{\cdot}Et_2O$, 1 or 2 equiv of H_2O, at 80 °C for 18 h (Table 1, entries 5 and 7). Importantly, as shown in Table 1, the same samples of BMIm-BF_4 were efficiently reused up to five times, without adversely affecting the reaction yields.

Screening of different ionic liquids as media for the hydration of diphenylacetylene

After the optimization of the reaction conditions in BMIm-BF_4, different ILs were considered as alternative solvent (Table 2 and Table 3). All the experiments were carried out under the conditions reported in entry 9 of Table 1, in order to observe possible variations in the yield of compound **2a**. ILs with different anions or cations (compared to BMIm-BF_4) were investigated to probe potential interactions with the reagents, the intermediates or the reaction product. All the ILs were dried under vacuum for 16 h, prior to use.

Considering the imidazolium tetrafluoroborate ILs, with the exception of BMIm-BF_4, a progressive decrease in the yield of **2a**, from 76% to 31%, was observed by increasing the length of the aliphatic chain linked to the imidazolic ring (Table 3, entries 1–5). Although BMIm-BF_4 gave a slightly higher yield than that obtained with EMIm-BF_4, the general trend suggests that probably the increase in the lipophilicity of the ILs impairs the reaction, hindering the attack of water to the triple bond. Furthermore, the reaction in BDMIm-BF_4, with an additional methyl group in 2 position of the imidazolic ring, gave **2a** with a lower yield compared to BMIm-BF_4 (Table 3, entry 6 vs 2). Replacing the imidazolium cation with 1-butyl-3-methylpyridinium led to a drastic reduction of the yield of **2a**, to 35% (Table 3, entry 7).

By keeping the 1-butyl-3-methylimidazolium cation unchanged, anion variation also affected the reaction yield. Indeed, in the presence of triflate, acetate or trifluoroacetate anions the desired product was obtained only in trace amounts (Table 3, entries

Table 2: Structure of the ILs used as solvent for the hydration reaction of diphenylacetylene (**1a**).

Structure	Acronym	R	R^1	X^-
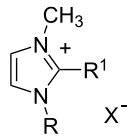	EMIm-BF_4	CH_3CH_2-	H-	BF_4^-
	BMIm-BF_4	$CH_3(CH_2)_3$-	H-	BF_4^-
	HMIm-BF_4	$CH_3(CH_2)_5$-	H-	BF_4^-
	OMIm-BF_4	$CH_3(CH_2)_7$-	H-	BF_4^-
	DMIm-BF_4	$CH_3(CH_2)_9$-	H-	BF_4^-
	BDMIm-BF_4	$CH_3(CH_2)_3$-	CH_3-	BF_4^-
	BMIm-Tf_2N	$CH_3(CH_2)_3$-	H-	$(CF_3SO_2)_2N^-$
	BMIm-PF_6	$CH_3(CH_2)_3$-	H-	PF_6^-
	BMIm-TfO	$CH_3(CH_2)_3$-	H-	$CF_3SO_3^-$
	BMIm-OAc	$CH_3(CH_2)_3$-	H-	CH_3COO^-
	BMIm-$OCOCF_3$	$CH_3(CH_2)_3$-	H-	CF_3COO^-
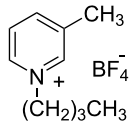	BMPy-BF_4			

Table 3: Hydration reaction of diphenylacetylene **1a** in different ILs[a].

Entry	Solvent[b]	Yield **2a** [%][c]	Recovered **1a** [%][c]
1	EMIm-BF_4	76	13
2 [d]	BMIm-BF_4	81	11
3	HMIm-BF_4	71	20
4	OMIm-BF_4	37	54
5	DMIm-BF_4	31	61
6	BDMIm-BF_4	64	28
7	BMPy-BF_4	35	60
8	BMIm-Tf_2N	87	4
9	BMIm-PF_6	87	3
10	BMIm-TfO	1	95
11	BMIm-OAc	traces	98
12	BMIm-$OCOCF_3$	traces	97
13	dioxane	10	90

[a]All the reactions were carried out with 0.3 mmol of diphenylacetylene (**1a**), 3 equiv of BF_3·Et_2O, 1 equiv of H_2O, at 80 °C for 18 h; [b]the ILs were kept under vacuum for 16 h before use; [c]yields calculated from the ^1H NMR spectra of the crude extracts; [d]replicate of experiment reported in entry 9 of Table 1, for comparison.

10–12). This could be explained by the fact that these anions could coordinate the Lewis acid BF_3 through the negatively charged oxygen [107], decreasing availability of BF_3 for catalysis.

Otherwise, ILs possessing bis(trifluoromeylsulfonyl)imide and hexafluorophosphate anions afforded hydrated product **2a** with slightly better yields (87%) compared to those achieved with the BF_4^- counter anion (Table 3, entries 8–9 vs 2), suggesting PF_6^- and Tf_2N^- do not hinder the reactivity of BF_3 in the hydration reaction.

Based on these results, considering the higher cost of BMIm-Tf_2N and BMIm-PF_6, the preferred IL among those tested, in terms of both yield and cost, is BMIm-BF_4.

The reaction was also carried out using dioxane as solvent [108]. In this case, the product was obtained with a very low yield of 10% (Table 3, entry 13). This result emphasizes the importance of the use of an IL as a solvent, not only for its green aspect, in particular for its very low vapour pressure and for the possibility of its recycling, but also for its ability to stabilize ionic or polar intermediates, improving the reaction efficiency.

Hydration of different alkynes catalysed by BF_3·Et_2O in BMIm-BF_4

Subsequently, the developed method was extended to different alkynes, both internal and terminal. The best results for the hydration reaction of each studied alkyne, catalysed by BF_3·Et_2O in BMIm-BF_4, are summarized in Table 4, while all the experiments carried out are reported in Table S1 in Supporting Information File 1. In order to avoid the use of a large excess of the Lewis acid, the conditions reported in entry 9 of Table 1 were chosen as reference for the study of the reactivity of different alkynes.

For the internal alkyl(aryl)alkynes a regioselective hydration occurred, with the only generation of the corresponding aryl ketones, formed after the attack of water to the pseudobenzylic position, as observed in Lewis acid-assisted Brønsted acid (LBA) catalysis [47-50]. Internal alkynes afforded the corresponding products in good to excellent yields (Table 4, entries 1–3). In particular, the unsymmetrical alkyl(aryl)alkynes **1b** and **1c** showed a higher reactivity compared to diphenylacetylene

Table 4: Hydration of different alkynes catalysed by BF_3–Et_2O in BMIm-BF_4[a].

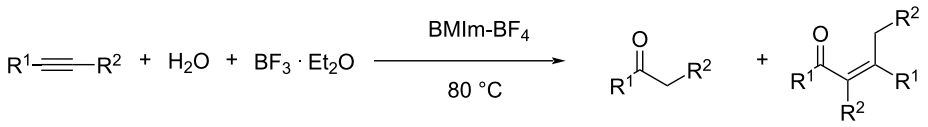

1 **2** **3**

Entry	Alkyne	BF_3·Et_2O[b]	Time	**2**, yield[c]	**3**, yield[c]
1[d]	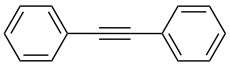	3	18 h	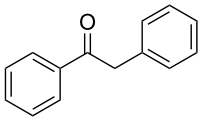	–
	1a			**2a**, 81%	
2	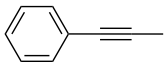	3	5 h	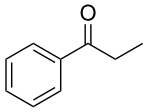	–
	1b			**2b**, 97%	
3	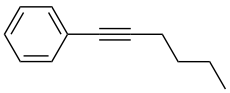	3	5 h	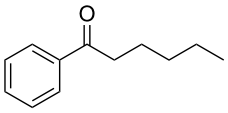	–
	1c			**2c**, 76%	
4	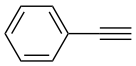	1	1 h	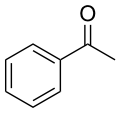	–
	1d			**2d**, 81%	
5	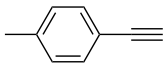	1	1 h	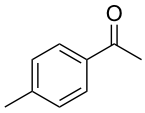	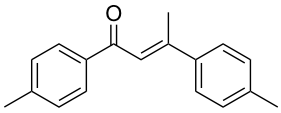
	1e			**2e**, 61%	**3e**, 38%
6	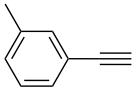	1	1 h	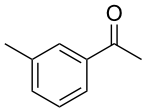	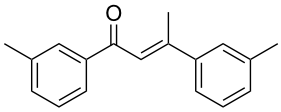
	1f			**2f**, 43%	**3f**, 56%
7	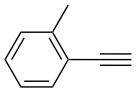	1	1 h	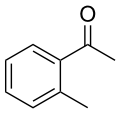	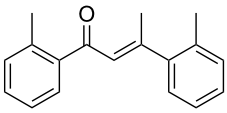
	1g			**2g**, 81%	**3g**, 4%

Table 4: Hydration of different alkynes catalysed by BF_3–Et_2O in BMIm-BF_4[a]. (continued)

8	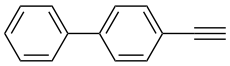 **1h**	1	1 h	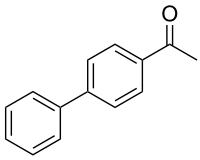 **2h**, 47%	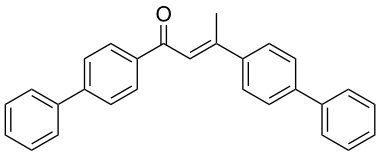 **3h**, 43%
9	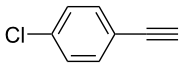 **1i**	1	1 h	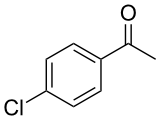 **2i**, 72%	–
10[e]	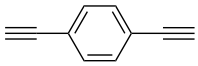 **1j**	2 [f]	1 h	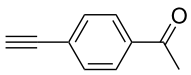 **2j**, 56% 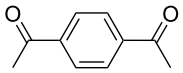 **2jj**, 22%	–
11	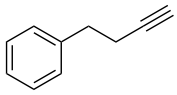 **1k**	3	18 h	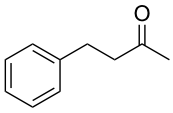 **2k**, 79%	–
12	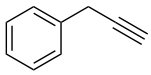 **1l**	2	18 h	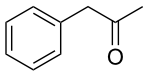 **2l**, 62%	–
13	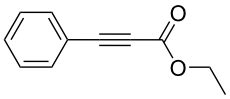 **1m**	5	18 h	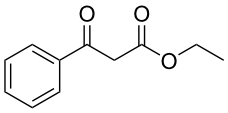 **2m**, 65%	–
14	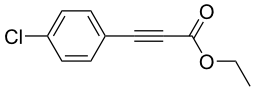 **1n**	5	18 h	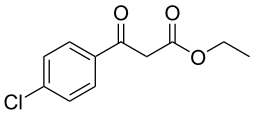 **2n**, 47%	–

[a]All the reactions were carried out at 80 °C in BMIm-BF_4, kept under vacuum for 16 h before each use, with 0.3 mmol of alkyne **1** and 0.3 mmol of H_2O; [b]equivalents with respect to **1**; [c]yields calculated from ^1H NMR spectra of the crude extracts; [d]replicate of the experiment reported in entry 9 of Table 1; [e]0.6 mmol of H_2O were used; [f]equivalents with respect to one alkyne group of **1j**.

(**1a**), affording the corresponding ketones in high yields after 5 h.

Otherwise, terminal alkynes generally showed higher reactivity compared to internal ones. For all the studied terminal alkynes, only ketone products (Markovnikov) were obtained, excluding the formation of the *anti*-Markovnikov ones. Hydration of phenylacetylene **1d** carried out with 3 equiv of $BF_3{\cdot}Et_2O$ for 5 h gave the aldol condensation product **3d** (58%) in addition to acetophenone **2d** with low yield (32%) (see Table S1, Supporting Information File 1). Assuming that enone **3d** is formed from acetophenone, catalysed by the excess Lewis acid present, the reaction was performed in presence of 1 equiv of $BF_3{\cdot}Et_2O$ and a reaction time of 1 h (Table 4, entry 4). In this way, the selec-

tivity was improved and only the hydration product **2d** was obtained in 81% yield.

For electron-rich terminal alkynes, the corresponding ketones could not be selectively obtained without the aldol condensation products. Considering 4-methylphenylacetylene (**1e**), the reaction carried out with 3 equiv of $BF_3{\cdot}Et_2O$ for 5 h gave only the condensation product **3e** (70%, see Table S1, Supporting Information File 1). Reducing the amount of $BF_3{\cdot}Et_2O$ to 1 equiv and the reaction time to 1 h (Table 4, entry 5) gave a mixture of ketones **2e** and **3e** (61% and 38%, respectively). Even reducing the amount of $BF_3{\cdot}Et_2O$ to 0.5 equiv did not improve the yield of the hydration product (see Table S1, Supporting Information File 1). The presence of a methyl group in the *meta* position in **1f** decreased the selectivity with respect to formation of the hydration product **2f**, favouring the condensation product **3f** (Table 4, entry 6). On the other hand, an *ortho* methyl group in **1g** favoured formation of the ketone **2g**, with a good yield, probably due to the steric hindrance of the aldol condensation (Table 4, entry 7). As expected, based on the above consideration, 4-ethynyl-1,1'-biphenyl (**1h**) afforded both hydration and condensation products **2h** and **3h** in similar amounts (Table 4, entry 8), while the presence of a chlorine in the *para* position of the phenyl ring allowed to obtain the hydration product **2i** with good yield, reducing its reactivity (Table 4, entry 9).

With 1,4-diethynylbenzene (**1j**) both the products of mono (**2j**) and bis hydration (**2jj**) were obtained under all conditions tested (see Table S1, Supporting Information File 1). The highest selectivity for the generation of **2j** was achieved with 2 equiv of $BF_3{\cdot}Et_2O$ for 1 h (Table 4, entry 10).

Aliphatic alkyne **1k** showed a different reactivity compared to the other terminal alkynes. Indeed, in this case the corresponding condensation product was never obtained, while the hydration product **2k** was obtained in good yield using 3 equiv of $BF_3{\cdot}Et_2O$ and extending the reaction time to 18 h (Table 4, entry 11).

The aliphatic alkyne **1l** gave the corresponding hydration product **2l** in good yield with 2 equiv of $BF_3{\cdot}Et_2O$ and a reaction time of 18 h (Table 4, entry 12).

The following step was to study the reactivity of $BF_3{\cdot}Et_2O$ in BMIm-BF_4 towards disubstituted alkynes containing a carbonyl group adjacent to the triple bond. This class of substrates, after water addition, yields 1,3-dicarbonyl compounds, which could yield BF_2-chelates under our experimental conditions [109]. In order to study their behaviour, we decided to avoid water during an initial work-up, to prevent a possible BF_2-chelate hydrolysis, and only ethereal extraction was carried out after the reaction.

When the reaction was carried out on ethyl 3-phenylpropiolate (**1m**, Table 4, entry 13), the analysis of the ethereal extracts showed the presence of the BF_2-chelate. In fact, the following convincing peaks were found in the NMR spectra: a singlet at 6.11 ppm, along with a quartet at 4.68 ppm (^{1}H NMR spectrum), a peak at 83.3 ppm (^{13}C NMR spectrum) and a singlet at −139.1 ppm (^{19}F NMR spectrum) [109]. A simple washing with distilled water gave the corresponding ethyl benzoylacetate (**2m**). Compared to the other studied alkynes, **1m** required a larger excess of $BF_3{\cdot}Et_2O$ (5 equiv) to give the corresponding hydration product with a satisfactory yield. Indeed, this behaviour could be explained by the formation of the BF_2-chelate, which reduces the amount of BF_3 available for catalysis.

A similar behaviour was observed with ethyl 3-(4-chlorophenyl)propiolate (**1n**), although with lower yield due to the deactivating effect of the chlorine substituent in the *para* position of the phenyl ring (Table 4, entry 14).

Importantly, for the experiments involving the same alkyne (see Table S1, Supporting Information File 1), the same sample of BMIm-BF_4 was effectively reused, up to five times, demonstrating the advantage of using this IL as medium for this reaction.

Hydration of alkynes in electrogenerated BF_3/BMIm-BF_4 system

Based on previous works, which demonstrated the possibility to electrogenerate BF_3 in tetrafluoroborate ILs [100], and to efficiently use it to carry out different Lewis acid catalysed organic reactions [101-103], we investigated the applicability of the electrogenerated BF_3/BMIm-BF_4 system for the hydration reaction of alkynes. The best results for the hydration reaction of each studied alkyne, catalysed by electrogenerated BF_3 in BMIm-BF_4, are summarized in Table 5, while all the experiments carried out are reported in Table S2 in the Supporting Information File 1.

Regarding internal alkynes, the electrogenerated BF_3 (4 F/mol)/BMIm-BF_4 system proved to be highly efficient for **1a**, **1b** and **1c**, delivering the corresponding ketones in excellent yields, which were comparable or better than those achieved using $BF_3{\cdot}Et_2O$ (Table 5, entries 1–3, and Figure 1).

In contrast to earlier results, an interesting behaviour was observed with the terminal alkynes. Indeed, the terminal arylalkynes **1d–h** afforded the corresponding hydration prod-

Table 5: Hydration of different alkynes catalysed by electrogenerated BF_3 in BMIm-BF_4.[a]

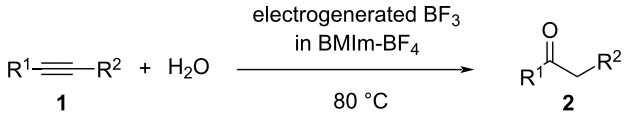

1 **2**

Entry	Alkyne	Electrogenerated BF_3 (F/mol)[b]	Time	Product **2**, yield[c]
1	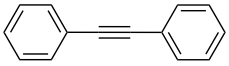 **1a**	4	18 h	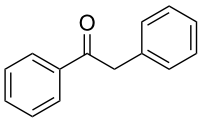 **2a**, 85%
2	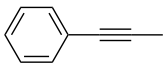 **1b**	4	5 h	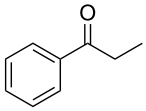 **2b**, 84%
3	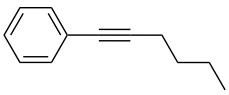 **1c**	4	5 h	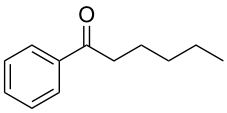 **2c**, 94%
4	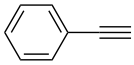 **1d**	1	1 h	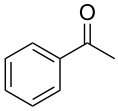 **2d**, 78%
5	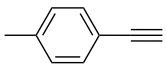 **1e**	1	1 h	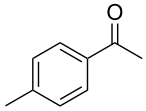 **2e**, 84%[d]
6	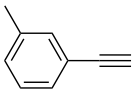 **1f**	1	1 h	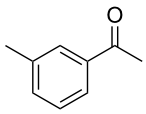 **2f**, 91%
7	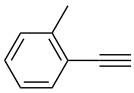 **1g**	1	1 h	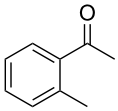 **2g**, 78%
8	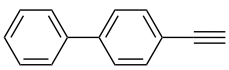 **1h**	1	1 h	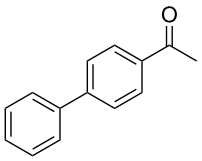 **2h**, 94%

Table 5: Hydration of different alkynes catalysed by electrogenerated BF_3 in BMIm-BF_4.[a] (continued)

9	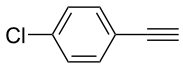 **1i**	2	18 h	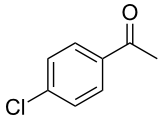 **2i**, 79%
10[e]	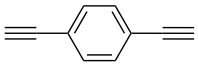 **1j**	4	5 h	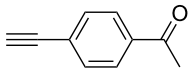 **2j**, 35% 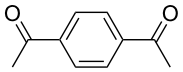 **2jj**, 53%
11	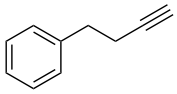 **1k**	2	18 h	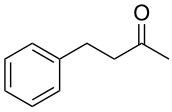 **2k**, 51%
12	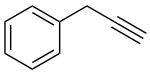 **1l**	4	18 h	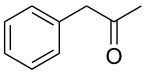 **2l**, 23%
13	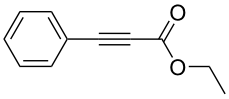 **1m**	4[f]	18 h	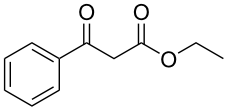 **2m**, 58%

[a]BMIm-BF_4, kept under vacuum for 16 h before each use, was electrolyzed (galvanostatic conditions: 10 mA·cm^{-2}) on platinum electrodes (rt, N_2) in divided cell configuration. At the end of electrolysis, alkyne **1** (0.3 mmol) and H_2O (0.3 mmol) were added to the anolyte. All the reactions were carried out at 80 °C for the time reported in table; [b]amount of electrogenerated BF_3 with respect to starting alkyne, admitting a 100% current efficiency (1 mF = 96.5 C = 1 mmol of BF_3); [c]yields calculated from ^{1}H NMR spectra of the crude extracts; [d]**3e**, 9%. [e]0.6 mmol of H_2O were used. [f]the electrolysis was carried out in the presence of the alkyne (0.3 mmol) in the anodic compartment. At the end of electrolysis, H_2O (0.3 mmol) was added to the anolyte, then the reaction was carried out at 80 °C for the time reported in table.

ucts selectively in good to excellent yields by exploiting the electrogeneration of BF_3 in BMIm-BF_4 at 1 F/mol (Table 5, entries 4–8). It is important to remember that with BF_3·Et_2O these alkynes gave mixtures with the corresponding aldol condensation products, in some cases in considerable amounts (Table 4, entries 5, 6, and 8). Reduction in the amount of BF_3·Et_2O to 0.5 equiv did not improve the yields of the hydration products (see Table S1, Supporting Information File 1).

Interestingly, the alkynes **1e**, **1f** and **1h**, which in the chemical route provided considerable amounts of the condensation products and moderate yields for the hydration products, with the electrochemical route gave the corresponding hydration products with excellent yields, significantly better compared to those obtained with BF_3·Et_2O (Table 5, entries 5, 6, 8, and Figure 1). By exploiting the electrochemical generation of BF_3, the alkynes **1d** and **1g** gave the corresponding ketones with similar yields compared to the chemical route (Table 5, entries 4 and 7, and Figure 1). The alkyne **1i** gave the ketone **2i** with a slightly better yield compared to the chemical route, when increasing the amount of the electrogenerated BF_3 to 2 F/mol and the reaction time to 18 h (Table 5, entry 9, and Figure 1).

The application of the electrochemical conditions to 1,4-diethynylbenzene (**1j**) using 2 F/mol selectively afforded ketone **2j** after 1 h, after hydration of one alkyne group, in low yield (39%), with the majority of the starting alkyne being recovered (46%) (see Table S2, Supporting Information File 1). Increasing the amount of electrogenerated BF_3 by applying 4 F/mol and extending the reaction time (5 h) reversed the selectivity in favour of the diketone **2jj** (Table 5, entry 10),

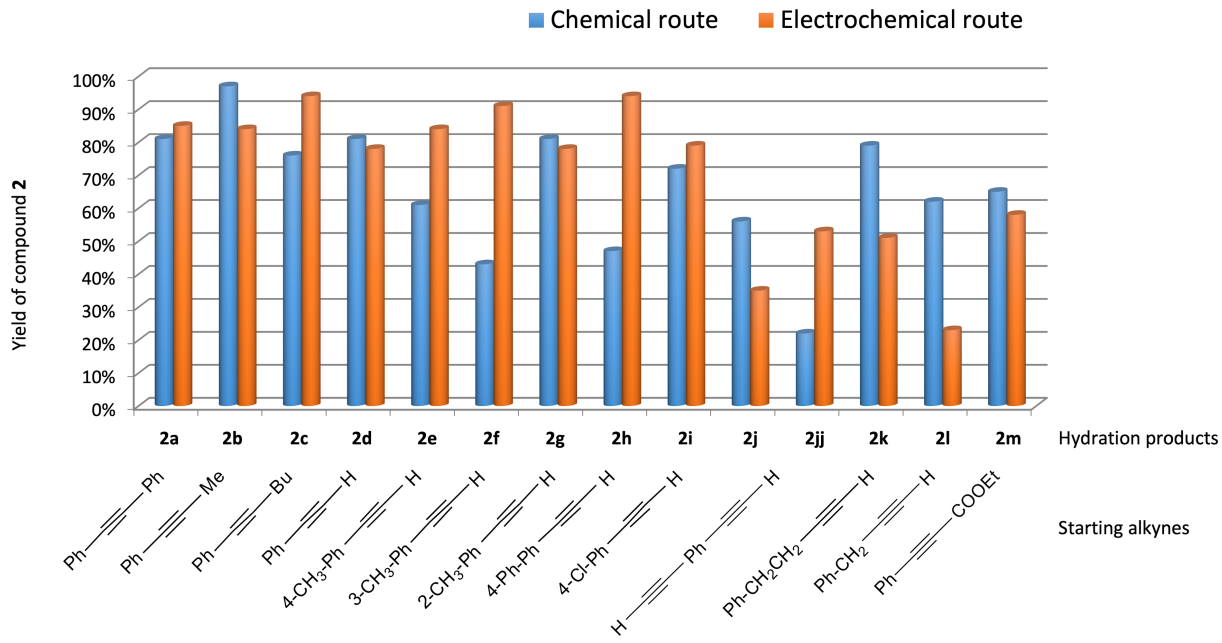

Figure 1: Comparison of the hydration reactions of different alkynes in BMIm-BF_4 catalysed by $BF_3{\cdot}Et_2O$ (blue) and by electrogenerated BF_3 (orange).

which had not been achieved using $BF_3{\cdot}Et_2O$ as a reagent (see Table 4, entry 10).

For the aliphatic alkyne **1k** the hydration product **2k** was obtained with moderate yield by exploiting the electrogeneration of 2 F/mol of BF_3 (Table 5, entry 11). Unfortunately, an increase in the amount of electrogenerated BF_3 did not improve the yield of the desired product (see Table S2, Supporting Information File 1).

By exploiting the electrogeneration of 4 F/mol of BF_3, with the aliphatic alkyne **1l** the corresponding hydration product **2l** was obtained with low yield (Table 5, entry 12).

Unfortunately, any attempt to hydrate disubstituted alkynes containing a carbonyl group adjacent to the triple bond (**1m**, **1n**) with electrogenerated BF_3, according to the procedure adopted for the other alkynes, failed, yielding only starting material.

We then tried to electrogenerate BF_3 in BMIm-BF_4, directly in the presence of the alkyne **1m** or **1n** in the anodic compartment. Surprisingly, for alkyne **1m** this approach has allowed to obtain the hydration product **2m**, with a yield (58%) slightly lower than that observed in the chemical route (Table 5, entry 13, and Figure 1). Otherwise, with the alkyne **1n**, also in this way, the hydration product was not obtained. In addition to the different reactivity, due to the presence or not of chlorine in the *para* position of the phenyl group, the different physical state (liquid for **1m** vs solid for **1n**) and the possible different solubility in BMIm-BF_4 at room temperature (according to the electrolysis conditions) may have affected the results obtained with these substrates. Further studies will be necessary to clarify the behaviour of alkynes containing a carbonyl group adjacent to the triple bond.

After work-up, the electrolysed IL was placed under vacuum to eliminate diethyl ether traces and then analysed by NMR to check for BMIm-F presence, whereas the fluoride ion could originate from IL decomposition in the presence of water or from the evolution of electrogenerated F_2. However, the ^{19}F NMR spectrum showed no detectable peak around −122 ppm, reported in the literature for BMIm-F [110]. The only difference between IL ^{19}F NMR spectra before and after electrolysis is a peak at −148.7 ppm (referred to BF_4^- at −150.6 ppm), possibly due to BF_3OH^- or $B_2F_7^-$ [111,112] (see Supporting Information File 1, Figure S1a vs f and b, c). This last hypothesis is corroborated by the ^{19}F NMR analysis of BMIm-BF_4 after anodic oxidation in a divided cell, which shows a peak at −147.3 ppm (besides the peak at −150.6 due to BF_4^-) (see Supporting Information File 1, Figure S1e), which is replaced by a peak at −144.0 ppm (referred to −150.6 ppm for BF_4^-) when the electrolysis is carried out in an undivided cell (see Supporting Information File 1, Figure S1d). In this last case, in fact, the NHC-BF_3 adduct is formed between anodically electrogenerated BF_3 and cathodically electrogenerated NHC [103].

Evaluation of the current efficiency in the electrogeneration of BF_3 in BMIm-BF_4

In order to have an idea of the current efficiency in the electrogeneration of BF_3 in BMIm-BF_4 (a monoelectronic process, Scheme 1), we tried to quantitatively capture the electrogenerated BF_3 with a tertiary base just at the end of the electrolysis.

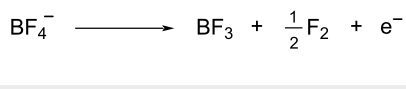

Scheme 1: Anodic oxidation of tetrafluoroborate anion.

By a comparison between the ^{13}C NMR peaks of the base and the base–BF_3 adduct, we should obtain an approximate current yield. Our first choice was *N*,*N*-diisopropylethylamine (DIPEA), as the DIPEA-BF_3 adduct is reported in the literature and fully characterized by NMR in $CDCl_3$ [113]. To be consistent with literature data, the BF_4^- peak in neat BMIm-BF_4 was set at −150.6 ppm in ^{19}F NMR spectrum [112].

We thus carried out the anodic oxidation of pure BMIm-BF_4 (divided cell, galvanostatic conditions) and stopped the electrolysis after 60 C (corresponding to 0.6 mmol of electrons). At the end of the electrolysis, 0.6 mmol of DIPEA were added to the anolyte and the mixture was kept under stirring at room temperature for 30 min. Then, the neat anolyte was analysed by NMR (^{19}F and ^{13}C). The ^{19}F NMR spectrum showed a new peak at −148.7 ppm and, to our great astonishment, we found only one set of signals in the ^{13}C NMR spectrum (55.0, 42.8, 17.4, 16.0, 12.2), apart from those of the IL cation (see Supporting Information File 1, Figure S2). These signals are quite different from those of DIPEA in $CDCl_3$ (48.5, 39.1, 20.6, 17.1) [114] (the ^{13}C NMR spectrum of DIPEA in pure BMIm-BF_4 is not reported), but quite similar to the ^{13}C NMR spectrum of DIPEA-BF_3 adduct in $CDCl_3$ (53.8, 41.6, 19.5, 18.9, 9.9), inducing us to think to have the DIPEA-BF_3 adduct in the solution. To confirm this assumption, we prepared a DIPEA solution in BMIm-BF_4 to record the ^{13}C NMR spectrum, but unfortunately DIPEA is not soluble enough in BMIm-BF_4 to obtain a decent spectrum. Therefore, while confirming the presence of the adduct, we could not quantify it.

The next choice was DBU (1,8-diazabicyclo[5,4,0]undec-7-ene). The DBU-BF_3 adduct is reported to be very stable in water and in air and not subjected to hydrolysis [115]. The DBU solubility in BMIm-BF_4 was confirmed by NMR analysis (amidine carbon atom at 161.6 ppm in BMIm-BF_4, taking as internal reference the imidazolium C2 at 136.4 ppm) [116]. The addition of an excess of $BF_3{\cdot}Et_2O$ to the solution of DBU in IL shifted the DBU amidine signal to 166.0 ppm, confirming the rapid formation of the adduct (see Supporting Information File 1, Figure S5c). Moreover, a new small peak at −146.1 ppm appeared in the ^{19}F NMR spectrum [115], in addition to the peaks at −150.6 ppm (BF_4^- signal), at −148.7 ppm (BF_3OH^-) and −153.6 ppm ($BF_3{\cdot}Et_2O$) (see Supporting Information File 1, Figures S3 and S4).

We thus carried out the anodic oxidation of pure BMIm-BF_4 (divided cell, galvanostatic conditions) and stopped the electrolysis after 60 C (corresponding to 0.6 mmol of electrons). At the end of the electrolysis, 0.6 mmol of DBU were added to the anolyte and the mixture was kept under stirring at room temperature for 30 min. Then the neat anolyte was analysed by NMR (^{19}F and ^{13}C). A peak at 166.0 ppm in the ^{13}C NMR spectrum appeared and no traces of starting DBU (peak at 161 ppm) were evidenced (see Supporting Information File 1, Figure S5a, b and d). As regards the ^{19}F NMR spectrum, a new peak at −148.6 ppm appeared, consistent with the formation of $B_2F_7^-$ or with the DBU-BF_3 adduct (a direct comparison with literature data is not possible in this case, as the NMR data reported in previous papers were obtained in molecular solvents, while we carried out the experiments in pure ionic liquid) [115].

To our surprise, the addition of additional DBU to this solution did not show the signal of DBU in the ^{13}C NMR spectrum (161 ppm), but increased the 166 ppm peak intensity (due to the DBU adduct) (see Supporting Information File 1, Figure S5e). We have no explanation for this behaviour, but the possibility of the coordination of more than one DBU molecule could be a hypothesis. In this regard, Hartman and co-workers reported the formation of BF_xDBU_y positively charged adducts (y from 1 to 3) [115]. Although we cannot exclude that the signal is due to the $[DBU\text{-}H]^+$, the ^{13}C NMR of the reaction mixture did not highlight the presence of the NHC derived from the IL deprotonation.

Conclusion

In conclusion, in this work we demonstrated the possibility to carry out the hydration of alkynes in imidazolium ILs, as alternative solvents until now still little explored for this reaction, employing the Lewis acid BF_3 as catalyst. The catalyst was used both as $BF_3{\cdot}Et_2O$ and as BF_3 directly electrogenerated in the IL. Among the investigated ILs, BMIm-BF_4 provided the best reaction yields and is preferred on the basis of cost. The results obtained with $BF_3{\cdot}Et_2O$ were compared with those achieved using BF_3 electrogenerated in BMIm-BF_4, demonstrating the possibility of employing a less harmful system to obtain the products of alkyne hydration with analogous or improved yields. On the basis of the results obtained with the

studied substrates, the electrochemical route would appear to be more advantageous for the more reactive terminal arylalkynes, in terms of selectivity and, in some cases, of yield.

The possibility of recycling the ionic liquid for subsequent reactions was successfully demonstrated, confirming the advantage of using BMIm-BF_4 as a green solvent for this reaction.

Together, these results demonstrate the promise of BMIm-BF_4/BF_3 (either with electrogenerated BF_3 or with $BF_3{\cdot}Et_2O$) as an efficient and less harmful alternative to expensive metal/ligand catalysts, while avoiding conventional toxic and volatile solvents commonly used for the hydration of alkynes.

Experimental

General Information

All chemicals were commercial (Fluorochem, Aldrich) and used without further purification. Ionic liquids (ILs, Iolitec) were kept under vacuum (7 mbar) under stirring at 40 °C for 16 h before use. NMR spectra were recorded at ambient temperature on Bruker Avance spectrometer operating at 400 MHz (^{1}H NMR) and 100 MHz (^{13}C{^{1}H} NMR) or on a Spinsolve 60 spectrometer operating at 62.5 MHz (^{1}H NMR), 15.7 MHz (^{13}C{^{1}H} NMR) and 58.8 MHz (^{19}F NMR) using the solvent as internal standard. All the NMR spectra of neat IL were performed on Spinsolve 60 spectrometer. The chemical shifts (δ) are given in ppm relative to TMS. Flash chromatography was carried out using silica (Merck; 40–63 μm particle size).

General procedures

General procedure for the hydration of alkynes catalysed by $BF_3{\cdot}Et_2O$ in ILs

In a 10 mL vial, 1 mL of the IL, a magnetic stirring bar and the amount of alkyne, water and $BF_3{\cdot}Et_2O$ reported in Tables 1, 3, and 4 were added. The vial was sealed with a screw cap and the mixture was stirred at 80 °C in an oil bath. After the time indicated in Tables 1, 3, and 4, the mixture was extracted with diethyl ether (3 × 8 mL). The combined organic phase was washed with water (3 × 20 mL), dried on Na_2SO_4, filtered and then the solvent was removed under reduced pressure. The crude was analysed by ^{1}H NMR and ^{13}C NMR and then the products were purified by column chromatography.

General procedure for the electrochemical generation of BF_3 in BMIm-BF_4

All the experiments were carried out in a home-made divided glass cell separated through a porous glass plug; Pt spirals (apparent area 0.8 cm^2) were used as anode and cathode. 2.0 mL of BMIm-BF_4 and the magnetic stirring bar were put in the anodic compartment (test tube, h = 10.5 cm, d = 1.7 cm), and 1.0 mL of the same IL in the cathodic one. Electrolyses were performed at constant current (I = 10 mA·cm^{-2}), under stirring at room temperature, under nitrogen atmosphere, using an Amel Model 552 potentiostat equipped with an Amel Model 731 integrator. When the desired Coulombs (reported in Table 5) had passed through the electrolysis cell, the current was switched off, the cathodic compartment removed and the amounts of alkyne and water reported in Table 5 were added to the anolyte. The test tube was sealed with a rubber cap and the mixture was stirred at 80 °C in an oil bath. After the time indicated in Table 5, the mixture was extracted with diethyl ether (3 × 8 mL). The combined organic phase was washed with water (3 × 20 mL), dried on Na_2SO_4, filtered and then the solvent was removed under reduced pressure. The crude was analysed by ^{1}H NMR and ^{13}C NMR and then the products were purified by column chromatography.

Procedure for the evaluation of the current efficiency in the electrogeneration of BF_3 in BMIm-BF_4

Electrolyses were performed as reported above and stopped after the passage of 60 C. At the end of the electrolysis the cathodic compartment was removed and 0.6 mmol of the appropriate tertiary amine (DIPEA or DBU) were added to the anolyte. The mixture was stirred at room temperature under inert atmosphere (N_2) for 30 min. Then the neat IL was analysed by ^{13}C NMR and ^{19}F NMR on Spinsolve 60 spectrometer. For the experiment with DBU, after the analysis of the sample thus prepared, another aliquot of DBU was added directly into the NMR test tube (about 0.1 mmol of DBU for 0.5 mL of IL).

The reference DIPEA/BMIm-BF_4 or DBU/BMIm-BF_4 solutions were prepared by mixing 0.1 mmol of the appropriate base with 0.5 mL of BMim-BF_4.

Recycling of ILs

The IL sample already used was recycled after the elimination of diethyl ether and water, by keeping the IL under vacuum (7 mbar) under stirring at 40 °C for 16 h.

Procedure for the hydration of diphenylacetylene in dioxane

Water (0.3 mmol) and $BF_3{\cdot}Et_2O$ (0.9 mmol) were added to a solution of diphenylacetylene (**1a**, 0.3 mmol) in dioxane (2 mL) in a 5 mL flask. The reaction mixture was stirred at 80 °C in an oil bath for 18 h. Then, the reaction mixture was diluted with diethyl ether (20 mL) and washed with water (3 × 20 mL). The organic phase was dried on Na_2SO_4, filtered and then the solvent was removed under reduced pressure. The crude was analysed by ^{1}H NMR and ^{13}C NMR.

Supporting Information

Integral tables of the experiments for the hydration of different alkynes catalysed by $BF_3{\cdot}Et_2O$ or by electrogenerated BF_3 in BMIm-BF_4. ^{19}F and ^{13}C NMR spectra for the evaluation of the current efficiency in the electrogeneration of BF_3 in BMIm-BF_4. Analytical data, ^1H and ^{13}C NMR spectra of synthetized compounds.

Supporting Information File 1

Additional experimental data.
[https://www.beilstein-journals.org/bjoc/content/supplementary/1860-5397-19-147-S1.pdf]

Acknowledgements

The authors thank Marco Di Pilato for his help with the electrochemical experiments.

Funding

Sapienza University, Project number RM12117A339284EE.

ORCID® iDs

Richard C. D. Brown - https://orcid.org/0000-0003-0156-7087
Marta Feroci - https://orcid.org/0000-0002-3673-6509
Fabrizio Vetica - https://orcid.org/0000-0002-7171-8779
Martina Bortolami - https://orcid.org/0000-0001-5740-6499

References

1. Bora, J.; Dutta, M.; Chetia, B. *Tetrahedron* **2023,** *132,* 133248. doi:10.1016/j.tet.2023.133248
2. Kaur, J.; Saxena, M.; Rishi, N. *Bioconjugate Chem.* **2021,** *32,* 1455–1471. doi:10.1021/acs.bioconjchem.1c00247
3. Gulevskaya, A. V.; Tonkoglazova, D. I. *Adv. Synth. Catal.* **2022,** *364,* 2502–2539. doi:10.1002/adsc.202200513
4. Kawamura, S.; Barrio, P.; Fustero, S.; Escorihuela, J.; Han, J.; Soloshonok, V. A.; Sodeoka, M. *Adv. Synth. Catal.* **2023,** *365,* 398–462. doi:10.1002/adsc.202201268
5. Rammohan, A.; Venkatesh, B. C.; Basha, N. M.; Zyryanov, G. V.; Nageswararao, M. *Chem. Biol. Drug Des.* **2023,** *101,* 1181–1203. doi:10.1111/cbdd.14148
6. Neto, J. S. S.; Zeni, G. *Asian J. Org. Chem.* **2021,** *10,* 1282–1318. doi:10.1002/ajoc.202100013
7. Wang, S. R. *Chem. – Asian J.* **2023,** *18,* e202300244. doi:10.1002/asia.202300244
8. Banjare, S. K.; Mahulkar, P. S.; Nanda, T.; Pati, B. V.; Najiar, L. O.; Ravikumar, P. C. *Chem. Commun.* **2022,** *58,* 10262–10289. doi:10.1039/d2cc03294e
9. Bortolami, M.; Petrucci, R.; Rocco, D.; Scarano, V.; Chiarotto, I. *ChemElectroChem* **2021,** *8,* 3604–3613. doi:10.1002/celc.202100497
10. Kutscheroff, M. *Ber. Dtsch. Chem. Ges.* **1884,** *17,* 13–29. doi:10.1002/cber.18840170105
11. Hintermann, L.; Labonne, A. *Synthesis* **2007,** 1121–1150. doi:10.1055/s-2007-966002
12. Salvio, R.; Bassetti, M. *Inorg. Chim. Acta* **2021,** *522,* 120288. doi:10.1016/j.ica.2021.120288
13. Gao, P.; Szostak, M. *Coord. Chem. Rev.* **2023,** *485,* 215110. doi:10.1016/j.ccr.2023.215110
14. Mariconda, A.; Sirignano, M.; Troiano, R.; Russo, S.; Longo, P. *Catalysts* **2022,** *12,* 836. doi:10.3390/catal12080836
15. Zuccaccia, D.; Del Zotto, A.; Baratta, W. *Coord. Chem. Rev.* **2019,** *396,* 103–116. doi:10.1016/j.ccr.2019.06.007
16. Segato, J.; Del Zotto, A.; Belpassi, L.; Belanzoni, P.; Zuccaccia, D. *Catal. Sci. Technol.* **2020,** *10,* 7757–7767. doi:10.1039/d0cy01343a
17. Goodwin, J. A.; Aponick, A. *Chem. Commun.* **2015,** *51,* 8730–8741. doi:10.1039/c5cc00120j
18. Gatto, M.; Del Zotto, A.; Segato, J.; Zuccaccia, D. *Organometallics* **2018,** *37,* 4685–4691. doi:10.1021/acs.organomet.8b00689
19. Ebule, R. E.; Malhotra, D.; Hammond, G. B.; Xu, B. *Adv. Synth. Catal.* **2016,** *358,* 1478–1481. doi:10.1002/adsc.201501079
20. Xu, Y.; Hu, X.; Shao, J.; Yang, G.; Wu, Y.; Zhang, Z. *Green Chem.* **2015,** *17,* 532–537. doi:10.1039/c4gc01322k
21. Nun, P.; Ramón, R. S.; Gaillard, S.; Nolan, S. P. *J. Organomet. Chem.* **2011,** *696,* 7–11. doi:10.1016/j.jorganchem.2010.08.052
22. Voloshkin, V. A.; Saab, M.; Van Hecke, K.; Lau, S. H.; Carrow, B. P.; Nolan, S. P. *Dalton Trans.* **2020,** *49,* 13872–13879. doi:10.1039/d0dt03330h
23. Singh, S.; Dobereiner, G. E. *Adv. Synth. Catal.* **2022,** *364,* 3551–3558. doi:10.1002/adsc.202200812
24. Arai, H.; Yoshida, T.; Nagashima, E.; Hatayama, A.; Horie, S.; Matsunaga, S.; Nomiya, K. *Organometallics* **2016,** *35,* 1658–1666. doi:10.1021/acs.organomet.6b00114
25. Saha, R.; Mukherjee, A.; Bhattacharya, S. *New J. Chem.* **2022,** *46,* 9098–9110. doi:10.1039/d1nj04736a
26. Mainkar, P.; Chippala, V.; Chegondi, R.; Chandrasekhar, S. *Synlett* **2016,** *27,* 1969–1972. doi:10.1055/s-0035-1561864
27. Sha, Y.; Bai, W.; Zhou, Y.; Jiang, J.; Ju, X. *ChemistrySelect* **2020,** *5,* 1994–1996. doi:10.1002/slct.202000498
28. Tyagi, D.; Rai, R. K.; Mobin, S. M.; Singh, S. K. *Asian J. Org. Chem.* **2017,** *6,* 1647–1658. doi:10.1002/ajoc.201700396
29. Boeck, F.; Kribber, T.; Xiao, L.; Hintermann, L. *J. Am. Chem. Soc.* **2011,** *133,* 8138–8141. doi:10.1021/ja2026823
30. Luo, D.; Li, Y.; Pullarkat, S. A.; Cockle, K. E.; Leung, P.-H. *Organometallics* **2010,** *29,* 893–903. doi:10.1021/om900958p
31. Kassie, A. A.; Wade, C. R. *Organometallics* **2020,** *39,* 2214–2221. doi:10.1021/acs.organomet.0c00164
32. Zhang, Z.; Wu, L.; Liao, J.; Wu, W.; Jiang, H.; Li, J.; Li, J. *J. Org. Chem.* **2015,** *80,* 7594–7603. doi:10.1021/acs.joc.5b01178
33. Kusakabe, T.; Ito, Y.; Kamimura, M.; Shirai, T.; Takahashi, K.; Mochida, T.; Kato, K. *Asian J. Org. Chem.* **2017,** *6,* 1086–1090. doi:10.1002/ajoc.201700138
34. Lin, H.-P.; Ibrahim, N.; Provot, O.; Alami, M.; Hamze, A. *RSC Adv.* **2018,** *8,* 11536–11542. doi:10.1039/c8ra00564h
35. Carlisle, S.; Matta, A.; Valles, H.; Bracken, J. B.; Miranda, M.; Yoo, J.; Hahn, C. *Organometallics* **2011,** *30,* 6446–6457. doi:10.1021/om2007908
36. Bassetti, M.; Ciceri, S.; Lancia, F.; Pasquini, C. *Tetrahedron Lett.* **2014,** *55,* 1608–1612. doi:10.1016/j.tetlet.2014.01.083
37. Wu, X.-F.; Bezier, D.; Darcel, C. *Adv. Synth. Catal.* **2009,** *351,* 367–370. doi:10.1002/adsc.200800666
38. Mei, Q.; Liu, H.; Hou, M.; Liu, H.; Han, B. *New J. Chem.* **2017,** *41,* 6290–6295. doi:10.1039/c7nj00486a

39. Niu, T.-f.; Jiang, D.-y.; Li, S.-y.; Shu, X.-g.; Li, H.; Zhang, A.-l.; Xu, J.-y.; Ni, B.-q. *Tetrahedron Lett.* **2017,** *58,* 1156–1159. doi:10.1016/j.tetlet.2017.02.004
40. Zou, H.; He, W.; Dong, Q.; Wang, R.; Yi, N.; Jiang, J.; Pen, D.; He, W. *Eur. J. Org. Chem.* **2016,** 116–121. doi:10.1002/ejoc.201501198
41. Hassam, M.; Li, W.-S. *Tetrahedron* **2015,** *71,* 2719–2723. doi:10.1016/j.tet.2015.03.034
42. Xie, Y.; Wang, J.; Wang, Y.; Han, S.; Yu, H. *ChemCatChem* **2021,** *13,* 4985–4989. doi:10.1002/cctc.202101180
43. Li, H.; Chen, J.; Liu, J.; Li, C.; Liu, L.; Yang, Q. *ChemNanoMat* **2022,** *8,* e202100386. doi:10.1002/cnma.202100386
44. Kang, S.-M.; Han, S.-S.; Zhu, Y.-Y.; Wu, Z.-Q. *ACS Catal.* **2021,** *11,* 13838–13847. doi:10.1021/acscatal.1c04062
45. Kaiser, D.; Veiros, L. F.; Maulide, N. *Chem. – Eur. J.* **2016,** *22,* 4727–4732. doi:10.1002/chem.201600432
46. Liu, H.; Wei, Y.; Cai, C. *Synlett* **2016,** *27,* 2378–2383. doi:10.1055/s-0035-1562779
47. Antenucci, A.; Flamini, P.; Fornaiolo, M. V.; Di Silvio, S.; Mazzetti, S.; Mencarelli, P.; Salvio, R.; Bassetti, M. *Adv. Synth. Catal.* **2019,** *361,* 4517–4526. doi:10.1002/adsc.201900633
48. Cabrero-Antonino, J. R.; Leyva-Pérez, A.; Corma, A. *Chem. – Eur. J.* **2012,** *18,* 11107–11114. doi:10.1002/chem.201200580
49. Liang, S.; Hammond, G. B.; Xu, B. *Chem. Commun.* **2015,** *51,* 903–906. doi:10.1039/c4cc08938c
50. Oss, G.; Ho, J.; Nguyen, T. V. *Eur. J. Org. Chem.* **2018,** 3974–3981. doi:10.1002/ejoc.201800579
51. Gao, Q.; Li, S.; Pan, Y.; Xu, Y.; Wang, H. *Tetrahedron* **2013,** *69,* 3775–3781. doi:10.1016/j.tet.2013.03.079
52. Rebacz, N. A.; Savage, P. E. *Ind. Eng. Chem. Res.* **2010,** *49,* 535–540. doi:10.1021/ie9017513
53. Zeng, M.; Huang, R.-X.; Li, W.-Y.; Liu, X.-W.; He, F.-L.; Zhang, Y.-Y.; Xiao, F. *Tetrahedron* **2016,** *72,* 3818–3822. doi:10.1016/j.tet.2016.04.049
54. Liu, W.; Wang, H.; Li, C.-J. *Org. Lett.* **2016,** *18,* 2184–2187. doi:10.1021/acs.orglett.6b00801
55. Gastaldi, C.; Taviot-Guého, C.; Guérard-Hélaine, C.; Forano, C. *Appl. Clay Sci.* **2023,** *238,* 106931. doi:10.1016/j.clay.2023.106931
56. Ventura-Espinosa, D.; Martín, S.; García, H.; Mata, J. A. *J. Catal.* **2021,** *394,* 113–120. doi:10.1016/j.jcat.2020.12.027
57. De Canck, E.; Nahra, F.; Bevernaege, K.; Vanden Broeck, S.; Ouwehand, J.; Maes, D.; Nolan, S. P.; Van Der Voort, P. *ChemPhysChem* **2018,** *19,* 430–436. doi:10.1002/cphc.201701102
58. Öztürk, B. Ö.; Çetinel, B.; Şehitoğlu, S. K. *Appl. Organomet. Chem.* **2020,** *34,* e5686. doi:10.1002/aoc.5686
59. Valverde-González, A.; Marchal, G.; Maya, E. M.; Iglesias, M. *Catal. Sci. Technol.* **2019,** *9,* 4552–4560. doi:10.1039/c9cy00776h
60. Cirujano, F. G.; López-Maya, E.; Navarro, J. A. R.; De Vos, D. E. *Top. Catal.* **2018,** *61,* 1414–1423. doi:10.1007/s11244-018-1039-6
61. Shen, L.; Han, X.; Dong, B.; Yang, Y.; Yang, J.; Li, F. *ACS Appl. Polym. Mater.* **2022,** *4,* 7408–7416. doi:10.1021/acsapm.2c01167
62. Srivastava, A. K.; Khandaka, H.; Joshi, R. K. *SynOpen* **2023,** *07,* 121–129. doi:10.1055/a-2025-2759
63. Ali, M.; Srivastava, A. K.; Upadhyay, N. S.; Satrawala, N.; Joshi, R. K. *Organics* **2023,** *4,* 251–264. doi:10.3390/org4020020
64. Sultana Poly, S.; Hakim Siddiki, S. M. A.; Touchy, A. S.; Yasumura, S.; Toyao, T.; Maeno, Z.; Shimizu, K.-i. *J. Catal.* **2018,** *368,* 145–154. doi:10.1016/j.jcat.2018.10.004
65. Lei, Y.; Zhang, M.; Li, Q.; Xia, Y.; Leng, G. *Polymers (Basel, Switz.)* **2019,** *11,* 2091. doi:10.3390/polym11122091
66. Rathnayake, D.; Perera, I.; Shirazi-Amin, A.; Kerns, P.; Dissanayake, S.; Suib, S. L. *ACS Appl. Mater. Interfaces* **2020,** *12,* 47389–47396. doi:10.1021/acsami.0c10757
67. Liu, Y.; Wang, B.; Kang, L.; Stamatopoulos, A.; Gu, H.; Wang, F. R. *Chem. Mater.* **2020,** *32,* 4375–4382. doi:10.1021/acs.chemmater.0c01763
68. Chen, J.; Zhang, J.; Zhu, D.; Li, T. *Gold Bull.* **2019,** *52,* 19–26. doi:10.1007/s13404-018-0249-9
69. Trentin, F.; Chapman, A. M.; Scarso, A.; Sgarbossa, P.; Michelin, R. A.; Strukul, G.; Wass, D. F. *Adv. Synth. Catal.* **2012,** *354,* 1095–1104. doi:10.1002/adsc.201100326
70. Deng, T.; Wang, C.-Z. *Catal. Sci. Technol.* **2016,** *6,* 7029–7032. doi:10.1039/c6cy01629d
71. Nairoukh, Z.; Avnir, D.; Blum, J. *ChemSusChem* **2013,** *6,* 430–432. doi:10.1002/cssc.201200838
72. Dandia, A.; Saini, P.; Chithra, M. J.; Vennapusa, S. R.; Parewa, V. *J. Mol. Liq.* **2021,** *331,* 115758. doi:10.1016/j.molliq.2021.115758
73. Zhao, J.; Yuan, H.; Chen, R.; Chen, H.; Zhang, Y. *Asian J. Org. Chem.* **2022,** *11,* e202100681. doi:10.1002/ajoc.202100681
74. Mallakpour, S.; Dinari, M. Ionic liquids as green solvents: progress and prospects. *Green Solvents II: properties and applications of ionic liquids;* Springer: Dordrecht, Netherlands, 2012; pp 1–32. doi:10.1007/978-94-007-2891-2_1
75. Silva, W.; Zanatta, M.; Ferreira, A. S.; Corvo, M. C.; Cabrita, E. J. *Int. J. Mol. Sci.* **2020,** *21,* 7745. doi:10.3390/ijms21207745
76. Vekariya, R. L. *J. Mol. Liq.* **2017,** *227,* 44–60. doi:10.1016/j.molliq.2016.11.123
77. Dong, K.; Liu, X.; Dong, H.; Zhang, X.; Zhang, S. *Chem. Rev.* **2017,** *117,* 6636–6695. doi:10.1021/acs.chemrev.6b00776
78. Xu, C.; Cheng, Z. *Processes* **2021,** *9,* 337. doi:10.3390/pr9020337
79. Sowmiah, S.; Srinivasadesikan, V.; Tseng, M.-C.; Chu, Y.-H. *Molecules* **2009,** *14,* 3780–3813. doi:10.3390/molecules14093780
80. Wang, B.; Qin, L.; Mu, T.; Xue, Z.; Gao, G. *Chem. Rev.* **2017,** *117,* 7113–7131. doi:10.1021/acs.chemrev.6b00594
81. Chiappe, C.; Pieraccini, D. *J. Phys. Org. Chem.* **2005,** *18,* 275–297. doi:10.1002/poc.863
82. Keaveney, S. T.; Haines, R. S.; Harper, J. B. *Pure Appl. Chem.* **2017,** *89,* 745–757. doi:10.1515/pac-2016-1008
83. Pandolfi, F.; Chiarotto, I.; Mattiello, L.; Petrucci, R.; Feroci, M. *ChemistrySelect* **2019,** *4,* 12871–12874. doi:10.1002/slct.201902841
84. Wong, W.-L.; Ho, K.-P.; Lee, L. Y. S.; Lam, K.-M.; Zhou, Z.-Y.; Chan, T. H.; Wong, K.-Y. *ACS Catal.* **2011,** *1,* 116–119. doi:10.1021/cs100016h
85. Kore, R.; Srivastava, R. *Tetrahedron Lett.* **2012,** *53,* 3245–3249. doi:10.1016/j.tetlet.2012.04.066
86. Kore, R.; Kumar, T. J. D.; Srivastava, R. *J. Mol. Catal. A: Chem.* **2012,** *360,* 61–70. doi:10.1016/j.molcata.2012.04.010
87. Chen, X.; Ye, X.; Liang, W.-Y.; Zhou, Q.; Vo-Thanh, G.; Liu, Y. *Mol. Catal.* **2018,** *448,* 171–176. doi:10.1016/j.mcat.2018.01.035
88. Tao, D.-J.; Liu, F.; Wang, L.; Jiang, L. *Appl. Catal., A* **2018,** *564,* 56–63. doi:10.1016/j.apcata.2018.07.018
89. Chen, B.; Wang, M.; Wang, X.; Zhao, Q.; Wang, Y.; Gao, G. *Polym. Chem.* **2021,** *12,* 2731–2742. doi:10.1039/d1py00377a
90. Banerjee, B. *ChemistrySelect* **2017,** *2,* 8362–8376. doi:10.1002/slct.201701700
91. Gauchot, V.; Gravel, J.; Vidal, M.; Charbonneau, M.; Kairouz, V.; Schmitzer, A. *Synlett* **2015,** *26,* 2763–2779. doi:10.1055/s-0035-1560182

92. Tiago, G. A. O.; Matias, I. A. S.; Ribeiro, A. P. C.; Martins, L. M. D. R. S. *Molecules* **2020,** *25,* 5812. doi:10.3390/molecules25245812
93. Kathiresan, M.; Velayutham, D. *Chem. Commun.* **2015,** *51,* 17499–17516. doi:10.1039/c5cc06961k
94. Feroci, M.; Chiarotto, I.; Inesi, A. *Curr. Org. Chem.* **2013,** *17,* 204–219. doi:10.2174/1385272811317030003
95. Feroci, M.; Chiarotto, I.; D'Anna, F.; Forte, G.; Noto, R.; Inesi, A. *Electrochim. Acta* **2015,** *153,* 122–129. doi:10.1016/j.electacta.2014.11.135
96. Rocco, D.; Folgueiras-Amador, A. A.; Brown, R. C. D.; Feroci, M. *Beilstein J. Org. Chem.* **2022,** *18,* 979–990. doi:10.3762/bjoc.18.98
97. Vetica, F.; Bortolami, M.; Petrucci, R.; Rocco, D.; Feroci, M. *Chem. Rec.* **2021,** *21,* 2130–2147. doi:10.1002/tcr.202000178
98. Feroci, M.; Chiarotto, I.; D'Anna, F.; Gala, F.; Noto, R.; Ornano, L.; Zollo, G.; Inesi, A. *ChemElectroChem* **2016,** *3,* 1133–1141. doi:10.1002/celc.201600187
99. Canal, J. P.; Ramnial, T.; Dickie, D. A.; Clyburne, J. A. C. *Chem. Commun.* **2006,** 1809–1818. doi:10.1039/b512462j
100. Xiao, L.; Johnson, K. E. *J. Electrochem. Soc.* **2003,** *150,* E307. doi:10.1149/1.1568740
101. Palombi, L. *Electrochim. Acta* **2011,** *56,* 7442–7445. doi:10.1016/j.electacta.2011.07.006
102. Bortolami, M.; Mattiello, L.; Scarano, V.; Vetica, F.; Feroci, M. *J. Org. Chem.* **2021,** *86,* 16151–16157. doi:10.1021/acs.joc.1c00932
103. Bortolami, M.; Magboo, F. J. P.; Petrucci, R.; Vetica, F.; Zollo, G.; Feroci, M. *J. Electrochem. Soc.* **2021,** *168,* 115501. doi:10.1149/1945-7111/ac39e2
104. Li, Y.; Thiemann, T.; Sawada, T.; Mataka, S.; Tashiro, M. *J. Org. Chem.* **1997,** *62,* 7926–7936. doi:10.1021/jo961985z
105. Freire, M. G.; Neves, C. M. S. S.; Marrucho, I. M.; Coutinho, J. A. P.; Fernandes, A. M. *J. Phys. Chem. A* **2010,** *114,* 3744–3749. doi:10.1021/jp903292n
106. Saihara, K.; Yoshimura, Y.; Fujimoto, H.; Shimizu, A. *J. Mol. Liq.* **2016,** *219,* 493–496. doi:10.1016/j.molliq.2016.03.036
107. Izquierdo, S.; Essafi, S.; del Rosal, I.; Vidossich, P.; Pleixats, R.; Vallribera, A.; Ujaque, G.; Lledós, A.; Shafir, A. *J. Am. Chem. Soc.* **2016,** *138,* 12747–12750. doi:10.1021/jacs.6b07999
108. Bandgar, B. P.; Sadavarte, V. S.; Uppalla, L. S. *Tetrahedron Lett.* **2001,** *42,* 951–953. doi:10.1016/s0040-4039(00)01953-5
109. Štefane, B. *Org. Lett.* **2010,** *12,* 2900–2903. doi:10.1021/ol100620j
110. Wang, G.; Li, Z.; Li, C.; Zhang, S. *Green Chem.* **2020,** *22,* 7913–7923. doi:10.1039/d0gc03133j
111. Sieland, M.; Schenker, M.; Esser, L.; Kirchner, B.; Smarsly, B. M. *ACS Omega* **2022,** *7,* 5350–5365. doi:10.1021/acsomega.1c06534
112. Tempel, D. J.; Henderson, P. B.; Brzozowski, J. R.; Pearlstein, R. M.; Cheng, H. *J. Am. Chem. Soc.* **2008,** *130,* 400–401. doi:10.1021/ja077233b
113. Iashin, V.; Berta, D.; Chernichenko, K.; Nieger, M.; Moslova, K.; Pápai, I.; Repo, T. *Chem. – Eur. J.* **2020,** *26,* 13873–13879. doi:10.1002/chem.202001436
114. Yoshida, K.; Morimoto, I.; Mitsudo, K.; Tanaka, H. *Tetrahedron* **2008,** *64,* 5800–5807. doi:10.1016/j.tet.2008.03.079
115. Hartman, J. S.; Yuan, Z.; Fox, A.; Nguyen, A. *Can. J. Chem.* **1996,** *74,* 2131–2142. doi:10.1139/v96-242
116. Schmitz, P.; Jakelski, R.; Jalkanen, K.; Winter, M.; Bieker, P. *Chem. – Eur. J.* **2017,** *23,* 2261–2264. doi:10.1002/chem.201604461

License and Terms

BEILSTEIN JOURNAL OF ORGANIC CHEMISTRY

Additive-controlled chemoselective inter-/intramolecular hydroamination via electrochemical PCET process

Kazuhiro Okamoto, Naoki Shida* and Mahito Atobe*

Full Research Paper

Open Access

Address:
Graduate School of Engineering, Yokohama National University, 79-7 Tokiwadai, Hodogaya-ku, Yokohama, Kanagawa 240-8501, Japan

Email:
Naoki Shida* - shida-naoki-gz@ynu.ac.jp; Mahito Atobe* - atobe@ynu.ac.jp

* Corresponding author

Keywords:
amidyl radical; cyclic voltammetry; electrosynthesis; hydroamination; proton coupled electron transfer

Beilstein J. Org. Chem. **2024,** *20,* 264–271.
https://doi.org/10.3762/bjoc.20.27

Received: 04 December 2023
Accepted: 01 February 2024
Published: 12 February 2024

This article is part of the thematic issue "Synthetic electrochemistry".

Guest Editor: K. Lam

Abstract

Electrochemically generated amidyl radical species produced distinct inter- or intramolecular hydroamination reaction products via a proton-coupled electron transfer (PCET) mechanism. Cyclic voltammetry (CV) analysis indicated that the chemoselectivity was derived from the size of the hydrogen bond complex, which consisted of the carbamate substrate and phosphate base, and could be controlled using 1,1,1,3,3,3-hexafluoro-2-propanol (HFIP) as an additive. These results provide fundamental insights for the design of PCET-based redox reaction systems under electrochemical conditions.

Introduction

Proton-coupled electron transfer (PCET) enables the generation of various radical species under ambient conditions (Figure 1, top) [1]. In PCET processes, hydrogen bond formation between weak bases and acidic X–H bonds (X = N, O, C) is a key step, which is followed by concerted proton- and electron-transfer to give the corresponding radical species through oxidative X–H bond cleavage. One such species is the amidyl radical, which is broadly synthetically useful as a nitrogen source in hydroamination reactions and as a hydrogen atom transfer (HAT) reagent for remote C–H activation [2-8]. Recent advances in photoredox and electrochemical PCET reactions have significantly expanded the substrate scope of amidyl-radical-based molecular transformations because the harsh acidic and high-temperature conditions required in the classical Hofmann–Löffler–Freytag reaction can be avoided [9].

The initial aim of this study was the electrochemical generation of an amidyl radical as a HAT source for the synthesis of 1'-*C* functionalized nucleosides via the generation of an anomeric radical species from uridine derivative **1** (Figure 1, bottom) [10]. Although the HAT reaction failed, remarkable inter- and intramolecular chemoselectivities were observed in the hydro-

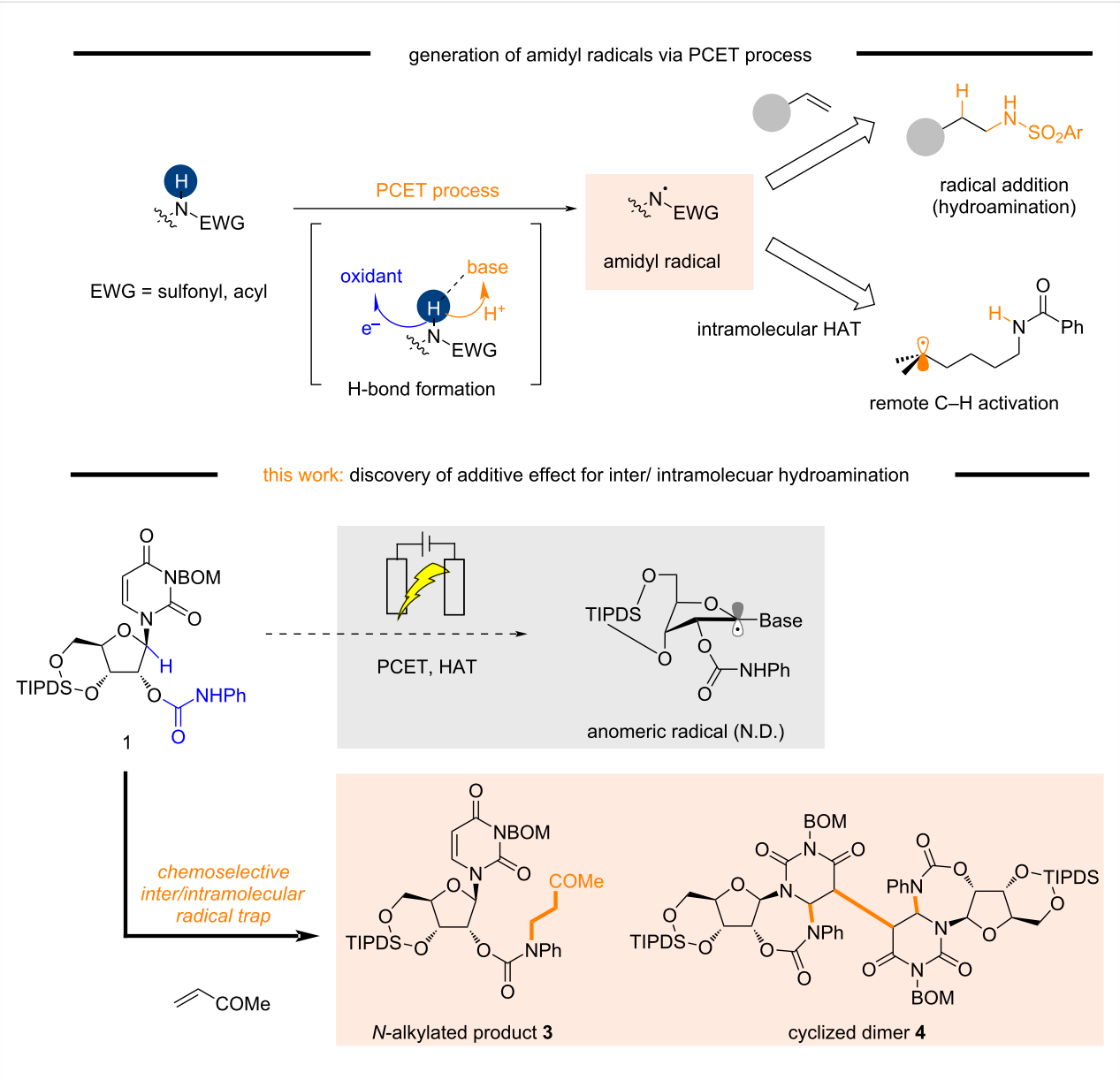

Figure 1: Application of amidyl radical species generated by PCET.

amination reaction. We investigated this phenomenon and found that complete inter-/intramolecular chemoselectivity could be achieved by modifying the reaction conditions, despite the presence of both inter- and intramolecular radical acceptor moieties. Therefore, we investigated the origin of this selectivity under electrochemical conditions.

Results and Discussion

Anodic oxidation of uridine derivative **1** was performed in a CH_2Cl_2/Bu_4NPF_6 (0.1 M) electrolyte system using a carbon felt (CF) anode and a Pt cathode in the presence of methyl vinyl ketone (MVK) as a radical acceptor (Table 1). Tetrabutylammonium dibutyl phosphate (phosphate base), which operates as a PCET initiator through hydrogen bond formation with the N–H bond of amide/carbamate [11], was used as an additive. As a result, *N*-alkylated product **3** was exclusively obtained, implying that the expected HAT at the 1'-*C* position to afford **2** (Table 1, entry 1) had not occurred. In contrast, the reaction efficiency was significantly decreased in the absence of the phosphate base (Table 1, entry 2), and electricity is necessary to proceed the reaction (Table 1, entry 3); thus, the phosphate base plays a crucial role in *N*-alkylation, while its basicity is insufficient to promote aza-Michael addition (pK_a of the conjugate acid of the phosphate base is 1.72 in H_2O) [12]. Furthermore, *N*-alkylation proceeded in a divided cell (anodic chamber); thus, the possibility of conjugate addition of a cathodically generated

Table 1: Electrochemical oxidation of **1** under varying conditions.

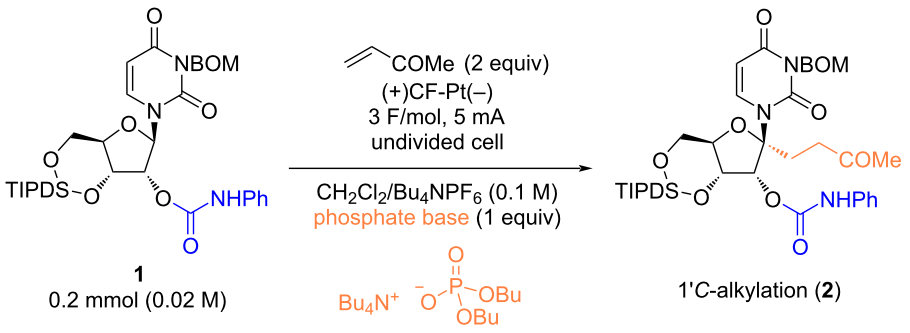

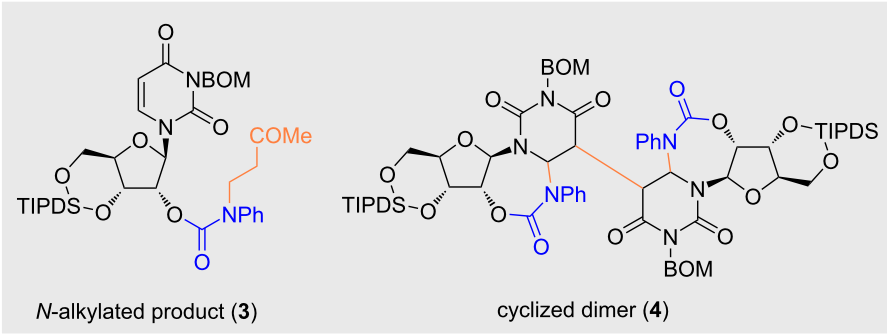

Entry	Deviation from standard conditions	Yield [%][a]	Recovered **1** [%][a]
1	none	57, 49[b] (**3**)	17
2	without phosphate base	13 (**3**)	76
3	without electricity	N.R.	92
4	divided cell (anodic chamber)	41 (**3**)	27
5	HFIP (2 equiv) as an additive	42, 27[b] (**4**)	32
6	AcOH (2 equiv) as an additive	10 (**3**)	51
7	MeCN instead of CH_2Cl_2	17 (**4**)	28

[a]Yield was determined based on ^{1}H NMR by using benzaldehyde as an internal standard, and recovery rate of **1** was determined by the integral of H-1' proton. [b]Isolated yield.

carbamate anion was ruled out, prompting us to consider that *N*-alkylation proceeded via a radical mechanism. On the other hand, the addition of 1,1,1,3,3,3-hexafluoro-2-propanol (HFIP) led to the predominant formation of cyclized dimer **4** without *N*-alkylation, whereas the use of AcOH provided *N*-alkylated product **3** (Table 1, entries 5 and 6). When acetonitrile (MeCN) was used as the solvent, cyclized dimer **4** was obtained (Table 1, entry 7).

Next, **1** was subjected to cyclic voltammetry (CV) measurements under varying conditions (Figure 2). An oxidation wave was observed at approximately +1.4 V (Figure 2A). The oxidation current of this wave decreased significantly in the presence of a phosphate base and the subsequent addition of HFIP enhanced this phenomenon (Figure 2B, grey line). In contrast, using AcOH instead of HFIP did not affect the oxidation current (Figure 2B, blue line). We considered that the inter- and intramolecular chemoselectivities were derived from the pK_a of the proton sources.

The pre-organization of the amide substrate and phosphate bases is an important process in PCET [13]. Recently, Gschwind et al. published a detailed NMR spectroscopic analysis of a PCET-mediated hydroamination reaction, which indicated that the pK_a of the proton source (PhSH or PhOH in the study) determines the size of the hydrogen bond complex. PhSH as the more acidic additive (pK_a = 6.62 in H_2O) provided better results in the PCET-induced intramolecular hydroamination reaction compared to the less acidic PhOH (pK_a = 9.95 in H_2O) because PhSH supplied free protons (H^+) and contributed to the

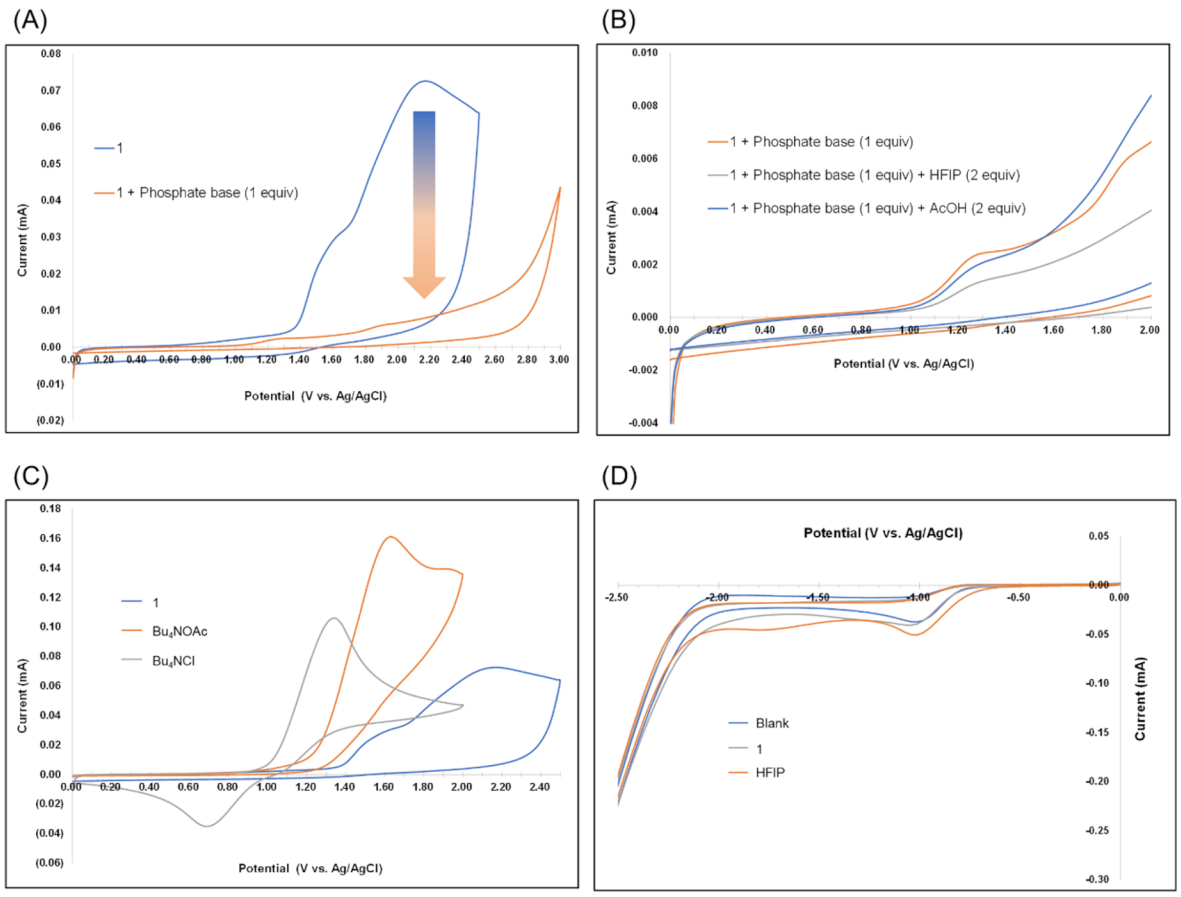

Figure 2: (A) Effect of phosphate base on the cyclic voltammogram of **1**. (B) Cyclic voltammograms of **1** in the presence of additives (AcOH or HFIP). (C) Comparison of oxidation potentials of **1** using Bu_4NOAc or Bu_4NCl. (D) Cyclic voltammograms for the cathodic side. All cyclic voltammograms were recorded in CH_2Cl_2/Bu_4NPF_6 (0.1 M). Sample concentration was 0.01 M. A glassy carbon anode (φ 3 mm) and Pt cathode (φ 3 mm) were used. Scan rate = 100 mV/s.

persistence of small aggregates composed of the amide and phosphate base [14]. On the other hand, owing to the insufficient dissociation constant between the proton and phenoxide in PhOH, the PhOH molecule is included in the hydrogen bond network along with the tetrabutylammonium cation (Bu_4N^+) to form a large aggregate. The hydrogen bonding between the amide and phosphate base in the small aggregates was stronger than in the large aggregates, which significantly enhanced amidyl radical generation through the PCET mechanism.

The above studies provided us with valuable insights into the intriguing electrochemical behavior of **1** (Figure 3). Hydrogen bond formation between **1** and the phosphate base yielded small aggregates, the interaction efficiency of which with the electrode surface was lower than that of **1** because the relatively large hydrodynamic radius of the aggregates decreased the number of electrode-accessible molecules. This increase in the hydrodynamic radius resulted in a decrease in the oxidation current. In the present study, HFIP (pK_a = 9.30 in H_2O) [15] is less acidic than AcOH (pK_a = 4.76 in H_2O) with a pK_a value similar to that of PhOH, which forms large aggregates under PCET conditions, as described above. Therefore, analogously, HFIP is expected to be included in the hydrogen-bonded complex. The resulting large aggregates further impeded access to the electrode surface, and a further decrease in the oxidation current was observed in the presence of HFIP (Figure 2B, grey line). In contrast, the more acidic AcOH supplied free protons, which enabled the persistence of small aggregates; thus, the current was not affected by the presence of AcOH (Figure 2B, blue line). However, in the presence of AcOH, the *N*-alkylation yield was low (Table 1, entry 6) owing to the competitive Kolbe oxidation of the cathodically generated acetate anion. In fact, the oxidation potential of Bu_4NOAc is lower than that of **1** (Figure 2C, orange line).

A decrease in the oxidation current can be considered as a decrease in the diffusion coefficient of the hydrogen bond complex; thus, we attempted to reproduce the CV pattern by compu-

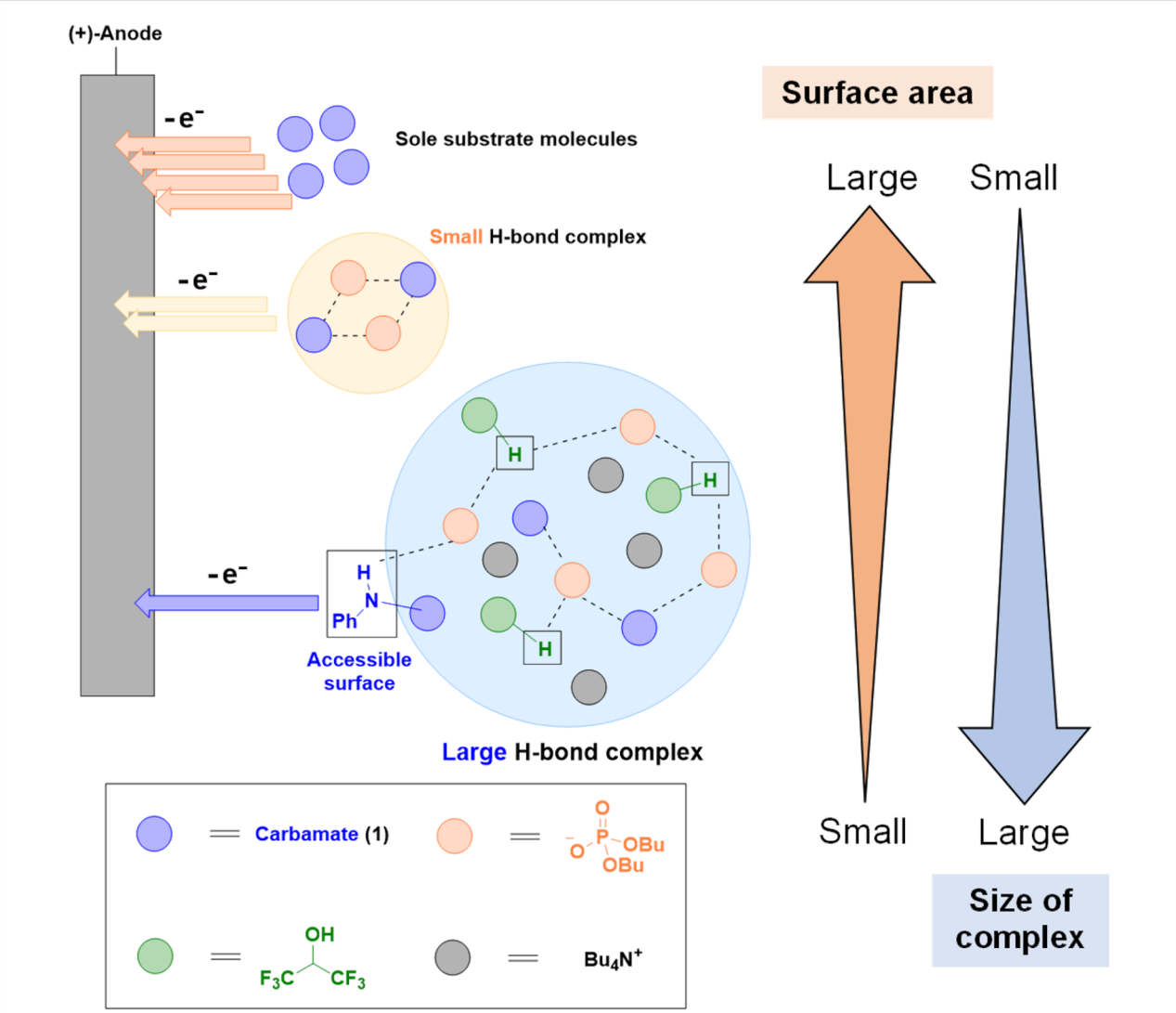

Figure 3: Plausible models illustrating the size effect of the hydrogen bond complex on the interaction efficiency with electrode surfaces.

tational simulation (Figures S1 and S2 in Supporting Information File 1) [16]. The results indicated that an excessively small diffusion coefficient (1/10- or 1/100-fold) is required to reproduce a CV pattern similar to that observed experimentally. Because the reported diffusion coefficient is only twice as small as that of the sole amide molecule [14], this simulated value is unrealistic, and we assumed that the diffusion coefficient did not affect the oxidation current.

In cathodic events, the reduction of CH_2Cl_2 primally occurred under standard conditions because the reduction wave of the blank solution appeared at approximately −1.0 V (Figure 2D, blue line). The resulting cathodically generated chloride ion (Cl^-) has a lower oxidation potential than **1** (Figure 2C, grey line); thus, it was subsequently oxidized on the anode to afford the halonium ion (Cl^+), which can react with **1** to form unstable N−Cl species (**B**) in situ (Figure 4). Although we cannot detect the chlorinated intermediate of **1**, electrolysis of *N*-propylcarbamate derivative under standard conditions gave the corresponding N−Cl species (**C**) as an unstable compound. We considered that this result as direct evidence for the plausibility of the existence of N−Cl species which driving the minor reaction pathway.

Further single-electron reduction affords the amidyl radical [17], which can react with MVK. Because *N*-alkylation also proceeded in the absence of a phosphate base but in a low yield (Table 1, entry 2), it can be concluded that only the N−Cl species contributed to *N*-alkylation in this case.

Based on the experimental and simulation results, we propose a plausible mechanism for the inter- and intramolecular hydroam-

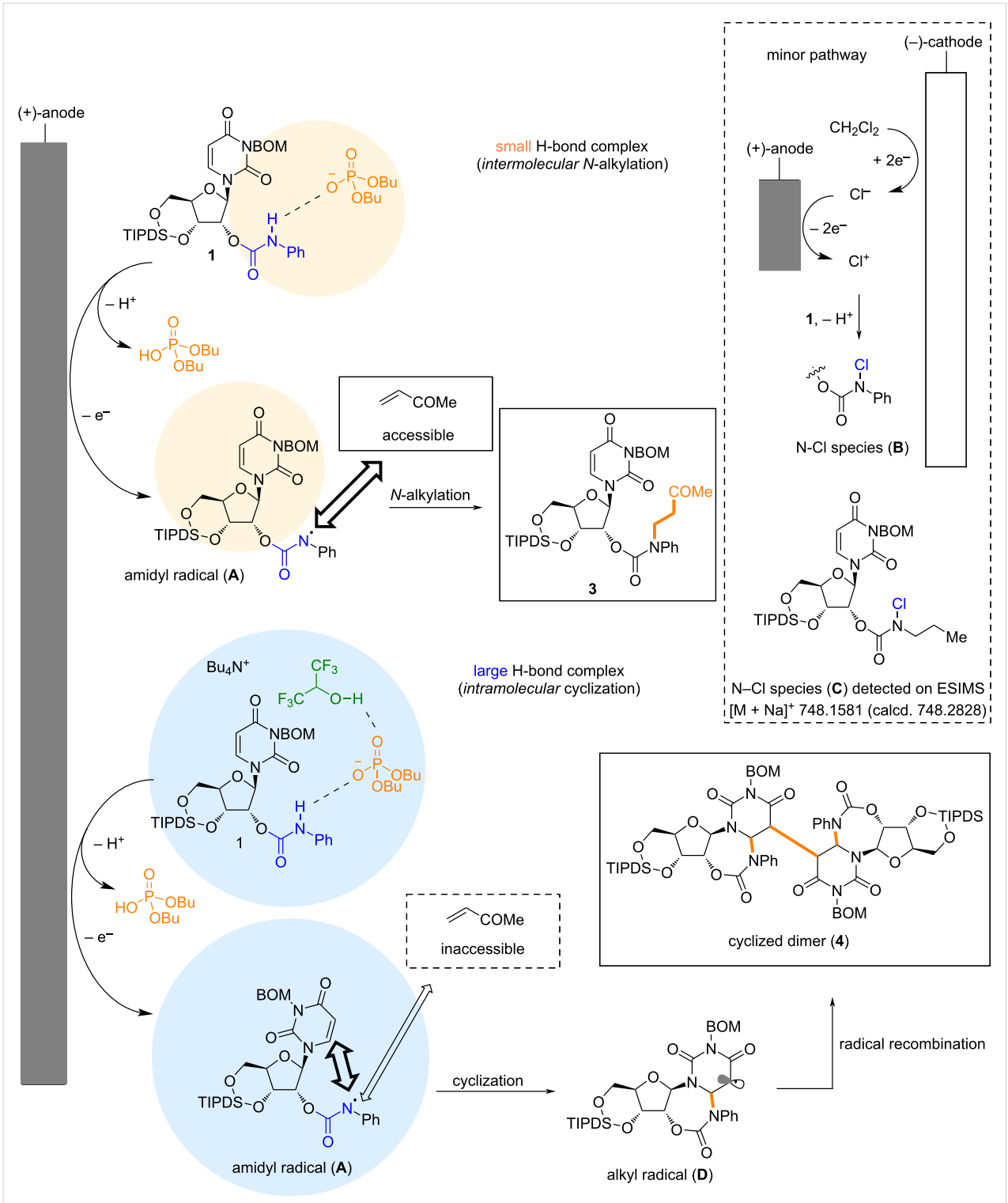

Figure 4: Plausible mechanism for the inter-/intramolecular hydroamination of **1**.

ination of **1** (Figure 4). In the *N*-alkylation reaction, anodic oxidation of a small hydrogen-bonded complex produces amidyl radical **A**. The hydrophobic MVK molecule was excluded from the highly polar environment of this complex, but the resulting amidyl radical could access MVK because it still had a large surface area for interaction with the solution interface. As mentioned above, the amidyl radical can also be generated through N–Cl species **B**.

However, the large hydrogen-bond complex, which included HFIP, prevented amidyl radical access to MVK. In this case, intramolecular radical trapping by the uracil nucleobase was preferred, leading to the formation of the cyclized alkyl radical **D**. Continuous radical recombination furnished dimer **4**.

Conclusion

We observed additive-controlled inter- and intramolecular chemoselectivity in the hydroamination of **1**. Detailed CV analysis indicated that the size of the hydrogen bond complex determined the selectivity, and HFIP played a crucial role in expanding the hydrogen bond network. These results provide fundamental insights beneficial for the design of PCET-based redox reaction systems under electrochemical conditions.

Experimental

General procedure of anodic oxidation

Compound **1** (145 mg, 0.2 mmol), Bu_4NPF_6 (387 mg, 1 mmol), CH_2Cl_2 (10 mL), phosphate base (90 mg, 0.2 mmol) and methyl vinyl ketone (32.7 μL, 0.4 mmol) were added to a test tube, which was then subjected to a constant electrical current of 5 mA (3 F/mol, 57.9 C) through the CF anode (1 × 1 cm) and the Pt cathode (1 × 1 cm). The reaction mixture was concentrated in vacuo and Et_2O (20 mL) was added. The resulting precipitate was removed by filtration through a short silica gel pad under reduced pressure. The filtrate was concentrated in vacuo and the resulting residue was subjected to ^1H NMR spectroscopy or column chromatography. A divided-cell experiment was performed using an H-type cell (4G glass filter). Compound **1** (0.2 mmol), Bu_4NPF_6 (387 mg, 1 mmol), phosphate base (90 mg, 0.2 mmol), CH_2Cl_2 (10 mL), and methyl vinyl ketone (32.7 μL, 0.4 mmol) were added to the anode chamber, and CH_2Cl_2 (10 mL), and Bu_4NPF_6 (387 mg, 1 mmol) were added to the cathode chamber. The anolyte was transferred to a round-bottomed flask, and the solvent was removed in vacuo. Et_2O (20 mL) was added to the crude mixture, and the resulting precipitate was removed by filtration through a short silica gel pad under reduced pressure. The filtrate was concentrated in vacuo and the resulting residue was subjected to ^1H NMR spectroscopy or column chromatography.

Supporting Information

Supporting Information File 1

Detailed experimental procedures, CV simulation, copies of NMR spectra.
[https://www.beilstein-journals.org/bjoc/content/supplementary/1860-5397-20-27-S1.pdf]

Funding

This work was supported by JSPS KAKENHI (Grant Nos. 22K18915 and 21H05215 to M.A. and 22H02118 23K17370, and 23H04916 to N.S.), a Grant-in-Aid for JSPS Fellows (Grant No. 22J00431 to K.O.), and JST CREST (Grant No. 18070940 to M.A.).

Author Contributions

Kazuhiro Okamoto: conceptualization; investigation; writing – original draft. Naoki Shida: conceptualization; project administration; writing – review & editing. Mahito Atobe: project administration; supervision; writing – review & editing.

ORCID® iDs

Kazuhiro Okamoto - https://orcid.org/0000-0002-3865-0362
Naoki Shida - https://orcid.org/0000-0003-0586-1216
Mahito Atobe - https://orcid.org/0000-0002-3173-3608

Data Availability Statement

All data that supports the findings of this study is available in the published article and/or the supporting information to this article.

References

1. Murray, P. R. D.; Cox, J. H.; Chiappini, N. D.; Roos, C. B.; McLoughlin, E. A.; Hejna, B. G.; Nguyen, S. T.; Ripberger, H. H.; Ganley, J. M.; Tsui, E.; Shin, N. Y.; Koronkiewicz, B.; Qiu, G.; Knowles, R. R. *Chem. Rev.* **2022,** *122,* 2017–2291. doi:10.1021/acs.chemrev.1c00374
2. Xiong, P.; Xu, H.-C. *Acc. Chem. Res.* **2019,** *52,* 3339–3350. doi:10.1021/acs.accounts.9b00472
3. Fazekas, T. J.; Alty, J. W.; Neidhart, E. K.; Miller, A. S.; Leibfarth, F. A.; Alexanian, E. J. *Science* **2022,** *375,* 545–550. doi:10.1126/science.abh4308
4. Wang, F.; Stahl, S. S. *Angew. Chem., Int. Ed.* **2019,** *58,* 6385–6390. doi:10.1002/anie.201813960
5. Zhu, Q.; Graff, D. E.; Knowles, R. R. *J. Am. Chem. Soc.* **2018,** *140,* 741–747. doi:10.1021/jacs.7b11144
6. Davies, J.; Svejstrup, T. D.; Fernandez Reina, D.; Sheikh, N. S.; Leonori, D. *J. Am. Chem. Soc.* **2016,** *138,* 8092–8095. doi:10.1021/jacs.6b04920
7. Choi, G. J.; Zhu, Q.; Miller, D. C.; Gu, C. J.; Knowles, R. R. *Nature* **2016,** *539,* 268–271. doi:10.1038/nature19811
8. Xu, F.; Zhu, L.; Zhu, S.; Yan, X.; Xu, H.-C. *Chem. – Eur. J.* **2014,** *20,* 12740–12744. doi:10.1002/chem.201404078
9. Hu, X.; Zhang, G.; Bu, F.; Nie, L.; Lei, A. *ACS Catal.* **2018,** *8,* 9370–9375. doi:10.1021/acscatal.8b02847
10. Gimisis, T.; Chatgilialoglu, C. *J. Org. Chem.* **1996,** *61,* 1908–1909. doi:10.1021/jo952218n
11. Gentry, E. C.; Knowles, R. R. *Acc. Chem. Res.* **2016,** *49,* 1546–1556. doi:10.1021/acs.accounts.6b00272
12. Kumler, W. D.; Eiler, J. J. *J. Am. Chem. Soc.* **1943,** *65,* 2355–2361. doi:10.1021/ja01252a028
13. Darcy, J. W.; Koronkiewicz, B.; Parada, G. A.; Mayer, J. M. *Acc. Chem. Res.* **2018,** *51,* 2391–2399. doi:10.1021/acs.accounts.8b00319

14. Berg, N.; Bergwinkl, S.; Nuernberger, P.; Horinek, D.; Gschwind, R. M. *J. Am. Chem. Soc.* **2021,** *143,* 724–735. doi:10.1021/jacs.0c08673
15. Dyatkin, B. L.; Mochalina, E. P.; Knunyants, I. L. *Tetrahedron* **1965,** *21,* 2991–2995. doi:10.1016/s0040-4020(01)96918-2
16. Izumiya, R.; Atobe, M.; Shida, N. *Electrochemistry* **2023,** *91,* 112003. doi:10.5796/electrochemistry.23-67010
17. Kim, H.; Kim, T.; Lee, D. G.; Roh, S. W.; Lee, C. *Chem. Commun.* **2014,** *50,* 9273–9276. doi:10.1039/c4cc03905j

License and Terms

BEILSTEIN JOURNAL OF ORGANIC CHEMISTRY

Transition-metal-catalyst-free electroreductive alkene hydroarylation with aryl halides under visible-light irradiation

Kosuke Yamamoto, Kazuhisa Arita, Masami Kuriyama and Osamu Onomura*

Letter

Open Access

Address:
Graduate School of Biomedical Sciences, Nagasaki University, 1-14 Bunkyo-machi, Nagasaki 852-8521, Japan

Email:
Osamu Onomura* - onomura@nagasaki-u.ac.jp

* Corresponding author

Keywords:
aryl halides; C–C bond formation; electroreduction; radicals; visible light

Beilstein J. Org. Chem. **2024,** *20,* 1327–1333.
https://doi.org/10.3762/bjoc.20.116

Received: 21 March 2024
Accepted: 22 May 2024
Published: 10 June 2024

This article is part of the thematic issue "Synthetic electrochemistry".

Guest Editor: K. Lam

Abstract

The radical hydroarylation of alkenes is an efficient strategy for accessing linear alkylarenes with high regioselectivity. Herein, we report the electroreductive hydroarylation of electron-deficient alkenes and styrene derivatives using (hetero)aryl halides under mild reaction conditions. Notably, the present hydroarylation proceeded with high efficiency under transition-metal-catalyst-free conditions. The key to success is the use of 1,3-dicyanobenzene as a redox mediator and visible-light irradiation, which effectively suppresses the formation of simple reduction, i.e., hydrodehalogenation, products to afford the desired products in good to high yields. Mechanistic investigations proposed that a reductive radical-polar crossover pathway is likely to be involved in this transformation.

Introduction

Alkene hydroarylation is an attractive method for the construction of alkylarenes, which serve as versatile building blocks in organic syntheses. To achieve this transformation with high efficiency and predictable regioselectivity, numerous efforts have been made to develop transition-metal-catalyzed reactions based on a C–H activation strategy [1-4] or the reductive coupling of aryl halides with a hydride donor [5-8]. On the other hand, aryl radical-involved hydroarylation would be a promising alternative for the synthesis of alkylarenes with high anti-Markovnikov selectivity [9,10]. Aryl halides have received increased attention as ideal radical precursors because of their beneficial features, such as higher chemical stability and wide commercial availability, compared with other precursors, e.g., diazonium salts [11]. Classical approaches toward aryl radical species from the corresponding halides would involve halogen abstraction or single-electron reduction processes using chemical reagents; however, these methods have some drawbacks, such as reagent toxicity/stability and limited substrate scope [12-14]. While recent advances in photochemistry have remarkably expanded the synthetic utility of (hetero)aryl radicals in

organic synthesis [15-20], visible-light-mediated alkene hydroarylation commonly requires external reductants and/or hydrogen atom sources to complete the catalytic cycle [21-25]. Over the past few decades, electrochemistry has proven to be an environmentally benign and convenient approach for accessing open-shell intermediates through a single-electron transfer process [26-31]. In particular, electroreductive transformations have recently received renewed attention from modern synthetic chemists as a safer protocol than conventional methods using chemical reductants such as metal hydride species [32-36]. In this context, the electrochemical single-electron reduction of aryl iodides, bromides, and activated (bearing at least one electron-withdrawing group) aryl chlorides has been demonstrated as a useful method to generate aryl radical species under mild reaction conditions [37]. Although the additional electron transfer to form the corresponding anions is a highly favorable pathway due to the more positive reduction potential of radicals than that of the starting halides [38], employing redox mediators enables the generated aryl radicals to participate in radical arylation reactions by preventing overreduction [39]. While the metal-catalyst-free radical cyclization of alkene-tethered aryl halides has been well documented in the literature [40-43], the efficient intermolecular hydroarylation of alkenes still relies on the use of transition-metal catalysts, including Pd [44], Ni [45], and Co [46] (Scheme 1a). The pioneering work by Savéant et al. demonstrated that electron-deficient (hetero)aromatics acted as efficient mediators for the metal-catalyst-free electroreductive hydroarylation of alkenes with some activated chloro-, bromo-, and iodoarenes, but the use of a Hg pool cathode and/or liquid NH_3 solvent would be problematic in terms of environmental and practical perspectives (Scheme 1b) [47]. Therefore, it is desirable to develop an efficient electroreductive protocol for alkene hydroarylation with a broad substrate scope under mild reaction conditions. Recently, the groups of Lin and Lambert [48] and Wickens [49] independently demonstrated that aryl chlorides with highly negative reduction potentials engaged in C–X (X = P, Sn, B) and C–C bond formation reactions involving aryl radical species by integrating photochemistry and electrochemistry [50-53]. Furthermore, odd-numbered [*n*]cumulenes have proven to be effective redox mediators for electroreductive radical borylation of unactivated aryl chlorides without visible-light irradiation by the group of Milner [54]. Herein, we report transition-metal-catalyst-free electroreductive alkene hydroarylation with (hetero)aryl halides using 1,3-dicyanobenzene as a redox mediator under visible-light irradiation.

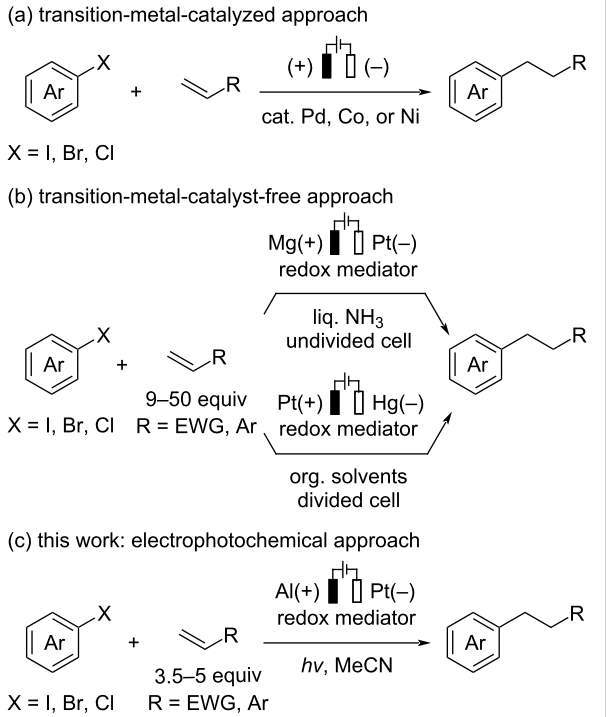

Scheme 1: Electrochemical hydroarylation of alkenes with aryl halides.

Results and Discussion

We began the investigation of the electroreductive hydroarylation using methyl 4-chlorobenzoate (**1a**) and methyl acrylate (**2a**) as model substrates (Table 1). After extensive efforts to screen the reaction parameters to achieve the desired transformation with high efficiency, we found that the electroreductive coupling of **1a** with **2a** proceeded smoothly to afford **3aa** in 82% yield under the conditions using an undivided cell equipped with Al(+)/Pt(−) electrodes in the presence of H_2O and 5 mol % of 1,3-dicyanobenzene (1,3-DCB) [55] under visible-light irradiation at 0 °C (Table 1, entry 1) [56]. Ammonium salts containing other counter anions also afforded **3aa** in slightly lower yields (Table 1, entries 2 and 3). Changing the sacrificial anode or cathode did not improve the reaction efficiency (Table 1, entries 4–7). The effects of a series of redox mediators on the reaction outcomes were examined, and none gave a better reaction outcome than 1,3-DCB (Table 1, entries 8–12). Control experiments revealed that both visible-light irradiation and the presence of 1,3-DCB were essential for achieving the hydroarylation in high efficiency (Table 1, entries 13–16). Furthermore, the different current density conditions provided the desired product in slightly decreased yields (Table 1, entries 17 and 18), and this transformation did not proceed in the absence of electric current (Table 1, entry 19).

With the optimized conditions in hand, the scope of aryl halides and alkenes was investigated (Scheme 2). The reaction of *para*-substituted aryl chlorides bearing pivaloyl and cyano groups proceeded smoothly to provide the desired coupling products in good to high yields (**3ba**, **3ca**). Products bearing *p*-methylsul-

Table 1: Evaluation of reaction conditions.[a]

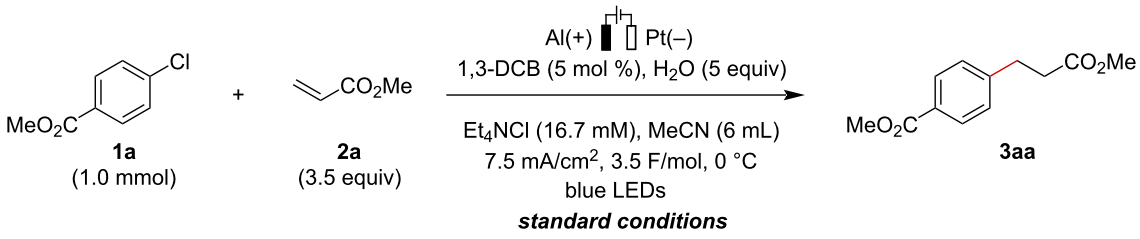

entry	variation from the standard conditions	yield (%)[b]
1	none	82
2	Et_4NBr instead of Et_4NCl	72
3	Et_4NOTs instead of Et_4NCl	76
4	Mg anode	50
5	Zn anode	44
6	Ni cathode	55
7	graphite cathode	50
8	1,2-DCB instead of 1,3-DCB	68
9	1,4-DCB instead of 1,3-DCB	75
10	9,10-DCA instead of 1,3-DCB	69
11	phenanthrene (1 equiv) instead of 1,3-DCB, without blue LEDs	60
12	9,9-diethylfluorene (1 equiv) instead of 1,3-DCB, without blue LEDs	65
13	without blue LEDs	55
14	without 1,3-DCB	46
15	without blue LEDs and 1,3-DCB	64
16	without blue LEDs and 1,3-DCB, 2.5 mA/cm^2	63
17	15 mA/cm^2	77
18	5 mA/cm^2	73
19	without electric current	n.r.

[a]Reaction conditions: **1a** (1.0 mmol), **2a** (3.5 mmol), 1,3-DCB (5 mol %), Et_4NCl (0.1 mmol), H_2O (5.0 mmol), MeCN (6 mL), Al(+)-Pt(–), 7.5 mA/cm^2, 3.5 F/mol, 0 °C, blue LEDs. [b]Isolated yield. DCB, dicyanobenzene; DCA, dicyanoanthracene; n.r., no reaction.

fonyl (**3da**) and *m*-methoxycarbonyl (**3ea**) groups were obtained from the corresponding aryl bromides instead of chlorides under otherwise identical reaction conditions. The steric hindrance of the *ortho*-substituent did not have a large influence on the reaction efficiency, affording **3fa** in 71% yield. Some heteroaryl chlorides including triazine, pyrimidine, and pyridazine skeletons were also effectively coupled with methyl acrylate to provide the desired products in good yields (**3ga**–**ja**). While unsubstituted chlorobenzene and bromobenzene were completely inert in this transformation, iodobenzene was successfully converted to the corresponding product **3ka** under slightly modified reaction conditions (see Table S1 in Supporting Information File 1 for optimization details). Under the modified conditions, aryl iodides with various electron-donating groups including a methoxy group were transformed into the products in good yields (**3la**–**na**). 4-(Trifluoromethoxy)iodobenzene also well participated in this reaction, affording **3oa** in 65% yield. Aryl iodides having fluoro and chloro substituents underwent selective C–I bond cleavage to provide monoalkylated products **3pa** and **3qa**, respectively. In addition to the successful transformations of heteroaryl iodides with indole or pyridine cores (**3ra**, **3sa**), the electroreductive synthesis of methaqualone derivatives was also achieved (**3ta**).

Pleasingly, a series of electron-deficient alkene and styrene derivatives were found to be suitable coupling partners. Aryl chloride **1a** reacted with *tert*-butyl acrylate (**2b**) without any difficulty, providing **3ab** in a high yield. Methacrylamide (**2c**) and acrylonitrile (**2d**) were transformed into the corresponding products in high yields, but with slightly lower Faradaic efficiency (**3ac**, **3ad**). In addition to styrene derivatives bearing α-substituents and electronically diverse functionalities, indene and 2-vinylpyridine were all compatible with the present electroreductive hydroarylation (**3ae**–**ak**). The reaction of iodo-

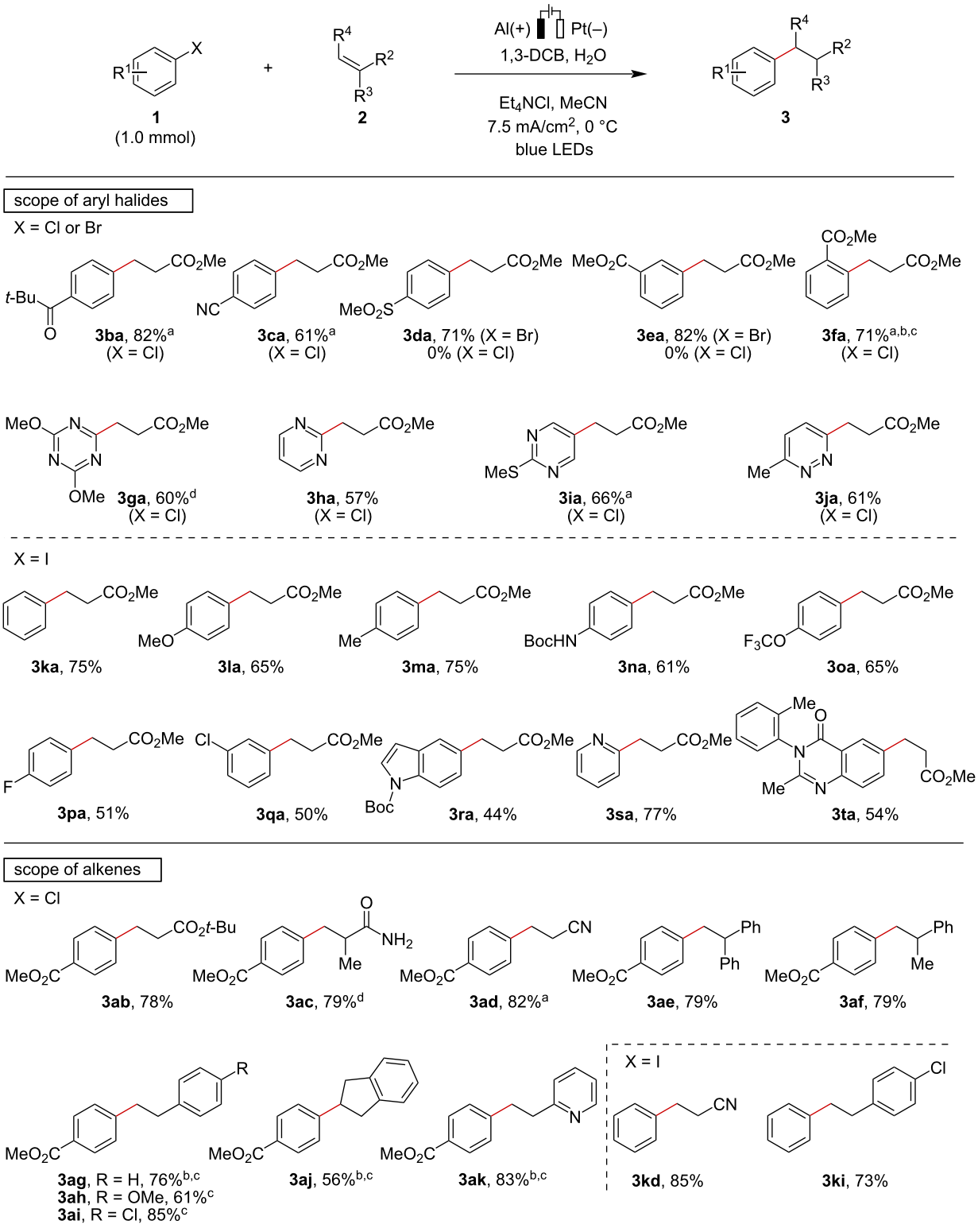

Scheme 2: Substrate scope. Reaction conditions for **1** (X = Cl, Br): **1** (1.0 mmol), **2** (3.5 mmol), 1,3-DCB (5 mol %), H_2O (5.0 mmol), Et_4NCl (0.1 mmol), MeCN (6 mL), Al(+)-Pt(−), 7.5 mA/cm^2, 3.5 F/mol, 0 °C, blue LEDs; reaction conditions for **1** (X = I): **1** (1.0 mmol), **2** (5.0 mmol), 1,3-DCB (50 mol %), H_2O (5.0 mmol), Et_4NCl (0.1 mmol), MeCN (3 mL), Al(+)-Pt(−), 7.5 mA/cm^2, 4.5 F/mol, 0 °C, blue LEDs. [a]4.5 F/mol. [b]**2** (5 equiv). [c]MeCN (3 mL). [d]5 F/mol. 1,3-DCB, 1,3-dicyanobenzene.

benzene with acrylonitrile and 4-chlorostyrene proceeded smoothly to afford **3kd** and **3ki** in 85% and 73% yields, respectively.

In order to demonstrate the scalability of this transformation, a gram-scale reaction was performed (Scheme 3a). The hydroarylation of **2a** with **1a** was successfully carried out in a simple glass beaker under the standard reaction conditions, providing the corresponding product **3aa** in 74% yield. Several control experiments were conducted to gain insight into the reaction mechanism of the electroreductive process. The hydroarylation of cyclopropane-substituted styrene **2l** resulted in the formation of ring-opening product **3al'**, and the simple hydroarylation product was not observed (Scheme 3b). This result strongly supported the involvement of radical intermediates in the present transformation. Next, a deuterium-labeling experiment was conducted to elucidate the H-source of this reaction (Scheme 3c). The reaction of **1a** and **2e** in MeCN with D_2O provided the coupling product with 51% deuterium incorporation, indicating that carbanion species would be generated in this reaction and that H_2O would serve as a major proton source. Et_4NCl may also provide protons to form the coupling product [47]. Taken these results together, the present electroreductive reaction would proceed through a reductive radical-polar crossover pathway [57].

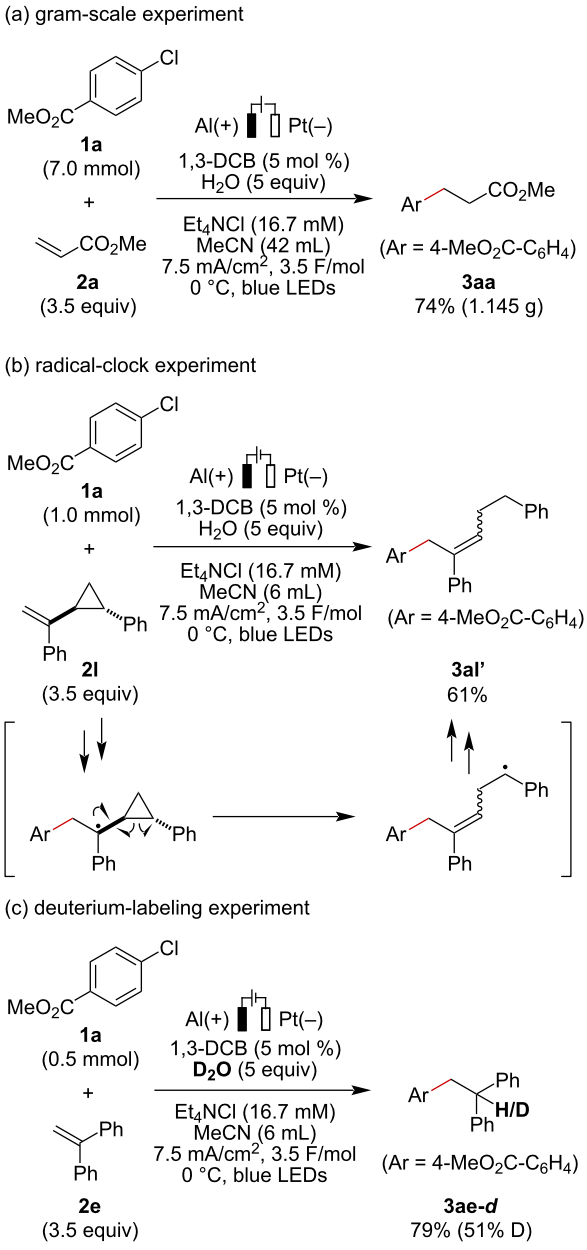

Scheme 3: Gram-scale reaction and control experiments.

On the basis of mechanistic investigations and a literature report [47], a plausible mechanism for this electroreductive hydroarylation is depicted in Scheme 4. 1,3-DCB ($E_{p/2}$ = −1.9 V vs SCE in MeCN) [58] undergoes single-electron reduction at the cathode to generate the radical anion species (1,3-DCB$^{\bullet-}$), which might act as a mediator to produce the radical anion **1**$^{\bullet-}$ through the homogeneous electron transfer in the bulk solution (representative reduction peak potential: **1a**, E_p = −1.98 V vs SCE in MeCN [59]; **1c**, E_p = −2.06 V vs SCE in MeCN [47]). In the case of the reaction with electron-deficient alkenes, e.g., methyl acrylate ($E_{1/2}$ = −2.1 V vs SCE) [60], reduction of alkenes is one of the competitive processes. Subsequent fragmentation of radical anion **1**$^{\bullet-}$ to form aryl radical species **A**, which then reacts with alkene **2** to provide alkyl radical species **B**. Further single-electron reduction by 1,3-DCB$^{\bullet-}$ or at the cathode followed by protonation of **B** provides hydroarylation product **3**. Meanwhile, the sacrificial anode is oxidized to form Al cations. Although the exact role of visible-light irradiation in the electroreductive hydroarylation is unclear, the generation of photoexcited radical anion species as potential reductants might be included in the present transformation.

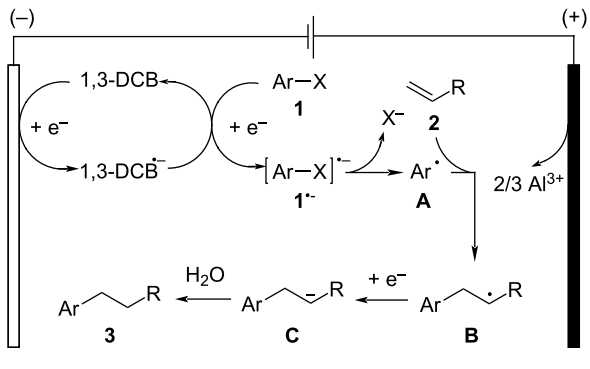

Scheme 4: Plausible mechanism.

Conclusion

In conclusion, we have developed a transition-metal-catalyst-free electroreductive hydroarylation of alkenes with aryl halides, including aryl chlorides, by employing 1,3-DCB under visible-light irradiation. The present transformation proceeded smoothly in a common organic solvent without transition-metal catalysts, and hydroarylation products were obtained from a variety of electron-deficient alkenes and styrene derivatives in good to high yields. A large-scale reaction was successfully carried out, highlighting the potential synthetic utility of the present transformation. The mechanistic study proposed that a reductive radical-polar crossover pathway would be involved in the present transformation.

Supporting Information

Supporting Information File 1

Experimental procedures, characterization data, and copies of NMR spectra of the products.
[https://www.beilstein-journals.org/bjoc/content/supplementary/1860-5397-20-116-S1.pdf]

Acknowledgements

The spectral data were collected with the research equipment shared in the MEXT Project for promoting public utilization of advanced research infrastructure (Program for supporting introduction of the new sharing system JPMXS0422500320).

Funding

This work was supported by JSPS (KAKENHI: 22K06528, 22K15255, and 19K05459).

ORCID® iDs

Kosuke Yamamoto - https://orcid.org/0000-0002-8189-7141
Masami Kuriyama - https://orcid.org/0000-0002-4871-6273
Osamu Onomura - https://orcid.org/0000-0003-3703-1401

Data Availability Statement

All data that supports the findings of this study is available in the published article and/or the supporting information to this article.

References

1. Kakiuchi, F.; Murai, S. *Acc. Chem. Res.* **2002,** *35,* 826–834. doi:10.1021/ar960318p
2. Foley, N. A.; Lee, J. P.; Ke, Z.; Gunnoe, T. B.; Cundari, T. R. *Acc. Chem. Res.* **2009,** *42,* 585–597. doi:10.1021/ar800183j
3. Crisenza, G. E. M.; Bower, J. F. *Chem. Lett.* **2016,** *45,* 2–9. doi:10.1246/cl.150913
4. Ketcham, H. E.; Bennett, M. T.; Reid, C. W.; Gunnoe, T. B. Advances in arene alkylation and alkenylation catalyzed by transition metal complexes based on ruthenium, nickel, palladium, platinum, rhodium and iridium. *Advances in Organometallic Chemistry;* Academic Press: Cambridge, MA, USA, 2023; Vol. 80, pp 93–176. doi:10.1016/bs.adomc.2023.01.002
5. Oxtoby, L. J.; Gurak, J. A., Jr.; Wisniewski, S. R.; Eastgate, M. D.; Engle, K. M. *Trends Chem.* **2019,** *1,* 572–587. doi:10.1016/j.trechm.2019.05.007
6. Nguyen, J.; Chong, A.; Lalic, G. *Chem. Sci.* **2019,** *10,* 3231–3236. doi:10.1039/c8sc05445b
7. Saper, N. I.; Ohgi, A.; Small, D. W.; Semba, K.; Nakao, Y.; Hartwig, J. F. *Nat. Chem.* **2020,** *12,* 276–283. doi:10.1038/s41557-019-0409-4
8. Richardson, G. M.; Douair, I.; Cameron, S. A.; Bracegirdle, J.; Keyzers, R. A.; Hill, M. S.; Maron, L.; Anker, M. D. *Nat. Commun.* **2021,** *12,* 3147. doi:10.1038/s41467-021-23444-x
9. Heinrich, M. R. *Chem. – Eur. J.* **2009,** *15,* 820–833. doi:10.1002/chem.200801306
10. Diesendorf, N.; Heinrich, M. R. *Synthesis* **2022,** *54,* 1951–1963. doi:10.1055/s-0040-1719893
11. Kvasovs, N.; Gevorgyan, V. *Chem. Soc. Rev.* **2021,** *50,* 2244–2259. doi:10.1039/d0cs00589d
12. Meijs, G. F.; Bunnett, J. F. *J. Org. Chem.* **1989,** *54,* 1123–1125. doi:10.1021/jo00266a024
13. Ohno, H.; Iwasaki, H.; Eguchi, T.; Tanaka, T. *Chem. Commun.* **2004,** 2228–2229. doi:10.1039/b410457a
14. Srikanth, G. S. C.; Castle, S. L. *Tetrahedron* **2005,** *61,* 10377–10441. doi:10.1016/j.tet.2005.07.077
15. Hari, D. P.; König, B. *Angew. Chem., Int. Ed.* **2013,** *52,* 4734–4743. doi:10.1002/anie.201210276
16. Zuo, Z.; Ahneman, D. T.; Chu, L.; Terrett, J. A.; Doyle, A. G.; MacMillan, D. W. C. *Science* **2014,** *345,* 437–440. doi:10.1126/science.1255525
17. Ghosh, I.; Marzo, L.; Das, A.; Shaikh, R.; König, B. *Acc. Chem. Res.* **2016,** *49,* 1566–1577. doi:10.1021/acs.accounts.6b00229
18. Kanegusuku, A. L. G.; Roizen, J. L. *Angew. Chem., Int. Ed.* **2021,** *60,* 21116–21149. doi:10.1002/anie.202016666
19. Lan, J.; Chen, R.; Duo, F.; Hu, M.; Lu, X. *Molecules* **2022,** *27,* 5364. doi:10.3390/molecules27175364
20. Piedra, H. F.; Valdés, C.; Plaza, M. *Chem. Sci.* **2023,** *14,* 5545–5568. doi:10.1039/d3sc01724a
21. Arora, A.; Teegardin, K. A.; Weaver, J. D. *Org. Lett.* **2015,** *17,* 3722–3725. doi:10.1021/acs.orglett.5b01711
22. Seath, C. P.; Jui, N. T. *Synlett* **2019,** *30,* 1607–1614. doi:10.1055/s-0037-1611527
23. Cheng, H.; Lam, T.-L.; Liu, Y.; Tang, Z.; Che, C.-M. *Angew. Chem., Int. Ed.* **2021,** *60,* 1383–1389. doi:10.1002/anie.202011841
24. Hendy, C. M.; Smith, G. C.; Xu, Z.; Lian, T.; Jui, N. T. *J. Am. Chem. Soc.* **2021,** *143,* 8987–8992. doi:10.1021/jacs.1c04427
25. Hou, J.; Hua, L.-L.; Huang, Y.; Zhan, L.-W.; Li, B.-D. *Chem. – Asian J.* **2023,** *18,* e202201092. doi:10.1002/asia.202201092
26. Schäfer, H. J. Electrochemical Generation of Radicals. In *Radicals in Organic Synthesis;* Renaud, P.; Sibi, M. P., Eds.; Wiley-VCH: Weinheim, Germany, 2001; Vol. 1, pp 250–297. doi:10.1002/9783527618293.ch14
27. Gandeepan, P.; Finger, L. H.; Meyer, T. H.; Ackermann, L. *Chem. Soc. Rev.* **2020,** *49,* 4254–4272. doi:10.1039/d0cs00149j

28. Chicas-Baños, D. F.; Frontana-Uribe, B. A. *Chem. Rec.* **2021,** *21,* 2538–2573. doi:10.1002/tcr.202100056
29. Kisukuri, C. M.; Fernandes, V. A.; Delgado, J. A. C.; Häring, A. P.; Paixão, M. W.; Waldvogel, S. R. *Chem. Rec.* **2021,** *21,* 2502–2525. doi:10.1002/tcr.202100065
30. Luo, M.-J.; Xiao, Q.; Li, J.-H. *Chem. Soc. Rev.* **2022,** *51,* 7206–7237. doi:10.1039/d2cs00013j
31. Mitsudo, K.; Okumura, Y.; Sato, E.; Suga, S. *Eur. J. Org. Chem.* **2023,** e202300835. doi:10.1002/ejoc.202300835
32. Zhu, C.; Ang, N. W. J.; Meyer, T. H.; Qiu, Y.; Ackermann, L. *ACS Cent. Sci.* **2021,** *7,* 415–431. doi:10.1021/acscentsci.0c01532
33. Park, S. H.; Ju, M.; Ressler, A. J.; Shim, J.; Kim, H.; Lin, S. *Aldrichimica Acta* **2021,** *54,* 17–27.
34. Claraz, A.; Masson, G. *ACS Org. Inorg. Au* **2022,** *2,* 126–147. doi:10.1021/acsorginorgau.1c00037
35. Zhang, W.; Guan, W.; Martinez Alvarado, J. I.; Novaes, L. F. T.; Lin, S. *ACS Catal.* **2023,** *13,* 8038–8048. doi:10.1021/acscatal.3c01174
36. K, B. B.; Lingden, C. P.; Pokhrel, T.; Paudel, M.; Sajid, K.; Adhikari, A.; Shirinfar, B.; Ahmed, N. *ChemElectroChem* **2023,** *10,* e202300289. doi:10.1002/celc.202300289
37. Xiang, H.; He, J.; Qian, W.; Qiu, M.; Xu, H.; Duan, W.; Ouyang, Y.; Wang, Y.; Zhu, C. *Molecules* **2023,** *28,* 857. doi:10.3390/molecules28020857
38. Koefoed, L.; Vase, K. H.; Stenlid, J. H.; Brinck, T.; Yoshimura, Y.; Lund, H.; Pedersen, S. U.; Daasbjerg, K. *ChemElectroChem* **2017,** *4,* 3212–3221. doi:10.1002/celc.201700772
39. Swartz, J. E.; Stenzel, T. T. *J. Am. Chem. Soc.* **1984,** *106,* 2520–2524. doi:10.1021/ja00321a005
40. Kurono, N.; Honda, E.; Komatsu, F.; Orito, K.; Tokuda, M. *Tetrahedron* **2004,** *60,* 1791–1801. doi:10.1016/j.tet.2003.12.038
41. Mitsudo, K.; Nakagawa, Y.; Mizukawa, J.-i.; Tanaka, H.; Akaba, R.; Okada, T.; Suga, S. *Electrochim. Acta* **2012,** *82,* 444–449. doi:10.1016/j.electacta.2012.03.130
42. Katayama, A.; Senboku, H.; Hara, S. *Tetrahedron* **2016,** *72,* 4626–4636. doi:10.1016/j.tet.2016.06.032
43. Folgueiras-Amador, A. A.; Teuten, A. E.; Salam-Perez, M.; Pearce, J. E.; Denuault, G.; Pletcher, D.; Parsons, P. J.; Harrowven, D. C.; Brown, R. C. D. *Angew. Chem., Int. Ed.* **2022,** *61,* e202203694. doi:10.1002/anie.202203694
44. Torii, S.; Tanaka, H.; Morisaki, K. *Chem. Lett.* **1985,** *14,* 1353–1354. doi:10.1246/cl.1985.1353
45. Condon, S.; Dupré, D.; Falgayrac, G.; Nédélec, J.-Y. *Eur. J. Org. Chem.* **2002,** 105–111. doi:10.1002/1099-0690(20021)2002:1<105::aid-ejoc105>3.0.co;2-j
46. Gomes, P.; Gosmini, C.; Nédélec, J.-Y.; Périchon, J. *Tetrahedron Lett.* **2000,** *41,* 3385–3388. doi:10.1016/s0040-4039(00)00420-2
47. Chami, Z.; Gareil, M.; Pinson, J.; Savéant, J.-M.; Thiébault, A. *J. Org. Chem.* **1991,** *56,* 586–595. doi:10.1021/jo00002a020
48. Kim, H.; Kim, H.; Lambert, T. H.; Lin, S. *J. Am. Chem. Soc.* **2020,** *142,* 2087–2092. doi:10.1021/jacs.9b10678
49. Cowper, N. G. W.; Chernowsky, C. P.; Williams, O. P.; Wickens, Z. K. *J. Am. Chem. Soc.* **2020,** *142,* 2093–2099. doi:10.1021/jacs.9b12328
50. Capaldo, L.; Quadri, L. L.; Ravelli, D. *Angew. Chem., Int. Ed.* **2019,** *58,* 17508–17510. doi:10.1002/anie.201910348
51. Liu, J.; Lu, L.; Wood, D.; Lin, S. *ACS Cent. Sci.* **2020,** *6,* 1317–1340. doi:10.1021/acscentsci.0c00549
52. Wu, S.; Kaur, J.; Karl, T. A.; Tian, X.; Barham, J. P. *Angew. Chem., Int. Ed.* **2022,** *61,* e202107811. doi:10.1002/anie.202107811
53. Huang, H.; Steiniger, K. A.; Lambert, T. H. *J. Am. Chem. Soc.* **2022,** *144,* 12567–12583. doi:10.1021/jacs.2c01914
54. Lai, Y.; Halder, A.; Kim, J.; Hicks, T. J.; Milner, P. J. *Angew. Chem., Int. Ed.* **2023,** *62,* e202310246. doi:10.1002/anie.202310246
55. Osaka, K.; Usami, A.; Iwasaki, T.; Yamawaki, M.; Morita, T.; Yoshimi, Y. *J. Org. Chem.* **2019,** *84,* 9480–9488. doi:10.1021/acs.joc.9b00970
    The group of Yoshimi reported that 1,3-DCB served as an efficient electron acceptor in the decarboxylative radical addition of carboxylic acids to alkenes through photoinduced electron-transfer process using a phenanthrene/1,3-DCB system.
56. Methyl benzoate (7% NMR yield) and dimethyl adipate (16% NMR yield) were observed in the crude reaction mixture, presumably formed through overreduction of the aryl radical species and reductive dimerization of methyl acrylate.
57. Zhang, W.; Lin, S. *J. Am. Chem. Soc.* **2020,** *142,* 20661–20670. doi:10.1021/jacs.0c08532
58. Roth, H. G.; Romero, N. A.; Nicewicz, D. A. *Synlett* **2016,** *27,* 714–723. doi:10.1055/s-0035-1561297
59. Connell, T. U.; Fraser, C. L.; Czyz, M. L.; Smith, Z. M.; Hayne, D. J.; Doeven, E. H.; Agugiaro, J.; Wilson, D. J. D.; Adcock, J. L.; Scully, A. D.; Gómez, D. E.; Barnett, N. W.; Polyzos, A.; Francis, P. S. *J. Am. Chem. Soc.* **2019,** *141,* 17646–17658. doi:10.1021/jacs.9b07370
60. Tyssee, D. A.; Baizer, M. M. *J. Org. Chem.* **1974,** *39,* 2819–2823. doi:10.1021/jo00933a001

License and Terms

BEILSTEIN JOURNAL OF ORGANIC CHEMISTRY

Synthesis of cyclic β-1,6-oligosaccharides from glucosamine monomers by electrochemical polyglycosylation

Md Azadur Rahman[1], Hirofumi Endo[1], Takashi Yamamoto[1], Shoma Okushiba[1], Norihiko Sasaki[1,2] and Toshiki Nokami[*1,2]

Full Research Paper

Open Access

Address:
[1]Department of Chemistry and Biotechnology, Tottori University, 4-101 Koyamacho-minami, Tottori city, 680-8552 Tottori, Japan and [2]Center for Research on Green Sustainable Chemistry, Faculty of Engineering, Tottori University, 4-101 Koyamacho-minami, Tottori city, 680-8552 Tottori, Japan

Email:
Toshiki Nokami* - tnokami@tottori-u.ac.jp

* Corresponding author

Keywords:
cyclic oligosaccharide; electrochemical glycosylation; glucosamine; polyglycosylation

Beilstein J. Org. Chem. **2024,** *20,* 1421–1427.
https://doi.org/10.3762/bjoc.20.124

Received: 15 April 2024
Accepted: 11 June 2024
Published: 26 June 2024

This article is part of the thematic issue "Synthetic electrochemistry".

Guest Editor: K. Lam

Abstract

The synthesis of protected precursors of cyclic β-1,6-oligoglucosamines from thioglycosides as monomers is performed by electrochemical polyglycosylation. The monomer with a 2,3-oxazolidinone protecting group afforded the cyclic disaccharide exclusively. Cyclic oligosaccharides up to the trisaccharide were obtained using the monomer with a 2-azido-2-deoxy group.

Introduction

Electrochemical polymerization of organic molecules is an important strategy for the preparation of functional materials, such as conducting polymers [1-5]. Electrochemical reactions can be controlled by electric potential or current, electrodes, and electrolytes, which are not available in conventional chemical reactions. Therefore, electrochemical polymerizations can be utilized for selective synthesis. Cyclic oligosaccharides are an important class of host molecules, and some natural cyclic oligosaccharides are produced by enzymatic processes. However, the corresponding chemical syntheses are still primitive [6-10]. Thus, chemical glycosylation has to be improved to be able to synthesize complex oligosaccharides, including cyclic oligosaccharides. In this context, electrochemical glycosylation is an important alternative to conventional chemical glycosylations because the precise control of reaction time and rate is possible under electrochemical conditions [11-13]. We have been interested in the preparation of cyclic oligosaccharides under electrochemical conditions and electrochemical conversion of linear oligosaccharides of glucosamine into the corresponding cyclic oligosaccharides by intramolecular glycosylation (Scheme 1a) [14]. One-pot two-step synthesis via electrochemical polyglycosylation and intramolecular glycosylation has also been achieved in order to synthesize unnatural cyclic oligosaccharides of glucosamine (Scheme 1b) [15]. Here, we

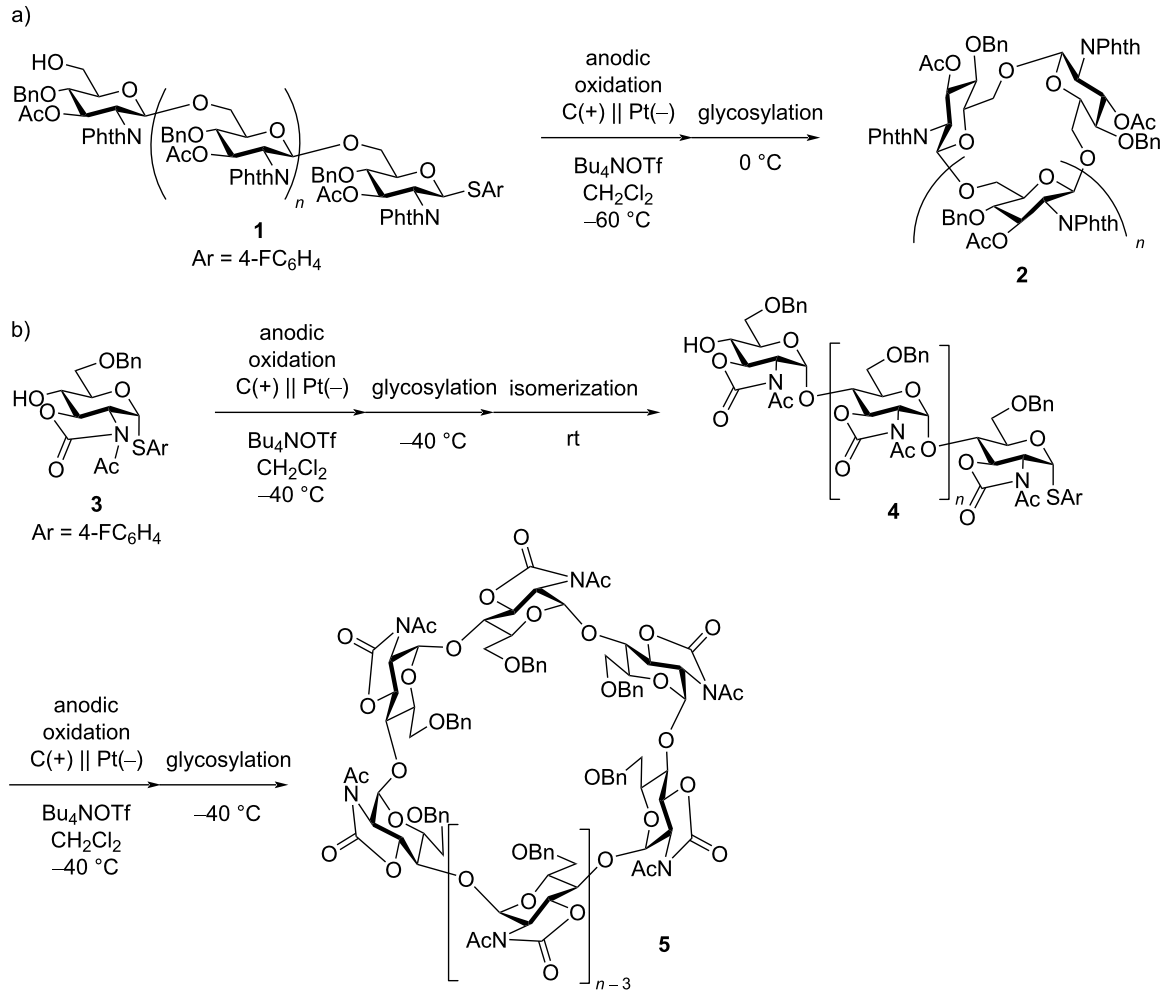

Scheme 1: Preparation of cyclic oligoglucosamines a) via intramolecular glycosylation and b) via polyglycosylation and intramolecular glycosylation.

report the direct synthesis of cyclic oligoglucosamines via electrochemical polymerization of thioglycoside monomers that are derived from glucosamine hydrochloride.

Results and Discussion

Electrochemical polyglycosylation of 2-deoxy-2-phthalimido-substituted thioglycoside monomers

We initiated our research with the electrochemical polyglycosylation of monomers **6** with a 2-deoxy-2-phthalimido (PhthN) group (Table 1). The influence of the anomeric leaving group was not investigated in this study. However, the *p*-ClC_6H_4S (ArS) group was used to avoid the exchange of the anomeric leaving group [16]. The monomer **6a** (R^3 = R^4 = Bz) was completely consumed with a slight excess of total charge (Q = 1.05 F/mol). However, 1,6-anhydrosugar **7a** (R^3 = R^4 = Bz) was formed as a major product, together with cyclic disaccharide **8a** (R^3 = R^4 = Bz) (Table 1, entry 1). The monosaccharide **6b** (R^3 = Ac, R^4 = Bn) was also completely consumed under the same reaction conditions. However, the yield of 1,6-anhydrosugar **7b** (R^3 = Ac, R^4 = Bn) was lower than that of **7a** (Table 1, entry 2). Because no linear oligosaccharides were obtained, we reduced the amount of total charge from 1.05 to 0.525 F/mol (Table 1, entry 3). Linear disaccharide **9b** (R^3 = Ac, R^4 = Bn) and trisaccharide **10b** (R^3 = Ac, R^4 = Bn) were obtained in 13% and 6% yield, respectively. The protecting group R^3 of 3-OH was changed from an acetyl to a benzyl group. However, conversion and yield of linear oligosaccharides **9c** and **10c** decreased, and the corresponding cyclic disaccharide **8c** was not obtained at all (Table 1, entry 4). The reasons for the lower conversion and yield are unclear. However, the lower yield may stem from the lower stability of glycosylation intermediates with a benzyl protecting group at C-3. In

Table 1: Electrochemical polyglycosylation of monomers **6** with a 2-PhthN group.

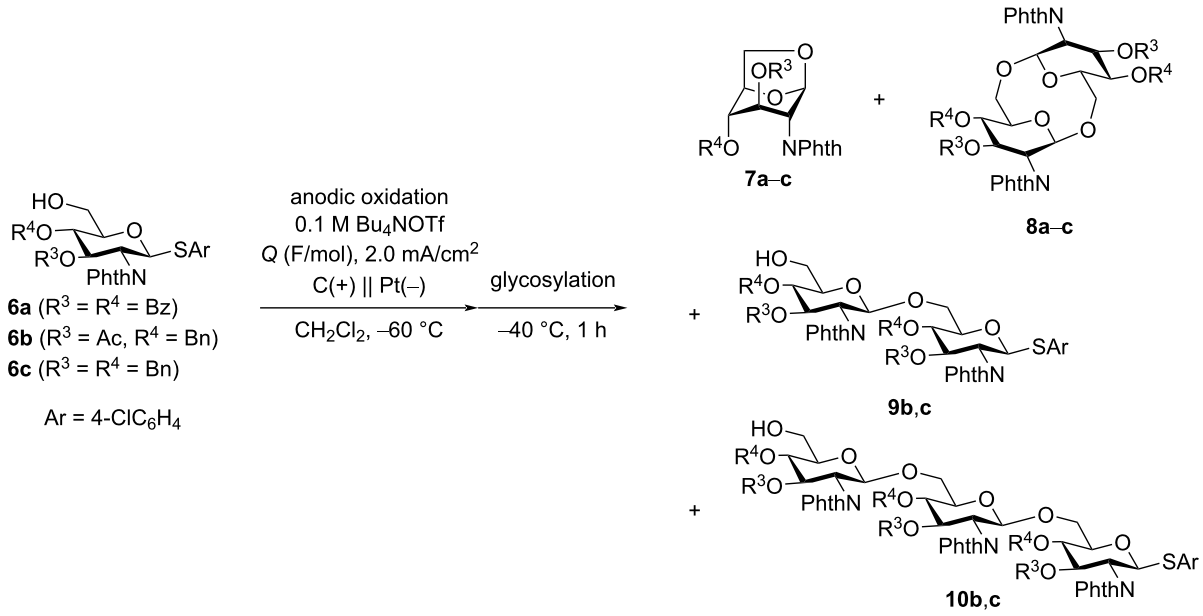

entry	R^3	R^4	total charge *Q* (F/mol)	conversion[a]	yield of **7**	yield of oligosaccharide		
						8	**9**	**10**
1	Bz	Bz	1.05	>99%	**7a** (73%)	**8a** (3%)	—	—
2	Ac	Bn	1.05	>99%	**7b** (28%)	**8b** (6%)	—	—
3	Ac	Bn	0.525	67%	**7b** (25%)	**8b** (7%)	**9b** (13%)	**10b** (6%)
4	Bn	Bn	0.525	59%	**7c** (25%)	—	**9c** (4%)	**10c** (2%)

[a]Based on recovered starting material **6a–c**.

all cases, the major product was 1,6-anhydrosugar **7**, which was the intramolecular glycosylation product of monomer **6**. The proposed mechanism is shown in Scheme 2. Anodic oxidation of thioglycoside **6** generated radical cation **11**, which was converted to glycosyl triflate **12**. 1,6-Anhydrosugar **7** was produced via $^4C_1$-to-$^1C_4$ conformational change of the pyran ring

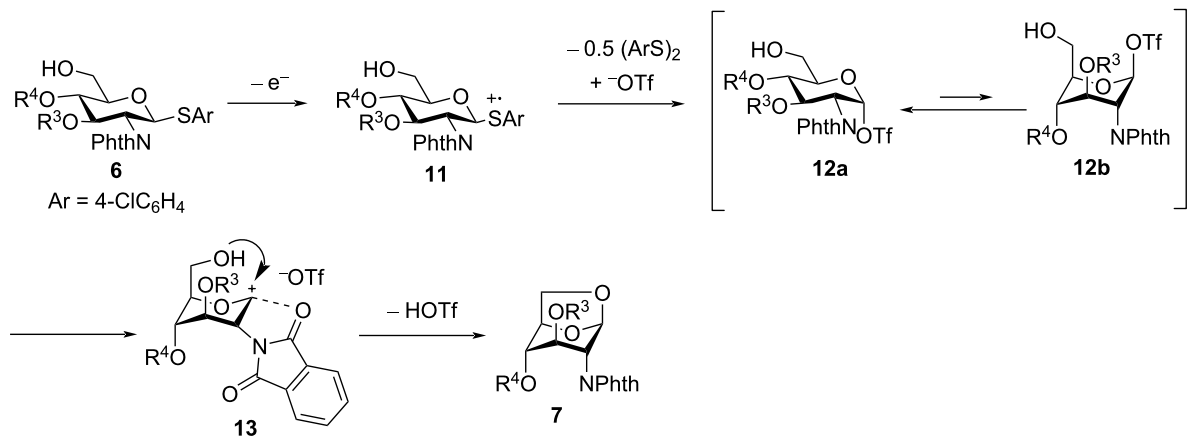

Scheme 2: Proposed reaction mechanism of the formation of 1,6-anhydrosugar **7**.

to generate cation intermediate **13**. Therefore, prevention of the conformational change might be necessary to synthesize larger cyclic oligosaccharides.

Electrochemical polyglycosylation of 2,3-oxazolidinone-substituted thioglycoside monomer

To avoid formation of 1,6-anhydrosugar, we introduced an *N*-acetyl-2,3-oxazolidinone protecting group to the thioglycoside monomer **14** (Scheme 3) [17,18]. The electrochemical polyglycosylation of **14** was carried out in the presence of 2,6-di-*tert*-butyl-4-methylpyridine (DTBMP) to ensure the formation of a β-glycosidic bonds [19]. Although we could suppress formation of 1,6-anhydrosugar **15**, cyclic disaccharide **16** was obtained as an exclusive product. The optimized structure of **15** calculated by DFT (B3LYP/6-31G(d)) suggested that the pyran ring preferred the boat conformation because the chair conformation of the pyran ring was controlled by the introduction of the 2,3-oxazolidinone protecting group (see DFT calculations in Supporting Information File 1). Therefore, it was proven that the 2,3-oxazolidinone protecting group was powerful enough to prevent intramolecular glycosylation of monomer **14**. However, it did not prevent intramolecular glycosylation of the linear disaccharide and promote the formation of larger cyclic oligosaccharides.

Electrochemical polyglycosylation of 2-azido-2-deoxy-substituted thioglycoside monomers

Based on the results shown in Table 1 and Scheme 3, we changed the substituent in position C-2 of the thioglycoside monomer from PhthN to azide, which has no neighboring group effect. Although glycosyl donors with an N_3 group in position C-2 have been used for α-selective glycosylation [20,21], we have already found that β-selective glycosylation proceeds using a glycosyl donor with an N_3 group under electrochemical conditions [22]. The results of the electrochemical polyglycosylation using the thioglycoside monomer **17** with an N_3 group are summarized in Table 2. Cyclic trisaccharide **19a** was obtained together with cyclic disaccharide **18a**, along with trace amount of linear and cyclic tetrasaccharides by introduction of an N_3 group (Table 2, entry 1). Cyclic disaccharide **18b** and linear trisaccharide **20b** were produced with monomer **17b** with a 3,4-di-*O*-benzyl group (Table 2, entry 2). Although the 3-hydroxy protecting group R^3 also affected the product distribution, formation of the corresponding 1,6-anhydrosugars was not observed in both cases. NMR data suggested that cyclic trisaccharide **19a** contained one α-glycosidic bond and two β-glycosidic bonds. Based on these results, we assumed that the formation of the α-glycosidic bond was crucial for producing the cyclic trisaccharide **19a** (Scheme 4). Moreover, the α-glycosidic bond might have formed in the first step, and linear disaccharide **21α**, which did not afford the cyclic disaccharide, should have been produced as an intermediate of **19a**.

The influence of the functional group in position C-2 on the formation of the cyclic products is summarized in Scheme 5. Notably, the C-2 position is the most influential because it is the closest to the anomeric carbon atom, which is the reaction site of the glycosylation. The PhthN group is known to be a strongly β-directing group, and 1,6-anhydrosugar **7b** was obtained as a major product (Scheme 5a). In this case, the competition between intramolecular glycosylation and intermolecular glycosylation (polyglycosylation) occurred, and intramolecular glycosylation was dominant because of the strong directing effect of the 2-PhthN group. By introducing a 2,3-oxazolidinone group at the C-2 and C-3 positions, the undesired intramolecular glycosylation of monomer **14** was suppressed. However, the intramolecular glycosylation of the disaccharide intermediate afforded cyclic disaccharide **16** exclusively (Scheme 5b). Only the C-2 azido group afforded cyclic trisaccharide **19**, which contained both α- and β-glycosidic linkages (Scheme 5c). Therefore, the synthesis of a cyclic trisaccharide with only β-glycosidic linkages by electrochemical polyglycosylation was not achieved. Further optimizations of the protection group are required to suppress the formation of 1,6-anhydrosugar and cyclic disaccharides.

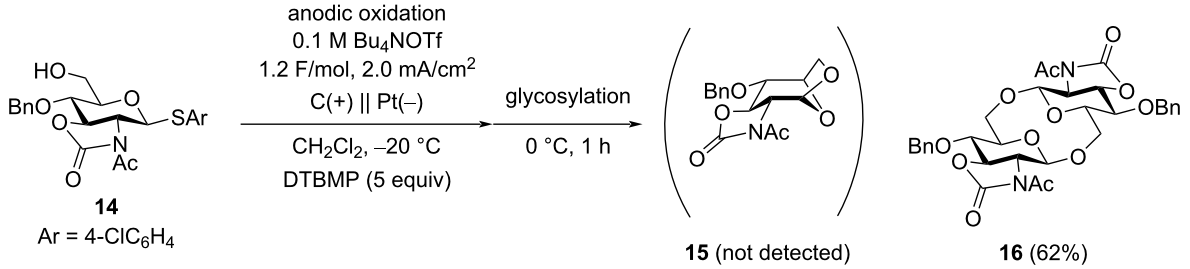

Scheme 3: Electrochemical polyglycosylation of monomer **14** with a 2,3-oxazolidinone protecting group.

Table 2: Electrochemical polyglycosylation of monomers **17** with a 2-azido group.

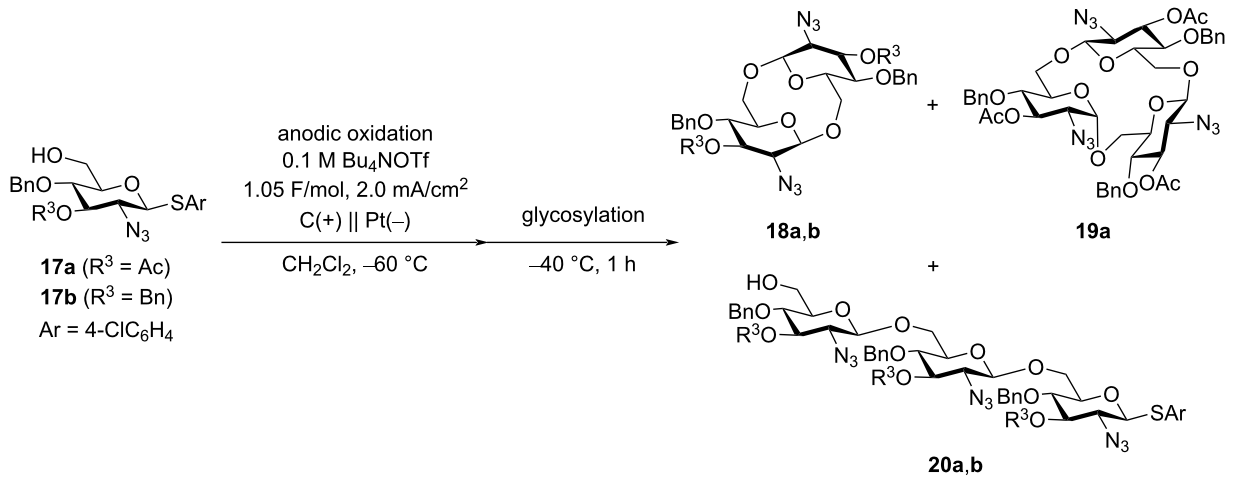

entry	R^3	conversion	yield of oligosaccharide		
			18	**19**	**20**
1	Ac	>99%	**18a** (49%)	**19a** (16%)	—
2	Bn	73%	**18b** (14%)	—	**20b** (13%)

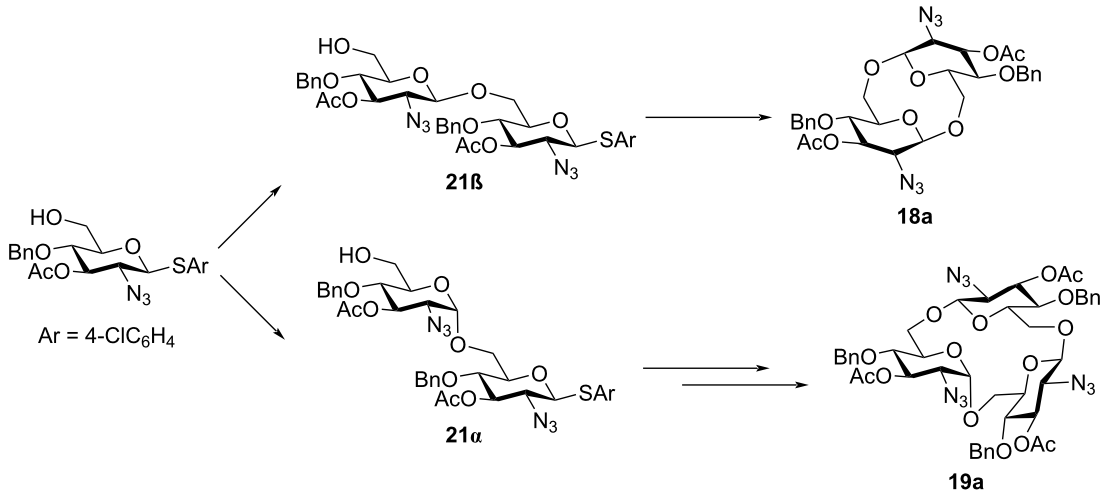

Scheme 4: Proposed reaction mechanism of the formation of cyclic trisaccharide **19a**.

Conclusion

We investigated the synthesis of cyclic β-1,6-oligoglucosamines by electrochemical polyglycosylation. The choice of the protecting group of the monomers was important to prevent intramolecular glycosylation, which formed 1,6-anhydrosugars as side products. It was revealed that the formation of cyclic disaccharides must be controlled to produce cyclic β-1,6-trisaccharides. Further optimizations of monomers and another synthetic approach using dimers for production of larger cyclic oligosaccharides are in progress in our laboratory.

Experimental

Electrochemical polyglycosylation (Scheme 3) was performed using our second-generation automated electrochemical synthesizer equipped with the H-type divided electrolysis cell. Thioglycoside **14** (0.40 mmol, 186 mg), Bu_4NOTf (1.0 mmol,

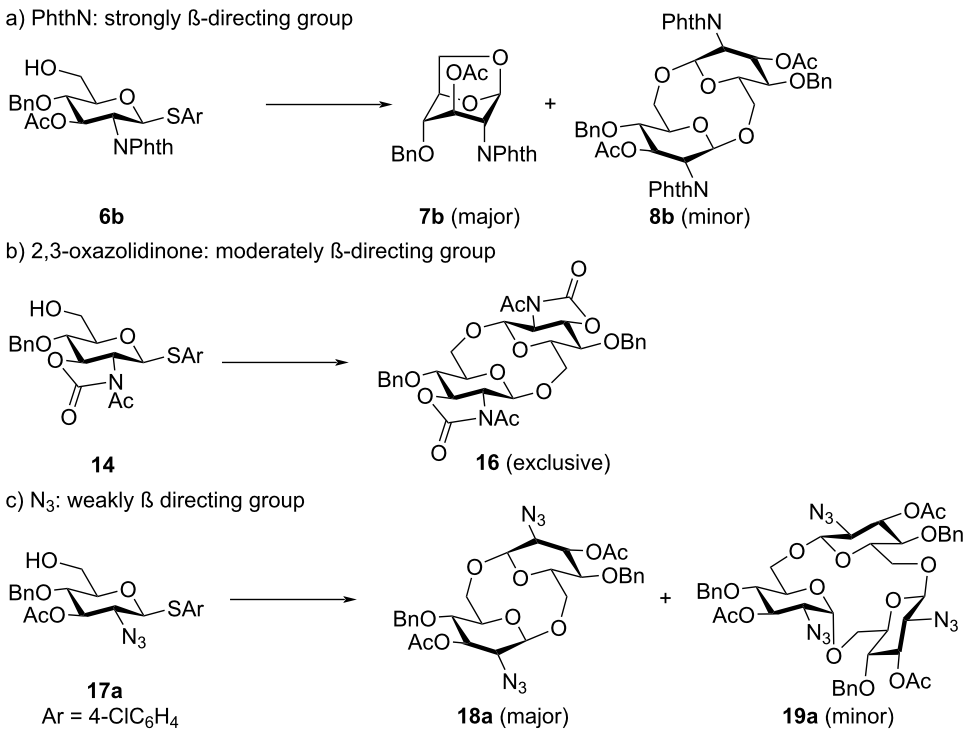

Scheme 5: Influence of the functional group in position C-2 on the formation of the cyclic product.

393 mg), DTBMP (2.0 mmol, 411 mg), and dry CH_2Cl_2 (10 mL) were added to the anodic chamber. Triflic acid (0.4 mmol, 35 µL) and CH_2Cl_2 (10 mL) were added to the cathodic chamber. Electrolysis was performed at −20 °C under constant current conditions until 1.2 F/mol of total charge had been consumed. Then, the reaction temperature was elevated to 0 °C, and this temperature was kept for 1 h. The reaction was quenched with Et_3N (0.5 mL), and the reaction mixture was dissolved in EtOAc and washed with water to remove electrolyte. It was further washed with aqueous 1 M HCl solution and dried over Na_2SO_4. Then, the solvent was removed under reduced pressure, and the crude product (220 mg) was purified with recycling preparative gel permeation chromatography equipped with two series-connected JAIGEL-2HH columns (eluent: $CHCl_3$, flow rate: 7.5 mL/min, recycle numbers: 3) to obtain pure cyclic oligosaccharide **16** (0.125 mmol, 79.7 mg, 62%).

Supporting Information

Supporting Information File 1

Synthetic details, DFT calculations, and compound characterization data.
[https://www.beilstein-journals.org/bjoc/content/supplementary/1860-5397-20-124-S1.pdf]

Acknowledgements

We thank Koganei Corporation (Tokyo, Japan) for donation of compound **6a**. The contents of this paper have been published by Md Azadur Rahman as a Ph.D. thesis at Tottori University in 2023.

Funding

The authors acknowledge financial support by the Grant-in-Aid for Scientific Research (JP23H01961 and JP22KK0078).

Author Contributions

Md Azadur Rahman: data curation; investigation; writing – original draft; writing – review & editing. Hirofumi Endo: formal analysis; investigation; writing – review & editing. Takashi Yamamoto: formal analysis; investigation; writing – review & editing. Shoma Okushiba: formal analysis; investigation; writing – review & editing. Norihiko Sasaki: methodology; project administration; supervision; validation; writing – review & editing. Toshiki Nokami: conceptualization; project administration; supervision; writing – original draft; writing – review & editing.

ORCID® iDs

Toshiki Nokami - https://orcid.org/0000-0001-5447-4533

Data Availability Statement

All data that supports the findings of this study is available in the published article and/or the supporting information to this article.

Preprint

A non-peer-reviewed version of this article has been previously published as a preprint: https://doi.org/10.3762/bxiv.2024.23.v1

References

1. Diaz, A. F.; Kanazawa, K. K.; Gardini, G. P. *J. Chem. Soc., Chem. Commun.* **1979,** 635–636. doi:10.1039/c39790000635
2. Tanaka, K.; Shichiri, T.; Wang, S.; Yamabe, T. *Synth. Met.* **1988,** *24,* 203–215. doi:10.1016/0379-6779(88)90258-5
3. Osaka, T.; Ogano, S.; Naoi, K.; Oyama, N. *J. Electrochem. Soc.* **1989,** *136,* 306–309. doi:10.1149/1.2096626
4. Heinze, J.; Frontana-Uribe, B. A.; Ludwigs, S. *Chem. Rev.* **2010,** *110,* 4724–4771. doi:10.1021/cr900226k
5. Hsiao, S.-H.; Lin, S.-W. *Polym. Chem.* **2016,** *7,* 198–211. doi:10.1039/c5py01407g
6. Gattuso, G.; Nepogodiev, S. A.; Stoddart, J. F. *Chem. Rev.* **1998,** *98,* 1919–1958. doi:10.1021/cr960133w
7. Maiti, K.; Jayaraman, N. *J. Org. Chem.* **2016,** *81,* 4616–4622. doi:10.1021/acs.joc.6b00462
8. Ikuta, D.; Hirata, Y.; Wakamori, S.; Shimada, H.; Tomabechi, Y.; Kawasaki, Y.; Ikeuchi, K.; Hagimori, T.; Matsumoto, S.; Yamada, H. *Science* **2019,** *364,* 674–677. doi:10.1126/science.aaw3053
9. Li, X.; Di Carluccio, C.; Miao, H.; Zhang, L.; Shang, J.; Molinaro, A.; Xu, P.; Silipo, A.; Yu, B.; Yang, Y. *Angew. Chem., Int. Ed.* **2023,** e20237851. doi:10.1002/anie.202307851
10. Wu, Y.; Aslani, S.; Han, H.; Tang, C.; Wu, G.; Li, X.; Wu, H.; Stern, C. L.; Guo, Q.-H.; Qiu, Y.; Chen, A. X.-Y.; Jiao, Y.; Zhang, R.; David, A. H. G.; Armstrong, D. W.; Stoddart, J. F. *Nat. Synth.* **2024,** *3,* 698–706. doi:10.1038/s44160-024-00495-8
11. Manmode, S.; Matsumoto, K.; Nokami, T.; Itoh, T. *Asian J. Org. Chem.* **2018,** *7,* 1719–1729. doi:10.1002/ajoc.201800302
12. Shibuya, A.; Nokami, T. *Chem. Rec.* **2021,** *21,* 2389–2396. doi:10.1002/tcr.202100085
13. Rahman, M. A.; Kuroda, K.; Endo, H.; Sasaki, N.; Hamada, T.; Sakai, H.; Nokami, T. *Beilstein J. Org. Chem.* **2022,** *18,* 1133–1139. doi:10.3762/bjoc.18.117
14. Manmode, S.; Tanabe, S.; Yamamoto, T.; Sasaki, N.; Nokami, T.; Itoh, T. *ChemistryOpen* **2019,** *8,* 869–872. doi:10.1002/open.201900185
15. Endo, H.; Ochi, M.; Rahman, M. A.; Hamada, T.; Kawano, T.; Nokami, T. *Chem. Commun.* **2022,** *58,* 7948–7951. doi:10.1039/d2cc02287g
16. Nokami, T.; Hayashi, R.; Saigusa, Y.; Shimizu, A.; Liu, C.-Y.; Mong, K.-K. T.; Yoshida, J.-i. *Org. Lett.* **2013,** *15,* 4520–4523. doi:10.1021/ol402034g
17. Manabe, S.; Ito, Y. *Pure Appl. Chem.* **2017,** *89,* 899–909. doi:10.1515/pac-2016-0917
18. Benakli, K.; Zha, C.; Kerns, R. J. *J. Am. Chem. Soc.* **2001,** *123,* 9461–9462. doi:10.1021/ja0162109
19. Nokami, T.; Shibuya, A.; Saigusa, Y.; Manabe, S.; Ito, Y.; Yoshida, J.-i. *Beilstein J. Org. Chem.* **2012,** *8,* 456–460. doi:10.3762/bjoc.8.52
20. Paulsen, H.; Kolář, Č.; Stenzel, W. *Chem. Ber.* **1978,** *111,* 2358–2369. doi:10.1002/cber.19781110630
21. Lemieux, R. U.; Ratcliffe, R. M. *Can. J. Chem.* **1979,** *57,* 1244–1251. doi:10.1139/v79-203
22. Nokami, T.; Shibuya, A.; Manabe, S.; Ito, Y.; Yoshida, J.-i. *Chem. – Eur. J.* **2009,** *15,* 2252–2255. doi:10.1002/chem.200802293

License and Terms

BEILSTEIN JOURNAL OF ORGANIC CHEMISTRY

Electrophotochemical metal-catalyzed synthesis of alkylnitriles from simple aliphatic carboxylic acids

Yukang Wang[1,2], Yan Yao[1,2] and Niankai Fu[*1,2]

Full Research Paper

Open Access

Address:
[1]Beijing National Laboratory for Molecular Sciences, CAS Key Laboratory of Molecular Recognition and Function, Institute of Chemistry, Chinese Academy of Sciences, Beijing 100190, China and [2]University of Chinese Academy of Sciences, Beijing 100049, China

Email:
Niankai Fu[*] - funiankai@iccas.ac.cn

* Corresponding author

Keywords:
aliphatic carboxylic acids; alkylnitriles; electroorganic synthesis; electrophotocatalysis; radical decarboxylation

Beilstein J. Org. Chem. **2024,** *20,* 1497–1503.
https://doi.org/10.3762/bjoc.20.133

Received: 10 April 2024
Accepted: 20 June 2024
Published: 03 July 2024

This article is part of the thematic issue "Synthetic electrochemistry".

Guest Editor: K. Lam

Abstract

We report a practical and sustainable electrophotochemical metal-catalyzed protocol for decarboxylative cyanation of simple aliphatic carboxylic acids. This environmentally friendly method features easy availability of substrates, broad functional group compatibility, and directly converts a diverse range of aliphatic carboxylic acids including primary and tertiary alkyl acids into synthetically versatile alkylnitriles without using chemical oxidants or costly cyanating reagents under mild reaction conditions.

Introduction

Alkylnitriles and their derivatives are widely found in pharmaceuticals and biologically active compounds [1-3]. In addition, within the field of synthetic organic chemistry, nitriles are synthetically useful handles that can be readily converted into a myriad of functional groups including carbonyls, amines, imines, and a variety of heterocyclic scaffolds with well-established procedures [4-9]. In particular, tertiary nitriles are common structural motifs in many bioactive compounds and are widely used as intermediates in organic synthesis for the construction of all-carbon-substituted quaternary centers (Figure 1A). However, conventional methods for the synthesis of tertiary alkylnitriles such as direct functionalization of alkylnitriles [10] and hydrocyanation of alkenes [11-14] are typically hindered by harsh reaction conditions, which reduces functional group compatibility and product diversity. As such, the development of practical methods for the preparation of alkylnitriles from readily available starting materials are particularly valuable in synthetic and medicinal applications [15-18].

Owing to the prevalence of aliphatic carboxylic acids in biomass and natural products, decarboxylative cyanation represents one of the most straightforward and attractive approaches to accessing alkylnitriles [19,20]. As an elegant example, Barton demonstrated the application of redox-active esters, the so called "Barton esters", for decarboxylative cyanation of aliphatic acids with tosyl cyanide as the nitrile source under

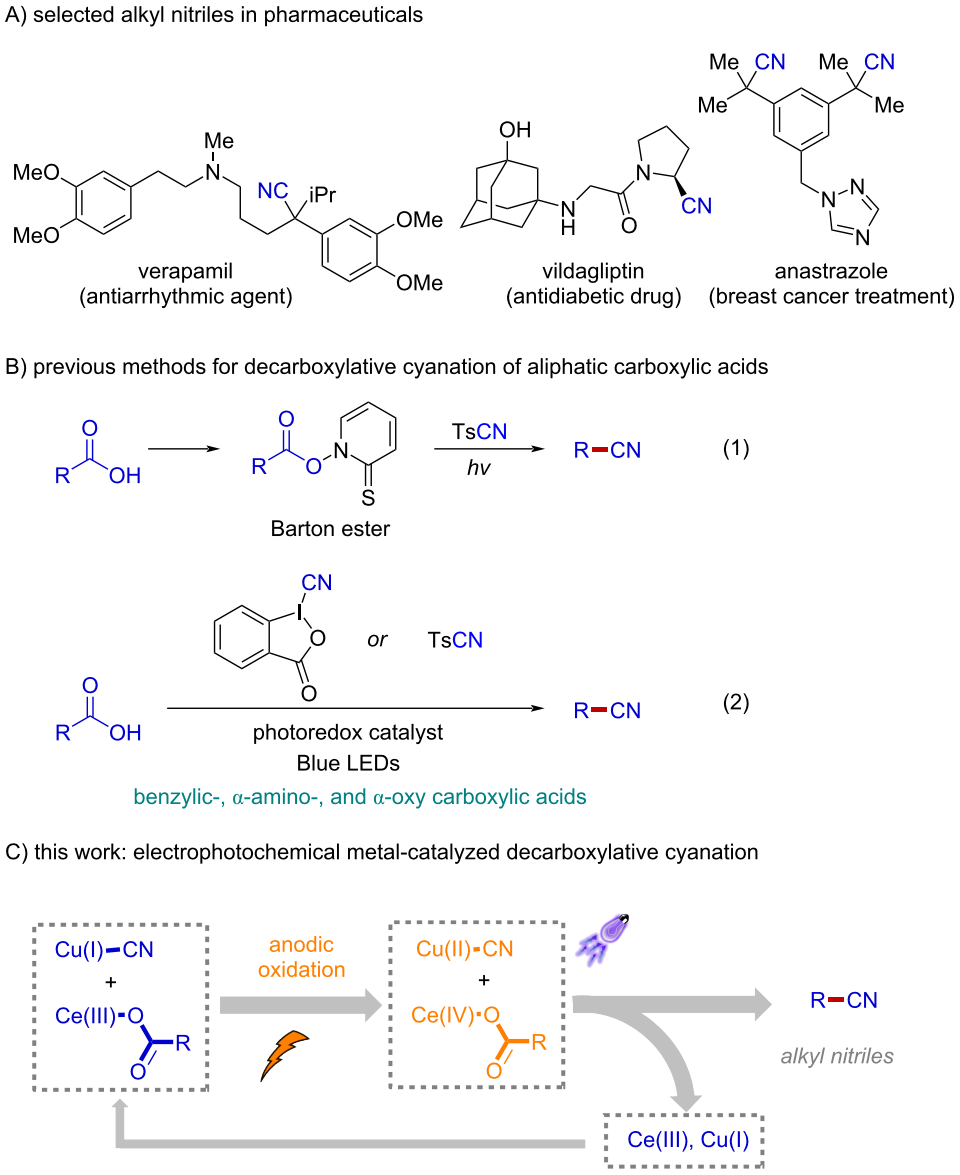

Figure 1: Decarboxylative cyanation: background and our working hypothesis.

visible light irradiation at room temperature [21,22]. Although two synthetic steps are required, this is the first practical decarboxylative cyanation protocol because different types of aliphatic acids including primary ones could be successfully employed (Figure 1B, reaction 1). The groups of Waser [23] and Gonzalez-Gomez [24] reported the direct conversion of aliphatic acids to the corresponding alkylnitriles by merging photoredox catalysis and radical cyanation processes using cyanobenziodoxolones and tosyl cyanide as the cyanating reagents, respectively (Figure 1B, reaction 2). Recently, the Rueping group demonstrated a distinctive use of 4-cyanopyridine as nitrile source for electrochemical decarboxylative cyanation of amino acids [25]. Although these methods have provided innovative strategies, substrates in all of these reaction systems are generally limited to benzylic, α-amino-, and α-oxy aliphatic acids, presumably due to the necessity of stabilized radical intermediates for the following radical cyanation step.

We and others have recently demonstrated electrophotochemical transition metal catalysis [26-31] as a unique and powerful synthetic platform for radical decarboxylative functionalization of aliphatic carboxylic acids [32-37]. In particular, the commonly required high activation energy for radical decarboxylation was provided by anodic oxidation and visible light irradiation of the Ce species in a sequential fashion [38-45]. Therefore, the

anodic electrode potential for this process could be substantially reduced. In doing so, a low working potential at the anode offers the opportunity for invention of cooperative catalysis with electrochemical transition metal catalysis, which generally has mild oxidation potential for the generation of persistent radicals in the form of nucleophile-bound metal complexes. We and other groups have successfully applied this reaction design to enantioselective decarboxylative cyanation of arylacetic acids [35-37]. Considering the widespread availability of aliphatic carboxylic acids and the significant synthetic and medicinal importance of alkylnitriles, we envisioned that the electrophotochemical Ce-catalyzed radical decarboxylation of alkyl carboxylic acids in combination with electrochemical copper catalysis might allow rapid access to alkylnitriles in a generic fashion (Figure 1C). Herein, we disclose the successful implementation of this strategy and present a mild, practical, and broadly applicable electrophotochemical metal-catalyzed protocol for the direct conversion of simple aliphatic carboxylic acids into alkylnitriles. Notably, this new decarboxylative cyanation protocol exhibited extraordinary insensitivity to substitution pattern of alkyl acids, affording the corresponding alkylnitriles including primary and tertiary alkylnitriles with good reaction efficiency.

Results and Discussion

Our study of this new electrophotochemical metal-catalyzed decarboxylative cyanation commenced with the evaluation of various combinations of Ce and Cu catalysts. A simple undivided cell using a carbon felt, inexpensive and practical porous material as the anode, and a Pt plate as the cathode, was electrolyzed with a cell potential of 2.3 V (corresponding to an initial anodic potential of 0.10 V versus the ferrocenium ion/ferrocene redox couple) under the irradiation of 400 nm light-emitting diodes (LEDs). Through systematic optimization, we found that the use of readily available $CeCl_3$ (10 mol %) and $Cu(OTf)_2$ (5.0 mol %) together with bidentate nitrogen ligands such as BPhen, Phen, dtbbpy, and bpy with TMSCN as the cyanating reagent promoted the direct conversion of flurbiprofen (**1**) to the desired product (**2**) in good yields (Table 1, entries 1 and 2).

Cu ions are well-known to be highly susceptible to electroplating on the cathode and thus require the use of ligands to avoid detrimental cathode deposition during electrolysis (Table 1, entry 3). In addition, we discovered that the additional use of DMF as co-solvent is beneficial to the reaction efficiency–reactions using acetonitrile as the solvent frequently led to the observation of Cu deposition at cathode (Table 1, entry 4). We reasoned that DMF could coordinate to the copper center, acting as a ligand to prevent copper from cathode reduction. Constant current electrolysis is also applicable to the reaction, the corresponding alkylnitrile product was obtained in 86% yield after electrolysis at 3.0 mA for 4 hours, demonstrating the high Faradaic efficiency of the reaction (Table 1,

Table 1: Reaction discovery and optimization.[a]

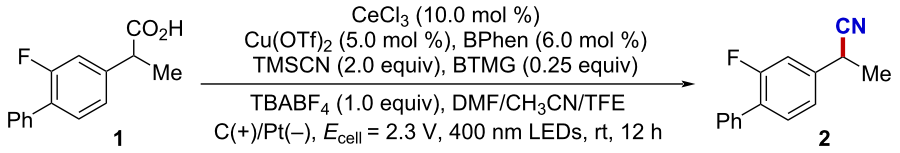

Entry	Variations	Yield (%)
1	**none**	**88 (86)**[b]
2	Phen, dtbbpy or bpy instead of BPhen	61–85
3	no BPhen	26
4	CH_3CN as solvent	64[c]
5	3 mA for 4 h	86
6	no Ce catalyst	16
7	no Cu/BPhen catalyst	<5
8	no light	0
9	no electricity	0
10	$[Mes\text{-}Acr]ClO_4$ instead of Ce	34

[a]Performed with **1** (0.2 mmol, 1.0 equiv) in DMF/CH_3CN (1:7, 4.0 mL), TFE (2.5 equiv), carbon felt anode, Pt cathode, undivided cell, 400 nm LEDs. Yields determined by ^1H NMR using 1,1,2,2-tetrachloroethane as the internal standard. [b]Isolated yield. [c]Due to the solubility issue of $CeCl_3$ in CH_3CN, $Ce(OTf)_3$ was used instead, see Supporting Information File 1 for more details. BTMG, 2-*tert*-butyl-1,1,3,3-tetramethylguanidine. BPhen, bathophenanthroline. Phen, 1,10-phenanthroline, TFE, 2,2,2-trifluoroethanol.

entry 5) [46]. Control experiments revealed that Ce catalyst, Cu catalyst, light, and electricity were all essential for the success of this transformation (Table 1, entries 6–9). We also tested other photoredox catalysts that are capable of driving the oxidative decarboxylation, only Fukuzumi catalyst [47] was able to deliver the product with a meaningful yield (Table 1, entry 10).

The scope of this transformation was next investigated (Figure 2). Arylacetic acids with relatively stable benzylic radicals as the corresponding intermediates have been proved to be suitable substrates to the reaction, providing the desired decarboxylative cyanation products with generally good yields (**2**–**18**). To show the synthetic potential of this method, we con-

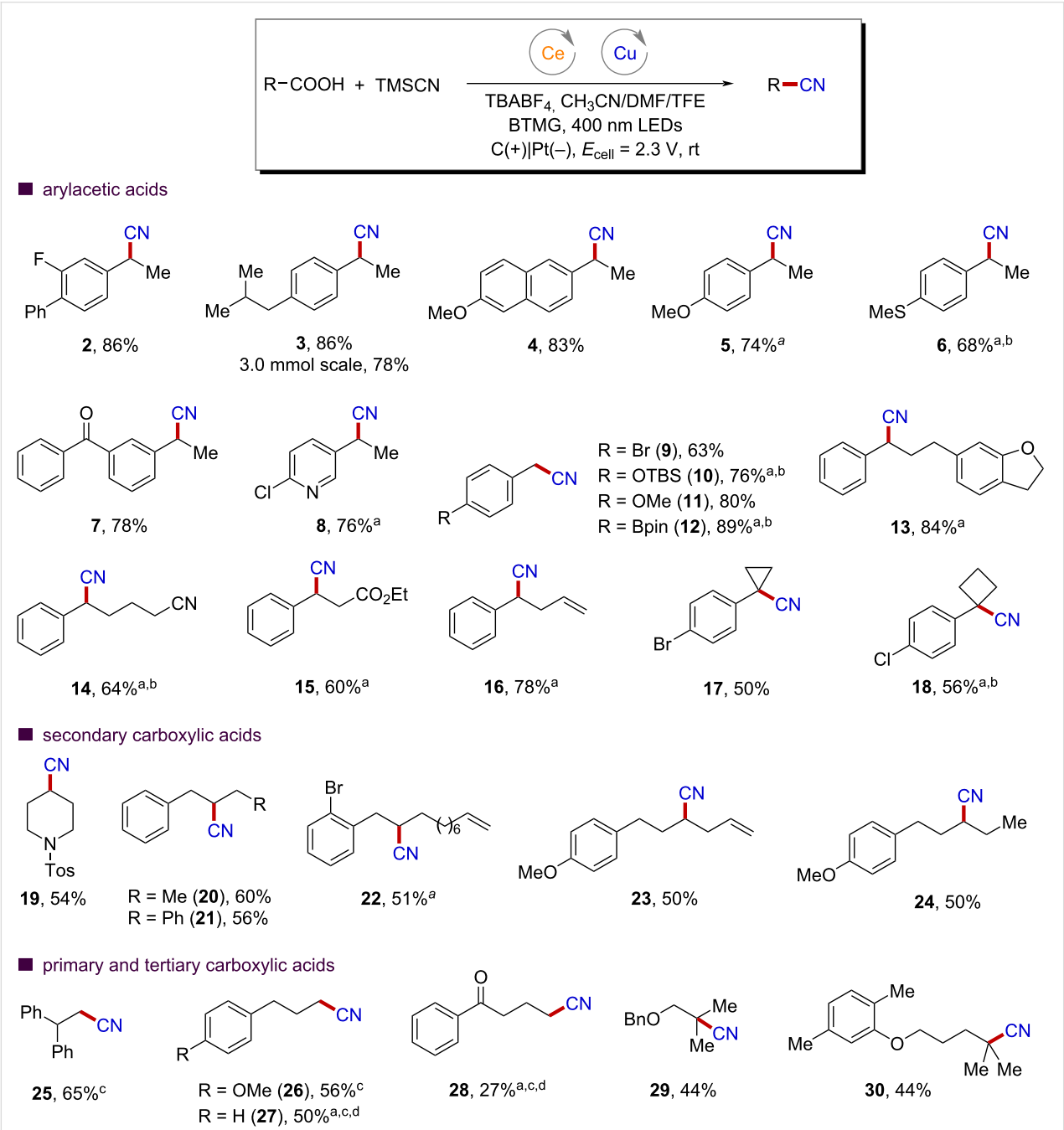

Figure 2: Scope of electrophotochemical decarboxylative cyanation of aliphatic carboxylic acids. All yields are of isolated products. Unless otherwise noted, reaction conditions were as follows: 0.2 mmol acids, 0.4 mmol TMSCN, $CeCl_3$ (10 mol %), $Cu(OTf)_2$/BPhen (5/6 mol %), 0.05 mmol BTMG, 0.2 mmol $TBABF_4$, 0.5 mmol TFE, 3.5 mL of CH_3CN, 0.5 mL of DMF, carbon felt as the anode, Pt as the cathode, under N_2, in an undivided cell, at 2.3 V cell potential, 400 nm LEDs, for 12 hours. [a]2,4,6-Collidine (1.0 equiv) was used instead of BTMG. [b]Phen was used instead of BPhen. [c]DMF/CH_3CN (1:15 v/v) was used as solvent. [d]Reactions were run with 0.4 mmol $LiClO_4$ instead of $TBABF_4$.

ducted the reaction with ibuprofen on a 3.0 mmol scale and obtained product **3** in 78% isolated yield. More importantly, the extremely mild reaction conditions imparted by the combination of electrochemistry and photochemistry made accessible a broad range of products with functionalities that are susceptible to oxidative degradation under traditional chemical conditions. For example, electron-rich arenes (**4**–**6**) can be smoothly obtained in synthetically useful yields. Electron-withdrawing groups at the phenyl ring are also compatible to give the products with good yields (**7**). Furthermore, the incorporation of pyridyl groups that are commonly found in pharmaceutically active compounds are also possible (**8**). In general, the catalytic efficiency of this new electrophotochemical protocol was found to be relatively independent of the electronic properties of the aryl substituents and the size of the alkyl side chain at the alpha position of arylacetic acids (**9**–**16**). These features offer great opportunities for the introduction of a wide range of functional groups, including bromide (**9**), boron (**12**), ether (**13**), nitrile (**14**), ester (**15**), and alkene (**16**) moieties, which are versatile functional handles for further elaboration. Notably, tertiary arylacetic acids can also be well tolerated to yield nitriles with quaternary carbon centers in good yields (**17** and **18**).

Simple carboxylic acids without functional groups at the alpha position to stabilize the corresponding carbon centered radicals are more challenging substrates. To our delight, both cyclic and acyclic secondary carboxylic acids performed well in our catalytic system, albeit with slightly reduced reaction efficiency (**19**–**24**). We also attempted simple primary carboxylic acids and got promising results. As outlined at the bottom of Figure 2, primary carboxylic acids can deliver the desired products with good yields in some cases (**25**–**27**). However, a large amount of hydrodecarboxylative products were observed, especially in the case of **28**. To our delight, tertiary carboxylic acids generally serve as better substrates (**29** and **30**). In these cases, a carbocation-involved pathway may be operative to yield the product. The successful and exclusive observation of product **29**, however, provided a piece of evidence to the objection of this possibility, as no carbocation-based rearrangement product was observed in our reaction system [48].

To probe the radical intermediate in the reaction, a radical rearrangement experiment with cyclopropane-derived acid **31** was subjected to the standard conditions, leading to the expected ring opening, alkene-containing nitrile product **32** in 62% isolated yield (Figure 3A). Moreover, experiments using stoichiometric Cu(II) and Ce(IV) indicated that the radical decarboxylative cyanation reaction can only occur under light irradiation. In contrast, reaction with Ce(III) exhibited nearly no reactivity, demonstrating the crucial roles of anodic oxidation and light irradiation to the transformation (Figure 3B).

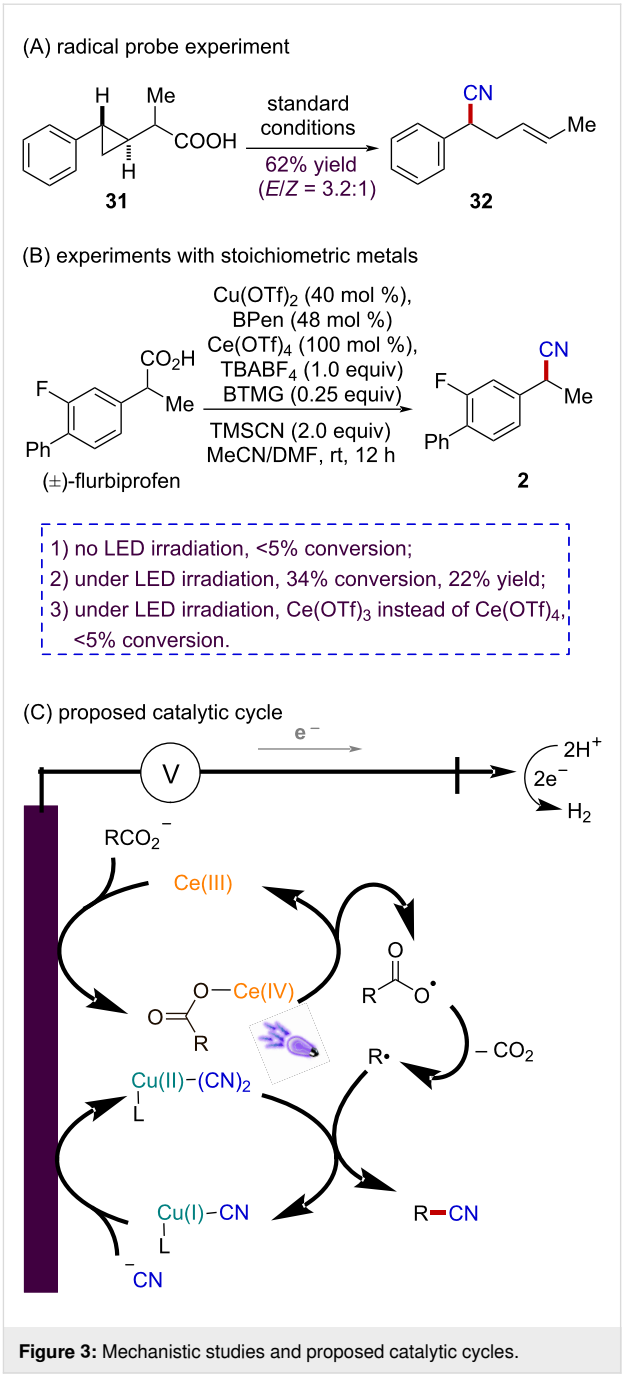

Figure 3: Mechanistic studies and proposed catalytic cycles.

Collectively, our experimental observations are in agreement with the proposed mechanistic picture detailed in Figure 3C. The anodically generated Ce(IV) carboxylates are able to undergo homolytic cleavage of the Ce–O bond upon light irradiation. The resulting carboxyl radical would then extrude CO_2 to generate the alkyl radical. Concurrently, Cu(II)–CN species are produced in the presence of cyanide anion through anodic oxidation. At this stage, Cu(II)–CN species are believed to capture alkyl radicals and the product would be readily generated via reductive elimination from the Cu(III) center [49-51].

Conclusion

In summary, we have developed an efficient and practical protocol for the synthesis of alkylnitriles directly from readily available aliphatic carboxylic acids. The reaction proceeds under mild conditions and exhibits exceptional substrate generality and functional group compatibility and is applicable to alkyl acids with all substitution pattern. Due to the wide utility of alkylnitriles, we expect this method to be widely adopted within the synthetic and medicinal chemistry communities. The present work also demonstrated electrophotochemical transition metal catalysis as a viable and potentially general approach for reaction discovery and would find broad application in new synthetic contexts.

Supporting Information

Supporting Information File 1

Experimental procedures, mechanistic studies, analytical data and copies of NMR spectra.
[https://www.beilstein-journals.org/bjoc/content/supplementary/1860-5397-20-133-S1.pdf]

Funding

We thank the National Natural Science Foundation of China (No. 22071252) and the Chinese Academy of Sciences for financial support.

Author Contributions

Yukang Wang: investigation; methodology. Yan Yao: investigation. Niankai Fu: conceptualization; funding acquisition; project administration; supervision; writing – review & editing.

ORCID® iDs

Niankai Fu - https://orcid.org/0000-0002-7453-3569

Data Availability Statement

All data that supports the findings of this study is available in the published article and/or the supporting information to this article.

References

1. Fleming, F. F. *Nat. Prod. Rep.* **1999,** *16,* 597–606. doi:10.1039/a804370a
2. Fleming, F. F.; Yao, L.; Ravikumar, P. C.; Funk, L.; Shook, B. C. *J. Med. Chem.* **2010,** *53,* 7902–7917. doi:10.1021/jm100762r
3. Wang, J.; Liu, H. *Chin. J. Org. Chem.* **2012,** *32,* 1643–1652. doi:10.6023/cjoc1202132
4. Fry, J. L.; Ott, R. A. *J. Org. Chem.* **1981,** *46,* 602–607. doi:10.1021/jo00316a023
5. Kornblum, N.; Singaram, S. *J. Org. Chem.* **1979,** *44,* 4727–4729. doi:10.1021/jo00393a063
6. Moorthy, J. N.; Singhal, N. *J. Org. Chem.* **2005,** *70,* 1926–1929. doi:10.1021/jo048240a
7. Haddenham, D.; Pasumansky, L.; DeSoto, J.; Eagon, S.; Singaram, B. *J. Org. Chem.* **2009,** *74,* 1964–1970. doi:10.1021/jo8023329
8. Himo, F.; Demko, Z. P.; Noodleman, L.; Sharpless, K. B. *J. Am. Chem. Soc.* **2002,** *124,* 12210–12216. doi:10.1021/ja0206644
9. Wen, Q.; Lu, P.; Wang, Y. *RSC Adv.* **2014,** *4,* 47806–47826. doi:10.1039/c4ra08675a
10. Christensen, S. B.; Guider, A.; Forster, C. J.; Gleason, J. G.; Bender, P. E.; Karpinski, J. M.; DeWolf, W. E., Jr.; Barnette, M. S.; Underwood, D. C.; Griswold, D. E.; Cieslinski, L. B.; Burman, M.; Bochnowicz, S.; Osborn, R. R.; Manning, C. D.; Grous, M.; Hillegas, L. M.; Bartus, J. O.; Ryan, M. D.; Eggleston, D. S.; Haltiwanger, R. C.; Torphy, T. J. *J. Med. Chem.* **1998,** *41,* 821–835. doi:10.1021/jm970090r
11. Yanagisawa, A.; Nezu, T.; Mohri, S.-i. *Org. Lett.* **2009,** *11,* 5286–5289. doi:10.1021/ol902244e
12. Bini, L.; Müller, C.; Vogt, D. *Chem. Commun.* **2010,** *46,* 8325–8334. doi:10.1039/c0cc01452d
13. Long, J.; Xia, S.; Wang, T.; Cheng, G.-J.; Fang, X. *ACS Catal.* **2021,** *11,* 13880–13890. doi:10.1021/acscatal.1c03729
14. Ding, Y.; Long, J.; Fang, X. *Org. Chem. Front.* **2021,** *8,* 5852–5857. doi:10.1039/d1qo01099a
15. Ellis, G. P.; Romney-Alexander, T. M. *Chem. Rev.* **1987,** *87,* 779–794. doi:10.1021/cr00080a006
16. Wang, T.; Jiao, N. *Acc. Chem. Res.* **2014,** *47,* 1137–1145. doi:10.1021/ar400259e
17. Patel, R. I.; Sharma, S.; Sharma, A. *Org. Chem. Front.* **2021,** *8,* 3166–3200. doi:10.1039/d1qo00162k
18. Wang, F.; Chen, P.; Liu, G. *Nat. Synth.* **2022,** *1,* 107–116. doi:10.1038/s44160-021-00016-x
19. Schwarz, J.; König, B. *Green Chem.* **2018,** *20,* 323–361. doi:10.1039/c7gc02949g
20. Li, L.; Yao, Y.; Fu, N. *Eur. J. Org. Chem.* **2023,** *26,* e202300166. doi:10.1002/ejoc.202300166
21. Barton, D. H. R.; Jaszberenyi, J. C.; Theodorakis, E. A. *Tetrahedron Lett.* **1991,** *32,* 3321–3324. doi:10.1016/s0040-4039(00)92696-0
22. Barton, D. H. R.; Jaszberenyi, J. C.; Theodorakis, E. A. *Tetrahedron* **1992,** *48,* 2613–2626. doi:10.1016/s0040-4020(01)88524-0
23. Le Vaillant, F.; Wodrich, M. D.; Waser, J. *Chem. Sci.* **2017,** *8,* 1790–1800. doi:10.1039/c6sc04907a
24. Ramirez, N. P.; König, B.; Gonzalez-Gomez, J. C. *Org. Lett.* **2019,** *21,* 1368–1373. doi:10.1021/acs.orglett.9b00064
25. Kumar, G. S.; Shinde, P. S.; Chen, H.; Muralirajan, K.; Kancherla, R.; Rueping, M. *Org. Lett.* **2022,** *24,* 6357–6363. doi:10.1021/acs.orglett.2c01897
26. Huang, H.; Steiniger, K. A.; Lambert, T. H. *J. Am. Chem. Soc.* **2022,** *144,* 12567–12583. doi:10.1021/jacs.2c01914
27. Barham, J. P.; König, B. *Angew. Chem., Int. Ed.* **2020,** *59,* 11732–11747. doi:10.1002/anie.201913767
28. Wu, S.; Kaur, J.; Karl, T. A.; Tian, X.; Barham, J. P. *Angew. Chem., Int. Ed.* **2022,** *61,* e202107811. doi:10.1002/anie.202107811
29. Liu, J.; Lu, L.; Wood, D.; Lin, S. *ACS Cent. Sci.* **2020,** *6,* 1317–1340. doi:10.1021/acscentsci.0c00549
30. Yu, Y.; Guo, P.; Zhong, J.-S.; Yuan, Y.; Ye, K.-Y. *Org. Chem. Front.* **2020,** *7,* 131–135. doi:10.1039/c9qo01193e
31. Li, L.; Yao, Y.; Fu, N. *Chem Catal.* **2024,** *4,* 100898. doi:10.1016/j.checat.2023.100898

32. Wang, Y.; Li, L.; Fu, N. *ACS Catal.* **2022,** *12,* 10661–10667. doi:10.1021/acscatal.2c02934
33. Yang, K.; Lu, J.; Li, L.; Luo, S.; Fu, N. *Chem. – Eur. J.* **2022,** *28,* e202202370. doi:10.1002/chem.202202370
34. Lu, J.; Yao, Y.; Li, L.; Fu, N. *J. Am. Chem. Soc.* **2023,** *145,* 26774–26782. doi:10.1021/jacs.3c08839
35. Yang, K.; Wang, Y.; Luo, S.; Fu, N. *Chem. – Eur. J.* **2023,** *29,* e202203962. doi:10.1002/chem.202203962
36. Lai, X.-L.; Chen, M.; Wang, Y.; Song, J.; Xu, H.-C. *J. Am. Chem. Soc.* **2022,** *144,* 20201–20206. doi:10.1021/jacs.2c09050
37. Yuan, Y.; Yang, J.; Zhang, J. *Chem. Sci.* **2023,** *14,* 705–710. doi:10.1039/d2sc05428k
38. Lai, X.-L.; Shu, X.-M.; Song, J.; Xu, H.-C. *Angew. Chem., Int. Ed.* **2020,** *59,* 10626–10632. doi:10.1002/anie.202002900
39. Tan, Z.; He, X.; Xu, K.; Zeng, C. *ChemSusChem* **2022,** *15,* e202102360. doi:10.1002/cssc.202102360
40. Yang, Z.; Yang, D.; Zhang, J.; Tan, C.; Li, J.; Wang, S.; Zhang, H.; Huang, Z.; Lei, A. *J. Am. Chem. Soc.* **2022,** *144,* 13895–13902. doi:10.1021/jacs.2c05520
41. Tsurugi, H.; Mashima, K. *J. Am. Chem. Soc.* **2021,** *143,* 7879–7890. doi:10.1021/jacs.1c02889
42. Sheldon, R. A.; Kochi, J. K. *J. Am. Chem. Soc.* **1968,** *90,* 6688–6698. doi:10.1021/ja01026a022
43. Yatham, V. R.; Bellotti, P.; König, B. *Chem. Commun.* **2019,** *55,* 3489–3492. doi:10.1039/c9cc00492k
44. Shirase, S.; Tamaki, S.; Shinohara, K.; Hirosawa, K.; Tsurugi, H.; Satoh, T.; Mashima, K. *J. Am. Chem. Soc.* **2020,** *142,* 5668–5675. doi:10.1021/jacs.9b12918
45. Hu, A.; Guo, J.-J.; Pan, H.; Zuo, Z. *Science* **2018,** *361,* 668–672. doi:10.1126/science.aat9750
46. Assuming that the overall reaction is a 2-electron oxidation process, the Faradaic efficiency was calculated to be 77%.
47. Fukuzumi, S.; Kotani, H.; Ohkubo, K.; Ogo, S.; Tkachenko, N. V.; Lemmetyinen, H. *J. Am. Chem. Soc.* **2004,** *126,* 1600–1601. doi:10.1021/ja038656q
48. Sheng, T.; Zhang, H.-J.; Shang, M.; He, C.; Vantourout, J. C.; Baran, P. S. *Org. Lett.* **2020,** *22,* 7594–7598. doi:10.1021/acs.orglett.0c02799
49. Zhang, W.; Wang, F.; McCann, S. D.; Wang, D.; Chen, P.; Stahl, S. S.; Liu, G. *Science* **2016,** *353,* 1014–1018. doi:10.1126/science.aaf7783
50. Wang, D.; Zhu, N.; Chen, P.; Lin, Z.; Liu, G. *J. Am. Chem. Soc.* **2017,** *139,* 15632–15635. doi:10.1021/jacs.7b09802
51. Wang, F.; Chen, P.; Liu, G. *Acc. Chem. Res.* **2018,** *51,* 2036–2046. doi:10.1021/acs.accounts.8b00265

License and Terms

BEILSTEIN JOURNAL OF ORGANIC CHEMISTRY

Electrocatalytic hydrogenation of cyanoarenes, nitroarenes, quinolines, and pyridines under mild conditions with a proton-exchange membrane reactor

Koichi Mitsudo[*1], Atsushi Osaki[1], Haruka Inoue[1], Eisuke Sato[1], Naoki Shida[2,3], Mahito Atobe[2] and Seiji Suga[*1]

Full Research Paper

Open Access

Address:
[1]Division of Applied Chemistry, Graduate School of Environmental, Life, Natural Science and Technology, Okayama University, 3-1-1 Tsushima-naka, Kita-ku, Okayama 700-8530, Japan, [2]Graduate School of Engineering Science and Advanced Chemical Energy Research Center, Yokohama National University, 79-5 Tokiwadai, Hodogaya-ku, Yokohama 240-8501, Japan and [3]PRESTO, Japan Science and Technology Agency (JST), 4-1-8 Honcho, Kawaguchi, Saitama 332-0012, Japan

Email:
Koichi Mitsudo[*] - mitsudo@okayama-u.ac.jp; Seiji Suga[*] - suga@cc.okayama-u.ac.jp

* Corresponding author

Keywords:
cyanoarene; nitroarene; PEM reactor; pyridine; quinoline

Beilstein J. Org. Chem. **2024,** *20,* 1560–1571.
https://doi.org/10.3762/bjoc.20.139

Received: 13 April 2024
Accepted: 25 June 2024
Published: 11 July 2024

This article is part of the thematic issue "Synthetic electrochemistry".

Guest Editor: K. Lam

Abstract

An electrocatalytic hydrogenation of cyanoarenes, nitroarenes, quinolines, and pyridines using a proton-exchange membrane (PEM) reactor was developed. Cyanoarenes were then reduced to the corresponding benzylamines at room temperature in the presence of ethyl phosphate. The reduction of nitroarenes proceeded at room temperature, and a variety of anilines were obtained. The quinoline reduction was efficiently promoted by adding a catalytic amount of *p*-toluenesulfonic acid (PTSA) or pyridinium *p*-toluenesulfonate (PPTS). Pyridine was also reduced to piperidine in the presence of PTSA.

Introduction

Nitrogen-containing molecules are important bioactive compounds and intermediates in chemical synthesis. Therefore, the chemical transformations of nitrogen-containing compounds have been widely studied in the field of organic synthesis [1-4]. For instance, the reduction of cyanoarenes is a straightforward and powerful method for the synthesis of primary amines [5], and the reduction of nitroarenes is useful for the synthesis of aniline derivatives [6-11]. Nitrogen-containing aliphatic heterocycles, such as piperidines and tetrahydroquinolines, are key motifs in pharmaceuticals, and the reductive syntheses of these heterocycles from pyridines and quinolines have been well studied [12]. Although these transformations have been studied

intensively, such reductive reactions usually require harsh reaction conditions such as high reaction temperatures and high pressure of hydrogen [13-18].

Meanwhile, electrochemical systems using solid polymer electrolytes (SPEs) have recently attracted significant attention [19]. Among these, proton-exchange membrane (PEM) reactors are powerful tools for hydrogenation [20-43]. The PEM reactor included a membrane electrode assembly (MEA) consisting of a PEM and an electro-catalyst supported on carbon (Figure 1). Humidified hydrogen gas (H_2) or H_2O was injected into the anodic chamber and the substrate passed through the cathodic chamber. The hydrogen (H_2) or H_2O were oxidized at the anode to form protons (H^+) that moved to the cathodic chamber, and the protons were reduced to monoatomic hydrogen species (absorbed hydrogen, H_{ad}). Thus-generated H_{ad} reduced the substrate passed through the cathodic chamber. MEA eliminates the need for a supporting electrolyte, which is necessary for conventional organic electrolysis, reduces the environmental impact, and facilitates product purification. In addition, using nanoparticles in the catalyst layer, which serve as the electrode, results in a large specific surface area and efficient reactions. As PEM reactors are flow reactors, they have an advantage over batch reactors in terms of continuous production.

Several reductive transformations taking advantage of the characteristics of the PEM reactor have been reported in recent years. For example, Atobe et al. reported the electrocatalytic semihydrogenation of alkynes to form *Z*-alkenes using a PEM reactor [31]. The Pd/C catalyst was essential for the reaction. They recently found that a PEM reactor with a Rh/C catalyst was effective for the stereoselective reduction of cyclic ketones [40]. Nagaki et al. reported the electrochemical deuteration of aryl halides [42]. PEM reactors are also gaining industrial attention. Weber et al. reported a series of large-scale syntheses using PEM reactors [43].

We studied electrochemical transformations [44-49] and recently reported the selective reduction of enones using a PEM reactor [50]. As mentioned above, there have been several reports on reductive reactions using PEM reactors; however, the application of PEM reactors for precise chemical transformations remains limited. To the best of our knowledge, no reports are available on the efficient reduction of cyanoarenes, quinolines, and pyridines using PEM reactors [51,52].

In this context, we have focused on the synthesis of nitrogen-containing molecules using a PEM reactor. Herein, we report the application of a PEM reactor for the reduction of cyanoarenes, nitroarenes, quinolines, and pyridines. These reductions proceeded smoothly to afford benzylamines, anilines, tetrahydroquinolines, and piperidines using a PEM reactor under ambient conditions.

Results and Discussion

Reduction of cyanoarenes to benzylamines

Benzonitrile (**1a**) was chosen as the model substrate, and the electroreductive hydrogenation of **1a** was performed with a PEM reactor (Table 1). Humidified hydrogen was used as a proton source, and 4.0 F mol^{-1} of electricity was passed to a circulated solution of **1a** (for the details, see the Supporting Information File 1). When Pd/C was used as the cathode catalyst, benzylamine (**2a**) was not obtained (Table 1, entry 1). Ru/C, Pt/C, and an alloy catalyst PtRu/C were also ineffective (Table 1, entries 2–4). Further screening revealed that trace amounts of **2a** were obtained when an alloy catalyst PtPd/C was used as the cathode catalyst (Table 1, entry 5). Although the

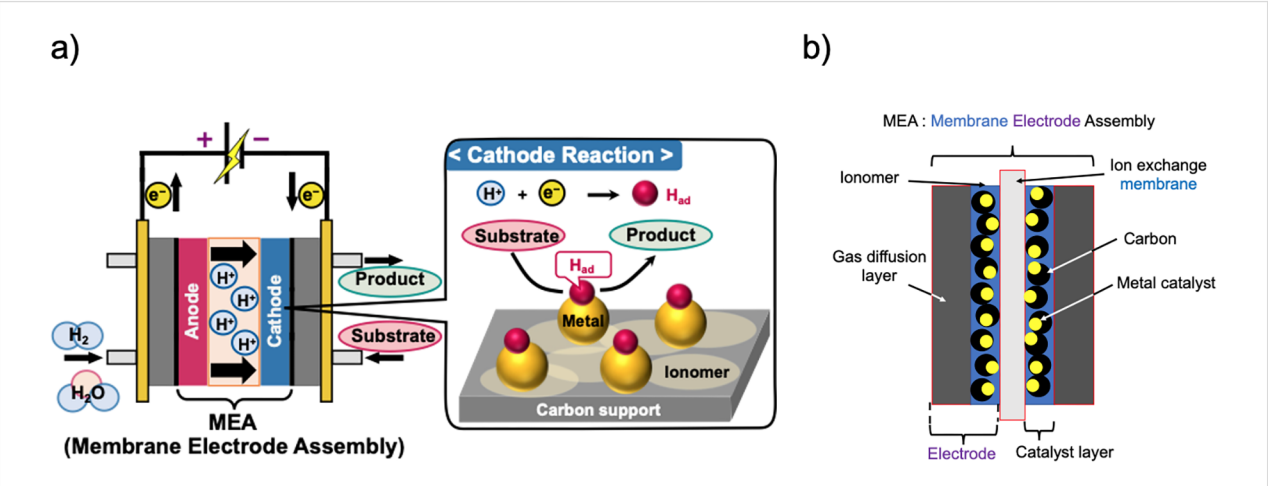

Figure 1: Schematic of (a) a PEM reactor and (b) MEA.

Table 1: Effect of cathode catalyst for the electrochemical reduction of **1a** using a PEM reactor[a].

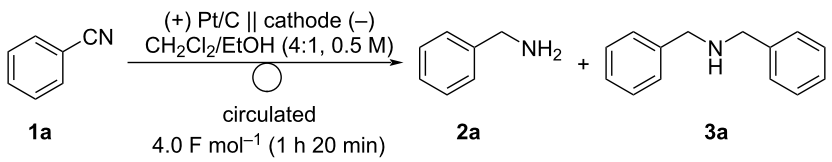

entry	cathode catalyst	**2a** (%)[b]	**3a** (%)[b]	recovered **1a** (%)[b]
1	Pd/C	N.D.[c]	N.D.	100
2	Ru/C	N.D.	N.D.	100
3	Pt/C	N.D.	N.D.	100
4	PtRu/C	N.D.	4	85
5	PtPd/C	4	18	78
6[d]	PtPd/C	11	7	79
7[e]	PtPd/C	13	19	65

[a]Reaction conditions: anode catalyst, Pt/C; **1a**, 2.5 mmol; solvent, CH_2Cl_2/EtOH (4:1, 0.5 M); flow rate of the solution of **1a**, 0.25 mL min^{-1}; flow rate of H_2 gas, 100 mL min^{-1}; reaction temperature, room temperature; current density, 50 mA cm^{-2}. The solution was circulated until the passage of 4.0 F mol^{-1} (1 h 20 min). [b]Area ratio determined by gas chromatography analysis. [c]Not detected. [d]Performed using HFIP instead of EtOH. [e]Performed using TFE instead of EtOH.

desired compound **2a** was obtained using PtPd/C, undesired dibenzylamine (**3a**), was obtained as a major product [53]. To suppress the generation of **3a**, we examined the effect of solvent (Table 1, entries 6 and 7). When the reaction was performed in a mixed solvent consisting of CH_2Cl_2 and 1,1,1,3,3,3-hexafluoropropan-2-ol (HFIP), the yield of **2a** increased; however, the generation of **3a** was not completely suppressed (Table 1, entry 6). The use of CH_2Cl_2/2,2,2-trifluoroethanol (TFE) gave similar results (Table 1, entry 7).

A plausible mechanism for the reduction of **1a** is shown in Scheme 1. First, the reduction of **1a** afforded phenylmethanimine (**A**). Further reduction of **A** afforded the desired benzylamine (**2a**). However, nucleophilic attack of **2a** on **A**, followed in situ by reduction, proceeded competitively to form dibenzylamine (**3a**). We considered that by protonating **2a** to form **2a-H$^+$**, its nucleophilic nature could be suppressed, thereby inhibiting the formation of **3a**.

Based on this hypothesis, we examined the reduction of **1a** in the presence of several acids (Table 2). First, electrochemical reduction was performed with 0.2 or 1.0 equiv of acetic acid, but the yield of **3a** did not decrease, suggesting that **2a** could not be trapped by acetic acid (pK_a = 4.75). To ensure the capture of **2a**, we performed reduction with phosphoric acid (pK_a = 2.12). Although the generation of **3a** was suppressed, only a trace amount of **2a** was obtained, and almost **1a** was recovered (Table 2, entry 4). This was probably because the presence of water inhibited the reaction. Therefore, it was necessary to perform the reaction under anhydrous conditions. Hence, we used ethyl phosphate (mono- and di-mixture) (pK_a = 1.42), which reacts easily under anhydrous conditions. As ex-

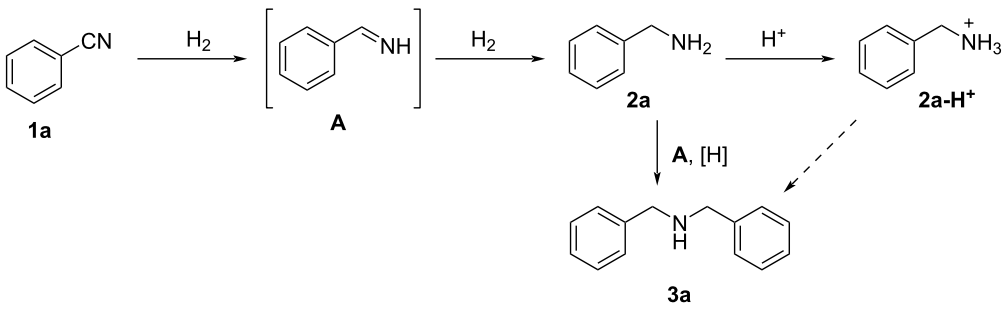

Scheme 1: Plausible mechanism for the reduction of **1a** leading to benzylamine **2a** and dibenzylamine **3a**.

Table 2: Electrochemical reduction of **1a** in the presence of acids[a].

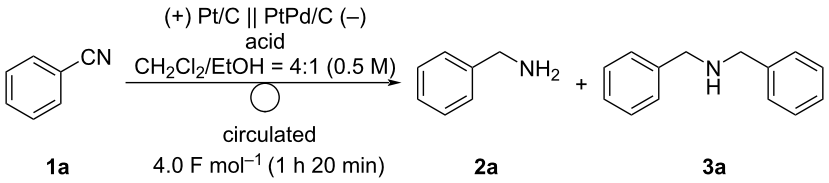

1a **2a** **3a**

entry	acid (equiv)	**2a** (%)[b]	**3a** (%)[b]	recovered **1a** (%)[b]
1	none	4	18	78
2	CH_3COOH (0.2)	2	15	82
3	CH_3COOH (1.0)	3	22	74
4	H_3PO_4 (1.0)	1	N.D.[c]	99
5	ethyl phosphate[d] (1.0)	18	trace	82
6[e]	ethyl phosphate[d] (1.0)	88[f]	trace[f]	7[f]

[a]Reaction conditions: anode catalyst, Pt/C; cathode catalyst, PtPd/C; **1a**, 2.5 mmol; solvent, CH_2Cl_2/EtOH (4:1, 0.5 M); flow rate of the solution of **1a**, 0.25 mL min^{-1}; flow rate of H_2 gas, 100 mL min^{-1}; reaction temperature, room temperature; current density, 50 mA cm^{-2}. The solution was circulated until the passage of 4.0 F mol^{-1} (1 h 20 min). [b]Area ratio determined by gas chromatography analysis. [c]Not detected. [d]Mono- and di- ester mixture. [e]16.0 F mol^{-1} (5 h 20 min). [f]GC yield determined by GC analysis using dodecane as an internal standard.

pected, the generation of **3a** was suppressed and **2a** was selectively obtained (Table 2, entry 5). With the increase of the electricity to 16.0 F mol^{-1}, **2a** was obtained selectively in 88% yield (Table 2, entry 6).

Next, we examined the scope of the electrochemical reduction of cyanoarenes under optimal conditions (Scheme 2). The reactions of cyanoarenes bearing electron-donating methyl, hydroxy, and methoxy groups proceeded smoothly to afford the corresponding benzylamines **2b–d** in moderate-to-good yields. Electron-withdrawing groups, such as esters, can be tolerated under these conditions. Unfortunately, the electrochemical reduction of 1,4-dicyanobenzene (**1f**) did not give the desired product **2f** probably due to the oligomerization of the substrate.

Reduction of nitroarenes to anilines

Next, we reduced nitroarenes using a PEM reactor. First, the electrocatalyst and solvent were optimized (Table 3). While 6.0 F mol^{-1} of electricity should be required for the reduction of

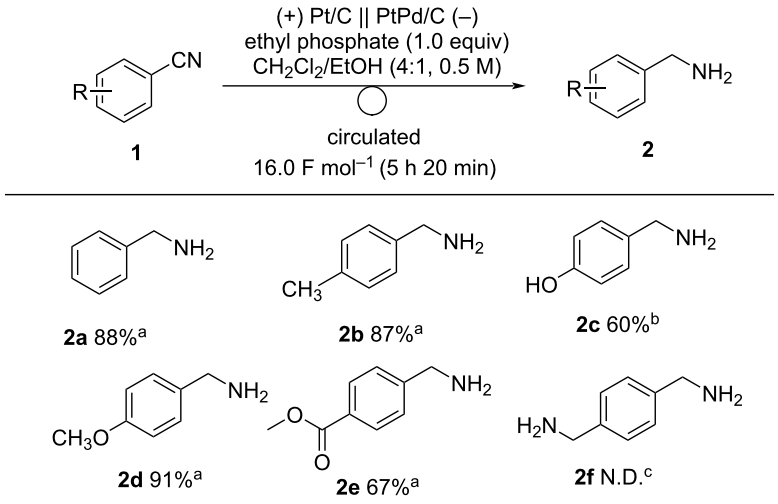

Scheme 2: Electrochemical reduction of cyanoarenes under optimal conditions. Reaction conditions: anode catalyst, Pt/C; cathode catalyst, PtPd/C; **1**, 2.5 mmol; solvent, CH_2Cl_2/EtOH (4:1); flow rate of the solution of **1**, 0.25 mL min^{-1}; flow rate of H_2 gas, 100 mL min^{-1}; reaction temperature, room temperature; current density, 50 mA cm^{-2}. The solution was circulated until the passage of 16.0 F mol^{-1} (5 h 20 min). [a]Determined by GC analysis using *n*-dodecane as an internal standard. [b]Determined by ^1H NMR analysis using 1,1,2,2-tetrachloroethane as an internal standard. [c]Not detected.

Table 3: Electrochemical reduction of **4a** with several cathode catalysts[a].

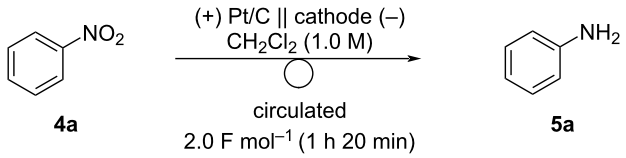

4a **5a**

entry	cathode catalyst	**5a** (%)[b]	current efficiency (%)[b]	recovered **4a** (%)[b]
1	Pd/C	N.D.[c]	–	–
2	Ru/C	25	79	65
3	Pt/C	30 (82)[d]	90 (20)[d]	76 (N.D.)[d]
4	Ir/C	6	18	70
5	Rh/C	29	90	59

[a]Reaction conditions: anode catalyst, Pt/C; **4a**, 5 mmol; solvent, CH_2Cl_2 (1.0 M); flow rate of the solution of **4a**, 0.25 mL min^{-1}; flow rate of H_2 gas, 100 mL min^{-1}; reaction temperature, room temperature; current density, 50 mA cm^{-2}. The solution was circulated until the passage of 2.0 F mol^{-1} (1 h 20 min). [b]Determined by GC using *n*-dodecane as an internal standard. [c]Not detected. [d]Performed until **4a** was consumed using 2.25 mmol of **4a** (7 h, 23.2 F mol^{-1}).

nitrobenzene (**4a**) to aniline (**5a**), the charge for screening was set to 2.0 F mol^{-1} for rapid evaluation, and several cathode catalysts were examined. When Pd/C was used as the cathode, the reaction did not proceed (Table 3, entry 1). The desired reduction proceeded with Ru/C and **5a** was obtained in 79% of current efficiency (Table 3, entry 2). Pt/C afforded the best result (90% current efficiency, Table 3, entry 3). To increase the yield, the reaction was carried out until **4a** was consumed. After 7 h of electrolysis (23.2 F mol^{-1}), **4a** was completely consumed and **5a** was obtained in 82% yield. Although Ir/C was inefficient (Table 3, entry 4), Rh/C was as efficient as Pt/C (Table 3, entry 5). As Rh is more expensive than Pt, Pt/C was selected as the best cathode catalyst.

Although **5a** was obtained in good yield with Pt/C, the current efficiency was low. We assumed that this was due to the recombination of H_{ad} to form hydrogen. To suppress hydrogen generation, we varied the flow rate of the reaction solution (Table 4). The reaction time was set to 2.5 h (2.25 mmol, 8.3 F mol^{-1}) and the flow rate of the reaction solution was changed from 0.25 to 1.0 mL min^{-1}. As expected, increasing the flow rate increased the current efficiency and yield of **5a**. With 0.75 mL min^{-1} of flow rate, **5a** was obtained in 88% yield with 62% of current efficiency (Table 4, entry 3). In contrast to the previous report on electrocatalytic hydrogenation of nitrobenzene using a PEM reactor [21], cyclohexylamine was not observed in each reaction.

Table 4: Effect of flow rate in the electrochemical reduction of **4a**[a].

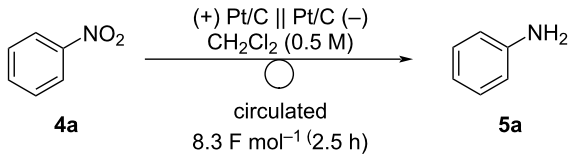

4a **5a**

entry	flow rate (mL min^{-1})	**5a** (%)[b]	current efficiency (%)[b]	recovered **4a** (%)[b]
1	0.25	75	53	14
2	0.50	78	56	7
3	0.75	88	62	3
4	1.0	88	63	2

[a]Reaction conditions: anode catalyst, Pt/C; cathode catalyst, Pt/C; **4a**, 2.25 mmol; solvent, CH_2Cl_2 (0.5 M); flow rate of the solution of **4a**, 0.25–1.0 mL min^{-1}; flow rate of H_2 gas, 100 mL min^{-1}; reaction temperature, room temperature; current density, 50 mA cm^{-2}. The solution was circulated for 2.5 h (8.3 F mol^{-1}). [b]Determined by GC analysis using *n*-dodecane as an internal standard.

Next, the scope of the nitroarene electro-reduction was explored (Scheme 3). To obtain products in high yields, the electrolysis was performed until the substrates were consumed. First, nitroarenes bearing electron-donating groups were investigated. Nitroarenes **4b**–**d** bearing methyl groups gave the corresponding anilines **5b–d** in 70–76% yield. *p*-Methoxyaniline (**5e**) was obtained in 83% yield. Nitroarenes bearing electron-withdrawing groups are also useful. Acetyl and cyano groups were tolerated under the reaction conditions and anilines **5f** and **5g** were obtained in 85% and 81% yields, respectively. 1-Naphthylamine, a more π-extended aniline was easily obtained in a high yield.

Reduction of quinolines to tetrahydroquinolines

The electrochemical reduction of quinolines was performed using a PEM reactor. First, several different cathode catalyst were examined for the reduction of quinoline (**6a**) (Table 5).

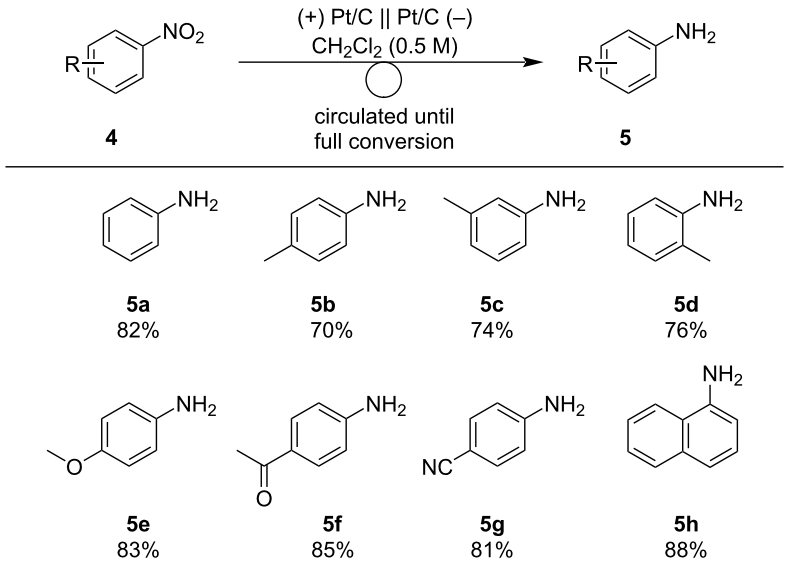

Scheme 3: Scope of the electrochemical reduction of nitroarenes. Reaction conditions: anode catalyst, Pt/C; cathode catalyst, Pt/C; **4**, 2.25 mmol; solvent, CH_2Cl_2 (0.5 M); flow rate of the solution of **4**, 0.75 mL min^{-1}; flow rate of H_2 gas, 100 mL min^{-1}; reaction temperature, room temperature; current density, 50 mA cm^{-2}. The solution was circulated until the full conversion of **4**. Isolated yield.

Table 5: Electrochemical reduction of **6a** with several cathode catalysts[a].

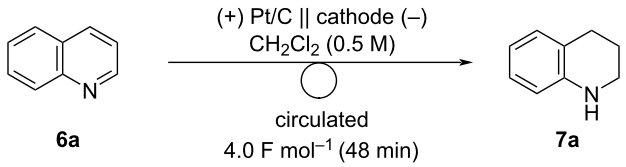

entry	cathode catalyst	**7a** (%)[b]	recovered **6a** (%)[b]
1	Pd/C	5	86
2	Ir/C	3	86
3	Ru/C	4	70
4	Pt/C	3	86
5[c]	Pt/C	96	N.D.[d]
6[e]	Pt/C	N.D.	N.D.

[a]Reaction conditions: anode catalyst, Pt/C; **6a**, 1.5 mmol; solvent, CH_2Cl_2 (0.5 M); flow rate of the solution of **6a**, 0.75 mL min^{-1}; flow rate of H_2 gas, 100 mL min^{-1}; reaction temperature, room temperature; current density, 50 mA cm^{-2}. The solution was circulated until the passage of 4.0 F mol^{-1} (48 min). [b]Determined by ^1H NMR spectroscopy using 1,1,2,2-tetrachloroethane as an internal standard. [c]50 F mol^{-1} (1st run). [d]Not detected. [e]50 F mol^{-1} (2nd run).

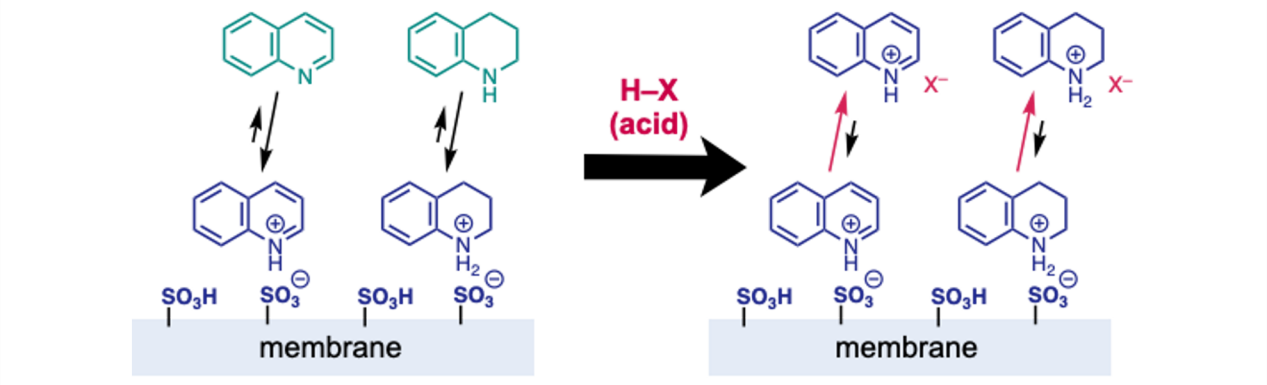

Figure 2: Hypothesis of the trap of quinoline on membrane and tetrahydroquinoline and the effect of adding an acid.

Because 4.0 F mol^{-1} of electricity should be required ideally to reduce quinoline (**6a**) to 1,2,3,4-tetrahydroquinoline (**7a**), 4.0 F mol^{-1} of electricity was applied for the reactions. Pd/C, Ir/C, Ru/C, and Pt/C were used as cathode catalysts, and 3–5% yields of **7a** were obtained by the use of each catalyst (Table 5, entries 1–4). We chose Pt/C, one of the most common catalysts used in fuel-cell reactors, and increased the charge to complete the reaction. With 50 F mol^{-1} of electricity, **6a** was completely consumed and **7a** was obtained in 96% yield (Table 5, entry 5). However, the electrochemical reaction of **6a** with reused MEA did not give **7a**, and MEA was torn after electrolysis, probably because **6a** and/or **7a** were trapped on the membrane having sulfonic acids, and the desired electrolysis was disturbed. We assumed that this could be resolved by adding a strong acid to liberate **6a** and/or **7a** from the membrane by the equilibrium (Figure 2).

Based on this hypothesis, we examined several acids and found that the addition of a catalytic amount (0.10 equiv) of *p*-toluenesulfonic acid (PTSA) was sufficient (Figure 3). The first run gave **7a** in 88% yield and the second run with the MEA gave **7a** in 85% yield. MEA was reused eight times, and **7a** was obtained in high yield in each run. The addition of pyridinium *p*-toluenesulfonate (PPTS) was also efficient, and MEA was repeatedly used to afford **7a** in high yield (Figure 4).

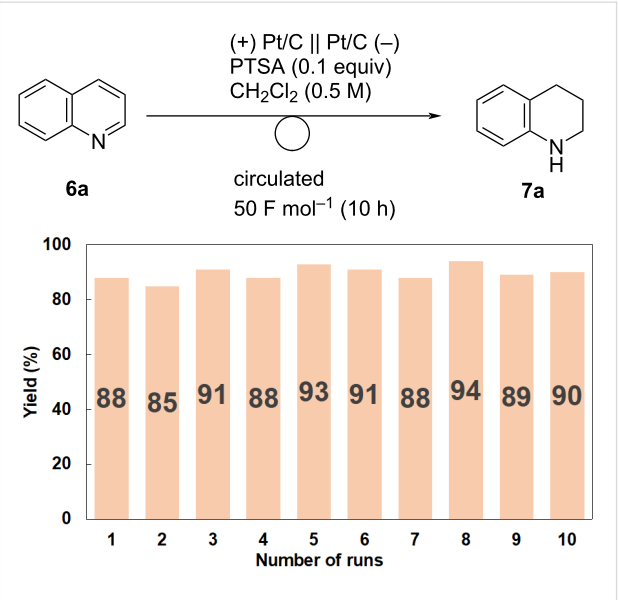

Figure 3: Recycled use of MEA for the electroreduction of **6a** in the presence of PTSA (0.10 equiv). Reaction conditions: anode catalyst, Pt/C; cathode catalyst, Pt/C; **6a**, 1.5 mmol; solvent, CH_2Cl_2 (0.5 M); flow rate of the solution of **6a**, 0.75 mL min^{-1}; flow rate of H_2 gas, 100 mL min^{-1}; reaction temperature, room temperature; current density, 50 mA cm^{-2}. The solution was circulated until the passage of 50 F mol^{-1} (10 h). The yields were determined by ^{1}H NMR analysis using 1,1,2,2-tetrachloroethane as an internal standard.

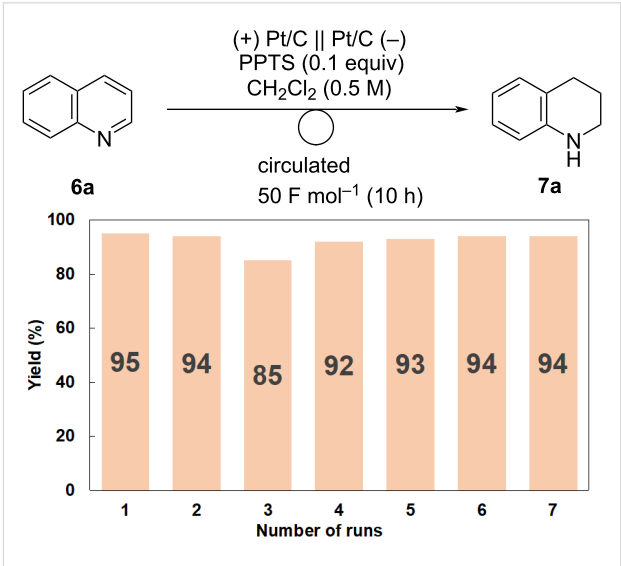

Figure 4: Recycled use of MEA for the electroreduction of **6a** in the presence of PPTS (0.10 equiv). Reaction conditions: anode catalyst, Pt/C; cathode catalyst, Pt/C; **6a**, 1.5 mmol; solvent, CH_2Cl_2 (0.5 M); flow rate of the solution of **6a**, 0.75 mL min^{-1}; flow rate of H_2 gas, 100 mL min^{-1}; reaction temperature, room temperature; current density, 50 mA cm^{-2} (10 h). The solution was circulated until the passage of 50 F mol^{-1}. The yields were determined by ^{1}H NMR analysis using 1,1,2,2-tetrachloroethane as an internal standard.

After further tunings, we found that the charge for electroreduction of **6a** could be reduced to 25 F mol^{-1} when decreasing the current density to 25 mA cm^{-2}, and **7a** was obtained in 90% yield (see the Supporting Information File 1). Next, the substrate scope was examined under optimal conditions (Scheme 4). Substrates bearing a methyl group afforded the corresponding products in high yields (**7a–e**, **7g**, and **7h**), except for **6f** which contained a methyl group at the 4-position. The reaction of 2,3-dimethylquinoline (**6i**) gave the desired product **7i** (*cis*/*trans* = 3:1) in 77% yield. Substrates bearing acetyl (**6k**), ester (**6l**), and amide (**6m**) groups were tolerated under these conditions and selectively afforded the desired products. A substrate with a methoxy group at the 8-position (**6o**) afforded the desired product **7o** in high yield. However, **6p** and **6q** with a methoxy group at the 6- and 3-position gave only a small amount of the target product, and **6r** with a methoxy group at the 4-position gave compound **7r′**, in which the benzene ring was hydrogenated. Substrates with chloro groups produced the dechlorinated products (**7t** and **7u**). Unfortunately, during the electrolysis of quinolines with cyano (**6v**), formyl (**6w** and **6x**), nitro (**6y**), and amino (**6z**) groups, the flow path was clogged probably due to the decomposition of the substrates, and the desired products were not obtained.

This system can be applied to large-scale syntheses. A similar yield of **7a** was obtained when the reaction was scaled up

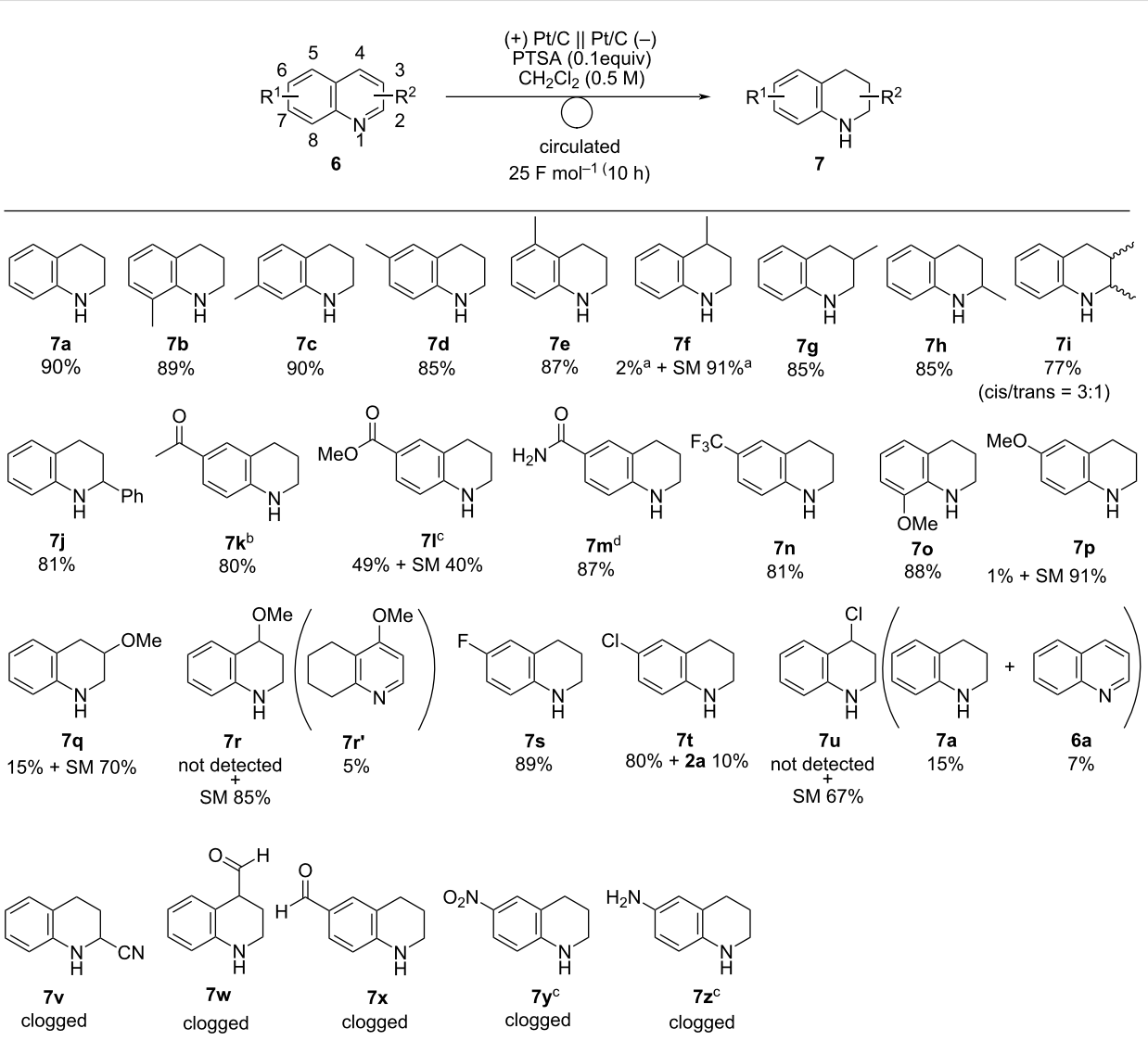

Scheme 4: Scope of the electroreduction of **6** in the presence of PTSA (0.10 equiv). Reaction conditions: anode catalyst, Pt/C; cathode catalyst, Pt/C; **6**, 1.5 mmol; solvent, CH_2Cl_2 (0.5 M); flow rate of the solution of **6**, 0.75 mL min^{-1}; flow rate of H_2 gas, 100 mL min^{-1}; reaction temperature, room temperature; current density, 25 mA cm^{-2}. The solution was circulated until the passage of 25 F mol^{-1} (10 h). Isolated yield. [a]Determined by ^1H NMR analysis using 1,1,2,2-tetrachloroethane as an internal standard. [b]0.125 M. [c]0.25 M. [d]1,4-dioxane/H_2O (7:1, 0.25 M).

(Scheme 5a). The electrolysis of 2.32 g of **6a** gave 2.12 g of **7a** (88% yield). Next, we examined the electroreduction of **6a** using an aqueous proton source instead of hydrogen. The use of DSE® as an anode and H_2SO_4 aq as an anolyte was effective, and **7a** was obtained in 80% yield (Scheme 5b).

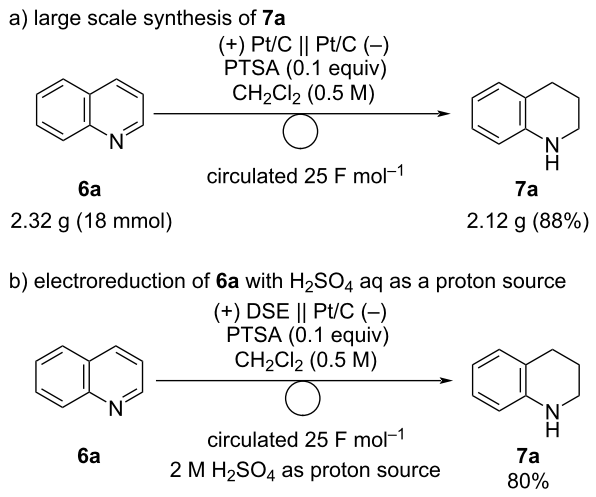

Scheme 5: a) Large scale synthesis of **7a** and b) electoreduction of **6a** using H_2SO_4 as a proton source.

Reduction of pyridines to piperidines

As mentioned previously, reduction of pyridines to piperidines is important for organic synthesis. Therefore, the electroreduction of pyridine (**8a**) was performed (Table 6). First, the electroreduction of **8a** was performed with 0.1 equiv of PTSA, and 1.0 equiv of PTSA was added after electrolysis to determine the yield by ^{1}H NMR analysis (Table 6, entry 1). The yield of **9a**·PTSA (26% yield) was low and **8a**·PTSA was obtained as the major product (60% yield), suggesting that the catalytic amount of PTSA was not sufficient because it would be completely trapped with **9a**. These results suggest that stoichiometric amount of PTSA was required to liberate **8a** from the membrane. As expected, the yield of **9a**·PTSA increased upon increasing the amount of PTSA used for electrolysis (Table 6, entries 1–4). Electrolysis with 1 equiv of PTSA afforded **9a**·PTSA quantitatively (Table 6, entry 4). MEA was used repeatedly, and the target compound was obtained quantitatively in each run (Table 6, entries 5 and 6). Finally, the reaction was examined using an aqueous proton source instead of humidified H_2 gas. Similar to the reaction of quinoline (**6a**), **9a**·PTSA was obtained in 85% yield (Table 6, entry 7) by the use of DSE® electrode and 2 M H_2SO_4 aq as a proton source.

The substrate scope was investigated under the optimized reaction conditions (Scheme 6). Electroreduction of 2-methylpyridine (**8b**) and 2-ethylpyridine (**8c**) afforded the corresponding 2-substituted piperidines **9b** and **9c** in 94% and 93% yields, respectively. The reaction of 3-methylpyridine (**8d**) gave 3-methylpiperidine (**9d**) in good yield. In contrast to quinolines, 4-methylpyridine (**8e**) gave 4-methylpiperidine (**9e**) in a moderate yield. 4-Phenylpyridine (**8f**) afforded a small amount of the target product **9f** and 91% of **8f** was recovered, probably

Table 6: Electroreduction of pyridine (**8a**) using a PEM reactor[a].

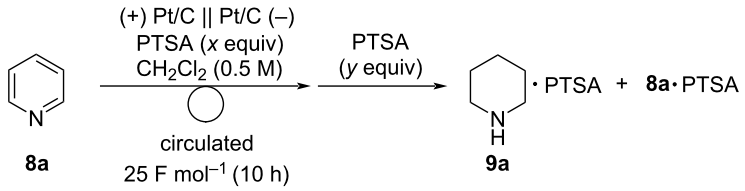

entry	*x* (equiv)	*y* (equiv)	**9a**·PTSA (%)[b]	**8a**·PTSA (%)[b]
1	0.1	1	26	60
2	0.5	0.5	48	47
3	0.75	0.25	77	23
4	1	0	quant	N.D.[c]
5[d]	1	0	99	N.D.
6[e]	1	0	quant	N.D.
7[f]	1	0	85	N.D.

[a]Reaction conditions: anode catalyst, Pt/C; cathode catalyst, Pt/C; **8a**, 1.5 mmol; solvent, CH_2Cl_2 (0.5 M); flow rate of the solution of **8a**, 0.75 mL min^{-1}; flow rate of H_2 gas, 100 mL min^{-1}; reaction temperature, room temperature; current density, 25 mA cm^{-2}. The solution was circulated until the passage of 25 F mol^{-1} (10 h). [b]Determined by ^{1}H NMR analysis using 1,1,2,2-tetrachloroethane as an internal standard. [c]Not detected. [d]2nd run. [e]3rd run. [f]Performed with DSE® electrode and 2 M H_2SO_4 aq was used instead of humidified H_2 gas.

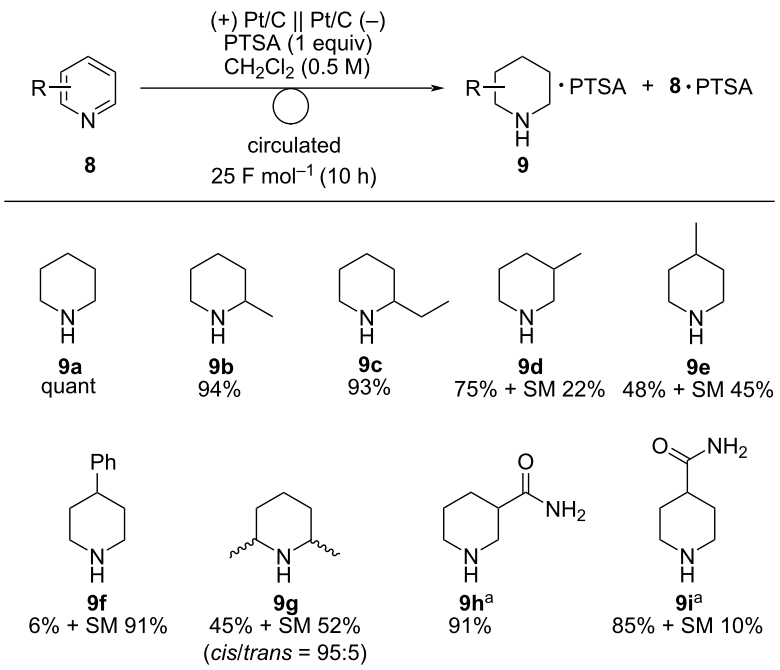

Scheme 6: Scope of the electroreduction of **6** in the presence of PTSA (1 equiv). Reaction conditions: anode catalyst, Pt/C; cathode catalyst, Pt/C; **8**, 1.5 mmol; solvent, CH_2Cl_2 (0.5 M); flow rate of the solution of **8**, 0.75 mL min^{-1}; flow rate of H_2 gas, 100 mL min^{-1}; reaction temperature, room temperature; current density, 25 mA cm^{-2}. The solution was circulated until the passage of 25 F mol^{-1} (10 h). Yields were determined by ^{1}H NMR analysis of PTSA salts using 1,1,2,2-tetrachloroethane as an internal standard. [a]Performed in 1,4-dioxane/H_2O (7:1), and the yield was determined by ^{1}H NMR analysis using ethylene carbonate as an internal standard.

because of steric hindrance of **8f**. 2,6-Disubstituted pyridine such as 2,6-lutidine (**8g**) was also applicable and 2,6-dimethylpiperidine (**9g**) was obtained in moderate yield. In contrast to quinolines, pyridines bearing an amide group were also applicable and amidylpiperidines **9h** and **9i** were obtained in high yields.

Conclusion

We established the electrochemical reduction of cyanoarenes, nitroarenes, quinolines, and pyridines using a PEM reactor. All the reactions proceeded under ambient conditions, and benzylamines, anilines, 1,2,3,4-tetrahydroquinolines, and piperidines were obtained. For the electrochemical reduction using a PEM reactor, the addition of an acid sometimes helped the progress of the reactions. For instance, the addition of ethyl phosphate is essential for the electroreduction of cyanoarenes. The generation of dibenzylamine was suppressed and benzylamines were obtained efficiently. The PEM system was effective in reducing nitroarenes. Several functional groups were tolerated under these conditions, and the nitro group was selectively reduced. The addition of an acid was also effective in reducing quinolines to 1,2,3,4-tetrahydroquinolines. In the presence a catalytic amount of PTSA, various 1,2,3,4-tetrahydroquinolines were obtained. Although a stoichiometric amount of PTSA was required, this system was applicable to the reduction of pyridines to quinolines. An aqueous proton source could also be used in this system. The fact that the addition of appropriate strength and amount of acid makes the reaction system more efficient is a key factor in the reduction of nitrogen-containing compounds with the PEM-type reactor. The chemoselective reduction of nitrogen-containing compounds under mild conditions is important for organic synthesis, and we believe that the PEM reaction system is a powerful tool that can be applied to a wide variety of nitrogen-containing compounds.

Supporting Information

Supporting Information File 1

Experimental part.
[https://www.beilstein-journals.org/bjoc/content/supplementary/1860-5397-20-139-S1.pdf]

Acknowledgements

The authors thank Prof. Yuta Nishina (Okayama University) and his group members for their help in preparing the MEA. The authors also thank Ishifuku Metal Industry Co., Ltd. and De Nora Permelec Ltd. for providing the catalysts and DSE® electrode, respectively.

Funding

This work was supported in part by JST CREST Grant No. JP65R1204400, Japan, JSPS KAKENHI Grant Numbers JP22H02122 (to K.M.), JP23K17917 (to K.M.), JP22K05115 (to S.S.), and JP21H05214 (Digitalization-driven Transformative Organic Synthesis) (to S.S.),

Author Contributions

Koichi Mitsudo: conceptualization; data curation; supervision; visualization; writing – original draft. Atsushi Osaki: investigation; visualization. Haruka Inoue: investigation. Eisuke Sato: writing – review & editing. Naoki Shida: writing – review & editing. Mahito Atobe: conceptualization; funding acquisition; writing – review & editing. Seiji Suga: conceptualization; funding acquisition; project administration; supervision.

ORCID® iDs

Koichi Mitsudo - https://orcid.org/0000-0002-6744-7136
Eisuke Sato - https://orcid.org/0000-0001-6784-138X
Naoki Shida - https://orcid.org/0000-0003-0586-1216
Mahito Atobe - https://orcid.org/0000-0002-3173-3608
Seiji Suga - https://orcid.org/0000-0003-0635-2077

Data Availability Statement

All data that supports the findings of this study is available in the published article and/or the supporting information to this article.

References

1. Nicolaou, K. C.; Sorensen, E. J. *Classics in Total Synthesis: Targets, Strategies, Methods;* Wiley-VCH: Weinheim, Germany, 1996.
2. Bhutani, P.; Joshi, G.; Raja, N.; Bachhav, N.; Rajanna, P. K.; Bhutani, H.; Paul, A. T.; Kumar, R. *J. Med. Chem.* **2021,** *64,* 2339–2381. doi:10.1021/acs.jmedchem.0c01786
3. Tang, P.; Wang, H.; Zhang, W.; Chen, F.-E. *Green Synth. Catal.* **2020,** *1,* 26–41. doi:10.1016/j.gresc.2020.05.006
4. Kibayashi, C. *Chem. Pharm. Bull.* **2005,** *53,* 1375–1386. doi:10.1248/cpb.53.1375
5. Das, S.; Zhou, S.; Addis, D.; Enthaler, S.; Junge, K.; Beller, M. *Top. Catal.* **2010,** *53,* 979–984. doi:10.1007/s11244-010-9526-4
6. Romero, A. H. *ChemistrySelect* **2020,** *5,* 13054–13075. doi:10.1002/slct.202002838
7. Waldvogel, S. R.; Streb, C. *Chem* **2022,** *8,* 2071–2073. doi:10.1016/j.chempr.2022.06.022
8. Begum, R.; Rehan, R.; Farooqi, Z. H.; Butt, Z.; Ashraf, S. *J. Nanopart. Res.* **2016,** *18,* 231. doi:10.1007/s11051-016-3536-5
9. Aditya, T.; Pal, A.; Pal, T. *Chem. Commun.* **2015,** *51,* 9410–9431. doi:10.1039/c5cc01131k
10. Roy, S. *J. Phys. Chem. C* **2020,** *124,* 28345–28358. doi:10.1021/acs.jpcc.0c07363
11. Sedghi, R.; Heravi, M. M.; Asadi, S.; Nazari, N.; Nabid, M. R. *Curr. Org. Chem.* **2016,** *20,* 696–734. doi:10.2174/1385272819666150907192826
12. Vitaku, E.; Smith, D. T.; Njardarson, J. T. *J. Med. Chem.* **2014,** *57,* 10257–10274. doi:10.1021/jm501100b
13. Ren, D.; He, L.; Yu, L.; Ding, R.-S.; Liu, Y.-M.; Cao, Y.; He, H.-Y.; Fan, K.-N. *J. Am. Chem. Soc.* **2012,** *134,* 17592–17598. doi:10.1021/ja3066978
14. Mao, S.; Ryabchuk, P.; Dastgir, S.; Anwar, M.; Junge, K.; Beller, M. *ACS Appl. Nano Mater.* **2022,** *5,* 5625–5630. doi:10.1021/acsanm.2c00601
15. Bourriquen, F.; Hervochon, J.; Qu, R.; Bartling, S.; Rockstroh, N.; Junge, K.; Fischmeister, C.; Beller, M. *Chem. Commun.* **2022,** *58,* 8842–8845. doi:10.1039/d2cc02928f
16. Murugesan, K.; Chandrashekhar, V. G.; Kreyenschulte, C.; Beller, M.; Jagadeesh, R. V. *Angew. Chem., Int. Ed.* **2020,** *59,* 17408–17412. doi:10.1002/anie.202004674
17. Wagener, T.; Heusler, A.; Nairoukh, Z.; Bergander, K.; Daniliuc, C. G.; Glorius, F. *ACS Catal.* **2020,** *10,* 12052–12057. doi:10.1021/acscatal.0c03278
18. Karakulina, A.; Gopakumar, A.; Akçok, İ.; Roulier, B. L.; LaGrange, T.; Katsyuba, S. A.; Das, S.; Dyson, P. J. *Angew. Chem., Int. Ed.* **2016,** *55,* 292–296. doi:10.1002/anie.201507945
19. Atobe, M.; Shida, N. *Curr. Opin. Electrochem.* **2024,** *44,* 101440. doi:10.1016/j.coelec.2024.101440
20. Langer, S. H.; Landi, H. P. *J. Am. Chem. Soc.* **1963,** *85,* 3043–3044. doi:10.1021/ja00902a052
21. Yuan, X.-Z.; Ma, Z.-F.; Jiang, Q.-Z.; Wu, W.-S. *Electrochem. Commun.* **2001,** *3,* 599–602. doi:10.1016/s1388-2481(01)00226-0
22. Fonocho, R.; Gardner, C. L.; Ternan, M. *Electrochim. Acta* **2012,** *75,* 171–178. doi:10.1016/j.electacta.2012.04.116
23. Green, S. K.; Tompsett, G. A.; Kim, H. J.; Kim, W. B.; Huber, G. W. *ChemSusChem* **2012,** *5,* 2410–2420. doi:10.1002/cssc.201200416
24. Takano, K.; Tateno, H.; Matsumura, Y.; Fukazawa, A.; Kashiwagi, T.; Nakabayashi, K.; Nagasawa, K.; Mitsushima, S.; Atobe, M. *Bull. Chem. Soc. Jpn.* **2016,** *89,* 1178–1183. doi:10.1246/bcsj.20160165
25. Takano, K.; Tateno, H.; Matsumura, Y.; Fukazawa, A.; Kashiwagi, T.; Nakabayashi, K.; Nagasawa, K.; Mitsushima, S.; Atobe, M. *Chem. Lett.* **2016,** *45,* 1437–1439. doi:10.1246/cl.160766
26. Ogihara, H.; Maezuru, T.; Ogishima, Y.; Yamanaka, I. *ChemistrySelect* **2016,** *1,* 5533–5537. doi:10.1002/slct.201601082
27. Nagasawa, K.; Kato, A.; Nishiki, Y.; Matsumura, Y.; Atobe, M.; Mitsushima, S. *Electrochim. Acta* **2017,** *246,* 459–465. doi:10.1016/j.electacta.2017.06.081
28. Ogihara, H.; Maezuru, T.; Ogishima, Y.; Yamanaka, I. *Electrocatalysis* **2018,** *9,* 220–225. doi:10.1007/s12678-017-0419-1
29. Fukazawa, A.; Takano, K.; Matsumura, Y.; Nagasawa, K.; Mitsushima, S.; Atobe, M. *Bull. Chem. Soc. Jpn.* **2018,** *91,* 897–899. doi:10.1246/bcsj.20180021
30. Sato, M.; Ogihara, H.; Yamanaka, I. *ISIJ Int.* **2019,** *59,* 623–627. doi:10.2355/isijinternational.isijint-2018-551
31. Fukazawa, A.; Minoshima, J.; Tanaka, K.; Hashimoto, Y.; Kobori, Y.; Sato, Y.; Atobe, M. *ACS Sustainable Chem. Eng.* **2019,** *7,* 11050–11055. doi:10.1021/acssuschemeng.9b01882
32. Fukazawa, A.; Tanaka, K.; Hashimoto, Y.; Sato, Y.; Atobe, M. *Electrochem. Commun.* **2020,** *115,* 106734. doi:10.1016/j.elecom.2020.106734
33. Nogami, S.; Nagasawa, K.; Fukazawa, A.; Tanaka, K.; Mitsushima, S.; Atobe, M. *J. Electrochem. Soc.* **2020,** *167,* 155506. doi:10.1149/1945-7111/abaae7
34. Fukazawa, A.; Shimizu, Y.; Shida, N.; Atobe, M. *Org. Biomol. Chem.* **2021,** *19,* 7363–7368. doi:10.1039/d1ob01197a
35. Kawaguchi, D.; Ogihara, H.; Kurokawa, H. *ChemSusChem* **2021,** *14,* 4431–4438. doi:10.1002/cssc.202101188

36. Ido, Y.; Fukazawa, A.; Furutani, Y.; Sato, Y.; Shida, N.; Atobe, M. *ChemSusChem* **2021,** *14,* 5405–5409. doi:10.1002/cssc.202102076
37. Ashikari, Y.; Tamaki, T.; Takahashi, Y.; Yao, Y.; Atobe, M.; Nagaki, A. *Front. Chem. Eng.* **2022,** *3,* 819752. doi:10.3389/fceng.2021.819752
38. Nogami, S.; Shida, N.; Iguchi, S.; Nagasawa, K.; Inoue, H.; Yamanaka, I.; Mitsushima, S.; Atobe, M. *ACS Catal.* **2022,** *12,* 5430–5440. doi:10.1021/acscatal.2c01594
39. Kondo, J. N.; Ge, S.; Suzuki, T.; Osuga, R.; Matsumoto, T.; Yokoi, T.; Shimizu, Y.; Fukazawa, A.; Shida, N.; Atobe, M. *J. Phys. Chem. C* **2022,** *126,* 19376–19385. doi:10.1021/acs.jpcc.2c05127
40. Shimizu, Y.; Harada, J.; Fukazawa, A.; Suzuki, T.; Kondo, J. N.; Shida, N.; Atobe, M. *ACS Energy Lett.* **2023,** *8,* 1010–1017. doi:10.1021/acsenergylett.2c02573
41. Ido, Y.; Shimizu, Y.; Shida, N.; Atobe, M. *Synthesis* **2023,** *55,* 2979–2984. doi:10.1055/a-2000-8231
42. Ashikari, Y.; Mandai, K.; Yao, Y.; Tsuchihashi, Y.; Nagaki, A. *ChemElectroChem* **2023,** *10,* e202300315. doi:10.1002/celc.202300315
43. Egbert, J. D.; Thomsen, E. C.; O'Neill-Slawecki, S. A.; Mans, D. M.; Leitch, D. C.; Edwards, L. J.; Wade, C. E.; Weber, R. S. *Org. Process Res. Dev.* **2019,** *23,* 1803–1812. doi:10.1021/acs.oprd.8b00379
44. Mitsudo, K.; Matsuo, R.; Yonezawa, T.; Inoue, H.; Mandai, H.; Suga, S. *Angew. Chem., Int. Ed.* **2020,** *59,* 7803–7807. doi:10.1002/anie.202001149
45. Mitsudo, K.; Okumura, Y.; Yohena, K.; Kurimoto, Y.; Sato, E.; Suga, S. *Org. Lett.* **2023,** *25,* 3476–3481. doi:10.1021/acs.orglett.3c01062
46. Mitsudo, K.; Tachibana, Y.; Sato, E.; Suga, S. *Org. Lett.* **2022,** *24,* 8547–8552. doi:10.1021/acs.orglett.2c03574
47. Kurimoto, Y.; Yamashita, J.; Mitsudo, K.; Sato, E.; Suga, S. *Org. Lett.* **2021,** *23,* 3120–3124. doi:10.1021/acs.orglett.1c00807
48. Mitsudo, K. *Chem. Rec.* **2021,** *21,* 2269–2276. doi:10.1002/tcr.202100033
49. Mitsudo, K.; Kaide, T.; Nakamoto, E.; Yoshida, K.; Tanaka, H. *J. Am. Chem. Soc.* **2007,** *129,* 2246–2247. doi:10.1021/ja069043r
50. Mitsudo, K.; Inoue, H.; Niki, Y.; Sato, E.; Suga, S. *Beilstein J. Org. Chem.* **2022,** *18,* 1055–1061. doi:10.3762/bjoc.18.107
51. Ma et al. reported the electrocatalytic reduction of nitrobenzene using a PEM reactor which afforded a mixture of cyclohexylamine and aniline, see ref [21].
52. Shida, N.; Shimizu, Y.; Yonezawa, A.; Harada, J.; Furutani, Y.; Muto, Y.; Kurihara, R.; Kondo, J. N.; Sato, E.; Mitsudo, K.; Suga, S.; Iguchi, S.; Kamiya, K.; Atobe, M. *ChemRxiv* **2024**. doi:10.26434/chemrxiv-2024-5c8lr
Quite recently, Atobe reported that an anion-exchange membrane (AEM) reactor is efficient for the electrocatalytic hydrogenation of pyridines and quinolines.
53. We considered that Pt site of PtPd/C was effective to generate H_{ad} and the hydrogenetaion would proceed on Pd site. For the behaviour of PtPd/C in a PEM reactor, see ref [38].

BEILSTEIN JOURNAL OF ORGANIC CHEMISTRY

Synthesis of polycyclic aromatic quinones by continuous flow electrochemical oxidation: anodic methoxylation of polycyclic aromatic phenols (PAPs)

Hiwot M. Tiruye[1], Solon Economopoulos[2] and Kåre B. Jørgensen[*1]

Full Research Paper

Open Access

Address:
[1]Department of Chemistry, Bioscience and Environmental Engineering, Faculty of Science and Technology, University of Stavanger, P.O Box 8600 Forus, N-4036 Stavanger, Norway and [2]Advanced Optoelectronic Nanomaterials Research Unit, Department of Chemistry, Norwegian University of Science and Technology, 7491 Trondheim, Norway

Email:
Kåre B. Jørgensen[*] - kare.b.jorgensen@uis.no

* Corresponding author

Keywords:
acetal formation; cyclic voltammetry; flow electrochemistry; green oxidation; polycyclic aromatic hydrocarbons

Beilstein J. Org. Chem. **2024,** *20,* 1746–1757.
https://doi.org/10.3762/bjoc.20.153

Received: 15 April 2024
Accepted: 08 July 2024
Published: 24 July 2024

This article is part of the thematic issue "Synthetic electrochemistry".

Guest Editor: K. Lam

Abstract

The electrochemical oxidation of polycyclic aromatic phenols (PAPs) has been developed in a microfluidic cell to synthesize polycyclic aromatic quinones (PAQs). Methanol was used as nucleophile to trap the phenoxonium cation formed in the oxidation as an acetal, that later were hydrolysed to the quinone. Formation of hydrogen gas as the cathode reaction caused challenges in the flow cell and were overcome by recycling the reaction mixture through the cell at increased flow rate several times. The specific quinones formed were guided by the position of an initial hydroxy group on the polycyclic aromatic hydrocarbon. An available *para*-position in the PAPs gave *p*-quinones, while hydroxy groups in the 2- or 3-position led to *o*-quinones. The substrates were analysed by cyclic voltammetry for estitmation of the HOMO/LUMO energies to shed more light on this transformation. The easy separation of the supporting electrolyte from the product will allow recycling and makes this a green transformation.

Introduction

Quinones and their derivatives are applied in various fields such as chemical, environmental, and pharmaceutical industries [1-4]. Their cyclic diketone structures can easily transform into intramolecular unsaturated structures, and their distinct physical properties make them privileged structures in medicinal chemistry [2]. Benzoquinone and naphthoquinone can exist as *ortho*-quinone and *para*-quinone, with the latter considered more stable [5]. Additionally, *p*- and *o*-quinones are formed in metabolism of drugs [6] as well as polycyclic aromatic hydrocarbons (PAHs) by cytochrome P450 (CYP) and other meta-

bolic enzymes [7,8]. Main metabolic pathways form quinone isomers of benzo[*a*]pyrene [8], naphthalene [9,10], and benzene [11].

Numerous methods for the oxidation of phenols or their derivatives to quinones have been described [12]. Oxidation with Fremy's radical (potassium nitrosodisulfonate) [13] or catalytic systems like methyltrioxorhenium(VII) ($MeReO_3$) [14] and 2-iodobenzenesulfonic acids (IBS)/Oxone® [15] led to either *p*-quinones or *o*-quinones, depending on the substituents in the *para*-position to the hydroxy group. Recently, hypervalent iodine reagents have been explored for the oxidation of polycyclic aromatic phenols (PAPs). Oxidation of 1-naphthol derivatives by bis(trifluoroacetoxy)iodobenzene (BTI) furnished *p*-naphthoquinones [16]. Other PAPs follow the same pattern forming *p*-quinones or *o*-quinones when the *para*-position is structurally blocked like in 2-naphthol (**1a**) [17]. Oxidation with iodoxybenzoic acid (IBX) [17] or stabilised IBX (SIBX) [18] form *o*-quinones selectively, even when the *p*-quinones are structurally feasible. However, all these methods constitute toxic hazards and/or produce stoichiometric amounts of waste products making them less desirable for industrial scale [19].

Electrochemical synthesis methods have a huge potential and this field is currently undergoing a renaissance [20-24]. Replacing chemical oxidants with electric current reduces waste production and gives a sustainable and inherently safe alternative to classical synthesis [25-28]. Electrochemical oxidation reactions are further used to emulate enzymatic oxidations of drugs and explore potential metabolites [29-31]. Electrochemical flow systems provide fast electrosynthesis with low cell resistance, large electrode area, and good control of the current [32-34].

Early studies on the electrochemical oxidation of phenols revealed that the oxidation passes through a phenoxonium ion and forms acetals in methanol but quinones in the presence of water [35-37]. However, the reaction is sometimes accompanied by the formation of dimers, which indicates a radical intermediate [36]. Swenton and co-workers [37] established evidence for the phenoxonium ion (Scheme 1), and were further able to divert the reaction into forming *ortho*-oxidation due to steric hindrance (Scheme 2). Cyclic voltammetry studies of the oxidation of 2-naphthol (**1a**) into *o*-quinone **5** revealed that the oxidation comprises two separate 1-electron oxidations [38]. Electrooxidative dearomatization has proven to be an effective synthetic tool [39]. However, we have not found examples of electrochemical oxidation of PAPs applied in synthesis. Here, we report the synthesis of polycyclic aromatic quinones by anodic oxidation as a green alternative to our previous synthesis with SIBX [18].

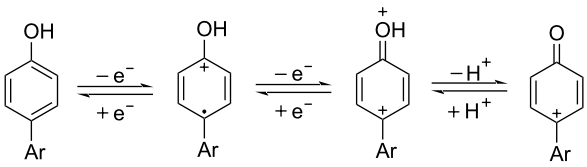

Scheme 1: Formation of phenoxonium cation in the anodic oxidation of phenol performed under neutral or weakly basic conditions.

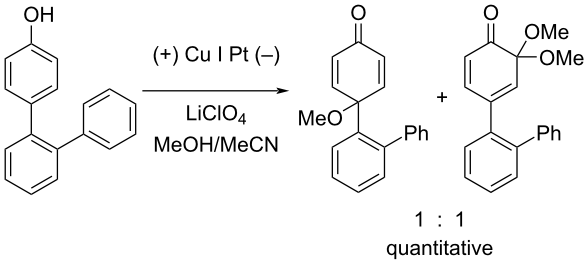

Scheme 2: Anodic oxidation reported by Swenton et al. [37].

Results and Discussion

The electrochemical reactions were performed in the Flux module of the Syrris automated modular flow system [40] which provides a controlled geometry with a short distance between the electrodes, and easily reproduceable conditions. The electrochemical oxidation of phenols has been performed with platinum anodes [37,41], and carbon/platinum worked well for the oxidation of toluene dissolved in methanol with tetraethylammonium tosylate (Et_4NOTs) as a supporting electrolyte within a flow system [32]. Et_4NOTs is highly soluble in these solvents and can easily be removed by filtration through a pad of silia gel. Initially, we did a short screening of available electrode materials on the oxidation of commercially available 2-naphthol (**1a**, Table 1) obtaining the four-electron oxidation product 1,1-dimethoxynaphthalen-2(1*H*)-one (**2**). Best results were obtained with a carbon/platinum electrode pair, although stainless steel (SS) could also be used as cathode. The experiments were conducted with a 3:1 mixture of methanol/tetrahydrofuran (optimization not shown), where methanol further served as nucleophile. Some THF was needed to improve the solubility of some of the substrates. Acidic conditions (Table 1, entry 5) or methanol/water (Table 1, entry 6) gave a complex mixture with overoxidized products.

Although the desired oxidation is a 4-electon process, there will always be some extra current passing the cell that does not contribute to the reaction. Our optimization of the current on 1-chrysenol (**3b**) is given in Table 2. The reaction mixtures were introduced via a 10 mL-injection loop into the stream that was flowing through the Flux cell at a flowrate of 100 µL/min.

Table 1: Electrode and electrolyte effects on the electrochemical oxidation of 2-naphthol (**1a**).[a]

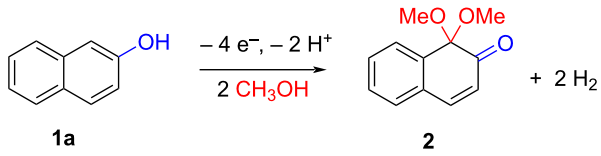

1a **2**

Entry	Electrolyte	Anode/cathode[b]	Solvent[c]	Yield (%)[d]
1	Et_4NOTS	C/C	MeOH/THF	0
2	Et_4NOTS	C/SS	MeOH/THF	65
3	Et_4NOTS	SS/C	MeOH/THF	0
4	Et_4NOTS	C/Pt	MeOH/THF	84
5	Et_4NOTS / TsOH	C/Pt	MeOH/THF	n/a[e]
6	Et_4NOTS	C/Pt	MeOH/H_2O	n/a[e]

[a]Experiments were conducted at room temperature with 0.01 M of **1a**, 0.05 M electrolyte, and 3.6 min residence time. [b]Electrode materials: C: carbon filled PPS (polyphenylene sulfide), SS: stainless steel, Pt: platinum. [c]Solvent ratio 3:1 (MeOH/THF) or 9:1 (MeOH/H_2O). [d]Isolated yield. [e]Complex mixture/over-oxidation.

Table 2: Anodic methoxylation of 1-chrysenol (**3b**) at different electron equivalents.[a]

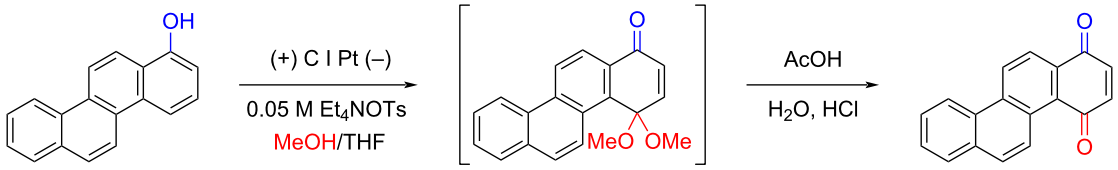

3b **4b**

Entry	Electrons (F/mol)	Current (mA)	Yield (%)[b]
1	1	2	33
2	2	3	31
3	4	6	40
4	6	9	47
5	7	11	42
6	8	13	34

[a]Conducted with 0.01 M substate and 100 µL/min flowrate (residence time 2.25 min). [b]Isolated yield of chrysen-1,4-dione (**4b**).

The current was increased from 1 mA to 13 mA to increase the electron equivalents from 1 F/mol to 8 F/mol at a potential of 1.7–3.0 V. The crudes, after evaporation of the solvents, were further hydrolysed with a mixture of HCl, acetic acid, and water to release the quinones before purification. Further experimental details are given in Supporting Information File 1. The best result was obtained at 6 F/mol equivalents, giving 47% of quinone **4b** (Table 2, entry 4).

These experiments, where the reaction mixture was passed through the cell a single time, gave rather low yields. This may be due to gas bubbles forming at the electrodes, disrupting the even distribution of electric current and potentially affecting the reaction [42,43]. When the size of a bubble is comparable to the width of a microchannel, the bubble tends to remain in the electrochemical cell and inhibits the reaction [44,45]. These gas slugs have been reported to block the ionic conduction path between electrodes and reduce the current down to 1/3 to 1/4 of its original value [43] and increase the activation overpotential of the cathode reaction [45].

To address these challenges in the single-pass operation, we directed our efforts toward recirculating the reaction mixture through the cell several times. This is often necessary to en-

hance the conversion of the electrochemical oxidation [46,47]. An increased electrolysis time is necessary as the conversion rate decreases significantly with the decay of the reactant concentration [46]. The reaction mixture was kept in a flask under stirring and pumped through the Flux cell and back to the flask. The flow rate was increased to 300 µL/min to faster flush out the evolved hydrogen gas from the cell. The Flux cell was operated in the galvanostatic mode at 9 mA until the substrate was consumed as monitored by TLC. Typically, the potential slowly increased from 1.7 V in the beginning of the experiments to approximately 2.9 V towards the end without any systematic variation between the compounds. The required residence time was mainly dependent on the conditions of the cell. It was building up in consecutive experiments but was reduced again by cleaning of the electrodes. The experiments collected in Table 3 and Table 4 typically had residence times between 3 and 7 minutes.

Substrates with the hydroxy group in the 2- or 3-position, i.e., **1a**, **3a**, **3c**, and **6a**, formed *o*-dimethoxylated products (Table 3). The oxidation of 2-naphthol (**1a**) to quinone acetal **2** by $PhI(OAc)_2$ (PIDA) has been reported to provide yields ranging

Table 3: Anodic methoxylation of PAPs followed by hydrolysis in two separate steps.[a]

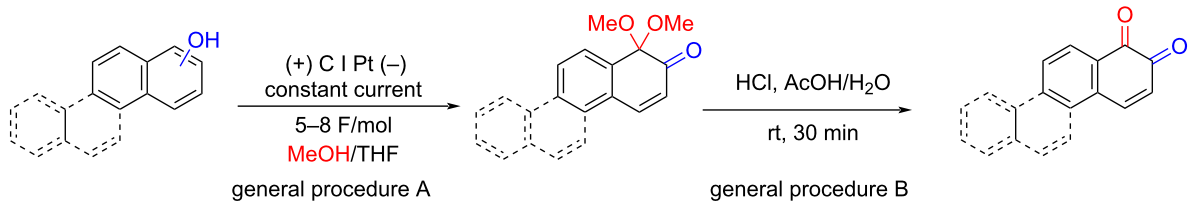

Entry	PAP	Quinone acetal[b]	Quinone[c]
1	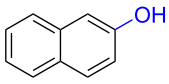 **1a**	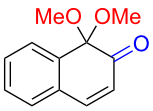 **2** (84%)	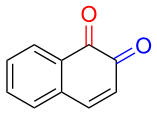 **5** (88%)
2	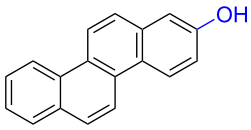 **3a**	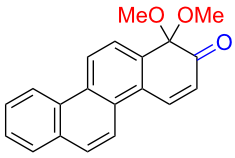 **7a** (72%)	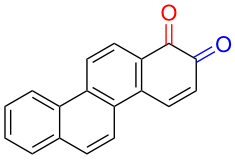 **4a** (69%)
3	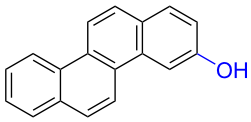 **3c**	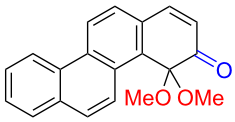 **7b** (79%)	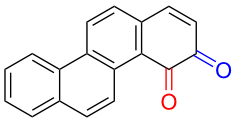 **4c** (96%)
4	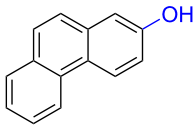 **6a**	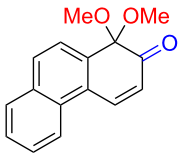 **8a** (57%)	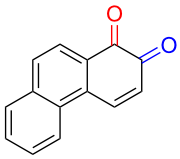 **9a** (90%)
5	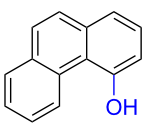 **6b**	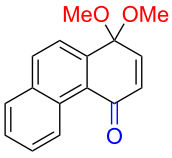 **8b** (66%)	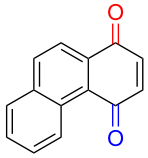 **9b** (93%)

[a]Reactions were carried out with 0.01 M substrate and 0.05 M of Et_4NOTs in 3:1 MeOH/THF that was recirculated through the cell with 300 µL/min flow rate and 9 mA current. [b]Isolated yields. [c]Isolated yields calculated with the acetals as starting material.

from 63% [48] to 76% [49], compared to 84% in our electrochemical oxidation that afforded 30 mg of **2** after 4 h (Table 3, entry 1). The dimethoxylated quinones are somewhat labile but can be purified by rapid silica gel chromatography and stored for a few weeks. The controlled current and anhydrous conditions helped avoiding overoxidation. The substrates leading to *p*-quinones were more prone to overoxidation. The electrochemical oxidation of phenanthren-4-ol (**6b**) provided the *p*-dimethoxylated product **8b** in 66% yield (87 mg), consuming 8 F/mol over a duration of 12.7 h (Table 3, entry 5). Next, quinone acetal **8b** was hydrolysed to phenanthrene-1,4-dione (**9b**) using aq acetic acid and HCl in 93% yield. The hydrolysis step went smoothly for all acetals. However, the methoxylated products from electrochemical oxidation of chrysen-1-ol (**3b**) and chrysen-6-ol (**3d**) rapidly hydrolysed to quinones during purification and could not be isolated. The attempted electrochemical oxidation of naphthalene-1-ol (**1b**) was unsuccessful; only small traces of multiple products were formed.

The lability of the acetals prompted us to submit the crude intermediate directly to hydrolysis without prior isolation (Table 4). As mentioned above, having an aqueous reaction mixture in the electrochemical oxidation will give reduced yields. The overall yield of **9b** from **6b** while isolating the acetal in between steps (Table 3, entry 5) was 57%, whereas the direct hydrolysis of the crude provided an increased yield of 74% (Table 4, entry 7). Further, chrysene-1,4-dione (**4b**) and chrysene-5,6-dione (**4d**) were obtainable this way (Table 4, entries 3 and 5), while **1b** continued to be overoxidized and provided only traces of multiple products. Some overoxidation of **4d** was observed as 12-methoxychrysene-5,6-dione (**10**), but the alternative product chrysene-6,12-dione was not formed. In contrast to the *ortho*-selective oxidations of PAPs with SIBX [18], the electrochemical oxidation forms the *p*-quinones when possible. However, the *o*-quinones are formed in good yields from substrates where the *para*-position of the phenol is part of the further polycyclic aromatic skeleton. The products could be separated from the

Table 4: Synthesis of *o*- and *p*-quinones without isolation of the acetal intermediate.[a]

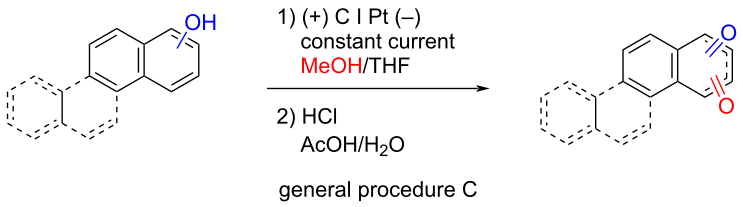

general procedure C

Entry	PAP	Quinone[b]
1	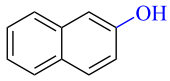 **1a**	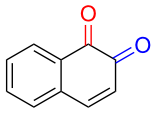 **5** (65%)
2	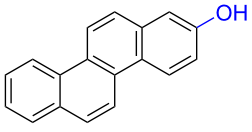 **3a**	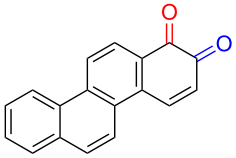 **4a** (63%)
3	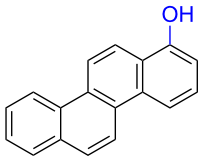 **3b**	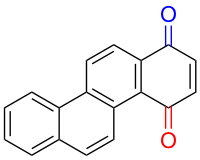 **4b** (65%)
4	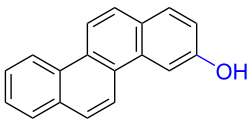 **3c**	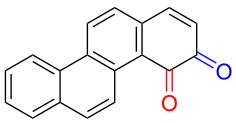 **4c** (58%)

Table 4: Synthesis of *o*- and *p*-quinones without isolation of the acetal intermediate.[a] (continued)

5	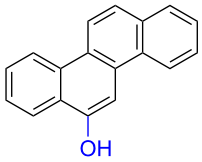 **3d**	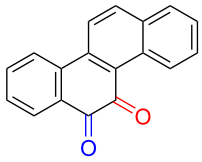 **4d** (72%)[c]
6	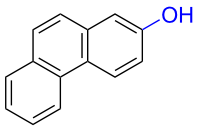 **6a**	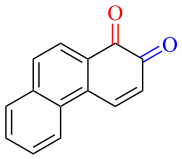 **9a** (49%)
7	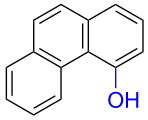 **6b**	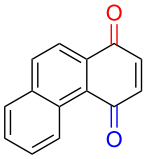 **9b** (74%)
8	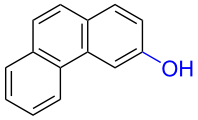 **6c**	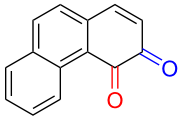 **9c** (81%)

[a]Reactions were carried out between 1.7 to 2.9 V with 0.01 M substrate and 0.05 M of Et_4NOTs in 3:1 MeOH/THF that was recirculated through the cell with 300 µL/min flow rate and 9 mA current. [b]Isolated yields. [c]The further oxidized compound **10** (12-methoxychrysene-5,6-dione) was also isolated in 22% yield.

supporting electrolyte by dispersing the solids in ethyl acetate after removal of solvents from the reaction mixture. Thus, Et_4NOTs can easily be recycled and reused for a greener reaction.

Voltammetric studies

To investigate their redox behaviour, PAPs **1a**,**b** (Figure 1A), **3a–c** (Figure 1C), and **6a–c** (Figure 1E) were scanned between +2.2 V and −1.5 V. All compounds showed irreversible oxidation processes within the oxidative potential window, scaling from 0.79 V to 1.10 V vs Fe/Fe^+. The oxidation peak potential difference between isomers of chrysenols **3** and phenanthrols **6** was 20–310 mV. No reduction peaks were observed in the reverse scan in solutions of neither chrysenols nor phenanthrols, suggesting a chemically irreversible reaction of the radical cation intermediate with the ensuing product no longer being electrochemically active within the potential window of the CV scans. However, a reduction peak was observed for compound **1b** (see Figure S2 in Supporting Information File 1). Naphthalene-1-ol (**1b**) gave a well-defined oxidation peak at 0.95 V (vs Fe/Fe^+) while naphthalene-2-ol (**1a)** showed an oxidation peak at 1.14 V (vs Fe/Fe^+). The oxidation peak potential difference between **1b** and **1a** was 190 mV.

PAHs undergo rapid irreversible chemical reactions upon electron transfer [50]. Unsubstituted PAHs display multielectron oxidation, but one-electron waves occur with electron-donating substituents in suitable positions. Panizza et al. [38] observed two one-electron oxidations in their cyclic voltammetry studies of **1a** in water and proposed the formation of a naphthyloxy radical and a naphthyloxy cation leading to the formation of **5**. Our CV studies exhibit oxidation peaks, which seem in line with what to expect for an electrochemical oxidation of PAPs.

Through the cyclic voltammetry experiments for the investigation of the redox behavior of the PAPs, an estimation of their highest occupied molecular orbital (HOMO) and lowest unoccupied molecular orbital (LUMO) energy levels can be derived via the oxidation onset potentials as shown in the literature [51]. The electrochemical properties of all products are summarized in Table 5. Individual CVs, with onset potentials indicated, are given in Supporting Information File 1. The optical properties of the PAPs were investigated by UV–vis absorption spectroscopy in 10^{-5} M solutions in CH_2Cl_2, as depicted in Figure 1. The UV–vis spectra of these compounds exhibited strong absorption in the region of 250–370 nm. These absorption bands are associated with π–π* and n–π* electronic transitions.

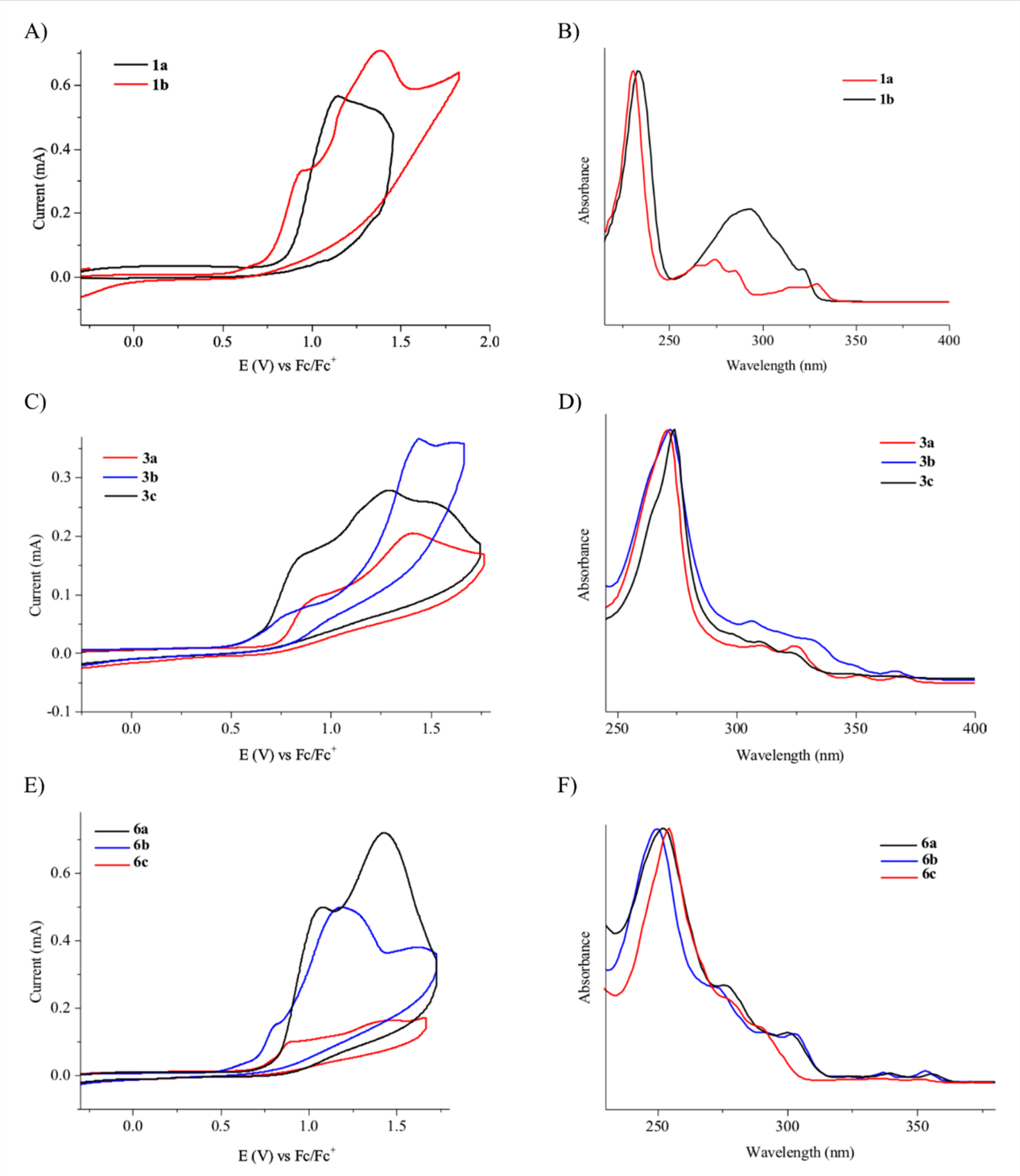

Figure 1: Cyclic voltammograms of PAPs first scan at 0.1 V/s in 0.1 M [NBu_4] [PF_6] in MeCN and UV–vis spectra of PAPs in DCM (≈10^{-5} M). A, B: naphthols **1a**,**b**. C, D: chrysenols **3a–c**. E, F: phenanthrols **6a–c**.

The optical bandgap ($E_{g\text{-}opt}$) values of the compounds determined from the absorption edge of the solution spectra are also summarized in Table 5. Although both HOMO and LUMO slightly vary between the compounds, the energy differences are quite the same for all compounds.

The oxidation is initiated by an electron transfer from the substrate where the substrate will loose an electron more easily [42], and the free electron pairs of the hydroxy group are usually more difficult to ionize than π-electrons of the aromatic systems [52]. Studies by Swenton's [41,53] and Barba's [54]

Table 5: Electrochemical properties of PAPs.

Compound	λ_{max}[a] (nm)	E_{P1}\V $_{onset-ox}$	E_{g-opt} (eV)[b]	E_{LUMO} (eV)[c]	E_{HOMO} (eV)[d]
1a	231	0.87	3.66	−2.31	−5.97
1b	233	0.75	3.76	−2.09	−5.85
3a	271	0.74	3.30	−2.54	−5.84
3b	272	0.57	3.29	−2.38	−5.67
3c	274	0.64	3.28	−2.46	−5.74
6a	252	0.76	3.43	−2.43	−5.86
6b	250	0.70	3.42	−2.38	−5.80
6c	254	0.75	3.41	−2.44	−5.85

[a]Absorption maxima measured in DCM solutions at room temperature. [b]The optical gap (E_{g-opt}) was calculated from the onset point of the absorption spectra: E_{g-opt} = 1240/λ_{onset}. [c]HOMO energy calculated from the oxidation potential: E_{HOMO} = −($V_{onset-ox}$ + 5.1) eV. [d]LUMO energy calculated from the difference between HOMO and optical gap (E_{g-opt}).

groups have established that a phenoxonium ion is formed, which is supported by further studies [37,39]. Based on this prior knowledge and our results, a mechanism for the anodic oxidation is proposed in Scheme 3. After two single-electron transfers [38], a cation is formed with two resonance structures (not counting further movement into the other aromatic rings

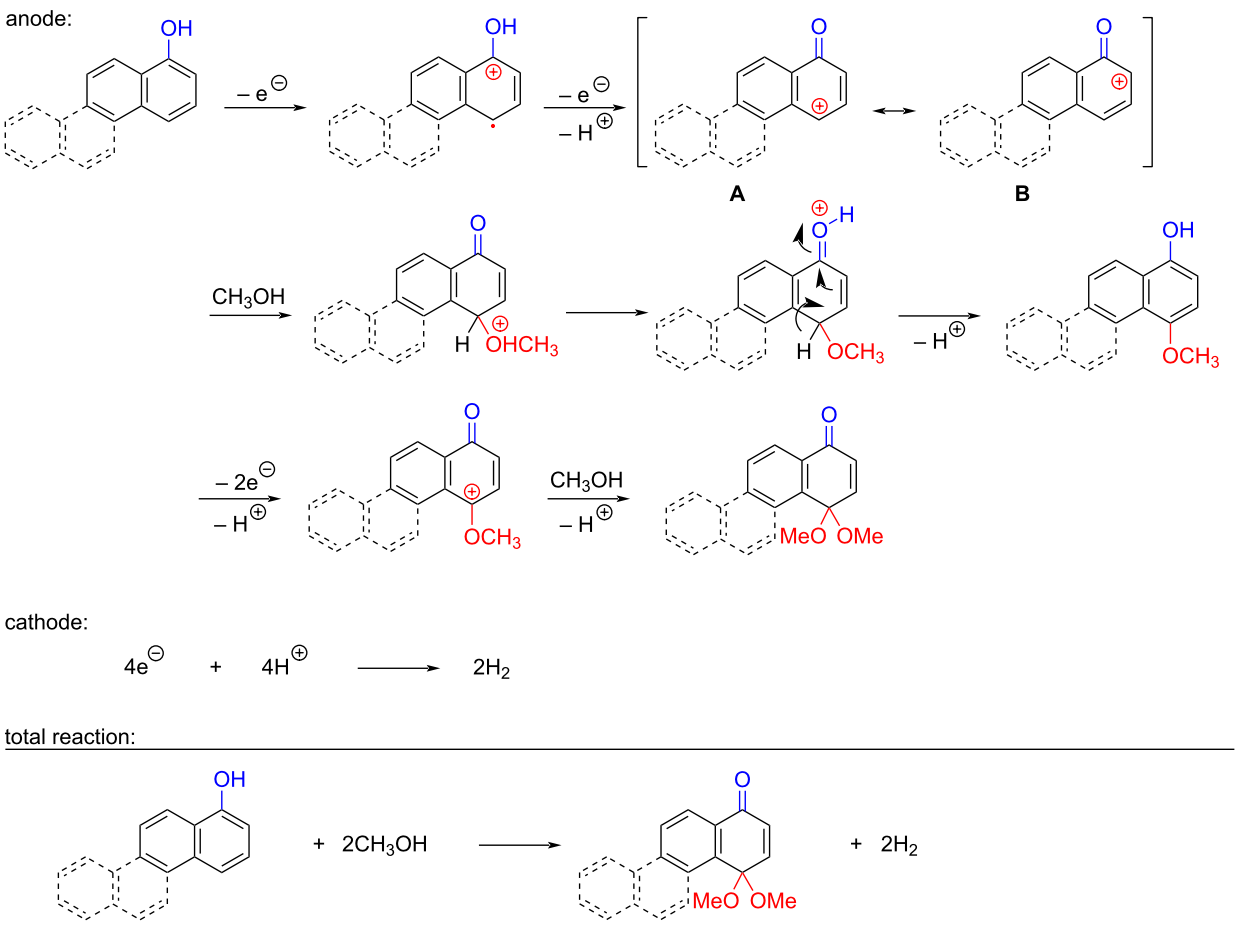

Scheme 3: Proposed mechanism for the formation of *p*-dimethoxy acetals in the anodic oxidation of **1b** and **3b**.

destroying the aromaticity of one more ring). Resonance structure **A** has the cation in a benzylic position and will be the preferred site for nucleophilic attack of methanol compared to resonance structure **B**, which is further destabilized by the neighbouring ketone. A similar resonance hybrid will be formed for molecules substituted in the 4-position, like **6b**, explaining the selectivity towards *p*-quinones. Abstraction of a proton rearomatizes the molecule before another cation is formed in the following two one-electron oxidations. The abstracted protons are reduced to hydrogen gas at the cathode.

The formation of *o*-dimethoxy acetals and thus *o*-quinones can be considered through Clar's aromatic sextet rules [55]. PAHs with more isolated and localized aromatic sextets are kinetically more stable than isomers with fewer aromatic π-sextets [56,57]. The relevant resonance structures of the phenoxonium ion of **3a**, and the Clar sextets of potential products are illustrated in Figure 2. The actual product, **7a**, has two isolated Clar sextets and should be favoured over the alternatives formed through cations **B** and **C** which have only one Clar sextet with two alternative positions.

Conclusion

The electrochemical oxidation of polycyclic aromatic phenols to quinones represents a green alternative to chemical oxidants. Hydrogen gas evolution can be handled by recycling of the reaction mixture through the electrochemical flow cell to achieve high yields. Better yields are obtained with C/Pt electrode pair and methanol in the absence of water during the oxidation. The position of the hydroxy group controls the position of the quinone acetal to form a single product. *p*-Quinones are formed when the *para*-position to the hydroxy group is available for oxidation, while *o*-quinones are formed when the *para*-position is part of the conserved polyaromatic skeleton. All results are in accordance with an oxidation mechanism going through a phenoxonium cation.

Experimental

The substrates **1a**,**b** and **6a**,**b** were obtained from our previous work [18]. Substrates **3a–c** and **6c** were synthesised by photochemical cyclisation of stilbenes [58], while **3d** was prepared according to literature [59]. The substrates were oxidized under galvanic (constant current) conditions in a Syrris Asia flow system with a 225 µL electrochemical flow cell equipped with a platinum-coated cathode and a carbon-filled PPS (polyphenylene sulfide) micro-channel anode separated by a polyetheretherketone (PEEK) gasket [40]. Further experimental details and characterization of new compounds are given in Supporting Information File 1.

General procedure A: anodic oxidation with recirculating reaction solution

The reaction solution of 0.01 M PAPs and 0.05 M Et_4NOTs was prepared by dissolving the chemicals in 3:1 MeOH/THF (10 mL). The reaction solution was circulated from a continuously stirred flask fitted with a slit septum, to the syringe pump, through the Flux cell, and back at 300 µL/min flow rate. The target current was set at 9 mA and when the voltage exceeded 3.2 V, the reaction would be stopped to avoid over-oxidation. The reaction was monitored by TLC until the substrate was consumed. After completed reaction, the system was flushed with methanol to collect all reaction mixture. The solvents were evaporated under reduced pressure, and the crude purified by column chromatography to isolate the product.

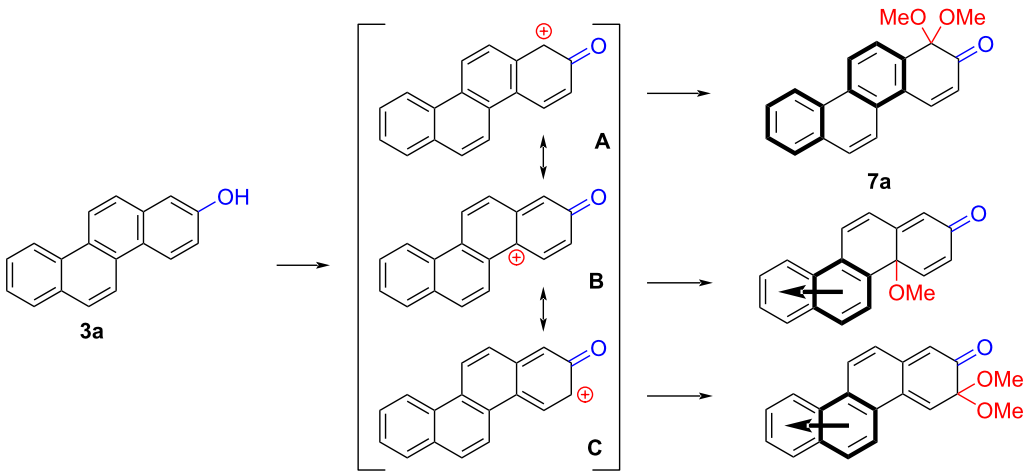

Figure 2: Resonance structures of the phenoxonium cation formed from 2-chrysenol (**3a**).

General procedure B: hydrolysis of acetals

To a solution of the quinone acetal (0.15 mmol) in acetic acid (4 mL) were added 2 drops of conc. HCl and 3–4 drops of water. The mixture was stirred at room temperature for 0.5 h and poured into ice water (5 mL). The precipitated quinone was filtered off, thoroughly washed with water, and dried under vacuum to yield the pure product.

General procedure C: combined electrochemical oxidation and hydrolysis

Following general procedure A, the reaction solution with the PAP was recirculated at 300 µL/min flow rate through the Flux Cell with 9 mA electrical current until the substrate was consumed. Solvents were removed under reduced pressure and the crude dispersed in ethyl acetate (3 × 3 mL) and filtered to remove the electrolyte. The filtrate was concentrated under reduced pressure and the crude dissolved in acetic acid (3 mL) before hydrolysis according to general procedure B.

Voltammetric studies

Voltammetric experiments were carried out using a Princeton Applied Research versaSTAT 3 potentiostat, connected to a three-electrode setup using Pt wires as working and pseudo reference electrodes and Pt mesh as counter electrode. The experimental conditions for the cyclic voltammetry (CV) scans were kept constant at 0.1 V/s. Voltammetric studies were conducted in 0.1 M tetrabutylammonium hexafluorophosphate ($[NBu_4]$ $[PF_6]$) solution in acetonitrile. The solvent was dried and degassed using N_2 prior to each experiment. All experiments were conducted at room temperature. All redox potentials were calibrated against ferrocene/ferrocenium (Fc/Fc^+) redox couple.

Supporting Information

Supporting Information File 1

Detailed experimental procedures and characterization data of new molecules together with individual cyclic voltagrams with onset potentials.
[https://www.beilstein-journals.org/bjoc/content/supplementary/1860-5397-20-153-S1.pdf]

Author Contributions

Hiwot M. Tiruye: conceptualization; data curation; investigation; resources; validation; visualization; writing – original draft. Solon Economopoulos: data curation; resources; supervision; validation; writing – review & editing. Kåre B. Jørgensen: conceptualization; data curation; funding acquisition; project administration; resources; supervision; validation; visualization; writing – review & editing.

ORCID® iDs

Hiwot M. Tiruye - https://orcid.org/0000-0002-4379-829X
Solon Economopoulos - https://orcid.org/0000-0002-2609-4602
Kåre B. Jørgensen - https://orcid.org/0000-0003-0662-1839

Data Availability Statement

All data that supports the findings of this study is available in the published article and/or the supporting information to this article.

References

1. Dahlem Junior, M. A.; Nguema Edzang, R. W.; Catto, A. L.; Raimundo, J.-M. *Int. J. Mol. Sci.* **2022,** *23,* 14108. doi:10.3390/ijms232214108
2. Zhang, L.; Zhang, G.; Xu, S.; Song, Y. *Eur. J. Med. Chem.* **2021,** *223,* 113632. doi:10.1016/j.ejmech.2021.113632
3. Patel, O. P. S.; Beteck, R. M.; Legoabe, L. J. *Eur. J. Med. Chem.* **2021,** *210,* 113084. doi:10.1016/j.ejmech.2020.113084
4. Pang, Y.; Huang, Y.; Li, W.; Feng, L.; Shen, X. *ACS Appl. Nano Mater.* **2019,** *2,* 7785–7794. doi:10.1021/acsanm.9b01821
5. Pereyra, C. E.; Dantas, R. F.; Ferreira, S. B.; Gomes, L. P.; Silva, F. P., Jr. *Cancer Cell Int.* **2019,** *19,* 207. doi:10.1186/s12935-019-0925-8
6. Klopčič, I.; Dolenc, M. S. *Chem. Res. Toxicol.* **2019,** *32,* 1–34. doi:10.1021/acs.chemrestox.8b00213
7. Flowers-Geary, L.; Bleczinski, W.; Harvey, R. G.; Penning, T. M. *Chem.-Biol. Interact.* **1996,** *99,* 55–72. doi:10.1016/0009-2797(95)03660-1
8. Shultz, C. A.; Quinn, A. M.; Park, J.-H.; Harvey, R. G.; Bolton, J. L.; Maser, E.; Penning, T. M. *Chem. Res. Toxicol.* **2011,** *24,* 2153–2166. doi:10.1021/tx200294c
9. Preuss, R.; Angerer, J.; Drexler, H. *Int. Arch. Occup. Environ. Health* **2003,** *76,* 556–576. doi:10.1007/s00420-003-0458-1
10. Zheng, J.; Cho, M.; Jones, A. D.; Hammock, B. D. *Chem. Res. Toxicol.* **1997,** *10,* 1008–1014. doi:10.1021/tx970061j
11. Snyder, R.; Witz, G.; Goldstein, B. D. *Environ. Health Perspect.* **1993,** *100,* 293–306. doi:10.1289/ehp.93100293
12. Gallagher, P. T. *Contemp. Org. Synth.* **1996,** *3,* 433–446. doi:10.1039/co9960300433
13. Zimmer, H.; Lankin, D. C.; Horgan, S. W. *Chem. Rev.* **1971,** *71,* 229–246. doi:10.1021/cr60270a005
14. Saladino, R.; Neri, V.; Mincione, E.; Marini, S.; Coletta, M.; Fiorucci, C.; Filippone, P. *J. Chem. Soc., Perkin Trans. 1* **2000,** 581–586. doi:10.1039/a908073b
15. Uyanik, M.; Mutsuga, T.; Ishihara, K. *Molecules* **2012,** *17,* 8604–8616. doi:10.3390/molecules17078604
16. Barret, R.; Daudon, M. *Tetrahedron Lett.* **1990,** *31,* 4871–4872. doi:10.1016/s0040-4039(00)97755-4
17. Wu, A.; Duan, Y.; Xu, D.; Penning, T. M.; Harvey, R. G. *Tetrahedron* **2010,** *66,* 2111–2118. doi:10.1016/j.tet.2009.12.022
18. Tiruye, H. M.; Jørgensen, K. B. *Tetrahedron* **2022,** *129,* 133144. doi:10.1016/j.tet.2022.133144
19. Schaub, T. *Chem. – Eur. J.* **2021,** *27,* 1865–1869. doi:10.1002/chem.202003544

20. Sperry, J. B.; Wright, D. L. *Chem. Soc. Rev.* **2006,** *35,* 605–621. doi:10.1039/b512308a
21. Yoshida, J.-i.; Kataoka, K.; Horcajada, R.; Nagaki, A. *Chem. Rev.* **2008,** *108,* 2265–2299. doi:10.1021/cr0680843
22. Yan, M.; Kawamata, Y.; Baran, P. S. *Chem. Rev.* **2017,** *117,* 13230–13319. doi:10.1021/acs.chemrev.7b00397
23. Möhle, S.; Zirbes, M.; Rodrigo, E.; Gieshoff, T.; Wiebe, A.; Waldvogel, S. R. *Angew. Chem., Int. Ed.* **2018,** *57,* 6018–6041. doi:10.1002/anie.201712732
24. Little, R. D. *J. Org. Chem.* **2020,** *85,* 13375–13390. doi:10.1021/acs.joc.0c01408
25. Frontana-Uribe, B. A.; Little, R. D.; Ibanez, J. G.; Palma, A.; Vasquez-Medrano, R. *Green Chem.* **2010,** *12,* 2099–2119. doi:10.1039/c0gc00382d
26. Wiebe, A.; Gieshoff, T.; Möhle, S.; Rodrigo, E.; Zirbes, M.; Waldvogel, S. R. *Angew. Chem., Int. Ed.* **2018,** *57,* 5594–5619. doi:10.1002/anie.201711060
27. Steckhan, E.; Arns, T.; Heineman, W. R.; Hilt, G.; Hoormann, D.; Jörissen, J.; Kröner, L.; Lewall, B.; Pütter, H. *Chemosphere* **2001,** *43,* 63–73. doi:10.1016/s0045-6535(00)00325-8
28. Horn, E. J.; Rosen, B. R.; Baran, P. S. *ACS Cent. Sci.* **2016,** *2,* 302–308. doi:10.1021/acscentsci.6b00091
29. Madsen, K. G.; Olsen, J.; Skonberg, C.; Hansen, S. H.; Jurva, U. *Chem. Res. Toxicol.* **2007,** *20,* 821–831. doi:10.1021/tx700029u
30. Stalder, R.; Roth, G. P. *ACS Med. Chem. Lett.* **2013,** *4,* 1119–1123. doi:10.1021/ml400316p
31. Torres, S.; Brown, R.; Szucs, R.; Hawkins, J. M.; Zelesky, T.; Scrivens, G.; Pettman, A.; Taylor, M. R. *J. Pharm. Biomed. Anal.* **2015,** *115,* 487–501. doi:10.1016/j.jpba.2015.08.010
32. Roth, G. P.; Stalder, R.; Long, T. R.; Sauer, D. R.; Djuric, S. W. *J. Flow Chem.* **2013,** *3,* 34–40. doi:10.1556/jfc-d-13-00002
33. Lehmann, M.; Scarborough, C. C.; Godineau, E.; Battilocchio, C. *Ind. Eng. Chem. Res.* **2020,** *59,* 7321–7326. doi:10.1021/acs.iecr.0c00431
34. Green, R. A.; Brown, R. C. D.; Pletcher, D. *J. Flow Chem.* **2015,** *5,* 31–36. doi:10.1556/jfc-d-14-00027
35. Nilsson, A.; Ronlán, A.; Parker, V. D. *J. Chem. Soc., Perkin Trans. 1* **1973,** 2337–2345. doi:10.1039/p19730002337
36. Nilsson, A.; Palmquist, U.; Pettersson, T.; Ronlán, A. *J. Chem. Soc., Perkin Trans. 1* **1978,** 696–707. doi:10.1039/p19780000696
37. Swenton, J. S.; Callinan, A.; Chen, Y.; Rohde, J. J.; Kerns, M. L.; Morrow, G. W. *J. Org. Chem.* **1996,** *61,* 1267–1274. doi:10.1021/jo951799d
38. Panizza, M.; Michaud, P. A.; Cerisola, G.; Comninellis, C. *J. Electroanal. Chem.* **2001,** *507,* 206–214. doi:10.1016/s0022-0728(01)00398-9
39. Shi, L.; Zheng, L.; Ning, S.; Gao, Q.; Sun, C.; Zhang, Z.; Xiang, J. *Org. Lett.* **2022,** *24,* 5782–5786. doi:10.1021/acs.orglett.2c02278
40. Asia Electrochemistry Flow Chemistry System by Syrris. https://www.syrris.com/product/asia-electrochemistry-flow-chemistry-system/ (accessed April 9, 2024).
41. Chen, C.-P.; Swenton, J. S. *J. Chem. Soc., Chem. Commun.* **1985,** 1291–1292. doi:10.1039/c39850001291
42. Hammerich, O.; Speiser, B., Eds. *Organic Electrochemistry: Revised and Expanded,* 5th ed.; CRC Press: Boca Raton, FL, USA, 2015. doi:10.1201/b19122
43. Fu, T.; Funfschilling, D.; Ma, Y.; Li, H. Z. *Microfluid. Nanofluid.* **2010,** *8,* 467–475. doi:10.1007/s10404-009-0471-0
44. Noël, T.; Cao, Y.; Laudadio, G. *Acc. Chem. Res.* **2019,** *52,* 2858–2869. doi:10.1021/acs.accounts.9b00412
45. Liu, X.; Zheng, S.; Wang, K. *Chem. Eng. J.* **2023,** *463,* 142453. doi:10.1016/j.cej.2023.142453
46. Pletcher, D.; Green, R. A.; Brown, R. C. D. *Chem. Rev.* **2018,** *118,* 4573–4591. doi:10.1021/acs.chemrev.7b00360
47. Pletcher, D.; Walsh, F. C. *Industrial Electrochemistry,* 2nd ed.; Springer Science & Business Media: Dordrecht, Netherlands, 1993. doi:10.1007/978-94-011-2154-5
48. Mascall, K. C.; Jacobi, P. A. *Tetrahedron Lett.* **2012,** *53,* 1620–1623. doi:10.1016/j.tetlet.2012.01.070
49. Mal, D.; Roy, H. N.; Hazra, N. K.; Adhikari, S. *Tetrahedron* **1997,** *53,* 2177–2184. doi:10.1016/s0040-4020(96)01119-2
50. Peover, M. E.; White, B. S. *J. Electroanal. Chem. Interfacial Electrochem.* **1967,** *13,* 93–99. doi:10.1016/0022-0728(67)80097-4
51. Cardona, C. M.; Li, W.; Kaifer, A. E.; Stockdale, D.; Bazan, G. C. *Adv. Mater. (Weinheim, Ger.)* **2011,** *23,* 2367–2371. doi:10.1002/adma.201004554
52. Mayeda, E. A.; Miller, L. L.; Wolf, J. F. *J. Am. Chem. Soc.* **1972,** *94,* 6812–6816. doi:10.1021/ja00774a039
53. Swenton, J. S.; Carpenter, K.; Chen, Y.; Kerns, M. L.; Morrow, G. W. *J. Org. Chem.* **1993,** *58,* 3308–3316. doi:10.1021/jo00064a017
54. Barba, I.; Chinchilla, R.; Gómez, C. *Tetrahedron* **1990,** *46,* 7813–7822. doi:10.1016/s0040-4020(01)90078-x
55. Clar, E. The Aromatic Sextet. In *Mobile Source Emissions Including Policyclic Organic Species;* Rondia, D.; Cooke, M.; Haroz, R. K., Eds.; Springer: Dordrecht, Netherlands, 1983; pp 49–58. doi:10.1007/978-94-009-7197-4_4
56. Solà, M. *Front. Chem. (Lausanne, Switz.)* **2013,** *1,* 22. doi:10.3389/fchem.2013.00022
57. Balaban, A. T.; Klein, D. J. *J. Phys. Chem. C* **2009,** *113,* 19123–19133. doi:10.1021/jp9082618
58. Jørgensen, K. B.; Joensen, M. *Polycyclic Aromat. Compd.* **2008,** *28,* 362–372. doi:10.1080/10406630802374580
59. Matsushima, T.; Kobayashi, S.; Watanabe, S. *J. Org. Chem.* **2016,** *81,* 7799–7806. doi:10.1021/acs.joc.6b01450

BEILSTEIN JOURNAL OF ORGANIC CHEMISTRY

Electrochemical radical cation aza-Wacker cyclizations

Sota Adachi and Yohei Okada*

Letter

Open Access

Address:
Department of Applied Biological Science, Tokyo University of Agriculture and Technology, 3-5-8 Saiwai-cho, Fuchu, Tokyo 183-8509, Japan

Email:
Yohei Okada* - yokada@cc.tuat.ac.jp

* Corresponding author

Keywords:
alkene; aza-Wacker cyclization; electrochemistry; radical cation; sulfonamide

Beilstein J. Org. Chem. **2024,** *20,* 1900–1905.
https://doi.org/10.3762/bjoc.20.165

Received: 15 April 2024
Accepted: 22 July 2024
Published: 05 August 2024

This article is part of the thematic issue "Synthetic electrochemistry".

Guest Editor: K. Lam

Abstract

Electrochemical or photochemical single-electron oxidation of bench-stable substrates can generate radical cations that offer unique reactivities as intermediates in various bond-formation processes. Such intermediates can potentially take part in both radical and ionic bond formation; however, the mechanisms involved are complicated and not fully understood. Herein, we report electrochemical radical cation aza-Wacker cyclizations under acidic conditions, which are expected to proceed via radical cations generated by single-electron oxidation of alkenes.

Introduction

Activating bench-stable substrates is the first step to driving bond formation and/or cleavage. Therefore, the discovery of new modes for activation leads to reaction advancements. Electrochemical [1-5] and photochemical [6-10] reactions that induce single-electron reduction and oxidation are widely used in modern synthetic organic chemistry [11-15]. Single-electron oxidation of bench-stable substrates can generate radical cations that offer unique reactivities as intermediates for various bond-formation processes (also true for reduction). Because the reactivities of radicals and ions are fundamentally different, their creative use may pave the way for complementary bond formation. This merging is unique and such intermediates could potentially take part in both radical and ionic bond formation. However, the mechanisms involved can be complicated and are not fully understood.

Alkenes and styrenes are representative radical cation precursors that are widely used to realize the formation of unique bonds. The respective radical cations are trapped by various nucleophiles under radical and/or ion control, where kinetic and/or thermodynamic effects are expected to be dominant. Typical examples that clearly show the difference in such reactivities are intramolecular cyclizations (Scheme 1). A radical cyclization generates a five-membered ring with a less-stable primary radical, while a six-membered ring with a secondary cation is obtained through ionic cyclization. When such intra-

molecular cyclizations are expected to proceed via radical cations, there are several interpretations of the mechanisms involved, since radical and ionic cyclizations are both possible.

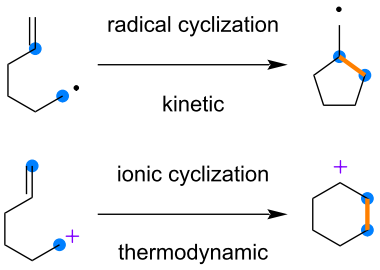

Scheme 1: Radical and ionic intramolecular cyclizations.

In this context, electrochemical and photochemical aza-Wacker cyclizations have provided interesting models for mechanistic discussion (Scheme 2). For example, Moeller reported electrochemical reactions under basic conditions, which were proposed to proceed via radicals [16-18]. Xu also reported electrochemical reactions via radicals, which were generated through proton-coupled electron transfer [19]. On the other hand, Yoon reported photochemical reactions under acidic conditions, which were proposed to proceed via radical cations [20]. Since electrochemical and photochemical aza-Wacker cyclizations can offer ring systems that are difficult to construct through state-of-the-art palladium-catalyzed methods, the mechanistic understanding of these cyclizations would be of great help to expand their synthetic utility. Described herein are electrochemical aza-Wacker cyclizations under acidic conditions, which are expected to proceed via radical cations.

Results and Discussion

The present work began by examining the electrochemical aza-Wacker cyclization using the alkene **1** as a model (Table 1). Based on the conditions reported by Yoon and Moeller, the initial screening was carried out using tetrabutylammonium triflate (Bu_4NOTf)/1,2-dichloroethane (1,2-DCE) solution. Carbon felt (CF) was used as an anode instead of reticulated vitreous carbon (RVC), with platinum (Pt) as a cathode. To our delight, a constant-current condition at 1 mA was productive, and the desired five-membered pyrrolidine **2** was obtained in high yield (Table 1, entry 2). During the screening of conditions, the addition of acetonitrile (CH_3CN) was found to be effective, probably due to the increased conductivity of the electrolyte solution (Table 1, entry 1). The reaction did not take place without electricity and most of the starting material was recovered (Table 1, entry 3). The addition of trifluoroacetic acid (TFA) was advantageous in terms of the reproducibility, which

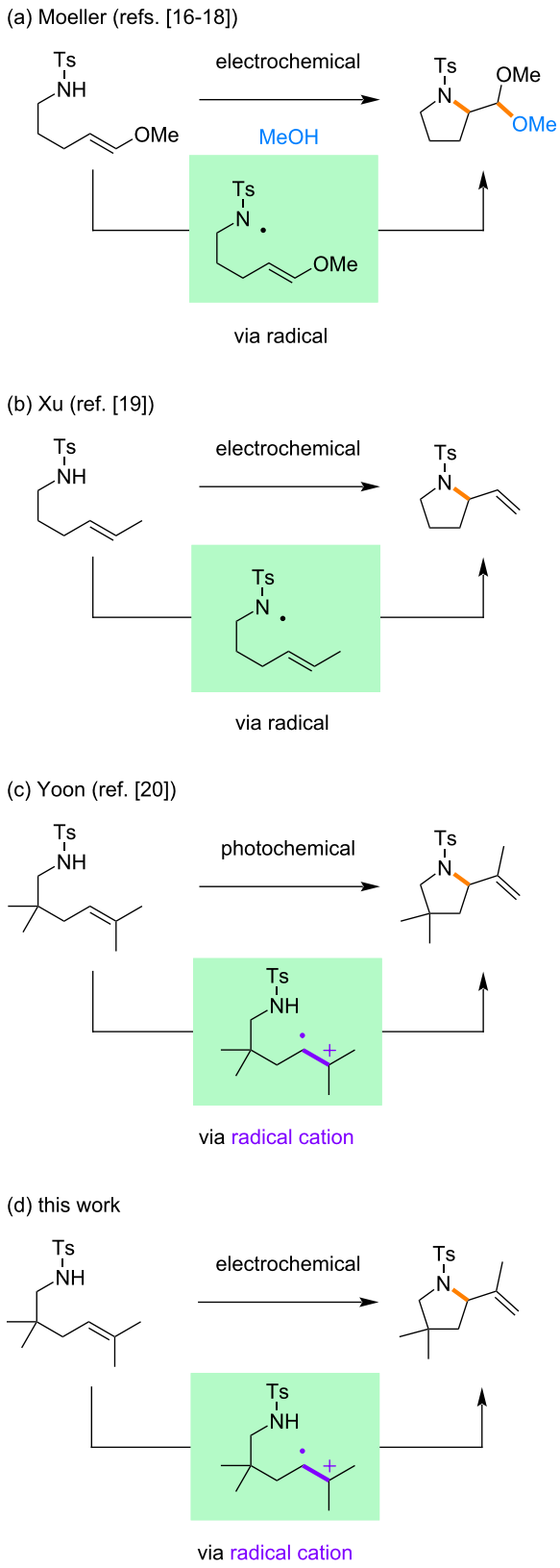

Scheme 2: Electrochemical and photochemical aza-Wacker cyclizations.

Table 1: Control studies for electrochemical aza-Wacker cyclization.[a]

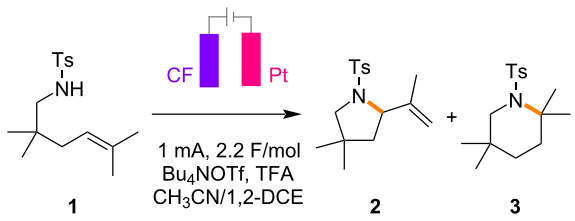

Entry	Deviation from the optimal condition	Yields of **2** + **3**[b]
1		97 (0) + 0
2	no CH_3CN	82 (0) + 0
3	no current	0 (75) + 0
4	no TFA	81 (3) + 0
5	AcOH instead of TFA	66 (5) + 0
6	constant potential at 1.8 V	74 (0) + 0
7[c]	$LiClO_4/CH_3NO_2$	0 (0) + 0
8[c]	$LiClO_4/CH_3NO_2$, no current	0 (0) + 96

[a]Reaction conditions: alkene **1** (0.20 mmol), Bu_4NOTf (0.1 M), TFA (1 equiv), CH_3CN (0.4 mL), and 1,2-DCE (3.6 mL). [b]Determined by NMR analysis. The recovered starting material is reported in parentheses. [c]$LiClO_4$ (1 M) instead of Bu_4NOTf (0.1 M).

was in good accordance with the observation reported by Yoon (Table 1, entry 4). The use of acetic acid (AcOH) instead of TFA gave a slightly lower yield of the five-membered pyrrolidine **2** (Table 1, entry 5). Although a constant-potential condition at 1.8 V was also productive, the constant-current condition gave better results (Table 1, entry 6). Previously, we reported that lithium perchlorate ($LiClO_4$)/nitromethane (CH_3NO_2) solution was an effective medium to facilitate radical cation reactions [21-25]. However, interestingly, it was not productive for the electrochemical aza-Wacker cyclization (Table 1, entry 7) and the six-membered piperidine **3**, instead of the five-membered pyrrolidine **2**, was obtained in excellent yield without electricity (Table 1, entry 8). Thus, it is proposed that the electrochemical aza-Wacker cyclization under acidic conditions proceeded via radical cations to give five-membered pyrrolidine **2**, while the six-membered piperidine **3** is formed through ionic cyclization under non-electrochemical conditions.

With the optimized conditions in hand, the scope of the electrochemical aza-Wacker cyclization was investigated (Scheme 3). Various aryl sulfonamides **4**–**6** were compatible to give the respective five-membered pyrrolidines, except for that

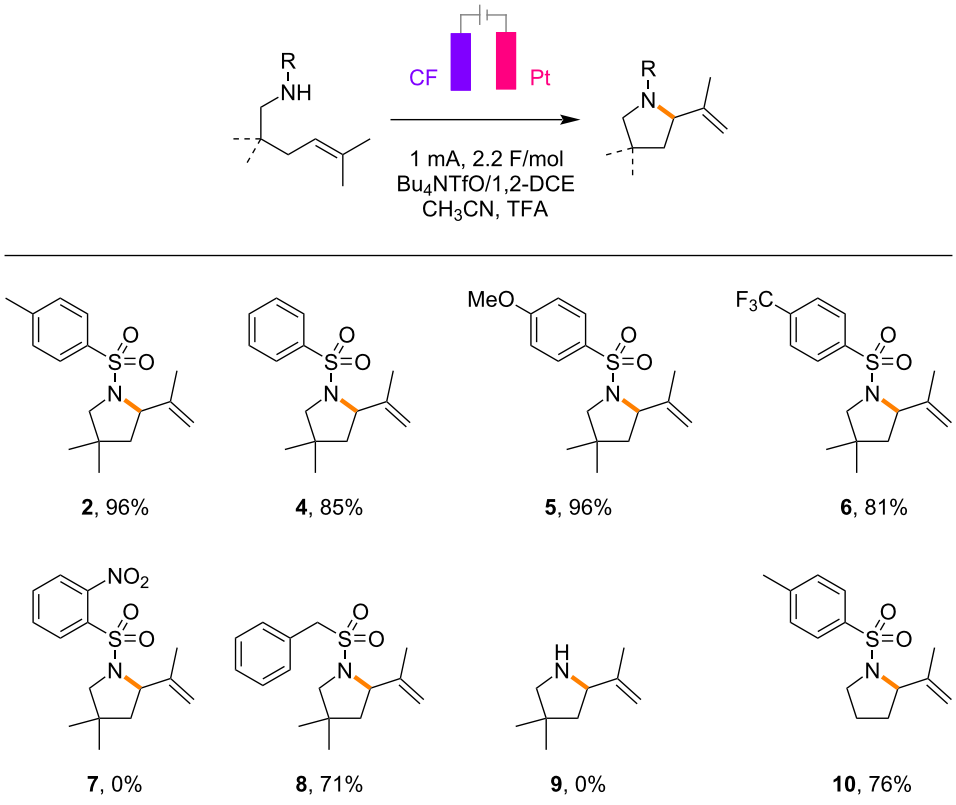

Scheme 3: Scope of electrochemical aza-Wacker cyclization. Reaction conditions: the alkene (0.20 mmol), Bu_4NOTf (0.1 M), TFA (1 equiv), CH_3CN (0.4 mL), and 1,2-DCE (3.6 mL). Yields reported here are isolated yields.

possessing a 2-nitro group **7**. As discussed later with cyclic voltammetric studies, the electron density in the aryl rings does not seem to have a significant impact on the reaction. While benzyl sulfonamide **8** was productive under the optimized conditions, unprotected amine **9** was not compatible. Although *gem*-dimethyl groups installed at the tether should have a positive impact on intramolecular cyclization, they were not essential for the reaction (**10**).

In order to obtain mechanistic insight into the aza-Wacker cyclization, differently substituted alkenes **11**, **14** were prepared and subjected to the reaction under electrochemical and non-electrochemical conditions (Scheme 4). In the case of the trisubstituted alkene **11**, the six-membered anti-Markovnikov product **12** was selectively obtained under electrochemical conditions, while the five-membered Markovnikov product **13** was obtained in good yield under non-electrochemical conditions. In the case of the tetrasubstituted alkene **14**, the five-membered pyrrolidine **15** was selectively obtained under electrochemical conditions, while both the five-membered pyrrolidine **16** and six-membered piperidine **17** were obtained in good mass balance under non-electrochemical conditions. Although the detailed mechanism remains an open question, the electrochemical aza-Wacker cyclizations might be radical reactions rather than ionic ones, since the six-membered piperidine was not obtained from the tetrasubstituted alkene **14**.

Cyclic voltammetric studies have provided further mechanistic insights into electrochemical aza-Wacker cyclizations. As reported by Yoon, a trisubstituted alkene is oxidized at significantly lower potential than aryl sulfonamides, suggesting that the reactions were initiated by single-electron oxidation of the alkenes. Although a drop in oxidation potential for the alkene was observed when tethered to an aryl sulfonamide, as detailed by Moeller, rapid intramolecular cyclization would be the key [26-28]. We also measured cyclic voltammograms for aryl sulfonamides with and without trisubstituted alkenes (Figure 1). As described above, the electron density in the aryl rings does not seem to have a significant impact on the reaction, since alkenes possessing methyl **2**, methoxy **5**, and trifluoromethyl **6** groups were all high yielding. This observation was supported by the cyclic voltammetric studies, namely, their oxidation potentials were similar. This suggests that the reactions are initiated by single-electron oxidation of alkenes instead of aryl sulfonamides, leading to unique radical cation aza-Wacker cyclizations. The cyclic voltammogram of the aryl sulfonamide without a trisubstituted alkene provides clear-cut experimental evidence of this, since the oxidation potential was recorded at a much higher value.

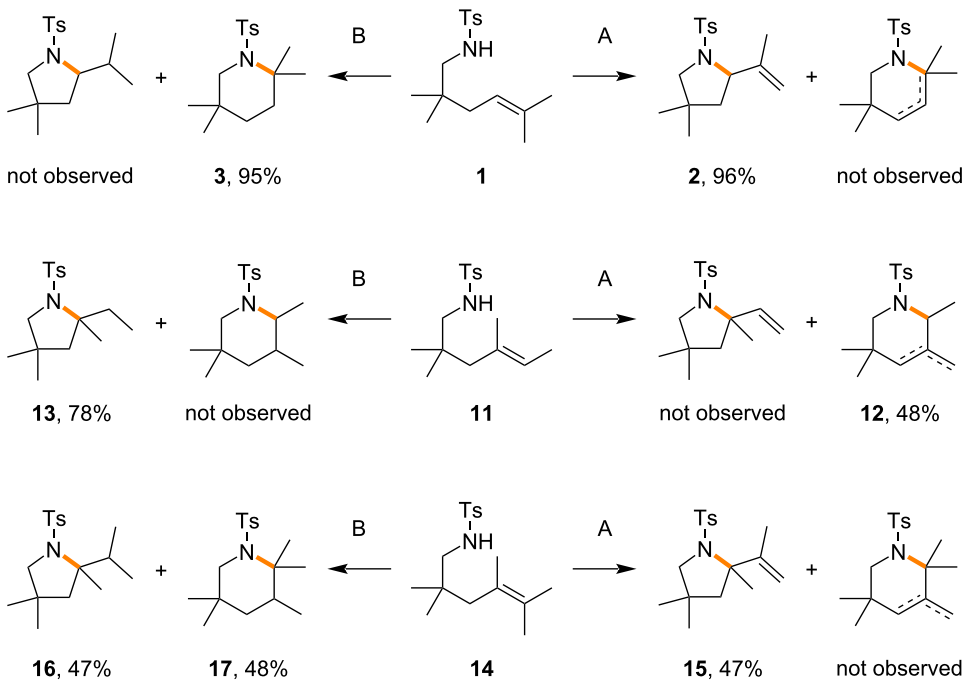

Scheme 4: Mechanistic studies of aza-Wacker cyclization. A: Electrochemical (Bu_4NOTf in CH_3CN/1,2-DCE), B: non-electrochemical ($LiClO_4$ in CH_3NO_2).

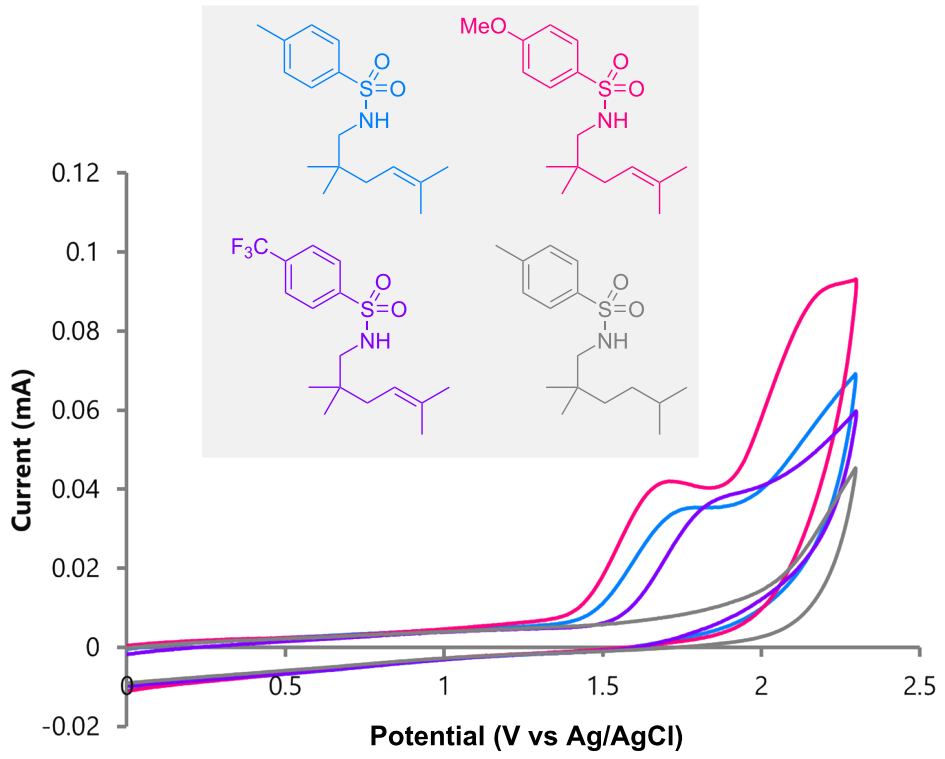

Figure 1: Cyclic voltammograms for aryl sulfonamides.

Conclusion

In conclusion, we have demonstrated that electrochemical aza-Wacker cyclizations are enabled under acidic conditions, and are expected to proceed via radical cations. Synthetic outcomes and cyclic voltammetric studies suggest that the reactions are initiated by single-electron oxidation of the alkenes instead of the aryl sulfonamides. Although the detailed mechanism remains an open question, the electrochemical radical cation aza-Wacker cyclizations might be radical reactions rather than ionic ones, since five-membered pyrrolidine formation is preferred over six-membered piperidine formation. Further mechanistic studies of the electrochemical radical cation aza-Wacker cyclizations are underway in our laboratory.

Experimental

Electrochemical aza-Wacker cyclizations: The appropriate alkene (0.20 mmol), TFA (0.20 mmol), and CH_3CN (0.4 mL) were added to a solution of Bu_4NOTf/1,2-DCE (0.10 M, 3.6 mL) while stirring at room temperature. The resulting reaction mixture was electrolyzed at 1 mA using a CF anode (10 mm × 10 mm) and a Pt cathode (10 mm × 20 mm) in an undivided cell with stirring. The solution was diluted with water and extracted with dichloromethane. The combined organic layers were dried over Na_2SO_4, filtered, and concentrated in vacuo. Yields were determined by ^1H NMR analysis using benzaldehyde as an internal standard (Table 1). Silica gel column chromatography (hexane/ethyl acetate) gave the corresponding ring compounds.

Supporting Information

Supporting Information File 1

General remarks and characterization data, including copies of ^1H and ^{13}C NMR spectra.
[https://www.beilstein-journals.org/bjoc/content/supplementary/1860-5397-20-165-S1.pdf]

Funding

This work was supported in part by JSPS KAKENHI Grant No. 22K05450 (to Y. O.), and TEPCO Memorial Foundation (to Y. O.).

Author Contributions

Sota Adachi: formal analysis; investigation; methodology. Yohei Okada: conceptualization; supervision; writing – original draft; writing – review & editing.

ORCID® iDs

Yohei Okada - https://orcid.org/0000-0002-4353-1595

Data Availability Statement

All data that supports the findings of this study is available in the published article and/or the supporting information to this article.

References

1. Chan, A. Y.; Perry, I. B.; Bissonnette, N. B.; Buksh, B. F.; Edwards, G. A.; Frye, L. I.; Garry, O. L.; Lavagnino, M. N.; Li, B. X.; Liang, Y.; Mao, E.; Millet, A.; Oakley, J. V.; Reed, N. L.; Sakai, H. A.; Seath, C. P.; MacMillan, D. W. C. *Chem. Rev.* **2022,** *122,* 1485–1542. doi:10.1021/acs.chemrev.1c00383
2. Genzink, M. J.; Kidd, J. B.; Swords, W. B.; Yoon, T. P. *Chem. Rev.* **2022,** *122,* 1654–1716. doi:10.1021/acs.chemrev.1c00467
3. Holmberg-Douglas, N.; Nicewicz, D. A. *Chem. Rev.* **2022,** *122,* 1925–2016. doi:10.1021/acs.chemrev.1c00311
4. Allen, A. R.; Noten, E. A.; Stephenson, C. R. J. *Chem. Rev.* **2022,** *122,* 2695–2751. doi:10.1021/acs.chemrev.1c00388
5. Twilton, J.; Le, C.; Zhang, P.; Shaw, M. H.; Evans, R. W.; MacMillan, D. W. C. *Nat. Rev. Chem.* **2017,** *1,* 0052. doi:10.1038/s41570-017-0052
6. Yan, M.; Kawamata, Y.; Baran, P. S. *Chem. Rev.* **2017,** *117,* 13230–13319. doi:10.1021/acs.chemrev.7b00397
7. Kärkäs, M. D. *Chem. Soc. Rev.* **2018,** *47,* 5786–5865. doi:10.1039/c7cs00619e
8. Malapit, C. A.; Prater, M. B.; Cabrera-Pardo, J. R.; Li, M.; Pham, T. D.; McFadden, T. P.; Blank, S.; Minteer, S. D. *Chem. Rev.* **2022,** *122,* 3180–3218. doi:10.1021/acs.chemrev.1c00614
9. Wiebe, A.; Gieshoff, T.; Möhle, S.; Rodrigo, E.; Zirbes, M.; Waldvogel, S. R. *Angew. Chem., Int. Ed.* **2018,** *57,* 5594–5619. doi:10.1002/anie.201711060
10. Möhle, S.; Zirbes, M.; Rodrigo, E.; Gieshoff, T.; Wiebe, A.; Waldvogel, S. R. *Angew. Chem., Int. Ed.* **2018,** *57,* 6018–6041. doi:10.1002/anie.201712732
11. Huang, H.; Steiniger, K. A.; Lambert, T. H. *J. Am. Chem. Soc.* **2022,** *144,* 12567–12583. doi:10.1021/jacs.2c01914
12. Murray, P. R. D.; Cox, J. H.; Chiappini, N. D.; Roos, C. B.; McLoughlin, E. A.; Hejna, B. G.; Nguyen, S. T.; Ripberger, H. H.; Ganley, J. M.; Tsui, E.; Shin, N. Y.; Koronkiewicz, B.; Qiu, G.; Knowles, R. R. *Chem. Rev.* **2022,** *122,* 2017–2291. doi:10.1021/acs.chemrev.1c00374
13. Tay, N. E. S.; Lehnherr, D.; Rovis, T. *Chem. Rev.* **2022,** *122,* 2487–2649. doi:10.1021/acs.chemrev.1c00384
14. Liu, J.; Lu, L.; Wood, D.; Lin, S. *ACS Cent. Sci.* **2020,** *6,* 1317–1340. doi:10.1021/acscentsci.0c00549
15. Barham, J. P.; König, B. *Angew. Chem., Int. Ed.* **2020,** *59,* 11732–11747. doi:10.1002/anie.201913767
16. Xu, H.-C.; Moeller, K. D. *J. Am. Chem. Soc.* **2008,** *130,* 13542–13543. doi:10.1021/ja806259z
17. Xu, H.-C.; Moeller, K. D. *J. Am. Chem. Soc.* **2010,** *132,* 2839–2844. doi:10.1021/ja910586v
18. Campbell, J. M.; Xu, H.-C.; Moeller, K. D. *J. Am. Chem. Soc.* **2012,** *134,* 18338–18344. doi:10.1021/ja307046j
19. Huang, C.; Li, Z.-Y.; Song, J.; Xu, H.-C. *Angew. Chem., Int. Ed.* **2021,** *60,* 11237–11241. doi:10.1002/anie.202101835
20. Reed, N. L.; Lutovsky, G. A.; Yoon, T. P. *J. Am. Chem. Soc.* **2021,** *143,* 6065–6070. doi:10.1021/jacs.1c02747
21. Okada, Y.; Chiba, K. *Chem. Rev.* **2018,** *118,* 4592–4630. doi:10.1021/acs.chemrev.7b00400
22. Okada, Y. *Electrochemistry* **2020,** *88,* 497–506. doi:10.5796/electrochemistry.20-00088
23. Okada, Y. *Chem. Rec.* **2021,** *21,* 2223–2238. doi:10.1002/tcr.202100029
24. Shida, N.; Imada, Y.; Okada, Y.; Chiba, K. *Eur. J. Org. Chem.* **2020,** 570–574. doi:10.1002/ejoc.201901576
25. Imada, Y.; Yamaguchi, Y.; Shida, N.; Okada, Y.; Chiba, K. *Chem. Commun.* **2017,** *53,* 3960–3963. doi:10.1039/c7cc00664k
26. Moeller, K. D.; Tinao, L. V. *J. Am. Chem. Soc.* **1992,** *114,* 1033–1041. doi:10.1021/ja00029a036
27. Xu, H.-C.; Moeller, K. D. *Angew. Chem., Int. Ed.* **2010,** *49,* 8004–8007. doi:10.1002/anie.201003924
28. Moeller, K. D. *Chem. Rev.* **2018,** *118,* 4817–4833. doi:10.1021/acs.chemrev.7b00656

License and Terms

BEILSTEIN JOURNAL OF ORGANIC CHEMISTRY

Novel oxidative routes to *N*-arylpyridoindazolium salts

Oleg A. Levitskiy, Yuri K. Grishin and Tatiana V. Magdesieva*

Full Research Paper

Open Access

Address:
Chemistry Department, Lomonosov Moscow State University, Leninskie Gory, 1/3, Moscow, 119234, Russia

Email:
Tatiana V. Magdesieva* - tvm@org.chem.msu.ru

* Corresponding author

Keywords:
anodic oxidation; diarylamines; electrochemical cyclization; pyridoindazolium salts; reversible ring closure

Beilstein J. Org. Chem. **2024,** *20,* 1906–1913.
https://doi.org/10.3762/bjoc.20.166

Received: 17 April 2024
Accepted: 25 July 2024
Published: 07 August 2024

This article is part of the thematic issue "Synthetic electrochemistry".

Guest Editor: K. Lam

Abstract

A novel facile approach to *N*-arylpyridoindazolium salts is proposed, based on direct oxidation of the *ortho*-pyridine substituted diarylamines, either using bis(trifluoroacetoxy)iodobenzene as an oxidant, or electrochemically, via potentiostatic oxidation. Electrochemical synthesis occurs under mild conditions; no chemical reagents are required except electric current. Both approaches can be considered as a late-stage functionalization; easily available *ortho*-pyridyl-substituted diarylamines are used as the precursors.

Introduction

Aromatic polyfused N-heterocycles are of interest as a popular structural motif of many biologically active alkaloids and other molecules of therapeutic interest [1-4]. Polycyclic N-heteroaromatics also often exhibit intercalating properties [5-9].

Pyridoindazolium salts can be considered as one of the typical representatives of polyfused N-heteroaromatics. However, this type of compounds is relatively rare. To the best of our knowledge, only three *N*-alkylpyridoindazolium salts [4,7,10,11] and the only *N*-aryl derivative [12] have been reported till now (Scheme 1). Meanwhile, these new ring systems are suitable for biological investigations, they exhibit significant bioactivity [4] and can be used as intercalating agents [7].

The very limited scope of these practically useful compounds is mainly attributed to the lack of convenient synthetic approaches to them. Thus, the only example of *N*-arylpyridoindazolium salts was obtained via intramolecular cyclization of perfluorinated phenylpyrilium salts using arylhydrazine [12]; the process is based on the fluorine nucleophilic substitution thus limiting its applicability to a wider range of substrates.

Pyridyl-substituted diarylamines may be considered as the possible precursors for *N*-arylpyridoindazolium salts. The oxidative behavior of substituted diarylamines is known to be very diverse and strongly influenced by the substituents in the phenyl rings as well as by the type of the oxidant. Diarylamines can serve as precursors for a wide variety of practically useful compounds such as diarylnitroxides [13-19], *N*,*N*-diarylbenzidines [20,21], *N*,*N*-diaryldihydrophenazines [20,21] and some others. Therefore, the selectivity issue is of primary importance. The

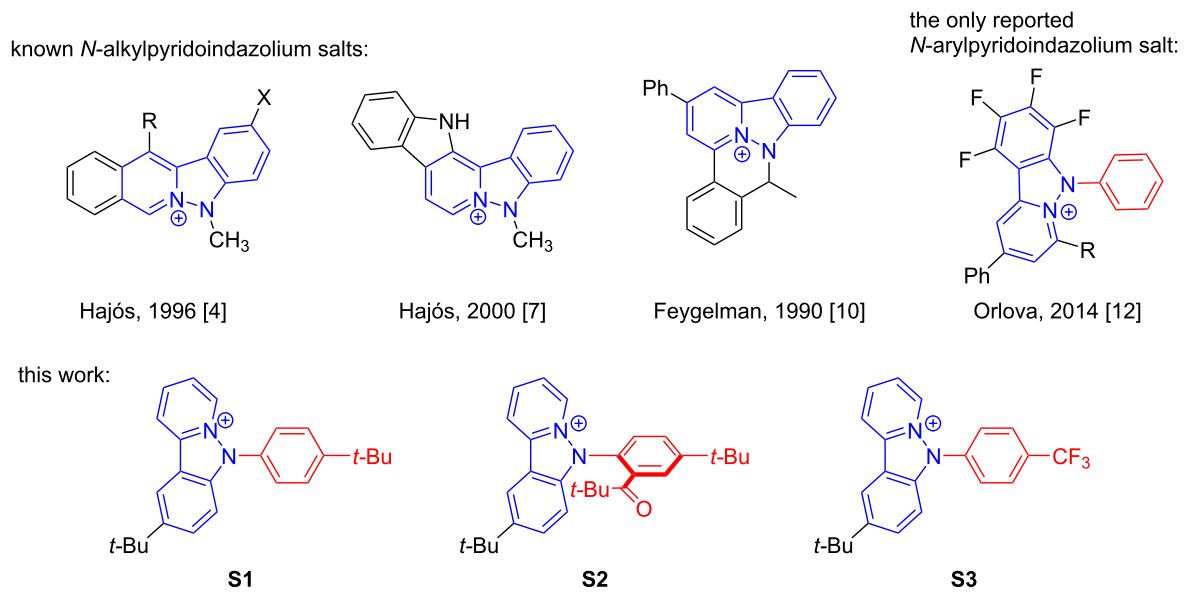

Scheme 1: Pyridoindazolium salts known to date and obtained in the present work.

guidelines for prediction of the dominant reaction path in the competing oxidative transformations of variously substituted diphenylamines yielding *N*,*N*-diarylbenzidines and *N*,*N*-diaryldihydrophenazines were reported in [21]. By varying the reaction conditions and additional substituents in the phenyl rings, a possibility for the selective oxidation of *ortho*-(2-pyridyl)diphenylamine to the corresponding nitroxide, as well as the oxidation of both N-centers was demonstrated in [19]. The wide variety of the subsequent reaction channels for the radical cations formed under chemical or electrochemical oxidation of diarylamines, as well as availability of variously substituted diarylamines make them perspective starting compounds for organic synthesis.

In the present paper, convenient, easily reproducible, straightforward synthetic routes to *N*-arylpyridoindazolium salts were elaborated, based on both electrochemical and chemical (using bis(trifluoroacetoxy)iodobenzene, PIFA) oxidation of the *ortho*-pyridine-substituted diarylamines. Voltammetry studies of the electrochemical behavior of the novel pyridoindazolium salts and the starting diarylamines were performed confirming a possibility for their reversible redox interconversion.

Results and Discussion

Chemical oxidation

Three previously reported *ortho*-pyridine-substituted diarylamines containing electron-donating and electron-withdrawing groups were taken as the starting compounds (Scheme 2). As an oxidant, bis(trifluoroacetoxy)iodobenzene (PIFA) was used. It allowed obtaining the targeted heterocyclic cations in practical 49–54% yield for all starting diarylamines. Notably, a minor amount (5%) of the *N*,*N*'-diaryldihydrophenazine radical cation that is the byproduct corresponding to the intermolecular oxidative C–N coupling of the diarylamine **A1** was detected in the reaction mixture. This emphasizes that the both processes are of the same nature and proceed through the same intermediate (i.e., the diarylamines' radical cation) and indicates the dominance of the intramolecular cyclization over the intermolecular C–N coupling process. Oxidation of diarylamines in the presence of an excess of trifluoroacetic acid gave no targeted pyridoindazolium salts, whereas the amount of diaryldihydrophenazine was increased (10%). Thus, protonation completely suppressed the intramolecular cyclization route.

Heterocyclic salts **S1**–**S3** were obtained as amorphous solids, soluble in polar solvents (acetonitrile, DMF, acetone) and chlorinated hydrocarbons ($CHCl_3$, CH_2Cl_2).

The structure of new *N*-arylpyridoindazolium salts **S1**–**S3** was confirmed with HRMS and ^1H, ^{13}C and ^{19}F NMR data; the complete assignment of the signals was performed using 2D NMR methods. The N–N bond formation was additionally confirmed via comparison of the ^1H spectra for the salts and their diarylamine precursors. The absence of the signals corresponding to the acidic protons in the spectra of the salts excluded protonation of the pyridyl or amino groups. The downfield shift of the signals of both the *N*-aryl ring (for 0.5–1 ppm) and the pyridyl moiety (for more than 1 ppm) confirmed the positive charge delocalization over both N atoms and

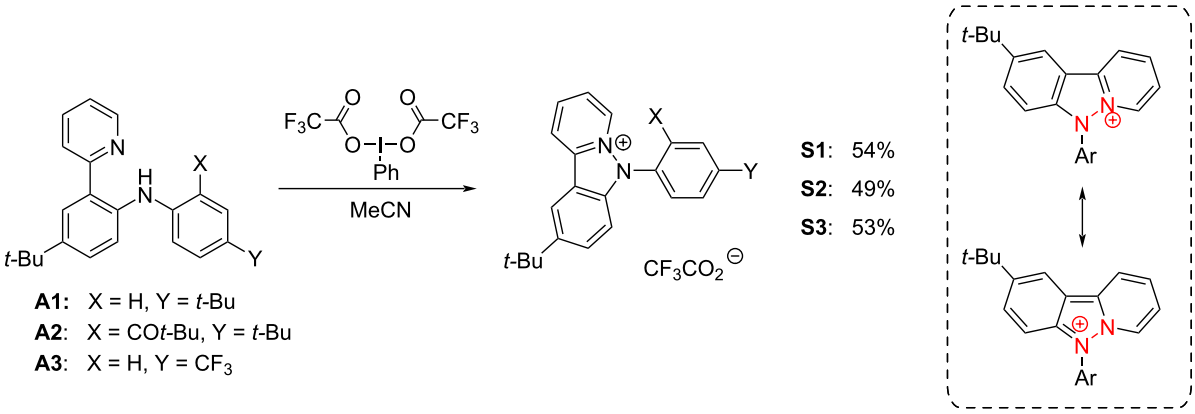

Scheme 2: Synthesis of **S1–S3** salts using PIFA as an oxidant and the resonance structures demonstrating the electron density distribution in pyridoindazolium salts.

the involvement of the amines' lone pair in the new 14-e aromatic system (Scheme 2).

One of the possible functionalities of the new compounds may be the utility of the charged aromatic fragment as an efficient leaving group in the $S_N(Ar)$ reactions, similarly to dibenzothiophenium triflates that have been recently reported as substrates for nucleophilic substitutions using potassium fluoride [22]. The study is in progress now.

Voltammetry characterization of the *N*-arylpyridoindazolium salts **S1–S3** and their precursors, diarylamines **A1–A3**

The electrochemical investigation of the new salts was performed at a Pt electrode in MeCN solution using Bu_4NBF_4 as a supporting electrolyte. Oxidation of the salts occurs at high positive potentials (>2 V vs Ag/AgCl, $KCl_{(sat.)}$, Figure 1a), in accordance with the cationic nature of the heterocycle. In the negative potential range, an irreversible peak can be observed in the −1.2V to −1.3 V region (Table 1). In case of **S2**, the second reduction peak corresponds to the reduction of the carbonyl group. Thus, the electrochemical window for the new salts exceeds 3.5 V; that makes their molten forms perspective for application as ionic liquids.

As follows from Table 1, oxidation of the starting amines **A1–A3** occurs at ca. 1–1.1 V vs Ag/AgCl, $KCl_{(sat.)}$. The electrochemical study of PIFA reduction showed a broad irreversible peak with the onset potential value of +0.93 V (vs Ag/AgCl, $KCl_{(sat.)}$). Thus, it is sufficiently strong to perform oxidation of diarylamines **A1–A3,** as it has been confirmed by the experimental results given in Scheme 2 above.

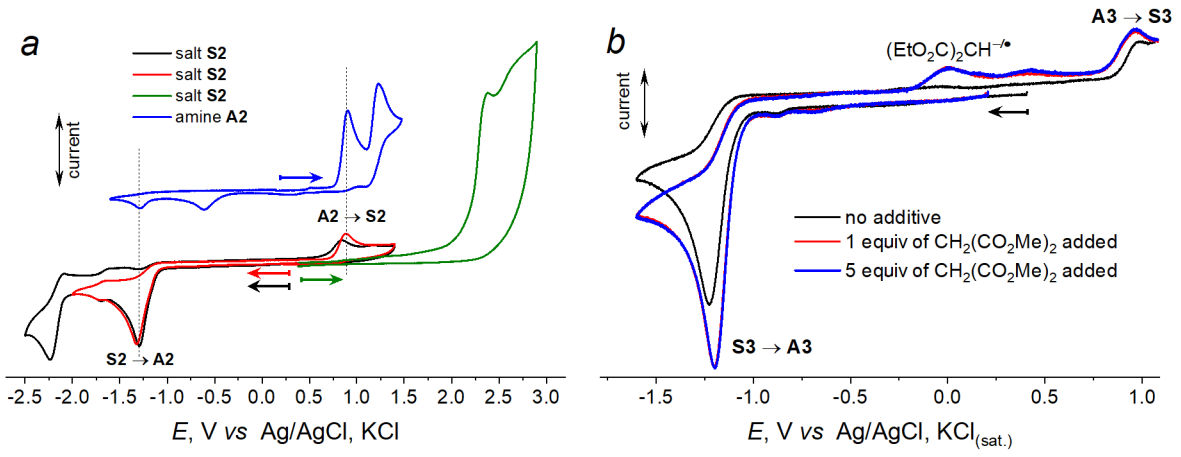

Figure 1: CV curves for salt **S2** and corresponding amine **A2** (left, Figure 1a) and salt **S3** with and without diethyl malonate additives (right, Figure 1b). (Pt, MeCN, 0.1 M Bu_4NBF_4, 0.1 V/s, vs Ag/AgCl, $KCl_{(sat.)}$.

Table 1: Peak potential values for the reduction of salts **S1**–**S3** (E^{pc}_{salt}, V) and oxidation of the corresponding diaryl amines **A1**–**A3** (E^{pa}_{amine}).

Salt	E^{pc}_{salt}, V[a]	Amine	E^{pa}_{amine}, V[b]
S1	–1.34	**A1**	1.03
S2	–1.29; –2.23	**A2**	1.07
S3	–1.23	**A3**	1.14

[a]In MeCN, 0.1 M Bu_4NBF_4, 0.1 V/s, glassy carbon disc electrode, vs Ag/AgCl, $KCl_{(sat.)}$; [b]in DMF, 0.1 M NaOTs, 0.1 V/s, Pt disc electrode, vs Ag/AgCl, $KCl_{(sat.)}$

Comparison of the CV curves measured for *N*-arylpyridoindazolium salts **S1**–**S3** and their precursors – the diarylamines – sheds light of the nature of the electrochemical process. In Figure 1a, it is shown for salt **S2**. If the direction of the potential sweep is changed after passing the first reduction peak of salt **S2**, the new peak appears at the potential of 0.89 V that completely coincides with the first oxidation peak of the amine precursor. The CV curve for the diarylamine, in its turn, exhibited (in the reverse scan after oxidation of the amine) a new reduction peak that coincides to the first reduction peak of the pyridoindazolium salt (one more peak at less negative potential in the reverse scan after amine oxidation corresponds to the reduction of the protonated pyridyl moiety of the diarylamine). Thus, the voltammetry testing confirmed that oxidation of the pyridyl-containing amines results in the intramolecular heterocyclization yielding pyridoindazolium salts. The reduction of *N*-arylpyridoindazoliums in the presence of a source of protons restores the starting diarylamines. Redox-interconversion between diarylamines **A1**–**A3** and *N*-arylpyridoindazoliums **S1**–**S3** can be presented in the following scheme (Scheme 3).

Anions formed after two-electron reduction of *N*-arylpyridoindazolium salts are strong bases and can be considered as electrogenerated proton sponges. That was demonstrated taken salt **S3** as an example. Addition of relatively weak H-donors such as diethyl malonate significantly increases the reduction current of **S3** and shifts the potential value for 30 mV toward positive potentials (Figure 1b). In the reverse scan, a new peak appears, corresponding to oxidation of the malonate anion [23]; the peak of the amine oxidation is increased.

Electrochemical synthesis of pyridoindazolium salts

The results of the voltammetry testing allowed to assume that pyridoindazolium salts can also be obtained using an anodic synthesis. Electric current as a reagent is inherently safe and easily scalable; electrosynthesis is in line with the green chemistry requirements [24]. To test the assumption, the preparative oxidation of amine **A1** was performed in the potentiostatic mode at 1.6 V (vs Ag/AgCl, $KCl_{(sat.)}$) in a two-compartment cell in DMF; sodium tosylate was used as a supporting electrolyte. After a charge corresponding to 2 F per mole of amine **A1** was passed through the solution, the targeted salt **S1** was isolated in a promising 45% yield (Scheme 4).

To find the optimal conditions, a base (2,6-lutidine) was added in the reaction mixture. A base is required to bind a proton released in the diarylamine oxidation. Our experiments with the acid additives (see above) showed that protonation of the pyridyl group suppresses the pyridoindazolium salt formation. Voltammetry testing also showed that 2,6-lutidine addition facilitates oxidation of the amine (Figure 2); the peak potential was of 100 mV shifted toward negative potentials. The pyridoindazolium salt reduction is also sensitive to the presence of a

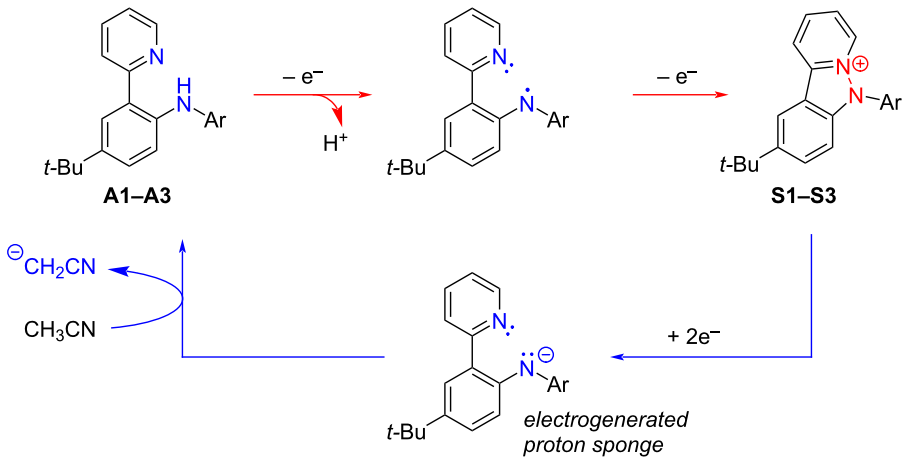

Scheme 3: Redox-interconversion between diarylamines **A1**–**A3** and *N*-arylpyridoindazoliums **S1**–**S3**.

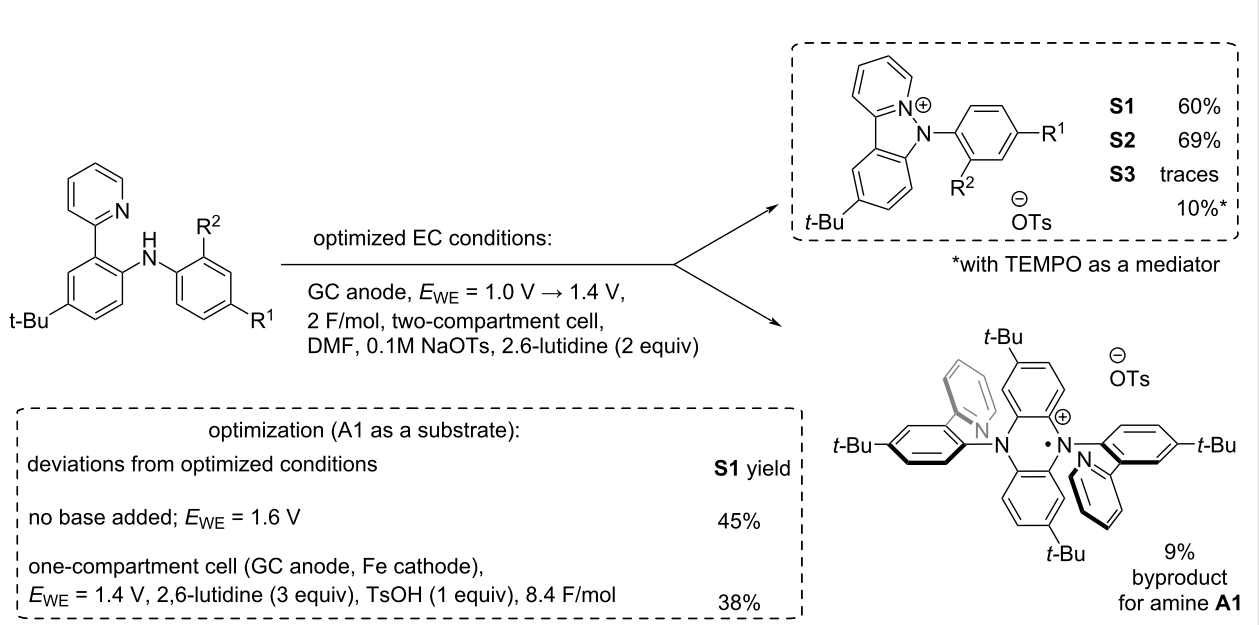

Scheme 4: Electrochemical approach to pyridoindazolium salts.

base since the electron transfer is followed by a protonation chemical step.

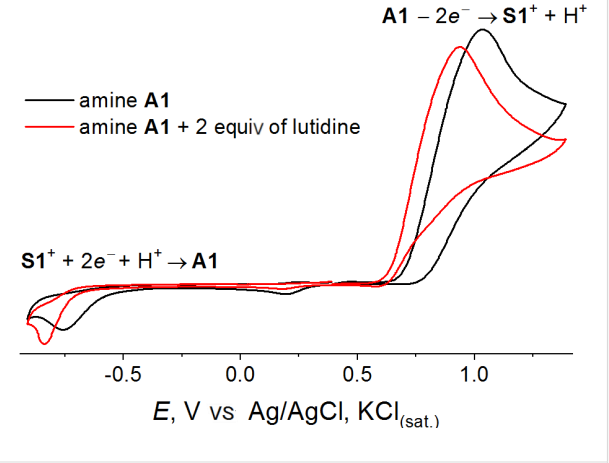

Figure 2: CV curves for amine **A1** without the lutidine additive (black curve) and after addition of 2 equiv (red curve). DMF, 0.1 M NaOTs, 0.1 V/s, Pt disc electrode, vs Ag/AgCl, $KCl_{(sat.)}$

Indeed, a bulk electrolysis of amine **A1** in the presence of 2,6-lutidine gave much better (60%) yield of salt **S1**. Additionally, the electrolysis potential was decreased (since lutidine facilitates amines' oxidation): the starting potential was set as 1.0 V and was gradually increased to 1.4 V. The attempt to perform the electrolysis in a one-compartment cell was unsuccessful: the yield of the salt dropped to 38%.

Thus, the optimized conditions of the potentiostatic electrolysis were the following: a two-compartment cell, a glassy carbon (GC) anode, DMF, the potential increased from 1.0 V to 1.4 V vs Ag/AgCl, $KCl_{(sat.)}$), 2 F per mol of amine electricity passed, sodium tosylate (0.1 M) as a supporting electrolyte, and 2 equiv of 2.6-lutidine added. Bulk oxidation of amine **A2** under the optimized conditions gave the corresponding pyridoindazolium salt **S2** in a practical 69% yield.

It should be noted that a small amount of the oxidized *N*,*N*-diaryldihydrophenazine (5–10%) was also detected in the reaction mixture after the electrolysis of **A1**, similarly to the chemical oxidation. The radical cation of dihydrophenazine formed was isolated and studied using ESR and HRMS methods. The ESR spectrum (see Supporting Information File 1) was typical for this type of compounds: a characteristic quintet due to hyperfine splitting on two equivalent nitrogen atoms (a_N = 6.56 G) as well as additional triplet splitting provided by hyperfine interaction with a pair of equivalent protons (a_H = 1.89 G). In contrast, only traces of this admixture were detected for the diarylamines with electron-withdrawing substituents. This is in line with our previous mechanistic study [20,21] which revealed that the intermolecular C–N and C–C couplings are disfavored in case of the diarylamines with two electron-deficient phenyl rings.

To our surprise, the procedure did not work in the case of amine **A3**: only traces of pyridoindazolium salt **S3** were detected in the post-electrolysis mixture. Instead, a complex mixture of prod-

ucts was obtained. It looks as if the oxidation is non-selective; not a single reaction path dominates. This is typical for diarylamines containing electron-withdrawing substituents in both rings; commonly, electrochemical oxidation yields an inseparable mixture [21]. In case of amine **S2**, the electron-donating *tert*-butyl group in the *para*-position compensates the electron-withdrawing influence of the *ortho*-acyl substituent. This prevents formation of the phenazine byproduct (the *ortho*-position is occupied) in favor of the targeted process of the pyridoindazolium salt formation.

It is not entirely clear why the electrochemical approach does not work for amine **A3** in contrast to its chemical oxidation that was successful. Our experiments with the variation of the solvent (CH_3CN and DMF), changing the supporting electrolyte (the replacement of NaOTs for more basic CF_3CO_2Na), addition of lutidine did not help.

To solve the problem, the mediatory oxidation of **A3** was also tried. Three possible mediators were tested: TEMPO, bis(4-*tert*-butylphenyl)nitroxide and tris(4-bromphenyl)amine. The voltammetry testing was performed in DMF using TsONa as a supporting electrolyte. As follows from Figure 3, the tertiary amine is inappropriate due to its too anodic oxidation potential whereas the two nitroxide radicals might be suitable. Indeed, an increase in the oxidation current of a mediator was observed in both cases after **A3** has been added into the reaction mixture (Figure 4a,b). Notably, the effect was more pronounced in the presence of lutidine, especially in the case of TEMPO. The difference between the oxidation potential of **A3** and the potential of the TEMPO/TEMPO$^+$ redox couple is rather significant (ca. 0.35 V); the base additives make oxidation of amines less anodic (due to the H-bonding and facilitation of deprotonation of the radical cations), thus narrowing the potential gap.

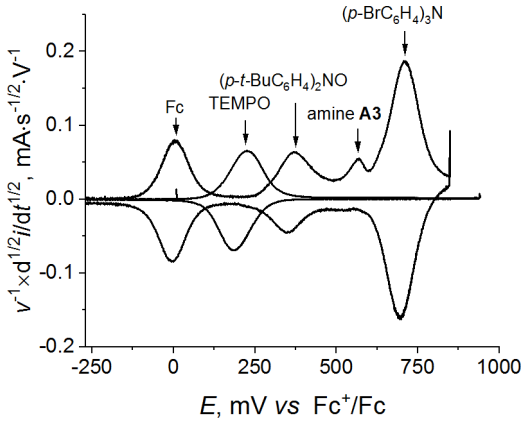

Figure 3: Semi-differential CV curves for the mediators (TEMPO, bis(4-*tert*-butylphenyl)nitroxide and tris(4-bromphenyl)amine) and amine **A3** in DMF/TsONa solution (0.1 V/s, Pt).

Preparative experiments were performed under the same conditions as described above: A one-compartment cell, DMF, 0.25 mol equiv of a mediator was added. Potentiostatic electrolyses were carried out at the potential of the mediator oxidation. The current was dropped down after ca. 1.5 equivalents of electricity has been passed through the solution. Analysis of the reaction mixtures showed that in both cases a certain amount of the target salt **S3** was formed. When TEMPO was used as a mediator, **S3** was isolated in 10% yield, along with the starting amine (18%) and the tetraarylhydrazine as the main product (50%). In the case of the diarylnitroxide, a complicated multicomponent reaction mixture was formed. Besides the products

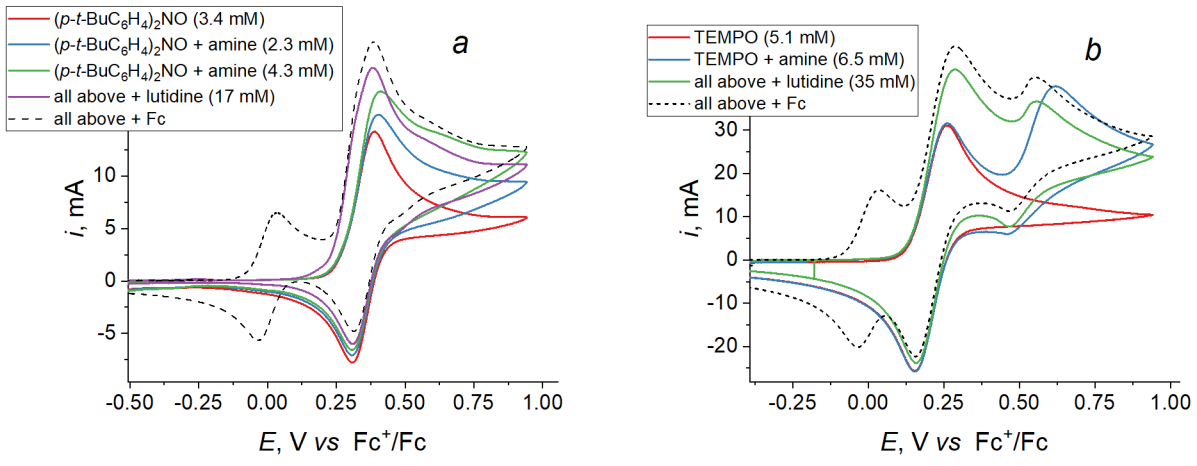

Figure 4: CV curves of bis(4-*tert*-butylphenyl)nitroxide (a) and TEMPO (b) with amine **A3** and 2,6-lutidine added (DMF/TsONa, 0.1 V/s, Pt).

mentioned above, it contained some other compounds, which have not been identified.

Among the amines studied, amine **A3** is less prone to oxidation (due to the electron-withdrawing effect of the trifluoromethyl group) and is the less basic; the presence of a lutidine base even more fastens deprotonation of the radical cation formed in oxidation. Since oxidation occurs in the bulk and the potential of the mediator is insufficient for the further oxidation of the electrophilic CF_3-substituted diarylaminyl radicals to the corresponding cations, the N–N coupling of thus formed aminyl radicals dominates over the intramolecular cyclization. This oxidation path is inherent to non-bulky amines of low basicity in the presence of a base [20,25]. In our case, the base is required to prevent acidification of the reaction mixture.

Conclusion

A novel facile approach to *N*-arylpyridoindazolium salts was proposed, based on direct oxidation of the *ortho*-pyridine-substituted diarylamines. The oxidation can be performed either chemically, using bis(trifluoroacetoxy)iodobenzene as the oxidant, or electrochemically, via potentiostatic oxidation. The electrochemical synthesis occurs under mild conditions; no chemical reagents are required except electric current. Both approaches can be considered as a late-stage functionalization; the easily available *ortho*-pyridyl-substituted diarylamines are used as the precursors. The direct approaches to *N*-arylpyridoindazolium salts elaborated herein open a route to broadening a scope of these practically useful compounds with multiple functionalities that were poorly available previously.

Supporting Information

Supporting Information File 1

Analytical data, NMR and MS spectra.
[https://www.beilstein-journals.org/bjoc/content/supplementary/1860-5397-20-166-S1.pdf]

Funding

This work was supported by Russian Science Foundation (Project number 22-73-00040). The NMR part of this work was supported by M. V. Lomonosov Moscow State University Program of Development.

Author Contributions

Oleg A. Levitskiy: funding acquisition; investigation; methodology. Yuri K. Grishin: investigation. Tatiana V. Magdesieva: conceptualization; writing – original draft; writing – review & editing.

ORCID® iDs

Tatiana V. Magdesieva - https://orcid.org/0000-0003-2173-652X

Data Availability Statement

All data that supports the findings of this study is available in the published article and/or the supporting information to this article.

References

1. Amariucai-Mantu, D.; Mangalagiu, V.; Bejan, I.; Aricu, A.; Mangalagiu, I. I. *Pharmaceutics* **2022,** *14,* 2026. doi:10.3390/pharmaceutics14102026
2. Taylor, A. P.; Robinson, R. P.; Fobian, Y. M.; Blakemore, D. C.; Jones, L. H.; Fadeyi, O. *Org. Biomol. Chem.* **2016,** *14,* 6611–6637. doi:10.1039/c6ob00936k
3. Khajuria, R.; Rasheed, S.; Khajuria, C.; Kapoor, K.; Das, P. *Synthesis* **2018,** *50,* 2131–2149. doi:10.1055/s-0036-1589533
4. Timári, G.; Soós, T.; Hajós, G.; Messmer, A.; Nacsa, J.; Molnár, J. *Bioorg. Med. Chem. Lett.* **1996,** *6,* 2831–2836. doi:10.1016/s0960-894x(96)00521-5
5. Julino, M.; Stevens, M. F. G. *J. Chem. Soc., Perkin Trans. 1* **1998,** 1677–1684. doi:10.1039/a800575c
6. Pastor, J.; Siró, J.; García-Navío, J.; Vaquero, J. J.; Melia Rodrigo, M.; Ballesteros, M.; Alvarez-Builla, J. *Bioorg. Med. Chem. Lett.* **1995,** *5,* 3043–3048. doi:10.1016/0960-894x(95)00532-4
7. Csányi, D.; Hajós, G.; Riedl, Z.; Timári, G.; Bajor, Z.; Cochard, F.; Sapi, J.; Laronze, J.-Y. *Bioorg. Med. Chem. Lett.* **2000,** *10,* 1767–1769. doi:10.1016/s0960-894x(00)00339-5
8. Sharma, V.; Gupta, M.; Kumar, P.; Sharma, A. *Curr. Pharm. Des.* **2021,** *27,* 15–42. doi:10.2174/1381612826666201118113311
9. Rescifina, A.; Zagni, C.; Varrica, M. G.; Pistarà, V.; Corsaro, A. *Eur. J. Med. Chem.* **2014,** *74,* 95–115. doi:10.1016/j.ejmech.2013.11.029
10. Tymyanskii, Y. R.; Feygelman, V. M.; Makarova, N. I.; Knyazhanskii, M. I.; Kharlanov, V. A.; Orekhovskii, V. S.; Zhdanova, M. P.; Zvezdina, E. A. *J. Photochem. Photobiol., A* **1990,** *54,* 91–97. doi:10.1016/1010-6030(90)87012-z
11. Messmer, A.; Hajós, G. Y.; Gelléri, A.; Radics, L. *Tetrahedron* **1986,** *42,* 5415–5426. doi:10.1016/s0040-4020(01)82093-7
12. Kargapolova, I. Y.; Shmuilovich, K. S.; Rybalova, T. V.; Orlova, N. A.; Shelkovnikov, V. V. *Russ. Chem. Bull.* **2014,** *63,* 723–730. doi:10.1007/s11172-014-0498-6
13. Magdesieva, T. *Electrochem. Sci. Adv.* **2022,** *2,* e2100182. doi:10.1002/elsa.202100182
14. Magdesieva, T. V.; Levitskiy, O. A. *Russ. Chem. Rev.* **2018,** *87,* 707–725. doi:10.1070/rcr4769
15. Dulov, D.; Levitskiy, O.; Bogdanov, A.; Magdesieva, T. *ChemistrySelect* **2021,** *6,* 9653–9656. doi:10.1002/slct.202102626
16. Levitskiy, O. A.; Dulov, D. A.; Bogdanov, A. V.; Magdesieva, T. V. *Eur. J. Org. Chem.* **2019,** 6225–6231. doi:10.1002/ejoc.201900961
17. Levitskiy, O. A.; Eremin, D. B.; Bogdanov, A. V.; Magdesieva, T. V. *Eur. J. Org. Chem.* **2017,** 4726–4735. doi:10.1002/ejoc.201700947
18. Levitskiy, O. A.; Sentyurin, V. V.; Bogdanov, A. V.; Magdesieva, T. V. *Mendeleev Commun.* **2016,** *26,* 535–537. doi:10.1016/j.mencom.2016.11.026
19. Levitskiy, O. A.; Bogdanov, A. V.; Klimchuk, I. A.; Magdesieva, T. V. *ChemPlusChem* **2022,** *87,* e202100508. doi:10.1002/cplu.202100508
20. Dulov, D.; Rumyantseva, A.; Levitskiy, O.; Nefedov, S.; Magdesieva, T. *ChemistrySelect* **2021,** *6,* 9769–9775. doi:10.1002/slct.202102906

21. Levitskiy, O. A.; Dulov, D. A.; Nikitin, O. M.; Bogdanov, A. V.; Eremin, D. B.; Paseshnichenko, K. A.; Magdesieva, T. V. *ChemElectroChem* **2018,** *5,* 3391–3410. doi:10.1002/celc.201801177
22. Schüll, A.; Grothe, L.; Rodrigo, E.; Erhard, T.; Waldvogel, S. R. *Org. Lett.* **2024,** *26,* 2790–2794. doi:10.1021/acs.orglett.3c02921
23. Cheng, S.; Hawley, M. D. *J. Org. Chem.* **1985,** *50,* 3388–3392. doi:10.1021/jo00218a028
24. Cembellín, S.; Batanero, B. *Chem. Rec.* **2021,** *21,* 2453–2471. doi:10.1002/tcr.202100128
25. Cauquis, G.; Delhomme, H.; Serve, D. *Electrochim. Acta* **1975,** *20,* 1019–1026. doi:10.1016/0013-4686(75)85066-3

BEILSTEIN JOURNAL OF ORGANIC CHEMISTRY

Harnessing the versatility of hydrazones through electrosynthetic oxidative transformations

Aurélie Claraz

Review

Open Access

Address:
Institut de Chimie des Substances Naturelles, CNRS, Univ. Paris-Saclay, 1 Avenue de la Terrasse, 91198 Gif-sur-Yvette Cedex, France

Email:
Aurélie Claraz - aurelie.claraz@cnrs.fr

Keywords:
C–H functionalization; diazo compound; electrosynthesis; hydrazone; nitrogen-containing heterocycle

Beilstein J. Org. Chem. **2024,** *20,* 1988–2004.
https://doi.org/10.3762/bjoc.20.175

Received: 14 April 2024
Accepted: 23 July 2024
Published: 14 August 2024

This article is part of the thematic issue "Synthetic electrochemistry".

Guest Editor: K. Lam

Abstract

Hydrazones are important structural motifs in organic synthesis, providing a useful molecular platform for the construction of valuable compounds. Electrooxidative transformations of hydrazones constitute an attractive opportunity to take advantage of the versatility of these reagents. By directly harnessing the electrical current to perform the oxidative process, a large panel of organic molecules can be accessed from readily available hydrazones under mild, safe and oxidant-free reaction conditions. This review presents a comprehensive overview of oxidative electrosynthetic transformations of hydrazones. It includes the construction of azacycles, the C(sp^2)−H functionalization of aldehyde-derived hydrazones and the access to diazo compounds as either synthetic intermediates or products. A special attention is paid to the reaction mechanism with the aim to encourage further development in this field.

Introduction

Hydrazones represent an important class of organic compounds. They can be readily prepared through the condensation of hydrazine derivatives with aldehydes or ketones. They have found widespread applications in materials sciences and supramolecular chemistry [1-5]. Importantly, they are versatile reagents in organic synthesis. They have for instance been frequently employed for the construction of azacycles through various cyclization protocols or cycloaddition reactions [6-10]. Early work in this field includes the well-known Fischer indole synthesis [11]. Additionally, they have been harnessed as valuable intermediates in Wolff–Kishner reduction reactions [12-14] or for the synthesis of various olefins via diazo or vinyllithium intermediates in the Bamford–Stevens reaction [15] and Shapiro reaction [16], respectively [17]. SAMP/RAMP ((*S*)/(*R*)-1-amino-2-methoxymethylpyrrolidine)hydrazones could be also key intermediates for the asymmetric synthesis of α-substituted aldehydes and ketones [18,19]. Interestingly, depending on the substitution pattern, the C=N bond can feature different electronic properties [20]. For instance, various hydrazones have been employed for the asymmetric preparation of chiral amines

through the addition of nucleophilic partners [21,22] while the azaenamine character of some aldehyde-derived hydrazones has been demonstrated in the coupling with suitable electrophiles such as Michael acceptors [23,24]. Last but not least, the C=N bond of hydrazones can act as radical acceptors for the synthesis of functionalized amines or hydrazones through reductive functionalization [21,25,26] or oxidative C(sp^2)–H functionalization [27,28], respectively. Consequently, given their rich reactivity profile, exploring new synthetic transformations of hydrazones is of significant importance and can contribute to the formation of novel organic compounds.

Electrosynthesis enables the generation of either radical, radical ionic or ionic species [29] under mild and environmentally friendly reaction conditions [30,31]. The direct use of electrical current to drive oxidative and reductive processes precludes the reliance on toxic or dangerous redox reagents [32]. The explosive renewal of interest in this technology and the resulting recent achievements have brought it at the forefront of organic synthesis. Electrooxidative transformations of hydrazones offer appealing opportunities to take advantage of the versatility of this reagent. Such an approach can either ameliorate the previous methods in a more sustainable and efficient fashion or provide a mean for the discovery of new reactivity. Herein, this review aims to give an overview of the state of the art in the electrochemical oxidative transformations of hydrazones. It is organized in four main parts: (i) synthesis of azacycles, (ii) synthesis of functionalized hydrazones through C(sp^2)–H functionalization of aldehyde-derived hydrazones, (iii) access to diazo compounds, and (iv) synthesis of miscellaneous compounds. For reactions carried out under constant current electrolysis, the reported current applied (in A or mA) is depicted. Additionally, when possible, and for better accuracy, the current density (in mA·cm^{-2}) has been calculated based on the size of the electrode portion immersed in the solution, as described in the experimental section. This information is provided in brackets.

Review

Synthesis of azacycles

Nitrogen-containing heterocyclic compounds possess numerous applications in various domains such as materials science, agrochemistry and medicinal chemistry. Especially, 60% of all FDA-approved drugs in the United States contain at least one azacycle [33]. Therefore, the development of gentle and efficient methods for accessing these heterocycles is an ongoing pursuit for synthetic chemists. As mentioned above, with their two nitrogen atoms, hydrazones constitute unique synthons for constructing azacycles. Resorting to electrochemical approaches furnishes original compounds. Although the first report dates back to 1974, this tool has only been seriously considered in the last 15 years.

Oxidative cyclization of hydrazones

In 1974, Tabaković et al. published the oxidative cyclization of 2-acetylpyridine-derived *N*-phenylhydrazone **1a** to form triazolopyridinium salt **2a** [34]. The process was further applied to various 2-acetylpyridine and 2-benzoylpyridine derivatives (Scheme 1) [35,36]. The corresponding pyridinium salts **2** were obtained in high yields when the electrolysis was conducted in a divided cell under potentiostatic conditions at 1.2–1.65 V vs SCE in acetonitrile.

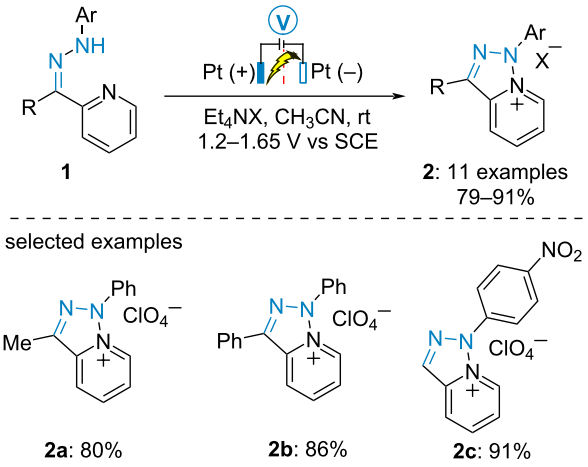

Scheme 1: Synthesis of triazolopyridinium salts [34-36].

In 1976, the same group reported the anodic cyclization of chalcone-derived *N*-phenylhydrazone **3** to pyrazole **4** in a divided cell at constant current (Scheme 2) [37]. The obtained poor yield was explained by the formation of dimeric side products. Cyclic voltammetry analysis suggested an initial anodic single electron transfer (SET) to radical cation **5**, cyclization and deprotonation. Subsequent SET oxidation in solution by **5** led to cation **7**. Final deprotonation furnished aromatic cycle **4**.

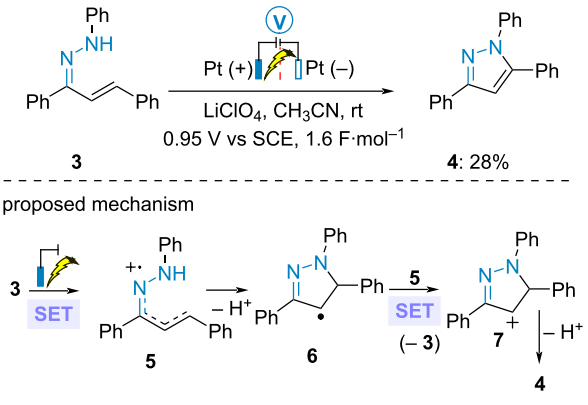

Scheme 2: Synthesis of pyrazoles [37].

In 2022, Zhang et al. documented the synthesis of 1*H*-indazoles **9** via the electrooxidative cyclization of (hetero)aromatic ketones-derived *N*-phenylhydrazones **8** (Scheme 3) [38]. In contrast with the above-mentioned works, the electrolysis was carried out in an undivided cell under galvanostatic conditions. High yields were obtained regardless of the electronic properties of the substituents on the *N*-phenyl ring. When dissymmetric diaryl ketone-derived substrates were employed, the C–N bond formation occurred selectively on the most electron rich aromatic ring. According to the proposed mechanism, this dehydrogenative cyclization of hydrazones initiated with the SET anodic oxidation of the hydrazone and deprotonation to form the *N*-centered radical **10**. After aza-cyclization on the aromatic ring, a second SET oxidation and deprotonation delivered the heterocycle **9**. This mechanism was supported by cyclic voltammetry analysis of a model substrate (1-(diphenylmethylene)-2-(4-nitrophenyl)hydrazine), which displayed three oxidation peaks (0.9, 1.7 and 2.2 V vs Ag^+/Ag in HFIP). The authors assumed that the two first peaks would correspond to the oxidation of **8** to **10** and **11** to **12** and that the oxidation of **10** would be responsible for the final one, which is consistent with the finding of ketone side-product.

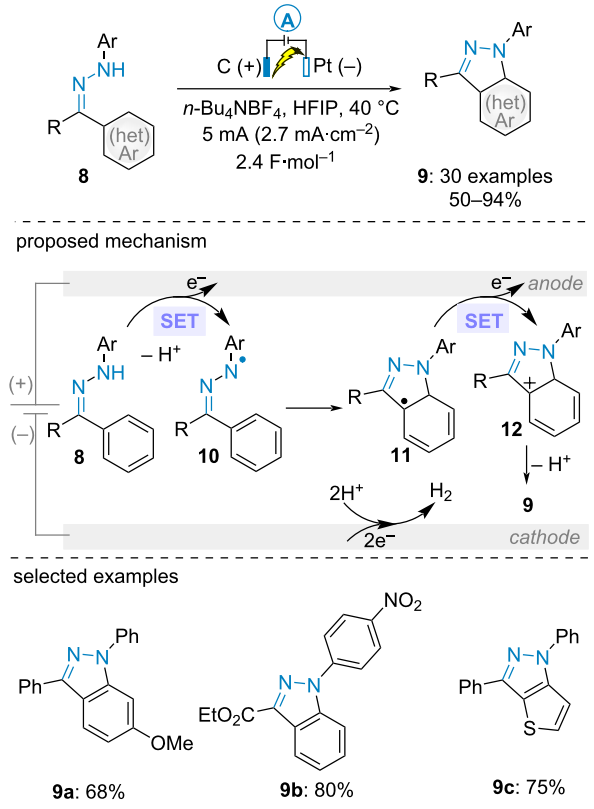

Scheme 3: Synthesis of indazoles from ketone-derived hydrazones [38].

In 2018, the group of Zhang established an intramolecular C(sp^2)–H functionalization of aldehyde-derived *N*-(2-pyridinyl)hydrazones **15** to produce 1,2,4-triazolo[4,3-*a*]pyridines **16** (Scheme 4) [39]. Interestingly, the hydrazone was in situ prepared prior to the electrolysis through the condensation of 2-hydrazinopyridine **13** and various aromatic, aliphatic and α,β-unsaturated aldehydes **14**. The electrooxidative transformation was performed under constant current at 7 mA in a mixture of acetonitrile and water under heating. From a mechanistic point of view, the authors proposed the formation of *N*-pyridyl radical **18** through the anodic oxidation of in situ-generated anion **17**. Subsequent radical cyclization, second anodic cyclization and deprotonation yielded the fused heterocycle **16**.

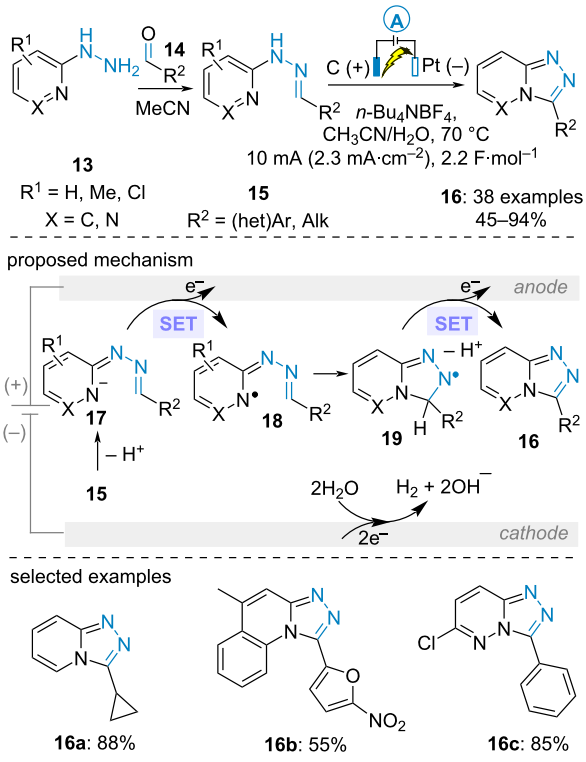

Scheme 4: Intramolecular C(sp^2)–H functionalization of aldehyde-derived *N*-(2-pyridinyl)hydrazones for the synthesis of 1,2,4-triazolo[4,3-*a*]pyridines [39].

Similarly, Youssef and Alajimi disclosed the electrochemical synthesis of pyrazolo[4,3-*c*]quinoline derivatives **22** from 7-chloro-4-hydrazinoquinolines **20** and aromatic aldehydes **21** (Scheme 5) [40].

In 1992, Chiba and Okimoto reported the electrooxidative cyclization of aldehyde and ketone-derived *N*-acylhydrazones **23a** and **23b** to build 1,3,4-oxadiazoles **24a** and Δ^3-1,3,4-oxadiazolines **24b**, respectively. Using sodium methoxide as basic sup-

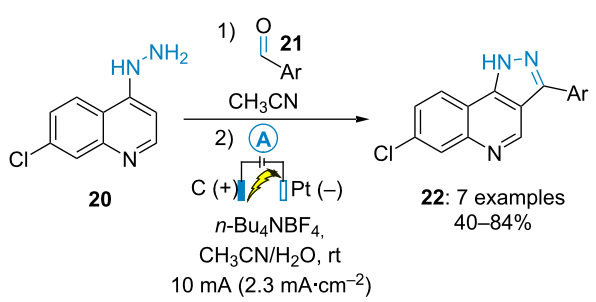

Scheme 5: Synthesis of pyrazolo[4,3-*c*]quinoline derivatives [40].

porting electrolyte in a divided cell equipped with carbon rod anodes and a platinium coil cathode, the transformation would involve cyclization of carbocationic species **25** to form the intermediate **26**. From **23a** (R^2 = H), the latter would undergo deprotonation delivering the oxadiazole **24a**. Alternatively, from **23b** ($R^2 \neq$ H), nucleophilic addition of methanol to oxycarbenium **26b** yielded the oxadiazoline **24b** (Scheme 6) [41,42].

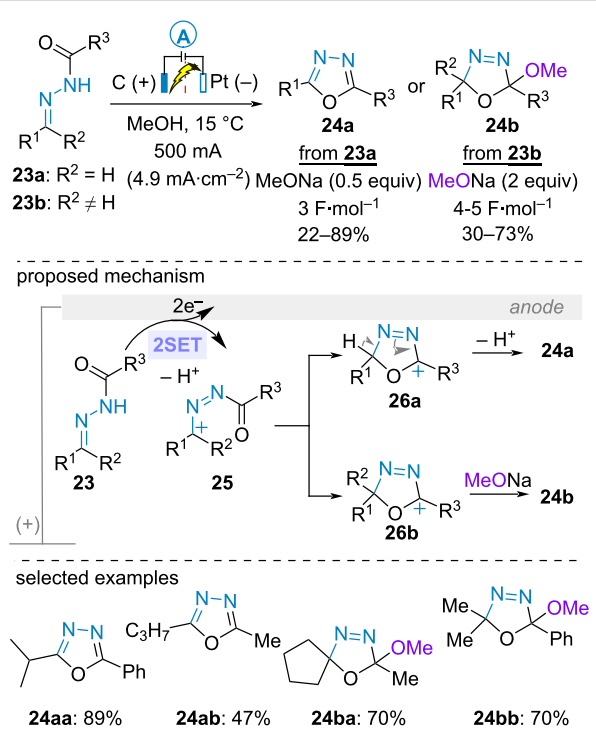

Scheme 6: Synthesis of 1,3,4-oxadiazoles and Δ^3-1,3,4-oxadiazolines [41].

In 2020, Lei, Zhang and Gao et al. described the electrooxidative cyclization of in situ-generated α-keto acid-derived *NH*-acylhydrazones to build 1,3,4-oxadiazole derivatives in good yields. The electrolysis was conducted under galvanostatic conditions in methanol using a carbon graphite anode and a platinum cathode. From a mechanistic point of view, in situ condensation of acylhydrazines **28** with α-keto acids **27** produced hydrazones **29**. After deprotonation, the authors proposed that the carboxylate anion underwent SET anodic oxidation/decarboxylation/radical cyclization sequence to form radical intermediates **34**. Subsequent second anodic oxidation and deprotonation yielded the desired heteroaromatic 5-membered rings **30**. Importantly, a control experiment using benzaldehyde-derived *N*-benzoylhydrazone delivered the corresponding 1,3,4-oxadiazole in only 25% yield. This result indicates that benzaldehyde-derived hydrazone is a less probable reaction intermediate, thereby supporting the proposed mechanism (Scheme 7) [43].

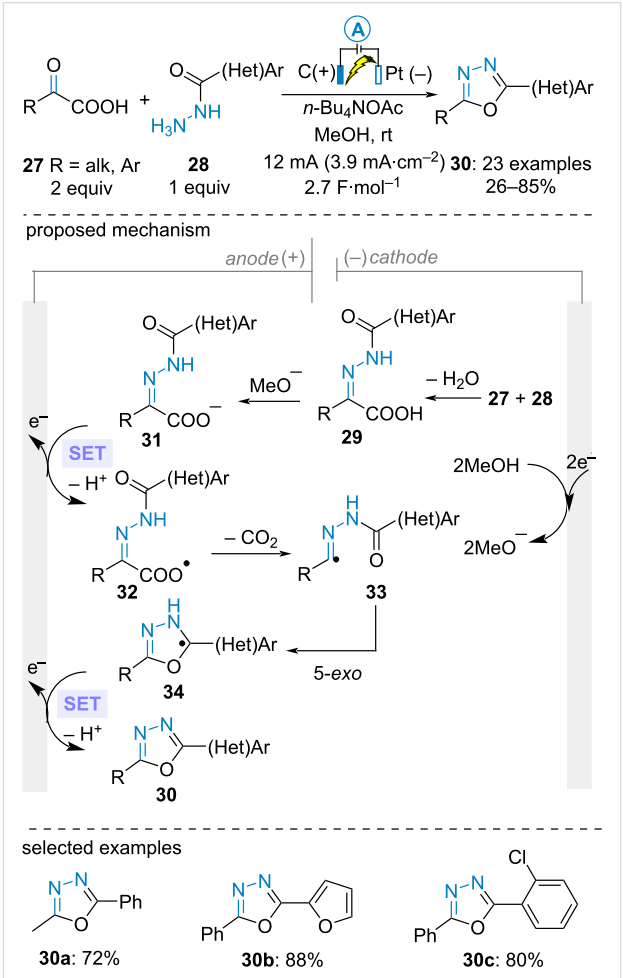

Scheme 7: Synthesis of 1,3,4-oxadiazoles [43].

In parallel, Sheng and Zhang et al. found that 2-(1,3,4-oxadiazol-2-yl)aniline derivatives **38** could be electrochemically synthesized from isatins **35** and acylhydrazine **36**. The transformation was carried out in an undivided cell at high temperature in DMSO using potassium iodide as supporting electrolyte with potassium carbonate as a base and two platinum electrodes.

Mechanistically, condensation of the two reactants formed isatin-derived acylhydrazone **37**. Hydrolysis of the latter in the presence of the inorganic base gave rise to potassium carboxylate **39**. Meanwhile, two consecutive SET oxidations of the iodide anion generated molecular iodine which reacted with **39** to furnish unstable hypoiodous anhydride **40**, thereby triggering the key CO_2 extrusion. The resulting C(sp^2)-centered radical **42** underwent a SET anodic oxidation/cyclization/deprotonation sequence to yield the oxadiazole derivative **38**. As such, the iodide electrolyte served as an electromediator to both promote the decarboxylation process and protect the aniline product from overoxidation. Importantly, a control experiment without electricity but in the presence of molecular iodine instead proceeded smoothly, thereby confirming the critical role of in situ-generated molecular iodine (Scheme 8) [44].

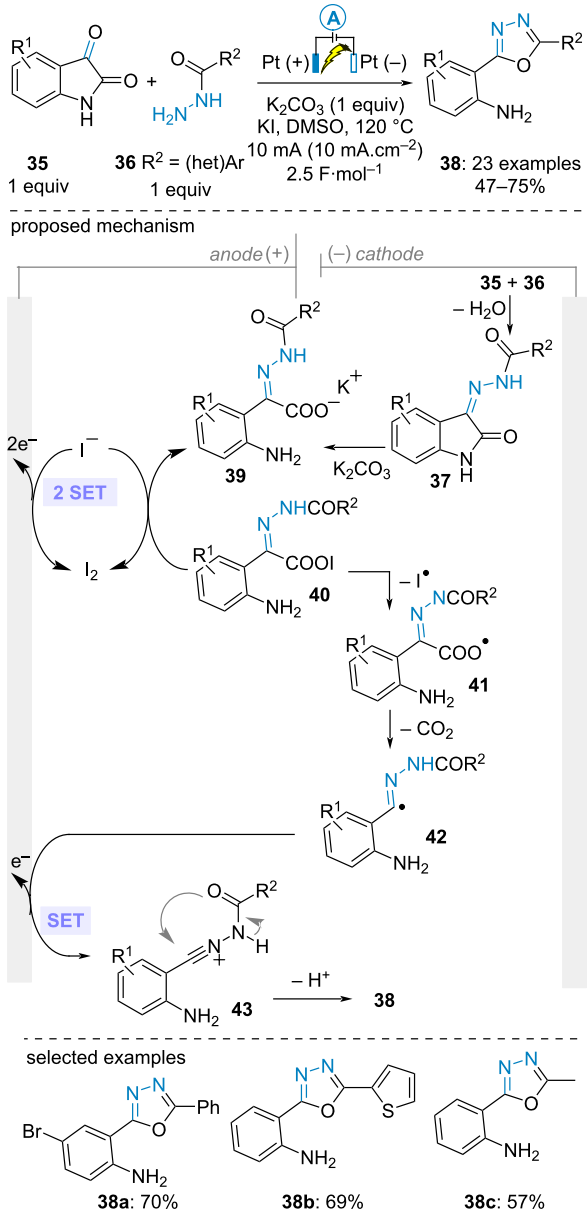

Scheme 8: Synthesis of 2-(1,3,4-oxadiazol-2-yl)anilines [44].

Formal cycloaddition

Hydrazones constitute a versatile building block for the construction of azacycles through formal cycloaddition reactions. Under oxidative electrochemical conditions, either the oxidation of the hydrazone or the partner might be investigated offering numerous possibilities for the assembly of heterocycles.

As early as 1988, Tabaković and Gunić examined the anodic oxidation of aldehyde-derived *NH*-arylhydrazones **44** in the presence of pyridine and (iso)quinolone derivatives **45** in acetonitrile-tetraethylammonium perchlorate solution under constant potential in a divided cell equipped with platinum gauze anode and nickel cathode. Such a transformation constituted a straightforward route to the corresponding fused *s*-triazolo perchlorates **46** in moderate to high yield. Coulometric analysis established that the electrolysis was a four-electron oxidative process. Based on this study, the authors proposed the initial anodic oxidation of hydrazone **44** through the loss of two electrons and one proton to form cation **47**. Subsequent nucleophilic addition of the azaarene led to new highly acidic cationic species **48**. The latter underwent deprotonation and cyclization to form fused system **49**. Final two-electron oxidation and deprotonation delivered the ionic product **46** (Scheme 9) [45].

For the construction of non-ionic azacycle from aldehyde-derived *NH*-arylhydrazones, the electrolysis is generally conducted in the presence of iodide anion as electromediator. An important challenge is to avoid the competitive formation of the corresponding methoxy(phenylazo)alkane [46,47] or carbonyl compound [48] upon SET anodic oxidation of the hydrazone and subsequent reaction with methanol or water, respectively. In 2018, Yuan and Yang developed a multicomponent synthesis of 1-aryl and 1,5-disubstitued 1,2,4-triazoles using tetrabutylammonium iodide as electromeditor [49]. 1-Methylene-2-arylhydrazine **52** was in situ generated through the condensation of paraformaldehyde **51** with arylhydrazines **50**, while the electrolyte ammonium acetate and the alcoholic solvent acted as N and C1 sources, respectively. The authors proposed the mechanism depicted in Scheme 10. The deprotonation of hydrazone **52** afforded anion **54** which underwent SET anodic oxidation to form radical **55**. In parallel, an elusive oxidation of alcohol electromediated by iodine would furnish aldehyde **56**. Electrogenerated iodine would further assist the reaction with ammonia to form *N*-iodo aldimine intermediate **57**. Subsequent radical cycloaddition between **56** and **57** would furnish cyclic hydrazinyl radical **58**. Finally, the triazole would be obtained

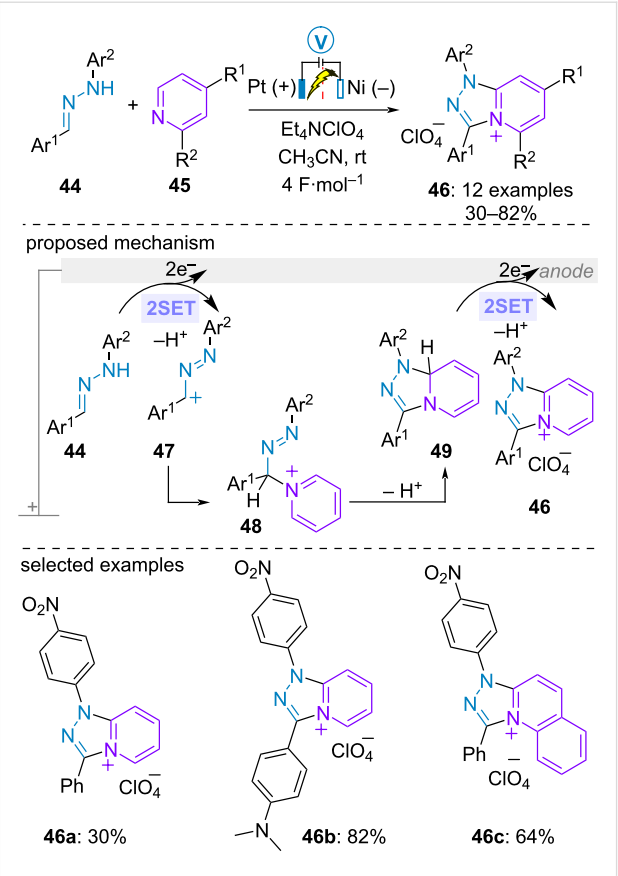

Scheme 9: Synthesis of fused *s*-triazolo perchlorates [45].

after hydrogen atom abstraction by iodide radical and deprotonation.

Inspired by these works, Li and Gu et al. proposed the electrosynthesis of 1,3,5-trisubstituted 1,2,4-triazoles from preformed aldehyde-derived *N*-arylhydrazones **60**, aldehydes **61** and ammonium acetate. Herein, the authors suggested the electromediated oxidation of *N*-arylhydrazone by electrogenerated iodide radical (Scheme 11) [50].

In parallel, the group of Yuan achieved the electrosynthesis of 1,3,5-trisubstituted 1,2,4-triazoles **67** from arylhydrazines **64**, aldehydes **65** and primary amines **66**. Iodine-mediated electrooxidation of in situ-generated aldehyde-derived hydrazones was also proposed as key initial step of the transformation (Scheme 12) [51]. Concurrently, similar formal electrochemical cycloaddition reactions between preformed aldehyde-derived hydrazones and aliphatic amines were investigated by the groups of D. Tang [52] and Pan [53]. The latter employed ferrocene as electrocatalyst instead of iodide salts. Additionally, Tang et al. demonstrated that amidines could react with preformed aldehydes-derived hydrazones to produce similar 1,3,5-trisubstituted 1,2,4-triazoles [54].

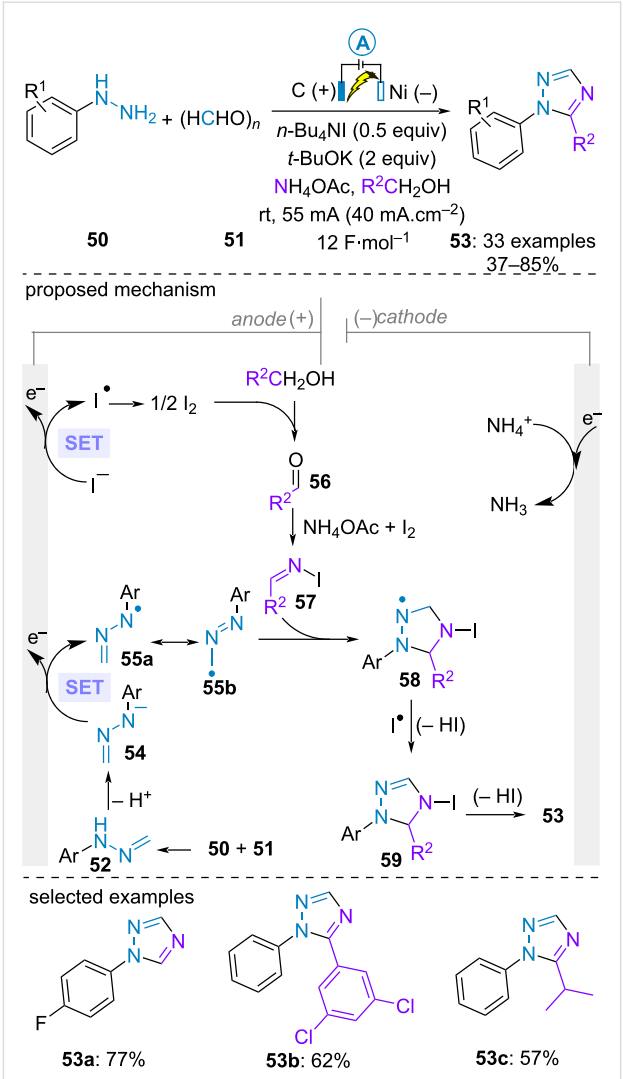

Scheme 10: Synthesis of 1-aryl and 1,5-disubstitued 1,2,4-triazoles [49].

The last example of electrochemical synthesis of trisubstituted 1,2,4-triazoles was accomplished by D. Tang et al. through the formal cycloaddition between in situ-generated aldehyde-derived hydrazones and cyanoamine (**70**). The 5-amino derivatives **71** were obtained in moderate to good yields by employing potassium iodide as electrocatalyst (Scheme 13) [55]. Herein, the electrochemical approach constitutes an advantageous alternative to previous methods, which required the preparation of difficult-to-handle hydrazonoyl halides for the synthesis of 1-aryl-5-amino-1,2,4-triazoles from cyanamide [56,57].

Pyrazolines are highly important heterocyclic motifs in pharmaceutical and agrochemical industries. The (3 + 2)-cycloaddition between nitrile imines and alkenes represents one of the most efficient strategies to prepare these azacycles. However,

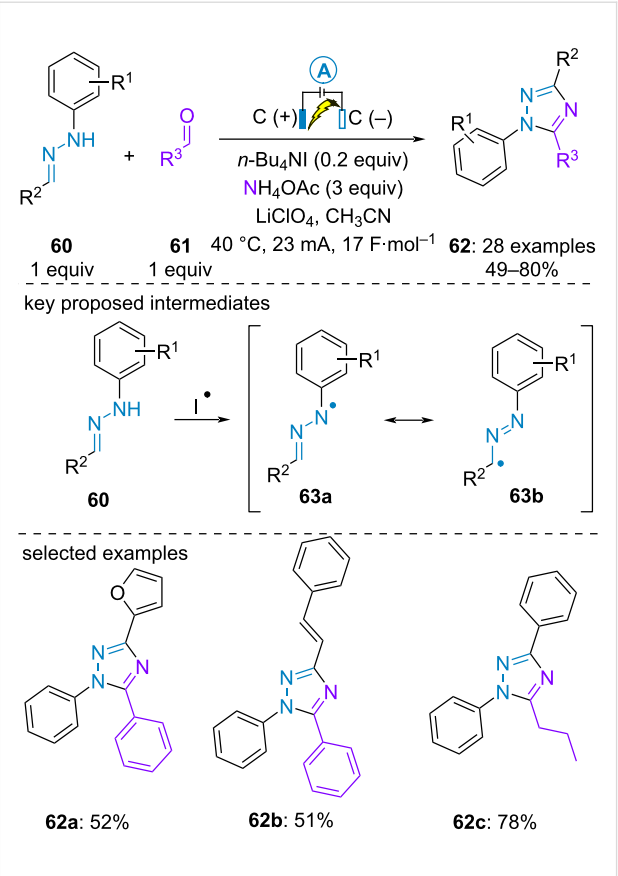

Scheme 11: Synthesis of 1,3,5-trisubstituted 1,2,4-triazoles [50].

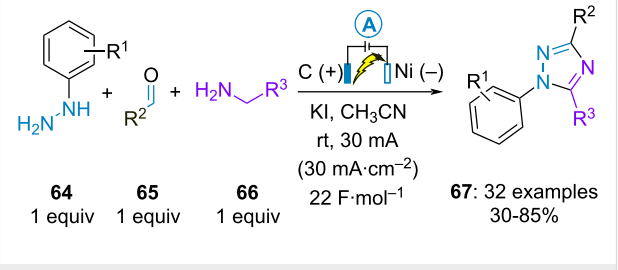

Scheme 12: Alternative synthesis of 1,3,5-trisubstituted 1,2,4-triazoles [51].

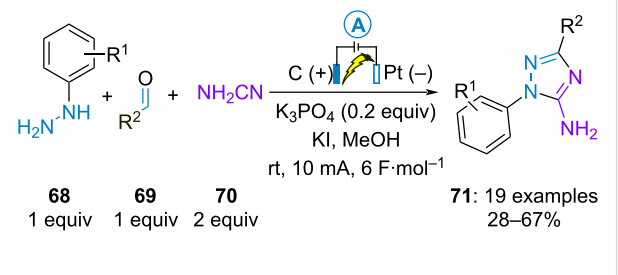

Scheme 13: Synthesis of 5-amino 1,2,4-triazoles [55].

conventional methods for the generation of the nitrile imine involved the use of unstable hydrazonoyl halides or the oxidation of aldehyde-derived hydrazones under harsh reaction conditions. In 2023, the group of Waldvogel presented a formal electrooxidative (3 + 2)-cycloaddition between aldehyde-derived hydrazones **72** and alkenes **73** to yield a large range of *N*-arylpyrazolines **74** under mild reaction conditions (Scheme 14) [58]. A biphasic system (aqueous/organic) was engineered during which the oxidation of the iodide mediator took place in the aqueous place, thereby protecting sensitive dipolarophiles such as styrenes from side reactions (e.g., overoxidation or polymerisation) in the organic phase. Ethyl acetate was employed as organic solvent for ethyl glyoxylate

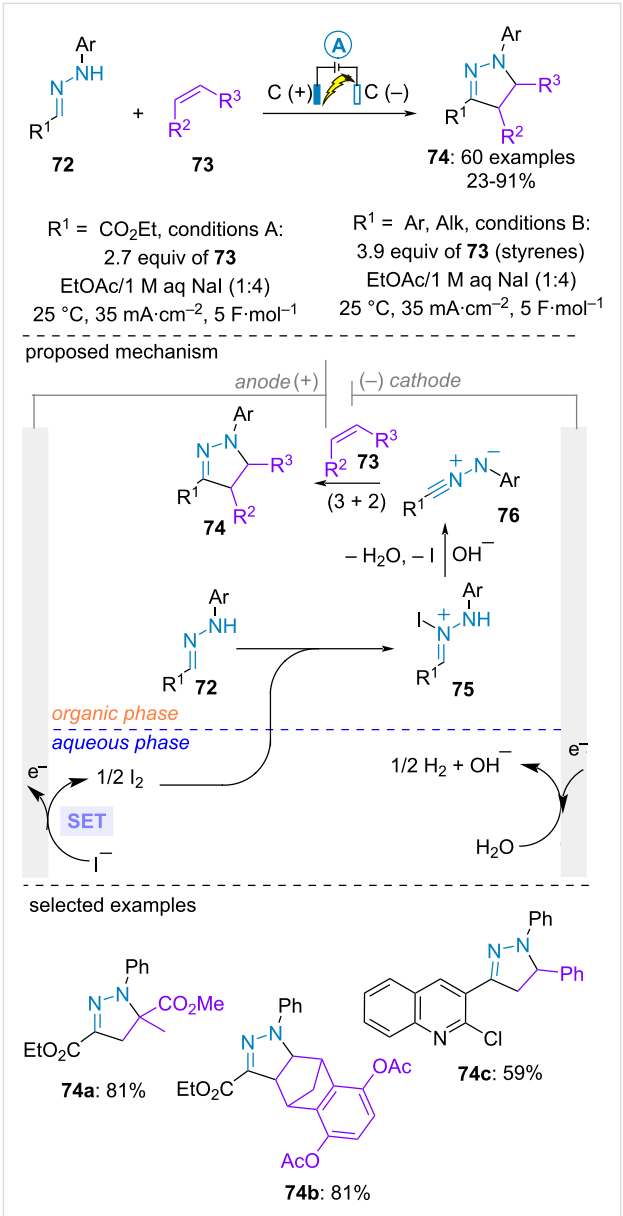

Scheme 14: Synthesis of 1-arylpyrazolines [58].

phenylhydrazone **72a** while methyl *tert*-butyl ether was preferred for aromatic and aliphatic aldehyde-derived hydrazones **72b**. Styrenes, enamines as well as electron poor aliphatic alkenes were all suitable dipolarophiles. From a mechanistic point of view, the authors proposed the electrogeneration of iodine in the aqueous phase. Under high stirring, the latter would react with *NH*-arylhydrazones **72** in the organic phase to furnish the *N*-iodo hydrazonium **75** and ultimately the nitrile imine **76** under basic conditions provided by the cathodic process. The critical role of the in situ cathodic generation of the base was supported by a control experiment in a divided cell, where no conversion was achieved. Final formal (3 + 2)-cycloaddition with the dipolarophiles **73** delivered the pyrazolines **74**. It is interesting to note that a complementary (3 + 2)-cycloaddition between aldehyde hydrazones and alkenes for the preparation of pyrazolines was proposed by Tong, Song, et al., achieving similar efficiency using oxone/KBr as an environmentally friendly oxidative system [59].

Most recently, Zhou and Ma et al. described the electrochemical access to 3-aminopyrazoles **79** from arylpropynal-derived *NH*-arylhydrazones **77** and secondary amines **78** in moderate to good yields. Potassium iodide was employed as electrolyte and mediator in ethanol in an undivided cell equipped with a carbon graphite and a platinium cathode. The transformation initiated with the electrochemical generation of iodonium through a two-electron process. Subsequent reaction with the hydrazone and deprotonation formed the *N*-iodo hydrazone intermediate **80**, triggering the reaction with the amine **78** through cationic species **81**. Final cyclization delivered the desired pyrazole **79** (Scheme 15) [60].

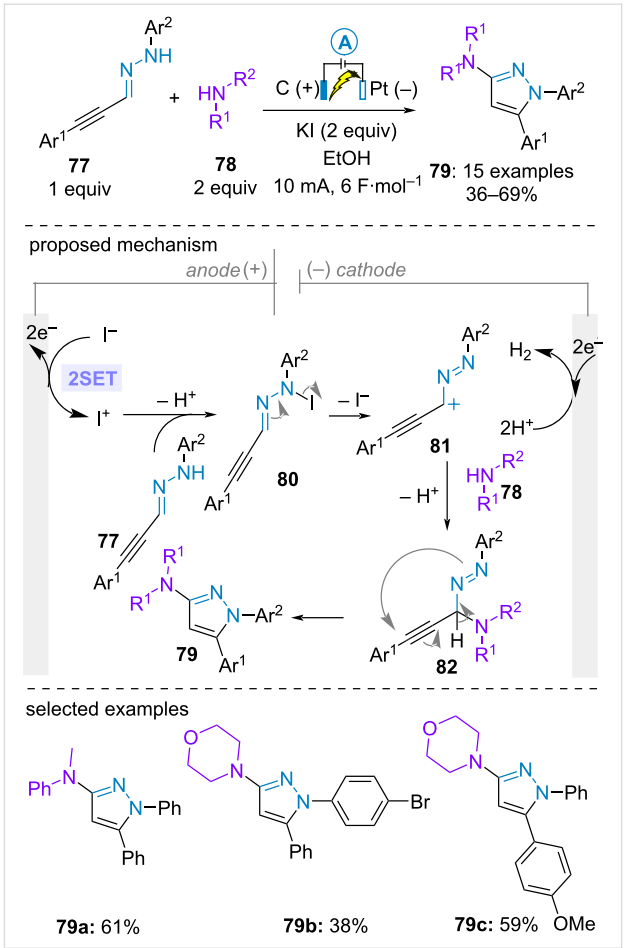

Scheme 15: Synthesis of 3-aminopyrazoles [60].

The group of D. Tang engaged aromatic aldehyde-derived *NH*-tosylhydrazones **83** in an iodide-catalyzed electrochemical formal (3 + 2)-cycloaddition with quinolines **84** to build [1,2,4]triazolo[4,3-*a*]quinoline derivatives **85**. Better yields were obtained with hydrazones bearing an electron-rich substituent on the aromatic ring. The reaction initiated with anodic formation of iodine. The latter would react with hydrazone **83** to form the zwitterionic species **86** under basic conditions. Subsequent formal (3 + 2)-cycloaddition with the quinoline **84** formed fused system **87** which underwent elimination of iodide and sulfinic acid to furnish the aromatic product **85**, thereby regenerating the catalyst (Scheme 16) [61].

Given its abundance, stability, and low price, elemental sufur (S_8) is an ideal source of sulfur atom to produce thiacycles [62]. In 2019, H.-T. Tang utilized this reagent in combination with (hetero)aromatic ketone-derived *NH*-tosylhydrazones **89** for the electrochemical construction of 1,2,3-thiadiazoles **91**. The electrolysis was conducted in an undivided cell at high temperature using ammonium iodide as electrocatalyst. Interestingly, no additional electrolyte was required. The transformation accommodated various substituents on the aromatic moiety regardless of their electronic properties. However, 4,5-disubstituted 1,2,3-thiadiazoles could not be accessed with this methodology. Mechanistically, control experiments with radical trapping agent such as TEMPO ((2,2,6,6-tetramethylpiperidin-1-yl)oxyl) or 1,1-diphenylethylene proceeded with similar efficiency, thereby excluding any radical pathway. As such, it was proposed that the catalytic electrooxidation of iodide (E_{NH4I} = 0.41 V and 0.75 V vs Ag/AgCl in dimethylacetamide for I^-/I^{3-} and I^{3-}/I_2 redox couples) into iodine provided a green and mild tool to in situ generate the α-iodo ketone-derived *NH*-tosylhydrazone **92** and ultimately the azadiene **93** upon elimination of HI. In agreement with a previous report [63], further formal (4 + 1) cycloaddition with S_8 followed by elimination of S_7 and sulfinic acid gave rise to the aromatic cycle **91** (Scheme 17) [64].

The direct C(sp^2)–H functionalization of aldehyde-derived *N,N*-dialkylhydrazones has been also explored for constructing

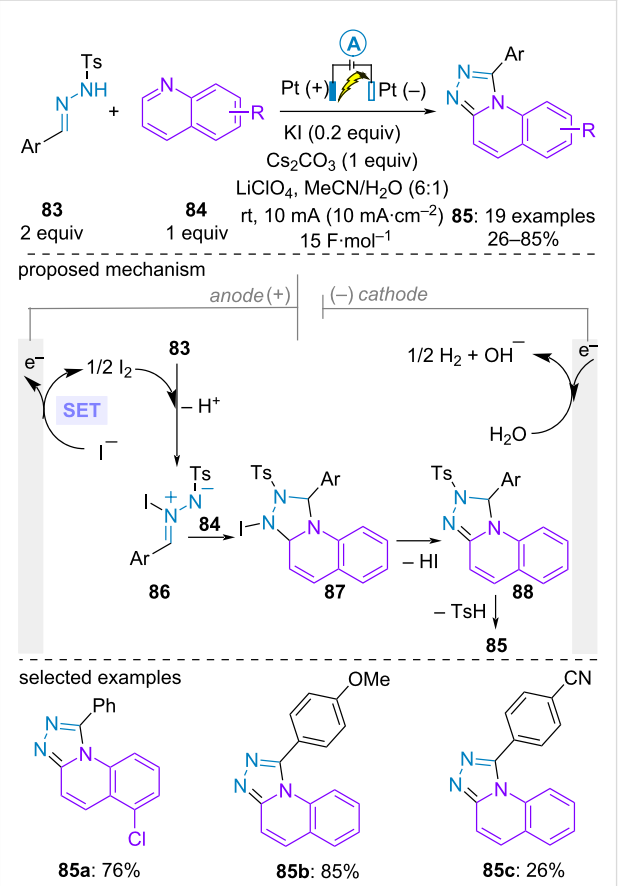

Scheme 16: Synthesis of [1,2,4]triazolo[4,3-*a*]quinolines [61].·

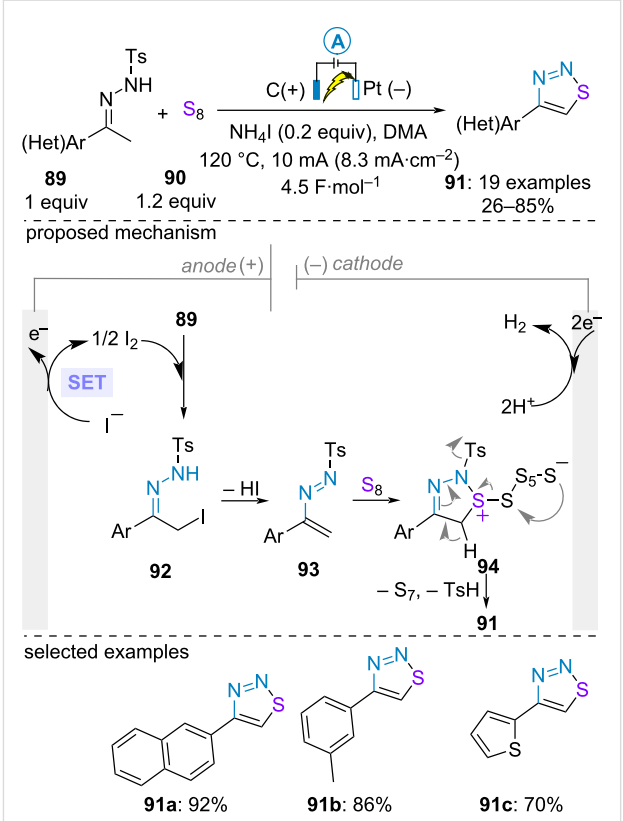

Scheme 17: Synthesis of 1,2,3-thiadiazoles [64].

various azacycles. In 2021, the group of Ruan and Feng studied the electrochemical C(sp^2)–H thiocyanation of aldehyde-derived *N*,*N*-dialkylhydrazones **95** with sodium thiocyanate (**96**) to prepare 5-thioxo-1,2,4-triazolium inner salts **97**. The electrolysis was conducted with two inexpensive graphite electrodes in the absence of additional supporting electrolyte. It could be easily performed on a gram scale, albeit with a slight decrease in the efficiency. It was compatible with a large array of aromatic aldehyde-derived hydrazones regardless of their electronic properties as well as aliphatic-aldehyde derived hydrazones. Cyclic voltammetry analysis showed that thiocyanate salt **96** possesses a lower oxidation potential than the hydrazone **95**. As such, the authors proposed the anodic generation of electrophilic thiocyanogen as the initial step. Further reaction with the hydrazone **95** and deprotonation led to hydrazonoyl thiocyanate intermediate **99**, which isomerized to the thermodynamically more stable isothiocyanate derivatives **100** through 1,3-shift. The latter underwent spontaneous ring closure to furnish the 1,2,4-triazolium **97** (Scheme 18) [65].

In the last example of this section, only one nitrogen atom of the hydrazone takes part in the cycloaddition reaction. In 2018, Zhang et al. realized the electrochemical (3 + 2)-cycloaddition of trimethylsilyl azide (**102**) with aldehyde-derived *N*,*N*-disubstituted hydazones **101** for synthesiszing tetrazoles **103**. Sodium azide could be an alternative source of azide, albeit with both slightly lower yields and Faradic efficiency. Remarkably, (hetero)aromatic as well as aliphatic aldehydes proved to be efficient. Various substituents on the N(sp^3) atom were well tolerated and the best result was obtained with a morpholine ring. Based on cyclic voltammetry studies, the transformation initiated with the anodic oxidation of hydrazone **101** to form highly electrophilic radical cationic species **104**. Subsequent addition of azide **102** and desilylation formed hydrazinyl radical **105** which underwent second anodic oxidation/cyclization and deprotonation sequence to build the 1-aminotetrazole **103** (Scheme 19) [66]. It is interesting to note that this mechanism differs from the one proposed by Zhu et al., who reported a hypervalent iodide-mediated similar cycloaddition through the generation of azide radical, although with similar yields [67].

Synthesis of functionalized hydrazones through C(sp^2)–H functionalization of aldehyde-derived hydrazones

The direct electrochemical C(sp^2)–H functionalization of aldehyde-derived *N*,*N*-disubstituted hydrazones provides an effi-

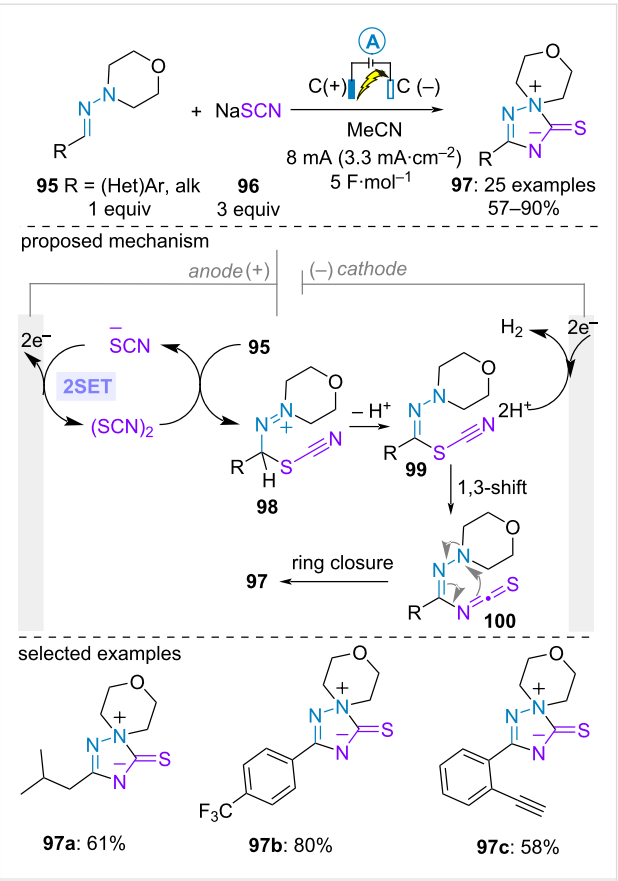

Scheme 18: Synthesis of 5-thioxo-1,2,4-triazolium inner salts [65].

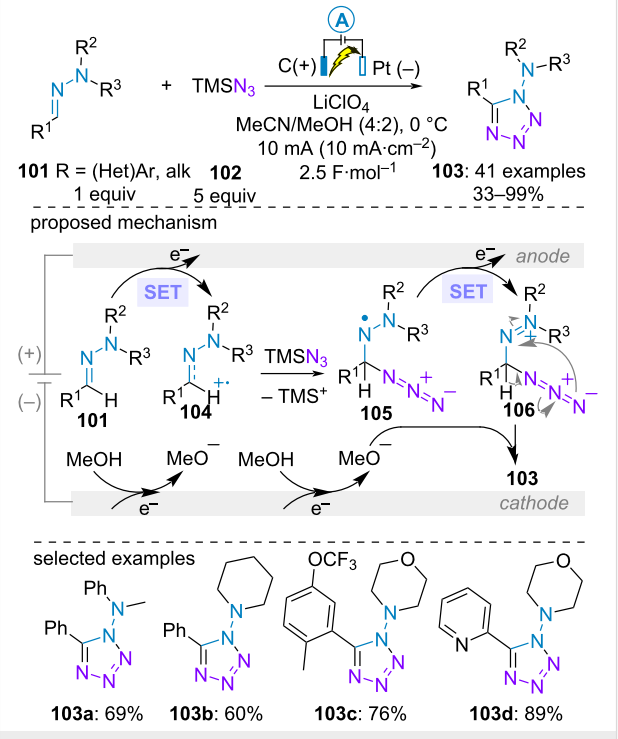

Scheme 19: Synthesis of 1-aminotetrazoles [66].

cient tool for accessing various hydrazones under mild reaction conditions and, to some extent, broadening the scope of more conventional radical approaches. Typically, two mechanistic pathways can be proposed depending on the oxidation potentials of each partner. If the hydrazone is the most readily species to be oxidized, initial SET anodic oxidation of the hydrazone furnishes the highly electrophilic radical cation species **D**, which undergo nucleophilic addition of the second partner and deprotonation to produce hydrazinyl radical **F** (route a). Alternatively, if the partner possesses a lower oxidation potential than the hydrazone, then the transformation initiates with the anodic generation of radical species Y•, that adds to the hydrazone leading ultimately to hydrazinyl radical **F** as well (route b). In both cases, a second SET anodic oxidation and deprotonation yields the functionalized hydrazone (Scheme 20).

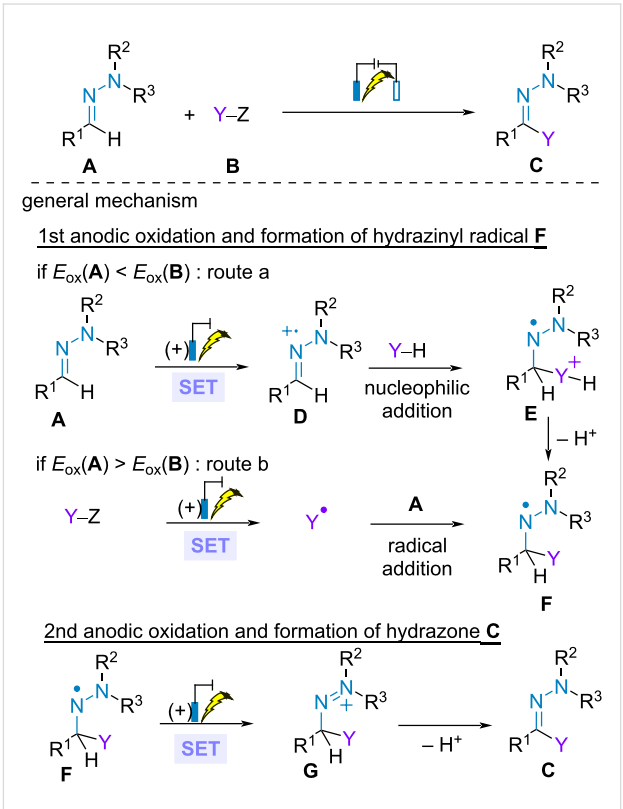

Scheme 20: C(sp^2)–H functionalization of aldehyde-derived hydrazones: general mechanisms.

Initial SET oxidation of the hydrazone

In 1973, Barbey and Caullet have shown that the benzaldehyde-derived *N,N*-diphenylhydrazone **107** dimerized upon electrochemical oxidation on platinum electrode [68]. The following year, they demonstrated that in the presence of an excess of pyridine, triphenylphosphine or tetraethylammonium cyanide, the corresponding pyridium **109**, phosphonium **111** and cyano hydrazones **113** were obtained, respectively (Scheme 21) [69].

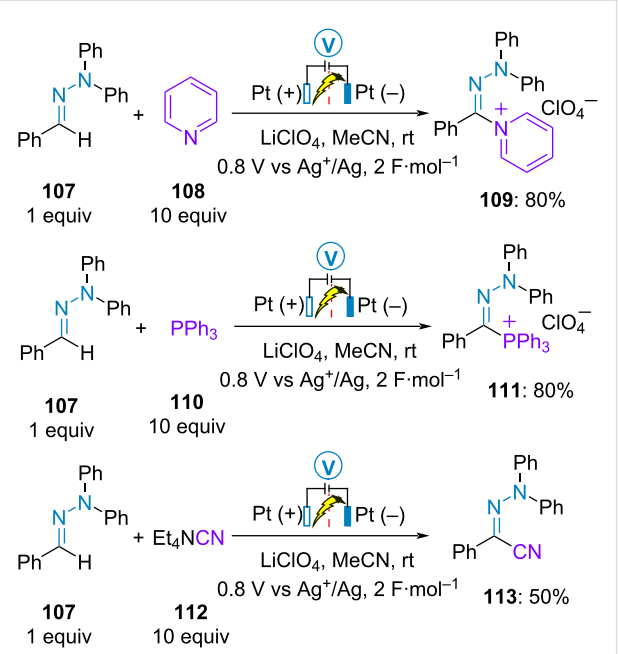

Scheme 21: C(sp^2)–H functionalization of benzaldehyde diphenyl hydrazone [68,69].

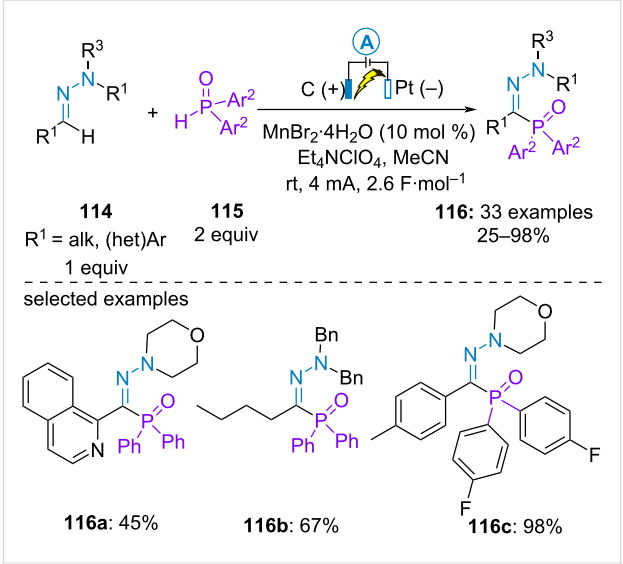

Scheme 22: Phosphorylation of aldehyde-derived hydrazones [70].

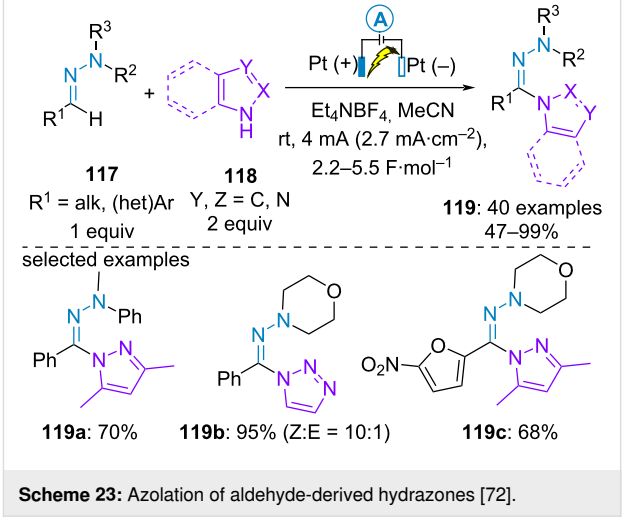

Scheme 23: Azolation of aldehyde-derived hydrazones [72].

In 2020, Ruan and Sun et al. communicated the electrochemical dehydrogenative coupling between (hetero)aromatic or aliphatic aldehyde-derived hydrazones **114** and diarylphosphine oxide **115**. The phosphorylation proceeded with slightly higher yield in the presence of a catalytic amount of manganese dibromide but its role was not clearly identified. Cyclic voltammetry analysis supported the initial oxidation of the hydrazone ($E_{p/2}$ of 4-methylbenzaldehyde-derived hydrazone = 0.89 V vs Ag/AgCl in CH_3CN and $E_{p/2}$ of diphenylphosphine oxide > 0.89 V vs Ag/AgCl in CH_3CN) (Scheme 22) [70]. Similar yields were previously obtained for the same transformation using a substoichiometric amount of potassium persulfate as oxidant [71].

In 2022, the group of Huang employed aromatic azoles **118** as additional suitable nucleophilic partners for C(sp^2)–H functionalization of aldehyde-derived *N,N*-disubstituted hydrazones **117**. A wide range of aldehyde-derived hydrazones reacted smoothly with various azoles including pyrazole derivatives, imidazole, pyrazole and triazoles (Scheme 23) [72]. Cyclic voltammetry studies confirmed that the azoles were redox inactive in the scan window while benzaldehyde-derived morpholino hydrazone could be readily oxidized at 1.18 V vs SCE in CH_3CN supporting the route (a) of the general mechanism in Scheme 20.

Initial SET oxidation of the partner

As mentioned above, if the partner is more readily oxidized than the hydrazone, then the general mechanism of the process is as described in Scheme 20, following route (b) for the first anodic oxidation. While investigating the electrochemical oxidative C(sp^2)–H thiocyanation of ketene dithioacetals, Wang and Yang et al. mentioned one example of thiocyanation of benzaldehyde-derived hydrazone **120** using potassium thiocyanate as a source of thiocyanate radical. The electrolysis was conducted in the presence of two equivalents of water in acetonitrile with lithium perchlorate as electrolyte. It is interesting to notice that the isomerization of the product and subsequent ring closure discussed above (see Scheme 17) did not occur under these conditions (Scheme 24) [73].

In 2023, Hajra et al. provided an electrochemical method for the C(sp^2)–H sulfonylation of aromatic aldehyde-derived *N,N*-dialkylhydrazones **123** under constant current with two carbon

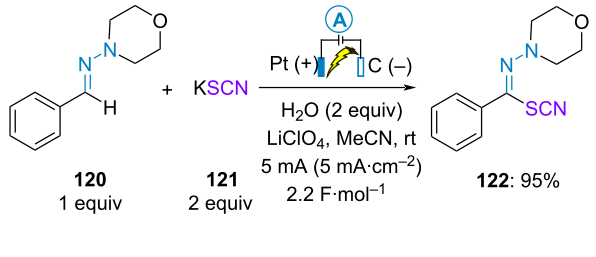

Scheme 24: Thiocyanation of benzaldehyde-derived hydrazone **122** [73].

electrodes. Aromatic and aliphatic sodium sulfinates **124** were employed as sources of sulfinate radicals under electrolyte-free reaction conditions. The targeted product was obtained in high yield regardless of the electronic properties of the substituents on the aromatic ring of either the hydrazone or the sulfinate salt (Scheme 25) [74]. In parallel, a similar transformation was developed by Guo and Yang et al. Using two platinum electrodes and *n*-Bu_4NBF_4 as supporting electrolyte in a 1:1 mixture of acetonitrile/water, heteroromatic aldehyde-derived hydrazones as well as heteroaromatic sodium sulfinate salts were additional compatible reagents [75].

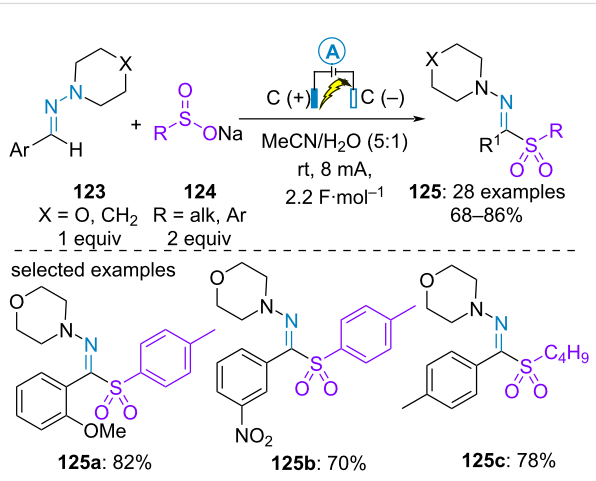

Scheme 25: Sulfonylation of aromatic aldehyde-derived hydrazones [74].

In 2022, Xie et al. achieved the electrochemical C(sp^2)–H trifluoromethylation of (hetero)aromatic aldehyde-derived hydrazones. The galvanostatic electrolysis was performed with two carbone graphite electrodes. The Togni reagent **127** was chosen as a source of trifluoromethyl radical with redox neutral and electron-rich hydrazones through a paired electrolysis. In contrast, the Langlois reagent **128** was preferred for electron-poor substrates through an electrooxidative process (Scheme 26) [76].

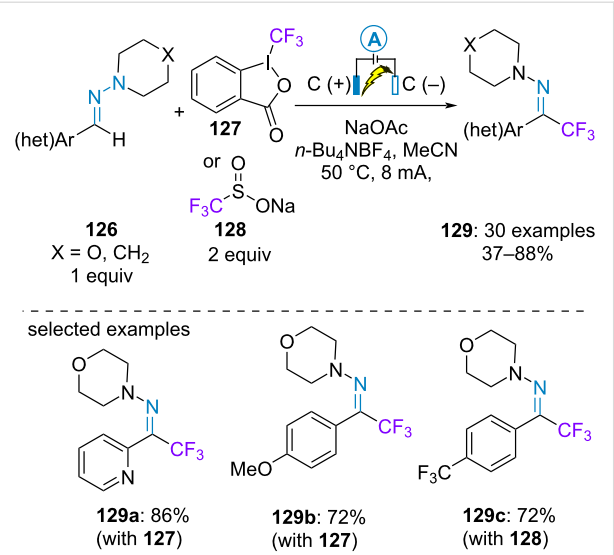

Scheme 26: Trifluoromethylation of aromatic aldehyde-derived hydrazones [76].

Electrochemical access to diazo compounds

Diazo compounds are highly useful synthetic reagents in organic chemistry. For instance, they are regularly utilized as 1,3-dipoles in cycloaddition reactions or as precursor of carbenes under thermal, photochemical, and catalytic transition-metal-based transformations. However, their use is significantly hampered by their inherent instability and hazardous nature. Therefore, it is endlessly highly demanding to find a new mode of generation of diazo compounds from stable and safe precursors. The third part of this review is dedicated to electrochemical synthesis of diazo compounds from hydrazones. Transformations involving diazo compounds as either products or intermediates are covered.

While investigating the electrochemical oxidation of benzophenone hydrazones **130**, Chiba et al. discovered that several products were obtained depending on the reaction conditions. For instance, the use of lithium perchlorate as supporting electrolyte in acetonitrile at room temperature in a divided cell equipped with two platinum electrodes led exclusively to diazines **131** in good yields. In contrast, when the electrolysis was conducted in methanol containing sodium methoxide in an undivided cell, three main products (namely benzophenone dimethyl acetals **133**, diphenylmethyl methyl ethers **134** and diphenylmethanes **135**) were obtained, the ratio of which was influenced by the electrode materials, the temperature and the amount of sodium methoxide. The range of isolated yields of the major products obtained under the appropriate reaction conditions is shown in Scheme 27. Based on control experiments, the authors proposed that **133**–**135** came from diazo intermediates **132**, which could not be isolated [77].

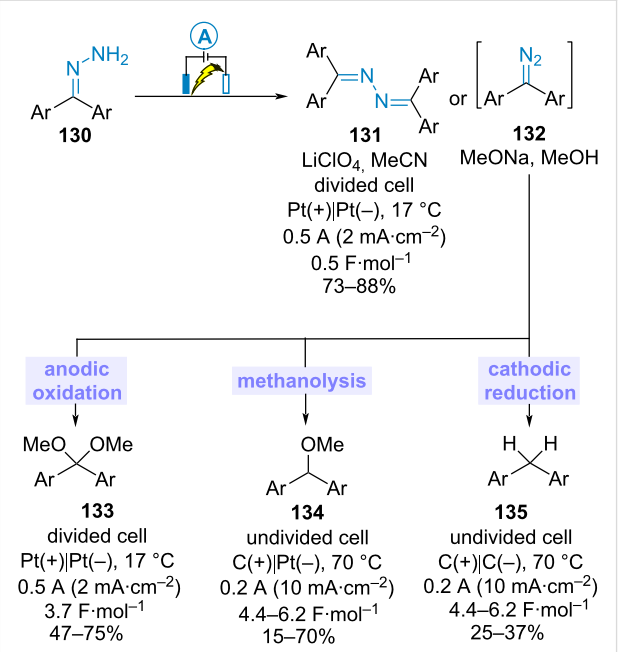

Scheme 27: Electrooxidation of benzophenone hydrazones [77].

Building on this study and considering the high ability of diazo compounds to react with alkenes, Chiba et al. developed the electrochemical construction of diphenylcyclopropanes **137** from benzophenone hydrazones **130** and methacrylic acid derivatives **136**. The transformation was conducted on a large scale (60 mmol) in an undivided cell using graphite anode and platinum cathode materials at 55 °C with a minimal amount of sodium methoxide, thereby limiting side products formation such as **133**–**135** or some oligomers of ethylenes (Scheme 28) [77].

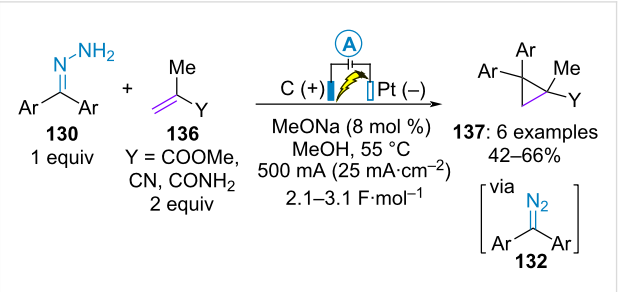

Scheme 28: Electrooxidative coupling of benzophenone hydrazones and alkenes [77].

In 2002, Okimoto et al. reported the indirect electrochemical oxidation of benzilhydrazones **138** using potassium iodide as electromediator for synthesising α-diazoketones **139** in good yields. The electrolysis was performed at low temperature in a divided cell equipped with a platinum anode and a nickel cathode. It was not possible to isolate the diazo compounds arising from the electrooxidation of 4,4'-dimethylbenzilhydrazone and 4,4'-dimethoxybenzilhydrazone (X = H, Cl). In these cases, the diazo compounds directly underwent both Wolff rearrangement and overoxidations to yield a mixture of the corresponding diphenyl acetal and benzil dimethyl acetal (akin to the conversion of **132** into **133** in Scheme 27), respectively (Scheme 29) [78]. Using a similar procedure, the same authors subsequently reported the electrochemical oxidation of dibenzoylbenzene dihydrazones into the corresponding bisdiazo compounds [79].

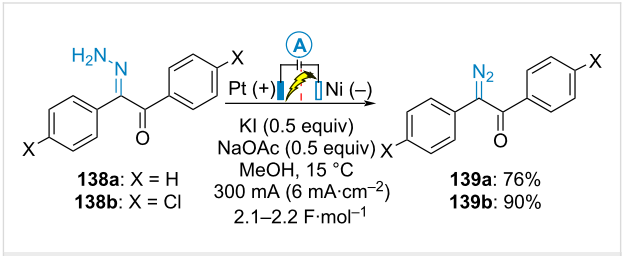

Scheme 29: Electrosynthesis of α-diazoketones [78].

In 2022, Ollevier and Lam et al. undertook an in-depth study for accessing stabilized diazo compounds through anodic oxidation of simple unsubstituted hydrazones **140**. After intensive parameter optimizations, good yields were achieved under galvanostatic conditions in a simple divided cell equipped with cheap carbon graphite anode and nickel cathode using potassium iodide and ammonium acetate as electrolyte. Cyclic voltammetry analysis suggested that potassium iodide would serve as an electromediator to oxidize the hydrazone through an inner-sphere electron transfer. Moreover, the electrolysis proceeded more efficiently in the presence of ammonium acetate since (i) the acetate anion would serve as a base to facilitate the oxidation of the hydrazone and (ii) the ammonium cation would provide a performant proton source to counterbalance the overall process, thereby protecting the diazo product from cathodic reduction (akin to the conversion of **132** into **135** in Scheme 27). Based on these studies, the authors proposed the initial anodic formation of the iodonium species [$(CH_3CN)_2I^+$], which would react with the hydrazone to furnish the protonated diazo compound **143** via the *N*-iodo hydrazone intermediate **142**. Further acetate anion-assisted deprotonation ultimately led to the desired diazo compounds **141** (Scheme 30) [80]. A nice application of this procedure involved the (3 + 2)-cycloaddition reaction between electrogenerated diphenyldiazomethane and methyl acrylate delivering the corresponding pyrazoline in good yield (68%).

Olefins are highly common structural motifs in natural and synthetic organic compounds. They are also often employed as pivotal element during the total synthesis of natural products. Therefore, the development of mild and efficient methods to

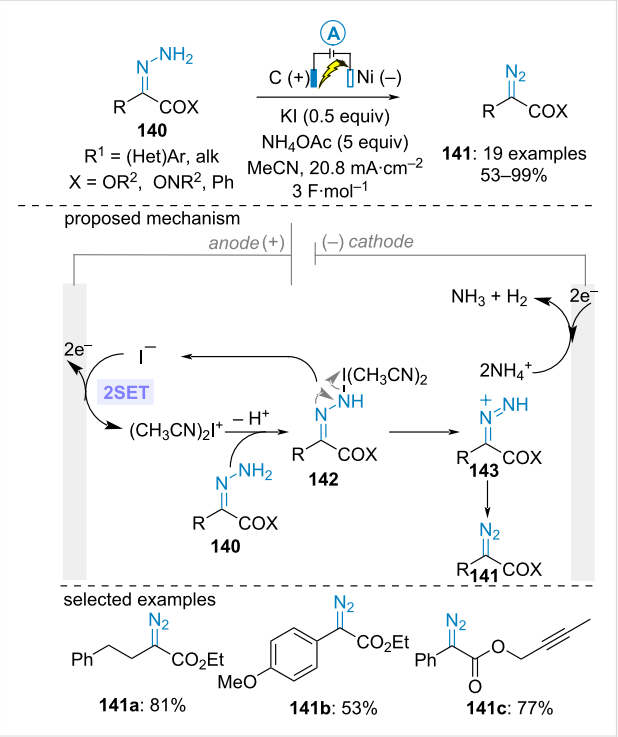

Scheme 30: Electrosynthesis of stable diazo compounds [80].

access this motif from readily available starting materials is a never-ending quest. With the aim to propose an alternative to the classical olefination of carbonyls through Wittig, Julia, Peterson and Tebbe-type reactions, the group of Lambert et al. implemented an elegant electrophotocatalytic carbonyl-olefin cross-coupling in an undivided cell equipped with a carbon felt anode and a platinum cathode in the presence of their own trisaminocyclopropenium cationic photocatalyst TAC^+. The electrolysis was carried out at a constant cell potential of 1.5 V under white light irradiation. The carbonyl compound **144** was initially treated with *tert*-butyl carbazate (**145**) in acetonitrile in the presence of molecular sieves, followed by the addition of trifluoroacetic acid (TFA) to yield the unsubstituted hydrazone **146**. Dropwise addition of this solution during the electrolysis to the anodic chamber containing the olefin **147**, lithium perchlorate and the photocatalyst in acetonitrile delivered the desired olefin product **148**. From a mechanistic point of view, the photoelectrochemical transformation began with the anodic oxidation of the hydrazone **146** to the corresponding diazo compound **149**, akin to Lam and Ollevier's work. Subsequent (3 + 2)-cycloaddition with the olefin partner **147** formed cyclic diazene **150**. Meanwhile, anodic oxidation of TAC^+ generated photosensitive TAC^{2+} ($E_{1/2}(TAC^{2+}/TAC^+)$ = +1.3 V vs SCE). Subsequent SET between highly oxidizing photoexcited species TAC^{2+*} ($E_{1/2}(TAC^{2+*}/TAC^+)$ = +3.3 V vs SCE) and **150** generated distonic species **151** by denitrogenation. After Wagner–Merweein shift, the resulting radical cation **152** would undergo SET reduction from an electron donor to furnish the olefin product **148**. In the cathodic chamber, reduction of the acidic proton of TFA counterbalance the overall transformation. A wide range of carbonyl compounds including aromatic and aliphatic aldehydes and ketones as well as various alkene partners were compatible. Of note, the most thermodynamically stable distonic radical was formed, thereby allowing the formation of only one isomer of the olefin product (Scheme 31) [81].

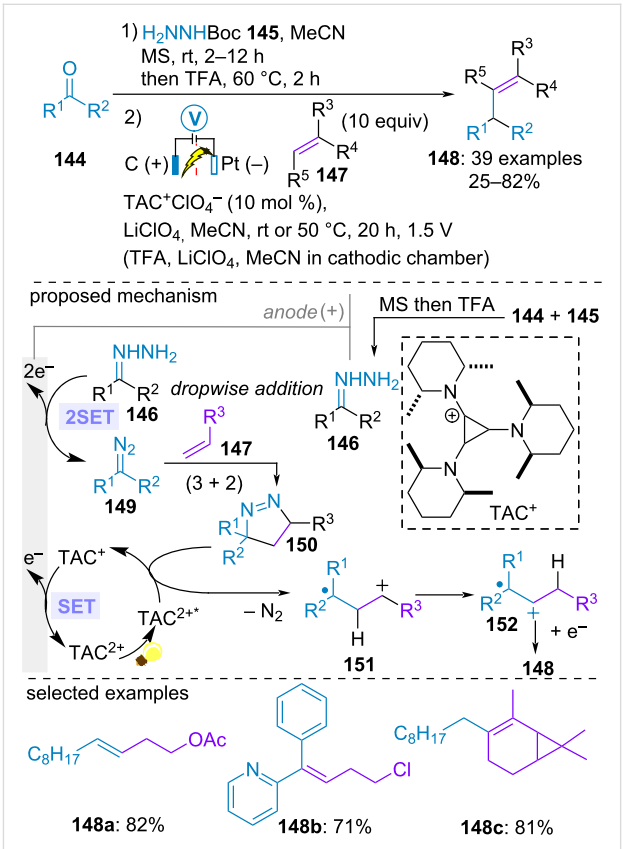

Scheme 31: Photoelectrochemical synthesis of alkenes through in situ generation of diazo compounds [81].

Miscellaneous

In 1990, Chiba and Okimoto established an electrosynthetic procedure to convert the carbonyl group of aliphatic ketones **153** into a cyanomethylene group. Condensation of **153** with methyl carbazate (**154**) furnished the corresponding methoxycarbonylhydrazone **155**. The latter was charged in the anolyte compartment of a divided cell containing sodium cyanide and acetic acid in methanol and was allowed to stand for several days in the dark in the absence of an electrical current, thus allowing the addition of in situ-generated HCN to the hydrazone **155**. After addition of a second equivalent of sodium cyanide, the resulting HCN adduct **156** was electrolyzed under constant current to form diazene **157**, which subsequently underwent addition of methanol/fragmentation and extrusion of

nitrogen to yield the nitrile derivative **159**. The transformation proceeded neither with aldehydes nor with aromatic ketones (Scheme 32) [82].

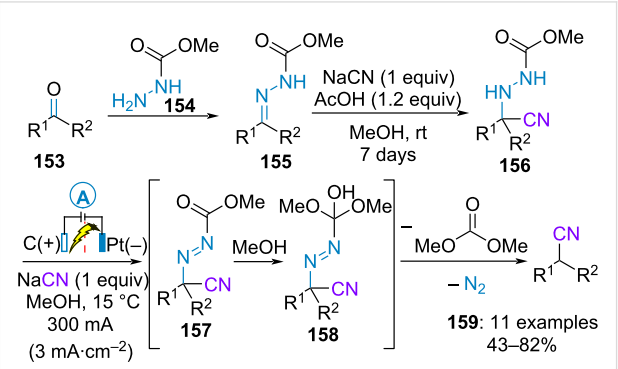

Scheme 32: Synthesis of nitriles [82].

In 2008, Okimoto et al. reported the electrochemical oxidation of ketone-derived *NH*-allylhydrazones **160** into the corresponding azines **161**. The electrolysis was conducted in a divided cell equipped with a nickel coil cathode and a platinum anode under constant current in methanol. Both potassium iodide and sodium methoxide were required as electrolyte supports to achieve high efficiency. The former would assist the oxidation of the hydrazone through the in situ generation of iodonium as oxidant while the latter would facilitate the deprotonation of iodoammonium **162** and the elimination of HI from *N*-iodo intermediate **163**. The best yields were obtained with aromatic ketone-derived hydrazones (Scheme 33) [83].

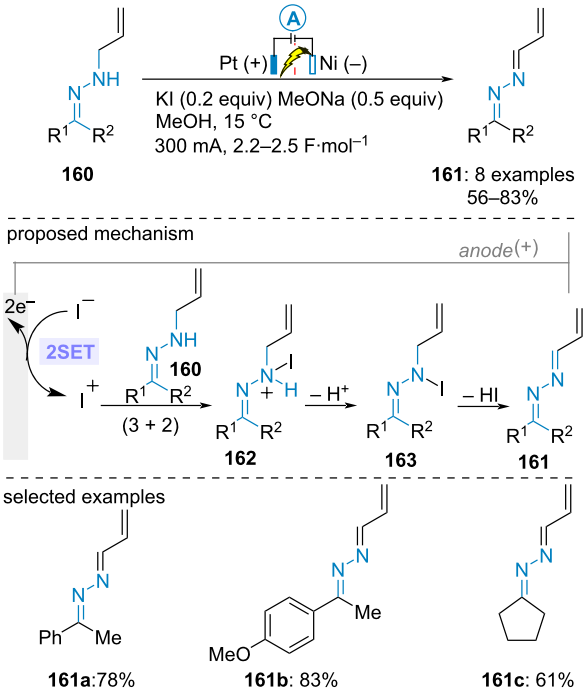

Scheme 33: Electrochemical oxidation of ketone-derived *NH*-allylhydrazone [83].

Conclusion

Given the rich reactivity profile of hydrazones, the electrooxidative transformations of such a molecular building block provides a fascinating route to valuable compounds under mild and safe reaction conditions. Alone, the electrooxidation of *NH*-aryl, -tosyl, and -acylhydrazones triggered the cyclization of a radical cation intermediate enabling the construction of pyrazole, triazole and oxadiazole derivatives, while the electrooxidation of unprotected NH_2 hydrazones constitutes a useful mean to access to relevant diazo compounds as products or synthetic intermediates. When coupled with a second reactant, electrooxidative processes gave rise to various azacycles or to functionalized hydrazones through C(sp^2)–H functionalization of aldehyde-derived hydrazones. In both cases, transformations involving either the initial oxidation of the hydrazone or the partner have been demonstrated by carefully adapting the reaction conditions to selectively oxidize the desired compound. In some cases, the use of an electromediatior such as an iodide anion helped in achieving the desired selectivity. In line with the continuing increasing interest for both electrosynthetic organic transformations and the chemistry of hydrazones, coupling with other partners or examination of different hydrazones, such as trifluoromethylated hydrazones, should enable the straightforward access to diversely functionalized molecules. Hopefully, this review will stimulate further development in this area which could eventually find useful applications in industry.

Funding

The CNRS and ICSN are gratefully acknowledged for financial support.

ORCID® iDs

Aurélie Claraz - https://orcid.org/0000-0002-0692-7830

Data Availability Statement

Data sharing is not applicable as no new data was generated or analyzed in this study.

References

1. Tatum, L. A.; Su, X.; Aprahamian, I. *Acc. Chem. Res.* **2014,** *47,* 2141–2149. doi:10.1021/ar500111f
2. Khattab, T. A. *Mater. Chem. Phys.* **2020,** *254,* 123456. doi:10.1016/j.matchemphys.2020.123456
3. Vantomme, G.; Lehn, J.-M. *Angew. Chem., Int. Ed.* **2013,** *52,* 3940–3943. doi:10.1002/anie.201210334

4. van Dijken, D. J.; Kovaříček, P.; Ihrig, S. P.; Hecht, S. *J. Am. Chem. Soc.* **2015,** *137,* 14982–14991. doi:10.1021/jacs.5b09519
5. Lygaitis, R.; Getautis, V.; Grazulevicius, J. V. *Chem. Soc. Rev.* **2008,** *37,* 770. doi:10.1039/b702406c
6. Lv, Y.; Meng, J.; Li, C.; Wang, X.; Ye, Y.; Sun, K. *Adv. Synth. Catal.* **2021,** *363,* 5235–5265. doi:10.1002/adsc.202101184
7. Xia, Y.; Wang, J. *Chem. Soc. Rev.* **2017,** *46,* 2306–2362. doi:10.1039/c6cs00737f
8. Neto, J. S. S.; Zeni, G. *Chem. – Eur. J.* **2020,** *26,* 8175–8189. doi:10.1002/chem.201905276
9. Si, Y.-F.; Lv, Q.-Y.; Yu, B. *Adv. Synth. Catal.* **2021,** *363,* 4640–4666. doi:10.1002/adsc.202100807
10. Yu, X.-Y.; Zhao, Q.-Q.; Chen, J.; Xiao, W.-J.; Chen, J.-R. *Acc. Chem. Res.* **2020,** *53,* 1066–1083. doi:10.1021/acs.accounts.0c00090
11. Fischer, E.; Jourdan, F. *Ber. Dtsch. Chem. Ges.* **1883,** *16,* 2241–2245. doi:10.1002/cber.188301602141
12. Kishner, N. *Zh. Russ. Fiz.-Khim. O-va., Chast Khim.* **1911,** *43,* 582.
13. Wolff, L. *Justus Liebigs Ann. Chem.* **1912,** *394,* 86–108. doi:10.1002/jlac.19123940107
14. Lewis, D. E. *The Wolff-Kishner Reduction and Related Reactions: Discovery and Development;* Elsevier: Amsterdam, Netherlands, 2019. doi:10.1016/c2017-0-03849-1
15. Bamford, W. R.; Stevens, T. S. *J. Chem. Soc.* **1952,** 4735. doi:10.1039/jr9520004735
16. Shapiro, R. H.; Heath, M. J. *J. Am. Chem. Soc.* **1967,** *89,* 5734–5735. doi:10.1021/ja00998a601
17. Shao, Z.; Zhang, H. *Chem. Soc. Rev.* **2012,** *41,* 560–572. doi:10.1039/c1cs15127d
18. Job, A.; Janeck, C. F.; Bettray, W.; Peters, R.; Enders, D. *Tetrahedron* **2002,** *58,* 2253–2329. doi:10.1016/s0040-4020(02)00080-7
19. Lim, D.; Coltart, D. M. *Angew. Chem., Int. Ed.* **2008,** *47,* 5207–5210. doi:10.1002/anie.200800848
20. Lazny, R.; Nodzewska, A. *Chem. Rev.* **2010,** *110,* 1386–1434. doi:10.1021/cr900067y
21. Friestad, G. K. *Eur. J. Org. Chem.* **2005,** 3157–3172. doi:10.1002/ejoc.200500232
22. Sugiura, M.; Kobayashi, S. *Angew. Chem., Int. Ed.* **2005,** *44,* 5176–5186. doi:10.1002/anie.200500691
23. Brehme, R.; Enders, D.; Fernandez, R.; Lassaletta, J. M. *Eur. J. Org. Chem.* **2007,** 5629–5660. doi:10.1002/ejoc.200700746
24. Lassaletta, J. M.; Fernández, R. *Synlett* **2000,** 1228–1240. doi:10.1055/s-2000-7122
25. Friestad, G. K. *Tetrahedron* **2001,** *57,* 5461–5496. doi:10.1016/s0040-4020(01)00384-2
26. Miyabe, H.; Yoshioka, E.; Kohtani, S. *Curr. Org. Chem.* **2010,** *14,* 1254–1264. doi:10.2174/138527210791330477
27. Prieto, A.; Bouyssi, D.; Monteiro, N. *Eur. J. Org. Chem.* **2018,** 2378–2393. doi:10.1002/ejoc.201701600
28. Xu, X.; Zhang, J.; Xia, H.; Wu, J. *Org. Biomol. Chem.* **2018,** *16,* 1227–1241. doi:10.1039/c8ob00056e
29. Chicas-Baños, D. F.; Frontana-Uribe, B. A. *Chem. Rec.* **2021,** *21,* 2538–2573. doi:10.1002/tcr.202100056
30. Frontana-Uribe, B. A.; Little, R. D.; Ibanez, J. G.; Palma, A.; Vasquez-Medrano, R. *Green Chem.* **2010,** *12,* 2099. doi:10.1039/c0gc00382d
31. Cembellín, S.; Batanero, B. *Chem. Rec.* **2021,** *21,* 2453–2471. doi:10.1002/tcr.202100128
32. Yan, M.; Kawamata, Y.; Baran, P. S. *Chem. Rev.* **2017,** *117,* 13230–13319. doi:10.1021/acs.chemrev.7b00397
33. Vitaku, E.; Smith, D. T.; Njardarson, J. T. *J. Med. Chem.* **2014,** *57,* 10257–10274. doi:10.1021/jm501100b
34. Laćan, M.; Jakopčić, K.; Rogić, V.; Damoni, S.; Rogić, O.; Tabaković, I. *Synth. Commun.* **1974,** *4,* 219–224. doi:10.1080/00397917408062076
35. Batusic, M.; Tabaković, I.; Crljenak, S. *Croat. Chem. Acta* **1981,** *54,* 397.
36. Crljenak, S.; Tabakovic, I.; Jeremic, D.; Gaon, I. *Acta Chem. Scand., Ser. B* **1983,** *37,* 527–535. doi:10.3891/acta.chem.scand.37b-0527
37. Tabaković, I.; Laćan, M.; Damoni, S. *Electrochim. Acta* **1976,** *21,* 621–626. doi:10.1016/0013-4686(76)85160-2
38. Zhang, H.; Ye, Z.; Chen, N.; Chen, Z.; Zhang, F. *Green Chem.* **2022,** *24,* 1463–1468. doi:10.1039/d1gc04534b
39. Ye, Z.; Ding, M.; Wu, Y.; Li, Y.; Hua, W.; Zhang, F. *Green Chem.* **2018,** *20,* 1732–1737. doi:10.1039/c7gc03739b
40. Alajmi, S. F.; Youssef, T. E. *Rev. Chim.* **2021,** *72,* 50–58. doi:10.37358/rc.21.2.8419
41. Chiba, T.; Okimoto, M. *J. Org. Chem.* **1992,** *57,* 1375–1379. doi:10.1021/jo00031a014
42. Hammerich, O.; Parker, V. D. *J. Chem. Soc., Perkin Trans. 1* **1972,** 1718. doi:10.1039/p19720001718
43. Lu, F.; Gong, F.; Li, L.; Zhang, K.; Li, Z.; Zhang, X.; Yin, Y.; Wang, Y.; Gao, Z.; Zhang, H.; Lei, A. *Eur. J. Org. Chem.* **2020,** 3257–3260. doi:10.1002/ejoc.202000311
44. Qian, P.; Zhou, Z.; Wang, L.; Wang, Z.; Wang, Z.; Zhang, Z.; Sheng, L. *J. Org. Chem.* **2020,** *85,* 13029–13036. doi:10.1021/acs.joc.0c01700
45. Gunić, E.; Tabaković, I. *J. Org. Chem.* **1988,** *53,* 5081–5087. doi:10.1021/jo00256a033
46. Okimoto, M.; Nagata, Y.; Takahashi, Y. *Bull. Chem. Soc. Jpn.* **2003,** *76,* 1447–1448. doi:10.1246/bcsj.76.1447
47. Okimoto, M.; Takahashi, Y.; Kakuchi, T. *Synthesis* **2003,** 2057–2063. doi:10.1055/s-2003-41048
48. Lin, E.-C.; Van De Mark, M. R. *J. Chem. Soc., Chem. Commun.* **1982,** 1176. doi:10.1039/c39820001176
49. Yang, N.; Yuan, G. *J. Org. Chem.* **2018,** *83,* 11963–11969. doi:10.1021/acs.joc.8b01808
50. Zhao, Z.; He, Y.; Li, M.; Xu, J.; Li, X.; Zhang, L.; Gu, L. *Tetrahedron* **2021,** *87,* 132111. doi:10.1016/j.tet.2021.132111
51. Yuan, L.; Yuan, G.-Q. *Tetrahedron* **2022,** *106-107,* 132647. doi:10.1016/j.tet.2022.132647
52. Zhou, P.; Li, H.; Jiang, R.; Wan, Y.; Hou, J.; Hong, Y.; Tang, D. *Asian J. Org. Chem.* **2023,** *12,* 10.1002/ajoc.202300421. doi:10.1002/ajoc.202300421
53. Li, W.; Xiong, M.; Liang, X.; Wang, D.; Zhu, H.; Pan, Y. *ChemistryOpen* **2022,** *11,* e202100268. doi:10.1002/open.202100268
54. Jiang, R.; Mu, Y.; Hou, J.; Wan, Y.; Hong, Y.; Yang, Z.; Tang, D. *Synlett* **2023,** *34,* 1804–1808. doi:10.1055/a-2082-0918
55. Yang, M.; Jiang, R.; Mu, Y.; Hong, Y.; Wan, Y.; Hou, J.; Tang, D. *Chem. Commun.* **2023,** *59,* 2303–2306. doi:10.1039/d2cc06277a
56. Catarzi, D.; Varano, F.; Poli, D.; Squarcialupi, L.; Betti, M.; Trincavelli, L.; Martini, C.; Dal Ben, D.; Thomas, A.; Volpini, R.; Colotta, V. *Bioorg. Med. Chem.* **2015,** *23,* 9–21. doi:10.1016/j.bmc.2014.11.033
57. Butler, R. N.; Fitzgerald, K. J. *J. Chem. Soc., Perkin Trans. 1* **1988,** 1587. doi:10.1039/p19880001587
58. Linden, M.; Hofmann, S.; Herman, A.; Ehler, N.; Bär, R. M.; Waldvogel, S. R. *Angew. Chem., Int. Ed.* **2023,** *62,* e202214820. doi:10.1002/anie.202214820

59. Song, L.; Lai, Y.; Li, H.; Ding, J.; Yao, H.; Su, Q.; Huang, B.; Ouyang, M.-A.; Tong, R. *J. Org. Chem.* **2022,** *87,* 10550–10554. doi:10.1021/acs.joc.2c01391
60. Tang, D.; Zhang, W.; Ji, J.; Jiang, R.; Wan, Y.; Ma, W.; Zhou, P. *J. Org. Chem.* **2024,** *89,* 6520–6526. doi:10.1021/acs.joc.3c02995
61. Zhang, W.; Jiang, R.; Mu, Y.; Hong, Y.; Wan, Y.; Yang, Z.; Tang, D. *Tetrahedron Lett.* **2023,** *114,* 154256. doi:10.1016/j.tetlet.2022.154256
62. Nguyen, T. B. *Adv. Synth. Catal.* **2017,** *359,* 1066–1130. doi:10.1002/adsc.201601329
63. Chen, J.; Jiang, Y.; Yu, J.-T.; Cheng, J. *J. Org. Chem.* **2016,** *81,* 271–275. doi:10.1021/acs.joc.5b02280
64. Mo, S.-K.; Teng, Q.-H.; Pan, Y.-M.; Tang, H.-T. *Adv. Synth. Catal.* **2019,** *361,* 1756–1760. doi:10.1002/adsc.201801700
65. Li, Y.; Huang, Z.; Mo, G.; Jiang, W.; Zheng, C.; Feng, P.; Ruan, Z. *Chin. J. Chem.* **2021,** *39,* 942–946. doi:10.1002/cjoc.202000586
66. Ye, Z.; Wang, F.; Li, Y.; Zhang, F. *Green Chem.* **2018,** *20,* 5271–5275. doi:10.1039/c8gc02889c
67. Wu, Z.; Xu, P.; Zhou, N.; Duan, Y.; Zhang, M.; Zhu, C. *Chem. Commun.* **2017,** *53,* 1045–1047. doi:10.1039/c6cc08779e
68. Barbey, G.; Genies, M.; Libert, M.; Caullet, C. *Bull. Soc. Chim. Fr.* **1973,** 1942.
69. Barbey, G.; Caullet, C. *Tetrahedron Lett.* **1974,** *15,* 1717–1719. doi:10.1016/s0040-4039(01)82562-4
70. Xu, Z.; Li, Y.; Mo, G.; Zheng, Y.; Zeng, S.; Sun, P.-H.; Ruan, Z. *Org. Lett.* **2020,** *22,* 4016–4020. doi:10.1021/acs.orglett.0c01343
71. Xu, P.; Wu, Z.; Zhou, N.; Zhu, C. *Org. Lett.* **2016,** *18,* 1143–1145. doi:10.1021/acs.orglett.6b00257
72. Fu, Z.-M.; Ye, J.-S.; Huang, J.-M. *Org. Lett.* **2022,** *24,* 5874–5878. doi:10.1021/acs.orglett.2c01782
73. Wen, J.; Zhang, L.; Yang, X.; Niu, C.; Wang, S.; Wei, W.; Sun, X.; Yang, J.; Wang, H. *Green Chem.* **2019,** *21,* 3597–3601. doi:10.1039/c9gc01351b
74. Sarkar, B.; Ghosh, P.; Hajra, A. *Org. Lett.* **2023,** *25,* 3440–3444. doi:10.1021/acs.orglett.3c00999
75. Yang, Q.-L.; Lei, P.-P.; Hao, E. J.; Zhang, B.-N.; Zhou, H.-H.; Li, W.-W.; Guo, W.-M. *SynOpen* **2023,** *7,* 535–547. doi:10.1055/s-0042-1751510
76. Shi, Y.; Wang, K.; Ding, Y.; Xie, Y. *Org. Biomol. Chem.* **2022,** *20,* 9362–9367. doi:10.1039/d2ob01734b
77. Chiba, T.; Okimoto, M.; Nagai, H.; Takata, Y. *J. Org. Chem.* **1983,** *48,* 2968–2972. doi:10.1021/jo00166a006
78. Okimoto, M.; Takahashi, Y. *Bull. Chem. Soc. Jpn.* **2002,** *75,* 2059–2060. doi:10.1246/bcsj.75.2059
79. Okimoto, M.; Numata, K.; Tomozawa, K.; Shigemoto, T.; Hoshi, M.; Takahashi, Y. *Aust. J. Chem.* **2005,** *58,* 560. doi:10.1071/ch05090
80. Tanbouza, N.; Petti, A.; Leech, M. C.; Caron, L.; Walsh, J. M.; Lam, K.; Ollevier, T. *Org. Lett.* **2022,** *24,* 4665–4669. doi:10.1021/acs.orglett.2c01803
81. Steiniger, K. A.; Lambert, T. H. *Sci. Adv.* **2023,** *9,* eadg3026. doi:10.1126/sciadv.adg3026
82. Okimoto, M.; Chiba, T. *J. Org. Chem.* **1990,** *55,* 1070–1076. doi:10.1021/jo00290a048
83. Okimoto, M.; Yoshida, T.; Hoshi, M.; Hattori, K.; Komata, M.; Tomozawa, K.; Chiba, T. *Synth. Commun.* **2008,** *38,* 3320–3328. doi:10.1080/00397910802136656

License and Terms

BEILSTEIN JOURNAL OF ORGANIC CHEMISTRY

Electrochemical allylations in a deep eutectic solvent

Sophia Taylor and Scott T. Handy*

Full Research Paper

Open Access

Address:
Department of Chemistry, Middle Tennessee State University, Murfreesboro, TN, USA

Email:
Scott T. Handy* - shandy@mtsu.edu

* Corresponding author

Keywords:
allylation; electrosynthesis; eutectic solvent; recycling; tin

Beilstein J. Org. Chem. **2024,** *20,* 2217–2224.
https://doi.org/10.3762/bjoc.20.189

Received: 02 July 2024
Accepted: 23 August 2024
Published: 02 September 2024

This article is part of the thematic issue "Synthetic electrochemistry".

Guest Editor: K. Lam

Abstract

Electrosynthesis is a technique that is attracting increased attention and has many appealing features, particularly its potential greenness. At the same time, electrosynthesis requires a solvent and a supporting electrolyte in order for current to pass through the reaction. These are effectively consumable reagents unless a convenient means of recycling can be developed. As part of our interest in unusual solvents and electrochemistry, we explored the application of simple, inexpensive, and recyclable deep eutectic solvents to the allylation of carbonyls. While several sets of conditions were developed, the goal of avoiding stoichiometric amounts of metal has proven elusive. Still, a deep eutectic solvent can be used to plate out and thus recover the metal used, offering an interesting new option for electrochemical allylations.

Introduction

The last several years have witnessed a tremendous resurgence of interest in electrochemistry in the area of organic synthesis [1]. While there are many reasons for this renewed interest, two major motivations are the unmatched control of oxidation or reduction potential that can be achieved and the environmentally friendly aspect of having electrons as the only consumed reagent. This latter reason is certainly an advantage in many cases, but its effective realization is limited by the need for both a solvent as well as a supporting electrolyte to allow for the flow of current through the reaction. Although some imaginative options have been reported, they tend to be quite limited in scope. Room temperature ionic liquids (RTILs) were viewed as interesting options that would combine both the solvent and the electrolyte into one component and could be readily recycled due to their non-volatile nature [2-15]. Further, many of these species featured very wide electrochemical windows. In practice, however, RTILs are expensive compared to conventional solvents. Most of them are also quite viscous, which severely limits their use in synthetic electrochemistry [16].

These same expense and viscosity issues plague the application of RTILs in any area. Driven by this limitation, deep eutectic solvents (DES) were reported and have been heavily promoted as cost-effective replacements for RTILs in many applications [17,18]. One of the early and very effective applications of DES was in the area of electroplating as well as metal recovery by

electrodeposition [19]. Despite this fascinating potential, very little has been reported in terms of their use in electrosynthesis [20-24].

Given our interest in both electrosynthesis and DES, we opted to explore this combination in the area of electrochemical allylation. The allylation of carbonyls is a valuable reaction that has been explored under a wide range of conditions, including several reports using electrochemical conditions [25,26]. Recently, an allylation in DES has also been reported, but using indium as the reducing metal under standard Barbier-type conditions, but not electrochemical ones [27]. While the unusual DES (acetylcholine chloride/acetamide 2:1 molar ratio with added ammonium chloride) could be recycled five times with a modest decrease in yield (99% to 65%), the requirement of using suprastoichiometric amounts of expensive indium metal for each reaction is a significant drawback. The potential to avoid this limitation by using electrochemistry with catalytic amounts of metal or perhaps by recovering and recycling the metal with a recyclable solvent was the goal motivating this project. With this as a background, we undertook an investigation of electrochemical allylation in DES.

Results and Discussion

While there are many potential DES that are known, one that would be stable to highly reducing conditions was desired for the allylation reaction. Further, to make the reaction conditions similar to standard electrochemical ones, a solvent with a tetraalkylammonium salt, the first DES that was studied was the 1:3 molar ratio of tetrabutylammonium bromide and ethylene glycol (TBAB/EG) [28]. Using the reaction of *p*-anisaldehyde with allyl bromide as a test case, reactions were performed using three sets of different sacrificial electrodes as well as non-sacrificial graphite. As can be seen in Table 1, tin (entry 1) resulted in good conversion to the allylation product, while zinc, magnesium, and graphite (Table 1, entries 3–5) displayed no reaction at all. This observation was somewhat surprising considering that both zinc and tin are very commonly used in conventional allylations in addition to as electrode materials for electrochemical allylations [29-48]. Further optimization employing tin (Table 1, entry 2) enabled near complete conversion to the desired product by using 2.5 F/mol of current passed through the solution at a constant current of 20 mA.

With this promising start, several other aldehydes and two ketones were explored under the same reaction conditions (Table 2). A range of aromatic aldehydes worked well as well as one aliphatic aldehyde (Table 2, entry 13) and one alkenyl aldehyde (Table 2, entry 10), although the highly electron-rich dimethylaminobenzaldehyde (Table 2, entry 4) afforded only recovered starting material. Both ketones (Table 2, entries 11 and 12) failed to react and resulted in just recovered starting material. 4-Nitrobenzaldehyde (Table 2, entry 5) also failed to afford any allylation product, although in this case, reduction of the nitro group to an amino group was observed and the resulting 4-aminobenzaldehyde is likely too electron-rich to undergo allylation.

Table 1: Influence of electrode material.

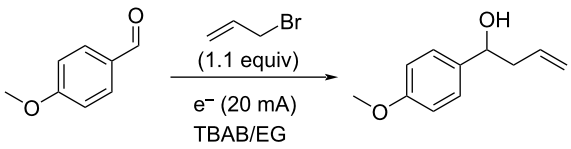

Entry	Electrode	F/mol	% Conversion
1	Sn/Sn	2	86
2	Sn/Sn	2.5	91[a]
3	Zn/Zn	2.5	0
4	Mg/Mg	2.5	0
5	C/C	2.5	0

[a]Isolated yield of product 78%.

Table 2: Aldehyde variations.

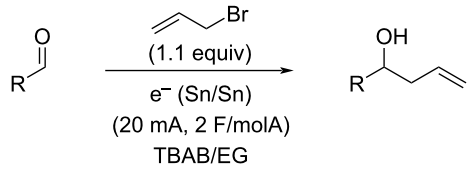

Entry	R	Isolated yield
1	*p*-$MeOC_6H_4$	78%
2	*p*-BrC_6H_4	82%
3	*p*-CNC_6H_4	80%
4	*p*-$Me_2NC_6H_4$	NR
5	*p*-$NO_2C_6H_4$	0%[a]
6	*p*-MeC_6H_4	85%
7	*m*-MeC_6H_4	79%
8	*o*-MeC_6H_4	76%
9	Ph	68%
10	cinnamyl	77%
11	acetophenone	NR
12	cyclohexanone	NR
13	C_6H_{11}	84%

[a]Only nitro group reduced, no allylation.

The use of other halides was also explored (Table 3). Switching to allyl chloride (Table 3, entry 2) did result in partial conver-

sion, but the reaction was much less efficient than for allyl bromide. More substituted allyl bromides, such as crotyl and prenyl bromide (Table 3, entries 3 and 4) did react, although they afforded only partial conversion when using 2.5 F/mol of current. In terms of regiochemistry, addition at the more substituted end (gamma addition) was the major product in both cases, although alpha addition was also observed. In the case of crotyl bromide, no diastereoselectivity was noted for the gamma product. Non-allylic halides such as benzyl bromide, propargyl bromide, and ethyl bromoacetate (Table 3, entries 5–7) did not result in carbonyl addition. The benzyl bromide was recovered intact, while for the other two, they are both sufficiently volatile that they would have been lost during the work-up. For all three, the aldehyde was recovered unreacted.

Table 3: Halide variations.

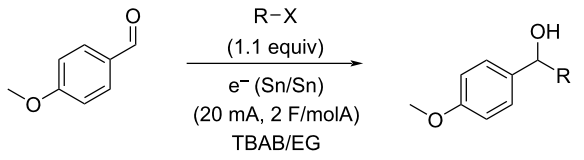

Entry	R–X	% Conversion[a]
1	allyl bromide	100%
2	allyl chloride	50%
3	crotyl bromide	85%[b]
4	prenyl bromide	45%[c]
5	ethyl bromoacetate	NR
6	benzyl bromide	NR
7	propargyl bromide	NR

[a]Determined by ^{1}H NMR of the crude extract; [b]γ to α addition 2.2:1.0, 1:1 diastereomeric mixture of the γ product; [c]γ to α addition 3:1.

While the use of DES as solvent and electrolyte for electrochemical allylation had been demonstrated, there was no particular advantage to this method over non-DES options without recycling of the DES. To explore this aspect, the allylation of anisaldehyde with allyl bromide was undertaken using TBAB/EG. As can be seen in Table 4, the DES could be recycled two times before incomplete conversion was noted. A more significant problem was the steady loss of DES during the product extraction stage. Using 3 mL of methoxycyclopentane in a single extraction, the amount of DES steadily decreased by roughly 0.5 mL for each recycling. This is likely due to partial solubility of ethylene glycol in methoxycyclopentane as ethylene glycol could be clearly seen in the ^{1}H NMR spectrum of the crude reaction extracts. It should also be noted that the lower isolated yields most likely reflect mechanical losses during extraction and chromatographic separation as the crude spectra do not show significant amounts of side products.

Table 4: Recycling for the allylation of *p*-anisaldehyde in TBAB/EG DES and Sn electrodes.

Cycle	Volume of DES recovered	Conversion/isolated yield[a]
1	2.5 mL	100%/78%
2	2.0 mL	100%/77%
3	1.5 mL	100%/79%
4	1.25 mL	80%/60%

[a]Determined by ^{1}H NMR of the crude extract.

Another problem that was noted in these recycling experiments was a build-up of tin salt byproducts that made the DES more and more viscous in each recycling. Avoiding the use of a sacrificial electrode could help this aspect as well as reducing the waste generated in these allylations. While non-sacrificial graphite electrodes had failed to result in any reaction, it seemed possible that the use of a catalytic amount of tin metal or a tin salt with graphite electrodes would result in a superior reaction due to in situ reduction and/or activation of the tin. This variation was explored as seen in Table 5. Use of 0.5 equivalents of tin metal (Table 5, entry 1) did result in partial conversion to product, which increased to complete conversion when 1.5 equivalents of tin were used (Table 5, entry 3). Upon attempted recycling of this reaction, very little conversion was noted, indicating that this method simply exchanged one form of consumed tin (the electrode) for another (the metal powder). We also explored the use of $SnCl_2$ as the tin source. Little to no reaction occurred under a variety of con-

Table 5: Tin metal with non-sacrificial electrodes.

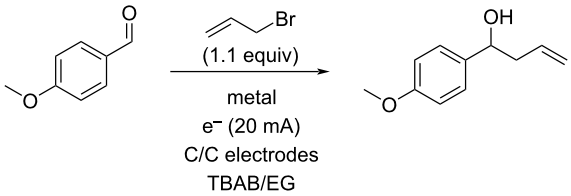

Entry	Tin source	Equivalents of tin	% Conversion[a]
1	Sn powder	0.5	15%
2	Sn powder	1	40%
3	Sn powder	1.5	100%
4	$SnCl_2$	1	10%
5	$SnCl_2$	2[b]	NR
6	$SnCl_2$	2[c]	NR
7	$SnCl_2$	2[d]	50%
8	$SnCl_2$	2[e]	100%

[a]Determined by ^{1}H NMR of the crude extract; [b]100 mA constant current; [c]50 mA constant current; [d]100 mA constant current and 10% by volume water added; [e]constant potential of 2 V.

stant current conditions (Table 5, entries 5 and 6), but using two equivalents at a constant potential of 2.0 V (Table 5, entry 8) resulted in complete conversion to the allylation product. As before, attempts to directly recycle the salt/DES mixture failed to afford any allylation.

Next, it was decided to compare the results of the sacrificial tin electrodes at a constant current of 20 mA with the non-sacrificial glassy carbon electrodes and tin(II) chloride at a constant potential of 2 V for a set of aldehydes. As can be seen in Table 6, three of the four cases (entries 1, 2, and 4), the glassy carbon conditions afforded better yields of the allylation product. Only in the case of the cyclohexanecarboxaldehyde (Table 6, entry 3) was the yield lower and in this case this lower yield was the result of incomplete conversion of the aldehyde.

Table 6: Electrode comparison in TBAB/EG.

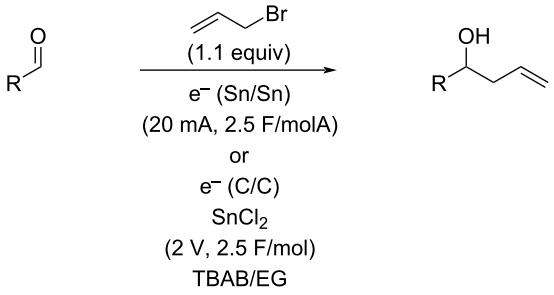

Entry	Aldehyde	Sn/Sn isolated yield	C/C with $SnCl_2$ isolated yield
1	*p*-anisaldehyde	83%	91%
2	*p*-tolualdehyde	77%	83%
3	cyclohexane-carboxaldehyde	68%	58%[a]
4	cinnamaldehyde	61%	85%

[a]12% recovered aldehyde.

For as successful as the TBAB/EG conditions were, TBAB is not inexpensive. Choline chloride is much less expensive and is particularly well known and frequently used in DESs. It is known that choline chloride and ethylene glycol will also form a DES when combined in a 1:2 molar ratio [49]. This solvent is much more viscous than the TBAB/EG one, and an initial attempt to use the same 20 mA constant current conditions with sacrificial tin electrodes resulted in 50% conversion to the allylation product and starting material after passing 2.5 F/mol of current. This poor conversion could be significantly improved by adding 10 volume percent of water to the reaction mixture, which also visibly decreased the viscosity. While complete conversion was still not achieved (67% conversion), it was a considerable improvement. Using glassy carbon electrodes with two equivalents of tin(II) chloride under a constant potential of 2 V, but still in CC/EG with 10 volume percent water, resulted in further improvement (75% conversion) for the same reaction with anisaldehyde. Comparing these two variations always resulted in improved conversions and yields for the glassy carbon conditions, although the results were generally not superior to those obtained in TBAB/EG (Table 7). Interestingly cyclohexanecarboxaldehyde (Table 7, entry 3) was again the outlier as it afforded an excellent yield and complete conversion in the case of glassy carbon in CC/EG.

Table 7: Electrode comparison in CC/EG.

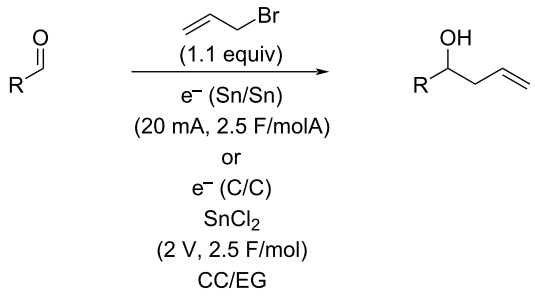

Entry	Aldehyde	Sn/Sn isolated yield	C/C with $SnCl_2$ isolated yield
1	*p*-anisaldehyde	34%[a]	62%[b]
2	*p*-tolualdehyde	24%[b]	67%[c]
3	cyclohexane-carboxaldehyde	52%[c]	96%
4	cinnamaldehyde	58%[d]	62%[b]

[a]Reaction 50% completion; [b]reaction 75% completion; [c]reaction 67% completion; [d]reaction 80% completion.

While the CC/EG system did not appear in general to be as successful as the TBAB/EG one in terms of yields and conversions, it was decided to explore DES recycling (Table 8). As with

Table 8: Recycling in CC/EG.

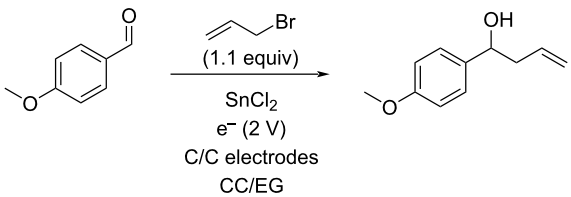

Cycle	Isolated yield
1	64%
2	68%
3	72%

TBAB/EG, the allylation of *p*-anisaldehyde with allyl bromide was conducted using 2 equivalents of tin(II) chloride in CC/EG with 10 volume percent water at a constant potential of 2 V until 2.5 F/mol of current had been passed through the reaction. The product and unreacted starting material were recovered via extraction with methoxycyclopentane and the CC/EG used in another cycle. Through two recyclings, the reactions were similar in efficiency, although the DES became increasingly viscous as the tin byproducts built up and it became impractical to recycle the DES further.

While the DES clearly had some ability to be recycled, the use of catalytic amounts of metal had uniformly failed. Recognizing that DES have been used extensively for electroplating and metal deposition, though it seemed that this might provide an opportunity for metal recovery and reuse [19]. To this end, the DES mixture from cycle 3 of Table 8 following product extraction was electrolyzed at 100 mA constant current using glassy carbon electrodes until 2 F/mol of current had passed. This deposited a metal clump on the electrode that was removed and then analyzed using X-ray fluorescent spectroscopy to determine that the deposited metal was tin, with traces of other metals consistent with the purity of the initial tin source. The tin recovery was 99% of the theoretical. To explore recycling of this recovered tin, 1 mmol was used in a 0.5 mmol scale allylation of anisaldehyde under the constant potential conditions with glassy carbon electrodes and fresh DES. This reaction afforded the anticipated product in 74% yield, thus demonstrating that the tin can be recovered and recycled.

Conclusion

In conclusion, we have demonstrated the ability to use DES as a combined solvent and electrolyte for electrosynthesis. It can be recycled, although product extraction does result in a slow but detectible loss of the ethylene glycol. Attempts to use catalytic amounts of metal with non-sacrificial electrodes in place of the sacrificial tin electrodes were not successful, but we were able to demonstrate efficient and near quantitative recovery of the metal by electrolysis after product extraction and this recovered metal can be used again for further allylations. Further efforts to improve the efficiency and enable catalytic metal use are underway.

Experimental

Preparation of deep eutectic solvents

Tetrabutylammonium bromide/ethylene glycol (1:3 molar ratio) deep eutectic solvent

To 8.0 grams of tetrabutylammonium bromide (TBAB) were added 4.7 grams of ethylene glycol (EG). The resulting mixture was heated to 70 °C until a homogeneous liquid formed. It was stored at this same temperature between uses.

Choline chloride/ethylene glycol (1:2 molar ratio) deep eutectic solvent

To 6.98 grams of choline chloride (CC) were added 6.2 grams of EG and the resulting mixture was heated to 70 °C until a homogeneous liquid formed. It was stored at this same temperature between uses.

General Sn/Sn procedure with TBAB/EG

To a 10 mL ElectraSyn 2.0 vial containing a magnetic stir bar, the carbonyl compound (0.5 mmol), allyl bromide (0.6 mmol), and TBAB/EG DES (2 mL) were added. Tin electrodes were used as the working and counter electrodes and were submerged into the reaction. The reaction was performed under constant current conditions of 20 mA with no reference electrode until 2.5 F/mol was passed. The current was programmed to alternate every five minutes to minimize any potential fouling of the electrode surface. Following completion of each reaction, the mixture was transferred to a separatory funnel with the aid of 10 mL of deionized (DI) water followed by 20 mL of diethyl ether. The organic layer was separated, dried with anhydrous magnesium sulfate, filtered, and the solvent removed in vacuo to afford the crude product, which was first analyzed by ^{1}H NMR spectroscopy and then purified using flash column chromatography. In between reactions, the tin electrodes were rinsed with DI water and acetone, then polished using diamond polish. This helped prevent buildup on the electrode surfaces.

General C/C procedure with TBAB/EG

To a 10 mL ElectraSyn 2.0 vial containing a magnetic stir bar were added the carbonyl compound (0.5 mmol), allyl bromide (0.6 mmol), and TBAB/EG DES (2 mL) along with $SnCl_2$ (0.1896 g, 1 mmol). Graphite electrodes were used as the working and counter electrodes and were submerged into the reaction. The ElectraSyn was programmed to run the reaction under constant potential conditions of 2 V with no reference electrode until 2.5 F/mol was passed. Following completion of each reaction, the mixture was transferred to a separatory funnel with the aid of 10 mL of DI water followed by 20 mL of diethyl ether. The organic layer was separated, dried with anhydrous magnesium sulfate, filtered, and the solvent removed in vacuo to afford the crude product, which was first analyzed by ^{1}H NMR spectroscopy and then purified using flash column chromatography. The graphite electrodes were not polished in between reactions, but were rinsed with DI water and then acetone.

General Sn/Sn procedure with CC/EG

To a 10 mL ElectraSyn 2.0 vial containing a magnetic stir bar, the carbonyl compound (0.5 mmol), allyl bromide (0.6 mmol), CC/EG DES (2 mL), and 10% DI water (0.2 mL) were added.

Tin electrodes were used as the working and counter electrodes and were submerged into the reaction. The ElectraSyn was programmed to run the reaction under constant current conditions of 20 mA with no reference electrode until 2.5 F/mol was passed. The current was programmed to alternate every five minutes. Following completion of each reaction, the mixture was transferred to a separatory funnel with the aid of 10 mL of DI water followed by 20 mL of diethyl ether. The organic layer was separated, dried with anhydrous magnesium sulfate, filtered, and the solvent removed in vacuo to afford the crude product, which was first analyzed by ^{1}H NMR spectroscopy and then purified using flash column chromatography. The electrodes were washed with DI water and acetone before polishing.

General C/C procedure with CC/EG

To a 10 mL ElectraSyn 2.0 vial containing a magnetic stir bar were added the carbonyl compound (0.5 mmol), allyl bromide (0.6 mmol), CC/EG DES (2 mL), and 10% DI water (0.2 mL) along with $SnCl_2$ (0.1896 g, 1 mmol). Graphite electrodes were used as the working and counter electrodes and were submerged into the reaction. The ElectraSyn was programmed to run the reaction under constant potential conditions of 2 V with no reference electrode until 2.5 F/mol was passed. Following completion of each reaction, the mixture was transferred to a separatory funnel with the aid of 10 mL of DI water followed by 20 mL of diethyl ether. The organic layer was separated, dried with anhydrous magnesium sulfate, filtered, and the solvent removed in vacuo to afford the crude product, which was first analyzed by ^{1}H NMR spectroscopy and then purified using flash column chromatography. The graphite electrodes were not polished in between reactions, but were rinsed with DI water and then acetone.

DES and tin metal recycling

For the recyclability trials, the electrolysis vial was opened and about 3 mL of methoxycyclopentane was pipetted directly onto the reaction solution. Then, the vial was capped with a rubber stopper. The methoxycyclopentane acted similarly to the diethyl ether in previous separatory methods by extracting the product from the DES. After letting the methyoxycyclopentane and DES layers separate, the methoxycyclopentane layer was removed using a pipette, placed into a round-bottomed flask, and concentrated in vacuo. This remaining DES could be used directly in subsequent reactions.

If $SnCl_2$ was used in the reaction, electrolysis of the tin metal could be achieved after workup with methoxycyclopentane. Once all product was extracted, the graphite electrodes were submerged in the remaining DES solution in the vial and the tin metal (around 3 mmol) was electrolyzed at 100 mA constant current until 2 F/mol had passed. The resulting metal clump on the electrode was removed using a scoopula for further use and analysis using a Thermo Scientific Niton XL3t X-Ray Fluorescent Spectroscopy analyzer.

Product characterization

1-(4-Methoxyphenyl)-3-buten-1-ol [39]: ^{1}H NMR (300 MHz, $CDCl_3$) 7.27 (d, *J* = 8.58, 2H), 6.86 (d, *J* = 5.82, 2H), 5.83–5.73 (m, 1H), 5.17–5.10 (m, 2H), 4.67 (t, *J* = 6.18, 1H), 3.80 (s, 3H), 2.49 (t, *J* = 4.8, 2H).

1-(4-Bromophenyl)-3-buten-1-ol [50]: ^{1}H NMR (300 MHz, $CDCl_3$) 7.43 (d, *J* = 8.58, 2H), 7.18 (d, *J* = 8.25, 2H), 5.80–5.65 (m, 1H), 5.13–5.07 (m, 2H), 4.64 (t, *J* = 6.51, 1H), 2.43 (t, *J* = 7.2, 2H).

4-(1-Hydroxybut-3-enyl)benzonitrile [51]: ^{1}H NMR (500 MHz, $CDCl_3$) 7.59 (d, *J* = 8.6, 2H), 7.44 (d, *J* = 7.45, 2H), 5.78–5.70 (m, 1H), 5.14–5.10 (m, 2H), 4.76 (t, *J* = 2.85, 1H), 2.48–2.41 (m, 2H).

1-Cyclohexyl-3-buten-1-ol [39]: ^{1}H NMR (300 MHz, $CDCl_3$) 6.0–5.7 (m, 1H), 5.2–5.0 (m, 1H), 3.5–3.3 (m, 1H), 2.4–2.2 (m, 1H), 2.1–2.0 (m, 1H), 1.9–1.6 (m, 4H), 1.5–1.0 (m, 4H).

1-(4-Methylphenyl)-3-buten-1-ol [39]: ^{1}H NMR (300 MHz, $CDCl_3$) 7.24 (d, *J* = 8.25, 2H), 7.16 (d, *J* = 8.22, 2H), 5.87–5.73 (m, 1H), 5.17–5.10 (m, 2H), 4.89 (s, 1H), 4.69 (t, *J* = 6.54, 1H), 2.51 (t, *J* = 6.6, 2H), 2.35 (s, 3H).

1-(3-Methylphenyl)-3-buten-1-ol [50]: ^{1}H NMR (500 MHz, $CDCl_3$) 7.24 (t, *J* = 7.45, 1H), 7.18 (s, 1H), 7.14 (d, *J* = 8.05, 1H), 7.09 (d, *J* = 7.45, 1H), 5.85–5.77 (m, 1H), 5.18–5.12 (m, 2H), 4.69 (t, *J* = 5.15, 1H), 2.50 (t, *J* = 7.45, 2H), 2.36 (s, 3H).

1-(2-Methylphenyl)-3-buten-1-ol [50]: ^{1}H NMR (300 MHz, $CDCl_3$) 7.27–7.14 (m, 4H), 5.91–5.80 (m, 1H), 5.22–5.14 (m, 2H), 4.97 (t, *J* = 3.6, 1H), 2.49 (t, *J* = 8.25, 2H), 2.34 (s, 3H).

1-Phenyl-3-buten-1-ol [39]: ^{1}H NMR (300 MHz, $CDCl_3$) 7.38–7.35 (m, 3H), 5.85–5.76 (m, 2H), 5.15–5.12 (m, 2H), 4.73 (t, *J* = 1.38, 1H), 2.51 (t, *J* = 1.02, 2H).

1-Phenyl-1,5-hexadien-3-ol [52]: ^{1}H NMR (300 MHz, $CDCl_3$) 7.41–7.22 (m, 5H), 6.61 (d, *J* = 16.5, 1H), 6.25 (dd, = 6.54, 15.78 Hz, 1H), 5.90–5.79 (m, 1H), 5.22–5.15 (m, 2H), 4.36 (q, *J* = 5.85, 1H), 2.41 (q, *J* = 8.94, 2H).

Acknowledgements

The authors acknowledge the assistance of Jessie Weatherly in obtaining the XFD results on the recovered tin.

Funding

The authors would like to thank the URECA program at Middle Tennessee State University for providing support for this research.

Author Contributions

Sophia Taylor: conceptualization; data curation; funding acquisition; investigation; methodology; writing – original draft. Scott T. Handy: conceptualization; data curation; funding acquisition; project administration; resources; supervision; writing – review & editing.

ORCID® iDs

Scott T. Handy - https://orcid.org/0000-0003-4199-7292

Data Availability Statement

The data that supports the findings of this study is available from the corresponding author upon reasonable request.

References

1. Yan, M.; Kawamata, Y.; Baran, P. S. *Chem. Rev.* **2017,** *117,* 13230–13319. doi:10.1021/acs.chemrev.7b00397
2. Nozaki, S.; Suzuki, Y.; Goto, T. *Electrochim. Acta* **2024,** *493,* 144431. doi:10.1016/j.electacta.2024.144431
3. Kong, X.; Liu, Q.; Chen, Y.; Wang, W.; Chen, H.-F.; Wang, W.; Zhang, S.; Chen, X.; Cao, Z.-Y. *Green Chem.* **2024,** *26,* 3435–3440. doi:10.1039/d3gc04528e
4. David, M.; Galli, E.; Brown, R. C. D.; Feroci, M.; Vetica, F.; Bortolami, M. *Beilstein J. Org. Chem.* **2023,** *19,* 1966–1981. doi:10.3762/bjoc.19.147
5. Witherspoon, E.; Ling, P.; Winchester, W.; Zhao, Q.; Ibrahim, A.; Riley, K. E.; Wang, Z. *ACS Omega* **2022,** *7,* 42828–42834. doi:10.1021/acsomega.2c04748
6. Rocco, D.; Chiarotto, I.; Mattiello, L.; Pandolfi, F.; Zane, D.; Feroci, M. *Pure Appl. Chem.* **2019,** *91,* 1709–1715. doi:10.1515/pac-2018-1118
7. Yimin, D.; Lanli, N.; Hui, L.; Jiaqi, Z.; Linping, Y.; Qiuju, F. *Int. J. Electrochem. Sci.* **2018,** *13,* 1084–1095. doi:10.20964/2018.01.85
8. Kathiresan, M.; Velayutham, D. *Chem. Commun.* **2015,** *51,* 17499–17516. doi:10.1039/c5cc06961k
9. Zhao, S.-F.; Horne, M.; Bond, A. M.; Zhang, J. *Phys. Chem. Chem. Phys.* **2015,** *17,* 19247–19254. doi:10.1039/c5cp00095e
10. Kronenwetter, H.; Husek, J.; Etz, B.; Jones, A.; Manchanayakage, R. *Green Chem.* **2014,** *16,* 1489–1495. doi:10.1039/c3gc41641k
11. Orsini, M.; Chiarotto, I.; Feeney, M. M. M.; Feroci, M.; Sotgiu, G.; Inesi, A. *Electrochem. Commun.* **2011,** *13,* 738–741. doi:10.1016/j.elecom.2011.04.025
12. Liu, Y.-Z.; Lin, M.-Y.; Xiao, L.-P.; Zhang, K.; Lu, J.-X. *Chin. J. Chem.* **2008,** *26,* 1168–1172. doi:10.1002/cjoc.200890214
13. Mellah, M.; Zeitouny, J.; Gmouh, S.; Vaultier, M.; Jouikov, V. *Electrochem. Commun.* **2005,** *7,* 869–874. doi:10.1016/j.elecom.2005.06.002
14. Doherty, A. P.; Brooks, C. A. *Electrochim. Acta* **2004,** *49,* 3821–3826. doi:10.1016/j.electacta.2003.12.058
15. Mellah, M.; Gmouh, S.; Vaultier, M.; Jouikov, V. *Electrochem. Commun.* **2003,** *5,* 591–593. doi:10.1016/s1388-2481(03)00136-x
16. Bornemann, S.; Handy, S. T. *Molecules* **2011,** *16,* 5963–5974. doi:10.3390/molecules16075963
17. Smith, E. L.; Abbott, A. P.; Ryder, K. S. *Chem. Rev.* **2014,** *114,* 11060–11082. doi:10.1021/cr300162p
18. Hansen, B. B.; Spittle, S.; Chen, B.; Poe, D.; Zhang, Y.; Klein, J. M.; Horton, A.; Adhikari, L.; Zelovich, T.; Doherty, B. W.; Gurkan, B.; Maginn, E. J.; Ragauskas, A.; Dadmun, M.; Zawodzinski, T. A.; Baker, G. A.; Tuckerman, M. E.; Savinell, R. F.; Sangoro, J. R. *Chem. Rev.* **2021,** *121,* 1232–1285. doi:10.1021/acs.chemrev.0c00385
19. Protsenko, V. *Coatings* **2024,** *14,* 375. doi:10.3390/coatings14040375
20. Mousa, M. O.; Adly, M. E.; Mahmoud, A. M.; El-Nassan, H. B. *ACS Omega* **2024,** *9,* 14198–14209. doi:10.1021/acsomega.3c09790
21. El-Nassan, H. B.; El-Mosallamy, S. S.; Mahmoud, A. M. *Sustainable Chem. Pharm.* **2023,** *35,* 101207. doi:10.1016/j.scp.2023.101207
22. Osman, E. O.; Mahmoud, A. M.; El-Mosallamy, S. S.; El-Nassan, H. B. *J. Electroanal. Chem.* **2022,** *920,* 116629. doi:10.1016/j.jelechem.2022.116629
23. Trujillo, S. A.; Peña-Solórzano, D.; Bejarano, O. R.; Ochoa-Puentes, C. *RSC Adv.* **2020,** *10,* 40552–40561. doi:10.1039/d0ra06871c
24. Golgovici, F.; Anicai, L.; Florea, A.; Visan, T. *Curr. Nanosci.* **2020,** *16,* 478–494. doi:10.2174/1573413715666190206145036
25. Yamamoto, Y.; Asao, N. *Chem. Rev.* **1993,** *93,* 2207–2293. doi:10.1021/cr00022a010
26. Denmark, S. E.; Fu, J. *Chem. Rev.* **2003,** *103,* 2763–2794. doi:10.1021/cr020050h
27. Gonzalez-Gallardo, N.; Saavedra, B.; Guillena, G.; Ramón, D. J. *Appl. Organomet. Chem.* **2021,** *35,* e6418. doi:10.1002/aoc.6418
28. Yusof, R.; Abdulmalek, E.; Sirat, K.; Rahman, M. B. A. *Molecules* **2014,** *19,* 8011–8026. doi:10.3390/molecules19068011
29. Zhang, J.; Zhang, L.; Xie, W.; Chen, M.; Zhang, C.; Qin, Y.; Zhao, J.; Wang, F.; Liu, Z.-Q. *Green Chem.* **2024,** *26,* 7002–7006. doi:10.1039/d4gc01838a
30. Zhang, Q.; Liang, K.; Guo, C. *Angew. Chem., Int. Ed.* **2022,** *61,* e202210632. doi:10.1002/anie.202210632
31. Torabi, S.; Jamshidi, M.; Amooshahi, P.; Mehrdadian, M.; Khazalpour, S. *New J. Chem.* **2020,** *44,* 15321–15336. doi:10.1039/d0nj03450a
32. Sinha, A. K.; Mondal, B.; Kundu, M.; Chakraborty, B.; Roy, U. K. *Org. Chem. Front.* **2014,** *1,* 1270–1275. doi:10.1039/c4qo00235k
33. Sun, L.; Sahloul, K.; Mellah, M. *ACS Catal.* **2013,** *3,* 2568–2573. doi:10.1021/cs400587s
34. de Souza, R. F. M.; Areias, M. C. C.; Bieber, L. W.; Navarro, M. *Green Chem.* **2011,** *13,* 1118–1120. doi:10.1039/c0gc00947d
35. Zhang, L.; Zha, Z.; Zhang, Z.; Li, Y.; Wang, Z. *Chem. Commun.* **2010,** *46,* 7196–7198. doi:10.1039/c0cc01964j
36. Huang, J.-M.; Ren, H.-R. *Chem. Commun.* **2010,** *46,* 2286–2288. doi:10.1039/b922897g
37. Zhang, L.; Zha, Z.; Wang, Z.; Fu, S. *Tetrahedron Lett.* **2010,** *51,* 1426–1429. doi:10.1016/j.tetlet.2010.01.026
38. Huang, J.-M.; Dong, Y. *Chem. Commun.* **2009,** 3943–3945. doi:10.1039/b905553c
39. Zha, Z.; Hui, A.; Zhou, Y.; Miao, Q.; Wang, Z.; Zhang, H. *Org. Lett.* **2005,** *7,* 1903–1905. doi:10.1021/ol050483h
40. Durandetti, M.; Meignein, C.; Périchon, J. *J. Org. Chem.* **2003,** *68,* 3121–3124. doi:10.1021/jo026782r

41. Hilt, G.; Smolko, K. I. *Angew. Chem., Int. Ed.* **2001,** *40,* 3399–3402. doi:10.1002/1521-3773(20010917)40:18<3399::aid-anie3399>3.0.co;2-t
42. Rollin, Y.; Derien, S.; Duñach, E.; Gebehenne, C.; Perichon, J. *Tetrahedron* **1993,** *49,* 7723–7732. doi:10.1016/s0040-4020(01)87246-x
43. Hebri, H.; Duñach, E.; Périchon, J. *Tetrahedron Lett.* **1993,** *34,* 1475–1478. doi:10.1016/s0040-4039(00)60322-2
44. Tokuda, M.; Uchida, M.; Katoh, Y.; Suginome, H. *Chem. Lett.* **1990,** *19,* 461–462. doi:10.1246/cl.1990.461
45. Tokuda, M.; Satoh, S.; Suginome, H. *J. Org. Chem.* **1989,** *54,* 5608–5613. doi:10.1021/jo00284a040
46. Durandetti, S.; Sibille, S.; Perichon, J. *J. Org. Chem.* **1989,** *54,* 2198–2204. doi:10.1021/jo00270a033
47. Minato, M.; Tsuji, J. *Chem. Lett.* **1988,** *17,* 2049–2052. doi:10.1246/cl.1988.2049
48. Uneyama, K.; Matsuda, H.; Torii, S. *Tetrahedron Lett.* **1984,** *25,* 6017–6020. doi:10.1016/s0040-4039(01)81748-2
49. Lapeña, D.; Lomba, L.; Artal, M.; Lafuente, C.; Giner, B. *Fluid Phase Equilib.* **2019,** *492,* 1–9. doi:10.1016/j.fluid.2019.03.018
50. Niharika, P.; Ramulu, B. V.; Satyanarayana, G. *ACS Omega* **2018,** *3,* 218–228. doi:10.1021/acsomega.7b01553
51. Dam, J. H.; Fristrup, P.; Madsen, R. *J. Org. Chem.* **2008,** *73,* 3228–3235. doi:10.1021/jo800180d
52. Smith, K.; Lock, S.; El-Hiti, G. A.; Wada, M.; Miyoshi, N. *Org. Biomol. Chem.* **2004,** *2,* 935–938. doi:10.1039/b400179f

License and Terms

BEILSTEIN JOURNAL OF ORGANIC CHEMISTRY

gem-Difluorination of carbon–carbon triple bonds using Brønsted acid/Bu_4NBF_4 or electrogenerated acid

Mizuki Yamaguchi[1], Hiroki Shimao[1], Kengo Hamasaki[1], Keiji Nishiwaki[2], Shigenori Kashimura[1] and Kouichi Matsumoto[*1]

Full Research Paper

Open Access

Address:
[1]Department of Chemistry, School of Science and Engineering, Kindai University, 3-4-1 Kowakae, Higashi-osaka, Osaka 577-8502, Japan and [2]Department of Pharmaceutical Sciences, Faculty of Pharmacy, Kindai University, 3-4-1 Kowakae, Higashi-osaka, Osaka, 577-8502, Japan

Email:
Kouichi Matsumoto[*] - kmatsumo@chem.kindai.ac.jp

* Corresponding author

Keywords:
carbon–carbon triple bonds; chemical method; electrochemistry; *gem*-difluorination

Beilstein J. Org. Chem. **2024,** *20,* 2261–2269.
https://doi.org/10.3762/bjoc.20.194

Received: 15 April 2024
Accepted: 08 July 2024
Published: 06 September 2024

This article is part of the thematic issue "Synthetic electrochemistry".

Guest Editor: K. Lam

Abstract

gem-Difluorination of carbon–carbon triple bonds was conducted using Brønsted acids, such as Tf_2NH and TfOH, combined with Bu_4NBF_4 as the fluorine source. The electrochemical oxidation of a Bu_4NBF_4/CH_2Cl_2 solution containing alkyne substrates could also give the corresponding *gem*-difluorinated compounds (*in-cell* method). The *ex-cell* electrolysis method was also applicable for *gem*-difluorination of alkynes.

Introduction

Organofluorine compounds have attracted great attention in various fields, such as organic materials and pharmaceuticals [1-3], because fluorinated compounds sometimes show specific properties [4]. So far, several methods have been developed for the synthesis of fluorinated compounds. Using nucleophilic fluorinating reagents, such as diethylaminosulfur trifluoride (DAST), HF, CsF, and AgF has been established as a reliable method. Electrophilic fluorinating reagents, such as 1-chloromethyl-4-fluoro-1,4-diazoniabicyclo[2.2.2]octane bis(tetrafluoroborate) (Selectfluor), *N*-fluorobenzenesulfonimide, and fluorobenziodoxole, are also utilized as F^+ equivalents to introduce fluorine atoms into organic molecules. In addition, various trifluoromethylation reagents have been developed so far [5-18]. Transition-metal-catalyzed fluorination and trifluoromethylation methods have also been proposed [19,20]. Thus, the synthesis of fluorinated compounds is an active research field. Among these compounds, skeletons bearing CF_2 units are important [21-24], because such molecules can change the physical properties and biological activity. They can also serve as building blocks for further transformations.

We have focused on the investigation of *gem*-difluorination of carbon–carbon triple bonds, because this procedure is one of the most simple but powerful and straightforward methods. In addition, there have been a few reports in the literature that seem to mainly rely on the use of HF or its complexes as a reagent. These reactions seem to proceed via the formation of the vinyl fluoride as the intermediate [25-28].

In the first example, Olah and co-workers reported the reaction of terminal alkynes with HF/pyridine (Olah reagent) (Figure 1, reaction 1) [29-32], although the original work was developed by Linn and Plueddeman using HF [33-35]. As another example, Renoux and co-workers developed the utility of SbF_5/HF (Figure 1, reaction 2) [36]. In 2014, the HF/*N*,*N*'-dimethylpropyleneurea (DMPU) complex in the presence of an Au catalyst was found to be a good reagent for the *gem*-difluorination of alkynes, reported by Hammond and Xu (Figure 1, reaction 3) [37]. HF/DMPU is easy to handle under experimental conditions. In addition, they recently reported the utilization of a combination of $KHSO_4$·13HF and DMPU·12HF under neat conditions for the *gem*-difluorination of alkynes (Figure 1, reaction 4) [38]. In 2020, the utility of 2,6-dichloropyridinium tetrafluoroborate was nicely demonstrated for the *gem*-difluorination by Liu and Wang (Figure 1, reaction 5) [39].

Although some procedures have been reported, the use of hazardous reagents such as HF is still inevitable [40,41]. Quite

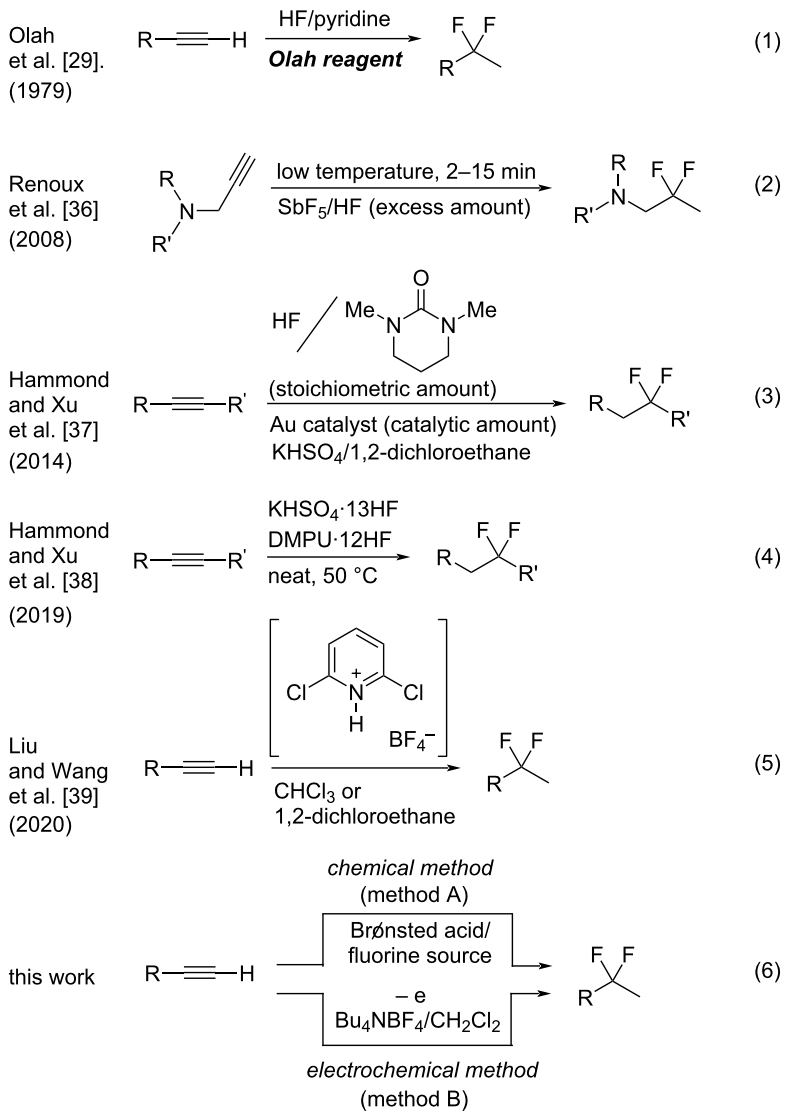

Figure 1: *gem*-Difluorination of carbon–carbon triple bonds. Selected examples from (1) to (5), and this work of (6).

recently, Crimmin and co-workers reported *gem*-difluorination by shuttling between fluoroalkanes and alkynes, in which catalytic HF played a key role [42]. In the course of our study on the fluorination reaction, we have envisioned that the combination of a Brønsted acid, such as Tf_2NH and TfOH, with Bu_4NBF_4 might be effective to promote the *gem*-difluorination of alkynes because of the in situ generation of HF equivalents (Figure 1, reaction 6, chemical method). In addition, the electrogenerated acid (EGA) [43-52] from a solution of Bu_4NBF_4/CH_2Cl_2 containing substrates might also promote the same reactions (Figure 1, reaction 6, electrochemical method). Currently, electrochemistry can be regarded as a promising technique in organic synthesis, because heavy-metal reagents can be avoided for the oxidation or reduction of organic molecules. Herein, we wish to report that the combination of the excess amount of Brønsted acid and Bu_4NBF_4 or the use of an EGA in Bu_4NBF_4/CH_2Cl_2 can serve as suitable reagents for the *gem*-difluorination of alkynes. These procedures are practical, simple and environmentally friendly, because HF or its equivalent is indirectly prepared and utilized in only solution phase.

Results and Discussion

First, we have chosen hex-5-yn-1-ylbenzene (**1a**) as the model substrate in the reaction optimization (Table 1, method A). The reaction was carried out as follows: Hex-5-yn-1-ylbenzene (**1a**, 0.5 mmol) was reacted with the Brønsted acid (*X* equiv) and the fluorine source (*Y* equiv) in the solvent (4 mL) at temperature of *T* (°C) for *Z* hours. The chemical yield of the desired product, (5,5-difluorohexyl)benzene (**2a**), was evaluated for reaction optimization by using the ^{19}F nuclear magnetic resonance (NMR) yield, in which trifluorotoluene ($CF_3C_6H_5$) was used as an internal standard. The use of Tf_2NH (5 equiv or 10 equiv) and Bu_4NBF_4 (5 equiv) in CH_2Cl_2 at room temperature gave the corresponding product **2a** in up to 83% yield (Table 1, entries 1–5). The use of CF_3COOH did not yield **2a** at all (Table 1, entry 6), but TfOH gave the product **2a** in 72% yield (Table 1, entry 7). As for the solvent, CH_3CN slightly afforded **2a**, although *N*,*N*-dimethylformamide (DMF) and dimethyl sulfoxide (DMSO) were not suitable for the reactions (Table 1, entries 8–10). A fluorine source, such as Bu_4NF or $BF_3{\cdot}Et_2O$, instead of Bu_4NBF_4 was not effective (Table 1, entries 11 and 12).

Table 1: Optimization of the *gem*-difluorination of hex-5-yn-1-ylbenzene (**1a**) to form difluorinated compound **2a** (method A).

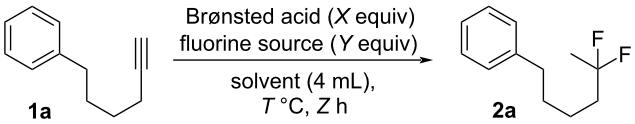

Entry	Brønsted acid	*X* (equiv)	Fluorine source	*Y* (equiv)	Solvent	Reaction time *Z* (h)	*T* (°C)	% Yield[a]
1	Tf_2NH	5	Bu_4NBF_4	5	CH_2Cl_2	8	rt	83
2	Tf_2NH	5	Bu_4NBF_4	5	CH_2Cl_2	16	rt	83 (72)[b]
3	Tf_2NH	5	Bu_4NBF_4	5	CH_2Cl_2	24	rt	82
4	Tf_2NH	3	Bu_4NBF_4	5	CH_2Cl_2	16	rt	75
5	Tf_2NH	10	Bu_4NBF_4	5	CH_2Cl_2	16	rt	46
6	CF_3COOH	5	Bu_4NBF_4	5	CH_2Cl_2	16	rt	n.r.[c]
7	TfOH	5	Bu_4NBF_4	5	CH_2Cl_2	16	rt	72
8	Tf_2NH	5	Bu_4NBF_4	5	CH_3CN	16	rt	6
9	Tf_2NH	5	Bu_4NBF_4	5	DMF	16	rt	n.r.[c]
10	Tf_2NH	5	Bu_4NBF_4	5	DMSO	16	rt	n.r.[c]
11[d]	Tf_2NH	5	Bu_4NF	5	CH_2Cl_2	16	rt	n.r.[c]
12	Tf_2NH	5	$BF_3{\cdot}Et_2O$	5	CH_2Cl_2	16	rt	n.d.[e]
13	Tf_2NH	5	Bu_4NBF_4	3	CH_2Cl_2	16	rt	50
14	Tf_2NH	5	Bu_4NBF_4	9	CH_2Cl_2	16	rt	89
15	Tf_2NH	5	Bu_4NBF_4	9	CH_2Cl_2	16	0	31
16	Tf_2NH	5	Bu_4NBF_4	9	CH_2Cl_2	16	–40	n.r.[c]
17	Tf_2NH	5	Bu_4NBF_4	9	CH_2Cl_2	16	40	82

[a]^{19}F NMR yields. Trifluorotoluene ($CF_3C_6H_5$) was used as an internal standard. [b]Isolated yield after silica gel column chromatography of crude product. [c]n.r. = no reaction. [d]A solution of Bu_4NF/THF underwent vacuum drying to prepare Bu_4NF without THF. Then, CH_2Cl_2 was added to Bu_4NF to prepare a solution. [e]n.d. = not detected.

Finally, investigations of the amount of Bu_4NBF_4 and the reaction temperature demonstrated that conditions including Bu_4NBF_4 (9 equiv) and room temperature gave the best result (Table 1, entries 13–17). Based on the above investigation, we decided to use the optimized conditions in entry 2, because reducing the amount of Bu_4NBF_4, for example, to 5 equiv is important from the viewpoint of eco-friendly chemical synthesis. The reaction time of 16 h also seems to be suitable for the investigation. Thus, the combination of Tf_2NH and Bu_4NBF_4 might generate HBF_4 in the solution.

Next, the electrochemical method was studied for *gem*-difluorination. In a previous report by us, we found that the electrogenerated acids of "$H^+BF_4^-$" equivalents can actually serve as H^+ equivalents [51,52]. We have envisioned that electrogenerated acids such as ''$H^+BF_4^-$'' equivalents might serve as good reagents for the *gem*-difluorination of alkynes. Thus, we have examined the electrochemical oxidation of a solution of Bu_4NBF_4/CH_2Cl_2 containing **1a** (0.5 mmol) in a divided cell using 8 mA or 16 mA (Scheme 1, method B, *in-cell* method). *In-cell* method means that EGA was generated in the presence of the substrate. The total electricity of 3.0 F/mol vs **1a** was passed to the solution. Interestingly, the result gave the corresponding difluorinated compound **2a** in 29% yield in the case of 8 mA, as shown by ^{19}F NMR analysis. In addition, **2a** was obtained in 42% yield by ^{19}F NMR analysis in the case of 16 mA [53].

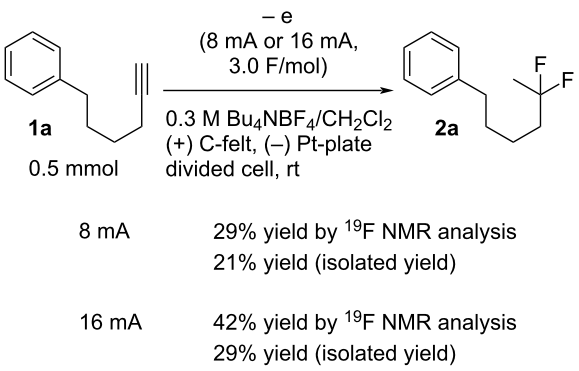

Scheme 1: *gem*-Difluorination promoted by electrogenerated acids (method B).

With the successful formation of (5,5-difluorohexyl)benzene (**2a**) by the chemical (method A) and electrochemical oxidation (method B) methods in hand, we have investigated the scope and limitations of *gem*-difluorination for various alkynes (Table 2). Electrochemical oxidation of method B was conducted by using 8 mA. The reaction of but-3-yn-1-ylbenzene (**1b**) in method A gave the corresponding compound **2b** in 21%

Table 2: Scope and limitations.

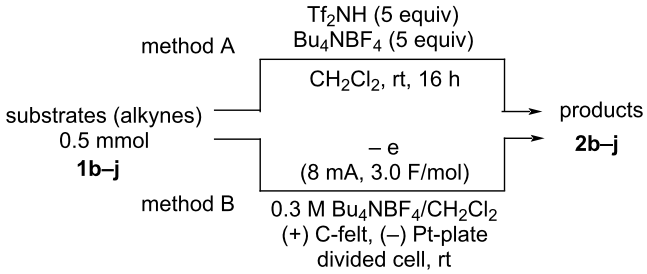

Entry	Substrate	Product	Method	% Yield[a]
1	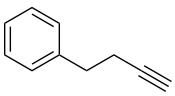 **1b**	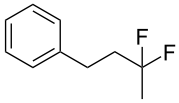 **2b**	A	21 (63)
2			B	6 (29)
3	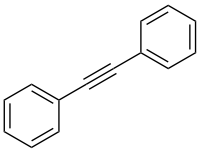 **1c**	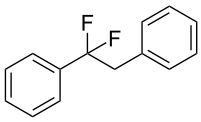 **2c**	A	n.d.[b]
4			B	n.d.[b]

Table 2: Scope and limitations. (continued)

5	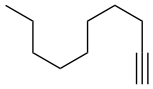 **1d**	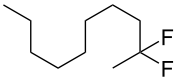 **2d**	A	–[c] (46)
6			A	4[c] (40)[d]
7			B	–[c] (35)
8	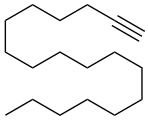 **1e**	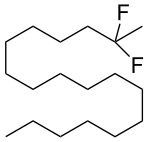 **2e**	A	67 (86)
9			B	50[e] (45)
10	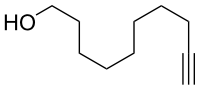 **1f**	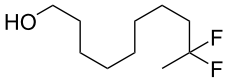 **2f**	A	47 (59)
11			B	41[e] (37)
12	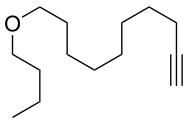 **1g**	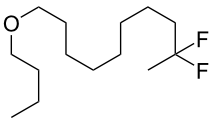 **2g**	A	58[e] (70)
13			B	40[e] (46)
14[f]	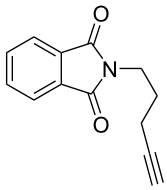 **1h**	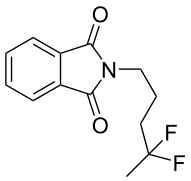 **2h**	A	37 (55)
15			B	15 (13)
16	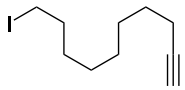 **1i**	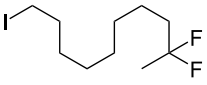 **2i**	A	60 (81)
17			B	–[c] (21)
18	 **1j**	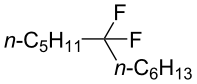 **2j**	A	38 (62)
19			B	10 (24)

[a]Isolated yields. Silica gel column chromatography and/or preparative GPC separation were/was conducted for the purification. ^{19}F NMR yields of the crude products are shown in parentheses. [b]n.d. = not detected. [c]It was impossible to purify and isolate the corresponding product, although the product was confirmed by NMR analysis, when the crude product was prepared. The reason might be due to volatility derived from the low molecular weight. [d]The reaction was conducted in the fourfold scale. [e]Isolated products contained a small amount of impurity. [f]The conditions such as Bu_4NBF_4 (9 equiv) and Tf_2NH (5 equiv) in CH_2Cl_2 at 40 °C for 16 h were used.

isolated yield (Table 2, entry 1). The ^{19}F NMR result indicated 63% yield. Because of the low molecular weight of **2b**, the isolated yield might be somewhat lower. In contrast, method B produced **2b** in 6% isolated yield (Table 2, entry 2). The ^{19}F NMR result indicated 29% yield. As for the internal carbon–carbon triple bonds, diphenylacetylene (**1c**) was tested, but the desired product **2c** was not obtained in any of the two methods (Table 2, entries 3 and 4). In the case of an aliphatic terminal alkyne, such as dec-1-yne (**1d**), the ^{19}F NMR study indicated 46% yield with method A (Table 2, entry 5), but it was

difficult to purify and isolate product **2d** because of the low molecular weight. Scale up conditions of method A, for the purpose of the isolation, led to the formation of the corresponding product **2d** in 40% yield as the ^{19}F NMR analysis (Table 2, entry 6), but the isolation of **2d** was difficult [54]. Method B gave **2d** in 35% yield, as shown by the ^{19}F NMR analysis (Table 2, entry 7). Another alkyne, namely, octadec-1-yne (**1e**), was found to be a nice substrate for *gem*-difluorination to yield the difluorinated compound **2e** (Table 2, entries 8 and 9). Interestingly, terminal alkynes bearing –OH and –O– functional groups, such as **1f** and **1g**, were used for reactions, and the corresponding products **2f** and **2g** were obtained by both methods (Table 2, entries 10–13). In addition, 2-(pent-4-yn-1-yl)isoindoline-1,3-dione (**1h**) was utilized for the construction of the CF_2 unit under the same conditions to give **2h** (Table 2, entries 14 and 15). The substrate bearing a halogen, such as 10-iododec-1-yne (**1i**) in method A, produced the corresponding **2i** in 60% isolated yield (Table 2, entry 16). Likewise, method B also gave **2i** in 21% yield, as shown by the ^{19}F NMR analysis (Table 2, entry 17), but it was difficult to purify and isolate the product **2i** in this case. Finally, the internal aliphatic alkyne such as dodec-6-yne (**1j**) was found to be effective for the *gem*-difluorination. Method A gave **2j** in 38% isolated yield, and method B produced **2j** in 10% isolated yield (Table 2, entries 18 and 19).

Another procedure involving electrochemical oxidation was also applied (the *ex-cell* method) [55,56]. *Ex-cell* method means that EGA was generated in the absence of the substrate, and the substrate was added to the solution after the electrolysis. Optimized conditions and the result are described in Scheme 2. Namely, the electrochemical oxidation of a 0.3 M Bu_4NBF_4/CH_2Cl_2 solution (8 mL) at 0 °C using 32 mA generated and accumulated the EGA as the pool. An electricity of 6.0 F/mol based on 0.5 mmol was passed to the solution. In order to suppress the increase of the solution temperature under the electrolysis, the electrolysis was conducted at 0 °C. Then, the solution containing EGA was allowed to react with **1a** (0.5 mmol) at 0 °C for 0.5 h, giving the corresponding product **2a** in 61% yield, as demonstrated by the ^{19}F NMR analysis. The result indicated that CH_2Cl_2 of the solvent might be oxidized and H^+ species (or equivalent units) might be generated by the electrolysis in this case. In addition, *ex-cell* method can avoid the overoxidation of **2a**, although the excess electricity was passed to the solution.

A plausible reaction mechanism for the current reactions is described in Scheme 3. The reaction of carbon–carbon triple bonds and H^+ species, which are derived from the Brønsted acid (in method A) or EGA (in method B), gives the vinylic carbocation intermediate **A**, which can react with BF_4^- to give fluorinated alkene **B** [57-60]. In the next step, **B** can undergo the second addition of H^+, followed by the incorporation of F^- into the carbocation intermediate **C**, forming the difluorinated compound **2a**. The carbocation adjacent to the F atom might be stabilized by the unshared electron pair of F. Thus, the chemical and electrochemical methods we developed here seem to be superior to the conventional method, because the chemical method requires a usual Brønsted acid and solid Bu_4NBF_4, which can avoid the use of dangerous HF solutions. The electrochemical method also needs only electricity and solid Bu_4NBF_4, which realizes in situ formation of "HBF_4" equivalents.

Conclusion

In summary, we have carried out the *gem*-difluorination of carbon–carbon triple bonds using Tf_2NH/Bu_4NBF_4 or EGA from Bu_4NBF_4/CH_2Cl_2. The feature superiority of these methods is that they do not directly require the use of hazardous HF reagents and expensive metal catalysts. The simple combination of a Brønsted acid with Bu_4NBF_4 as the fluorine source as

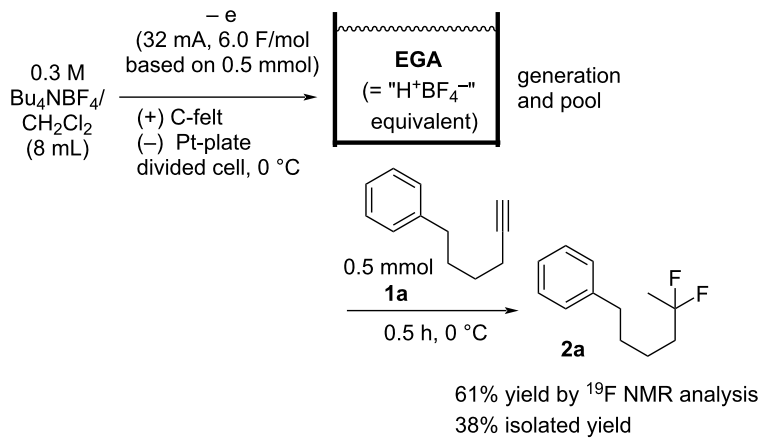

Scheme 2: Generation and accumulation of EGA followed by the reaction with **1a** for **2a**.

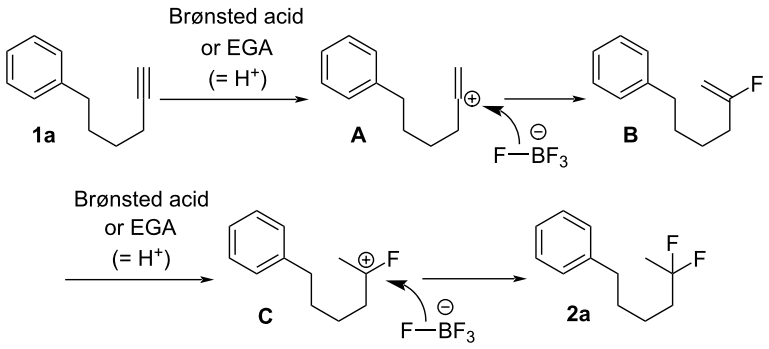

Scheme 3: Plausible reaction mechanism.

well as a simple electrolysis in Bu_4NBF_4/CH_2Cl_2 represent new routes to synthesize CF_2-incorporated organic molecules from alkynes. Further synthetic applications are in progress in our laboratory.

Supporting Information

Supporting Information File 1

Experimental procedure, characterization data of compounds and copies of spectra of ^{1}H NMR and ^{13}C NMR.
[https://www.beilstein-journals.org/bjoc/content/supplementary/1860-5397-20-194-S1.pdf]

Acknowledgements

We are grateful for Kindai University Joint Research Center for use of facilities.

Funding

This work was supported in part by JSPS KAKENHI Grants JP20K05588 (Grant-in-Aid for Scientific Research (C)). We appreciate 2021 Kindai University Research Enchancement Grants (KD2106 and KD2104).

Data Availability Statement

All data that supports the findings of this study is available in the published article and/or the supporting information to this article.

References

1. Zhou, Y.; Wang, J.; Gu, Z.; Wang, S.; Zhu, W.; Aceña, J. L.; Soloshonok, V. A.; Izawa, K.; Liu, H. *Chem. Rev.* **2016,** *116,* 422–518. doi:10.1021/acs.chemrev.5b00392
See for a selected review of fluorine chemistry for organic materials, pharmaceuticals, and chemical biology.
2. Hird, M. *Chem. Soc. Rev.* **2007,** *36,* 2070–2095. doi:10.1039/b610738a
See for a selected review of fluorine chemistry for organic materials, pharmaceuticals, and chemical biology.
3. O'Hagan, D.; Harper, D. B. *J. Fluorine Chem.* **1999,** *100,* 127–133. doi:10.1016/s0022-1139(99)00201-8
See for a selected review of fluorine chemistry for organic materials, pharmaceuticals, and chemical biology.
4. Krafft, M. P.; Riess, J. G. *Chem. Rev.* **2009,** *109,* 1714–1792. doi:10.1021/cr800260k
See for a review for understanding of basic properties for fluorine compounds.
5. Zhu, Y.; Han, J.; Wang, J.; Shibata, N.; Sodeoka, M.; Soloshonok, V. A.; Coelho, J. A. S.; Toste, F. D. *Chem. Rev.* **2018,** *118,* 3887–3964. doi:10.1021/acs.chemrev.7b00778
See for a selected review for the synthesis of fluorine molecules including CF_3-incorporated compounds.
6. Xu, X.-H.; Matsuzaki, K.; Shibata, N. *Chem. Rev.* **2015,** *115,* 731–764. doi:10.1021/cr500193b
See for a selected review for the synthesis of fluorine molecules including CF_3-incorporated compounds.
7. Neumann, C. N.; Ritter, T. *Acc. Chem. Res.* **2017,** *50,* 2822–2833. doi:10.1021/acs.accounts.7b00413
See for a selected review for the synthesis of fluorine molecules including CF_3-incorporated compounds.
8. Koike, T.; Akita, M. *Org. Biomol. Chem.* **2019,** *17,* 5413–5419. doi:10.1039/c9ob00734b
See for a selected review for the synthesis of fluorine molecules including CF_3-incorporated compounds.
9. Umemoto, T. *Chem. Rev.* **1996,** *96,* 1757–1778. doi:10.1021/cr941149u
See for a selected review of fluorinating and trifluoromethylation methods.
10. Hafner, A.; Jung, N.; Bräse, S. *Synthesis* **2014,** *46,* 1440–1447. doi:10.1055/s-0033-1341223
See for a selected review of fluorinating and trifluoromethylation methods.
11. Barata-Vallejo, S.; Lantaño, B.; Postigo, A. *Chem. – Eur. J.* **2014,** *20,* 16806–16829. doi:10.1002/chem.201404005
See for a selected review of fluorinating and trifluoromethylation methods.

12. Yang, X.; Wu, T.; Phipps, R. J.; Toste, F. D. *Chem. Rev.* **2015,** *115,* 826–870. doi:10.1021/cr500277b
See for a selected review of fluorinating and trifluoromethylation methods.
13. Charpentier, J.; Früh, N.; Togni, A. *Chem. Rev.* **2015,** *115,* 650–682. doi:10.1021/cr500223h
See for a selected review of fluorinating and trifluoromethylation methods.
14. Ni, C.; Hu, M.; Hu, J. *Chem. Rev.* **2015,** *115,* 765–825. doi:10.1021/cr5002386
See for a selected review of fluorinating and trifluoromethylation methods.
15. Umemoto, T. *J. Fluorine Chem.* **2014,** *167,* 3–15. doi:10.1016/j.jfluchem.2014.07.029
See for a selected review of fluorinating and trifluoromethylation methods.
16. Egami, H.; Sodeoka, M. *Angew. Chem., Int. Ed.* **2014,** *53,* 8294–8308. doi:10.1002/anie.201309260
See for a selected review of fluorinating and trifluoromethylation methods.
17. Liang, T.; Neumann, C. N.; Ritter, T. *Angew. Chem., Int. Ed.* **2013,** *52,* 8214–8264. doi:10.1002/anie.201206566
See for a selected review of fluorinating and trifluoromethylation methods.
18. Fuchigami, T.; Inagi, S. *Chem. Commun.* **2011,** *47,* 10211–10223. doi:10.1039/c1cc12414e
See for a selected review of fluorinating and trifluoromethylation methods.
19. Li, X.; Shi, X.; Li, X.; Shi, D. *Beilstein J. Org. Chem.* **2019,** *15,* 2213–2270. doi:10.3762/bjoc.15.218
See for a review of transition metal-catalyzed fluorination and trifluoromethylation.
20. Ogiwara, Y.; Sakai, N. *Angew. Chem., Int. Ed.* **2020,** *59,* 574–594. doi:10.1002/anie.201902805
See for a review of transition metal-catalyzed fluorination and trifluoromethylation.
21. Wu, Y.-b.; Wan, L.; Lu, G.-p.; Cai, C. *J. Fluorine Chem.* **2018,** *206,* 125–127. doi:10.1016/j.jfluchem.2017.08.017
See for a recent and selected report for the construction of CF_2 units.
22. Keereewan, S.; Soorukram, D.; Kuhakarn, C.; Reutrakul, V.; Pohmakotr, M. *Eur. J. Org. Chem.* **2018,** 295–305. doi:10.1002/ejoc.201701106
See for a recent and selected report for the construction of CF_2 units.
23. Masusai, C.; Soorukram, D.; Kuhakarn, C.; Reutrakul, V.; Pohmakotr, M. *Eur. J. Org. Chem.* **2018,** 160–169. doi:10.1002/ejoc.201701415
See for a recent and selected report for the construction of CF_2 units.
24. Lv, W.-X.; Li, Q.; Li, J.-L.; Li, Z.; Lin, E.; Tan, D.-H.; Cai, Y.-H.; Fan, W.-X.; Wang, H. *Angew. Chem., Int. Ed.* **2018,** *57,* 16544–16548. doi:10.1002/anie.201810204
See for a recent and selected report for the construction of CF_2 units.
25. Besset, T.; Poisson, T.; Pannecoucke, X. *Eur. J. Org. Chem.* **2015,** 2765–2789. doi:10.1002/ejoc.201403507
See for a review for vinyl fluorides.
26. Landelle, G.; Bergeron, M.; Turcotte-Savard, M.-O.; Paquin, J.-F. *Chem. Soc. Rev.* **2011,** *40,* 2867–2908. doi:10.1039/c0cs00201a
See for a review for vinyl fluorides.
27. Che, J.; Li, Y.; Zhang, F.; Zheng, R.; Bai, Y.; Zhu, G. *Tetrahedron Lett.* **2014,** *55,* 6240–6242. doi:10.1016/j.tetlet.2014.09.072
See for an example of hydrofluorination of alkynes.
28. Gauthier, R.; Mamone, M.; Paquin, J.-F. *Org. Lett.* **2019,** *21,* 9024–9027. doi:10.1021/acs.orglett.9b03425
See for an example of hydrofluorination of alkynes.
29. Olah, G. A.; Welch, J. T.; Vankar, Y. D.; Nojima, M.; Kerekes, I.; Olah, J. A. *J. Org. Chem.* **1979,** *44,* 3872–3881. doi:10.1021/jo01336a027
30. Olah, G. A.; Li, X.-Y.; Wang, Q.; Prakash, G. K. S. *Synthesis* **1993,** 693–699. doi:10.1055/s-1993-25924
31. Olah, G. A.; Mathew, T.; Goeppert, A.; Török, B.; Bucsi, I.; Li, X.-Y.; Wang, Q.; Marinez, E. R.; Batamack, P.; Aniszfeld, R.; Prakash, G. K. S. *J. Am. Chem. Soc.* **2005,** *127,* 5964–5969. doi:10.1021/ja0424878
32. Yamauchi, Y.; Fukuhara, T.; Hara, S.; Senboku, H. *Synlett* **2008,** 438–442. doi:10.1055/s-2008-1032069
33. Grosse, A. V.; Linn, C. B. *J. Am. Chem. Soc.* **1942,** *64,* 2289–2292. doi:10.1021/ja01262a019
34. Henne, A. L.; Plueddeman, E. P. *J. Am. Chem. Soc.* **1943,** *65,* 587–589. doi:10.1021/ja01244a026
35. Bello, D.; Cormanich, R. A.; O'Hagan, D. *Aust. J. Chem.* **2015,** *68,* 72–79. doi:10.1071/ch14298
36. Cantet, A.-C.; Carreyre, H.; Gesson, J.-P.; Jouannetaud, M.-P.; Renoux, B. *J. Org. Chem.* **2008,** *73,* 2875–2878. doi:10.1021/jo702441p
37. Okoromoba, O. E.; Han, J.; Hammond, G. B.; Xu, B. *J. Am. Chem. Soc.* **2014,** *136,* 14381–14384. doi:10.1021/ja508369z
38. Lu, Z.; Bajwa, B. S.; Liu, S.; Lee, S.; Hammond, G. B.; Xu, B. *Green Chem.* **2019,** *21,* 1467–1471. doi:10.1039/c8gc03876g
39. Guo, R.; Qi, X.; Xiang, H.; Geaneotes, P.; Wang, R.; Liu, P.; Wang, Y.-M. *Angew. Chem., Int. Ed.* **2020,** *59,* 16651–16660. doi:10.1002/anie.202006278
40. Wang, Z.-X.; Livingstone, K.; Hümpel, C.; Daniliuc, C. G.; Mück-Lichtenfeld, C.; Gilmour, R. *Nat. Chem.* **2023,** *15,* 1515–1522. doi:10.1038/s41557-023-01344-5
See for a related and recent work.
41. Gauthier, R.; Paquin, J.-F. *Chem. – Eur. J.* **2023,** *29,* e202301896. doi:10.1002/chem.202301896
See for a recent review.
42. Farley, S. E. S.; Mulryan, D.; Rekhroukh, F.; Phanopoulos, A.; Crimmin, M. R. *Angew. Chem., Int. Ed.* **2024,** *63,* e202317550. doi:10.1002/anie.202317550
43. Jiao, K.-J.; Xing, Y.-K.; Yang, Q.-L.; Qiu, H.; Mei, T.-S. *Acc. Chem. Res.* **2020,** *53,* 300–310. doi:10.1021/acs.accounts.9b00603
See for a recent review of electro-organic chemistry.
44. Leech, M. C.; Lam, K. *Acc. Chem. Res.* **2020,** *53,* 121–134. doi:10.1021/acs.accounts.9b00586
See for a recent review of electro-organic chemistry.
45. Yan, M.; Kawamata, Y.; Baran, P. S. *Chem. Rev.* **2017,** *117,* 13230–13319. doi:10.1021/acs.chemrev.7b00397
See for a recent review of electro-organic chemistry.
46. Yoshida, J.-i.; Shimizu, A.; Hayashi, R. *Chem. Rev.* **2018,** *118,* 4702–4730. doi:10.1021/acs.chemrev.7b00475
See for a recent review of electro-organic chemistry.
47. Atobe, M.; Shida, N. *Curr. Opin. Electrochem.* **2024,** *44,* 101440. doi:10.1016/j.coelec.2024.101440
See for a recent review of electro-organic chemistry.
48. Senboku, H. *Chem. Rec.* **2021,** *21,* 2354–2374. doi:10.1002/tcr.202100081
See for a recent review of electro-organic chemistry.

49. Uneyama, K.; Isimura, A.; Torii, S. *Bull. Chem. Soc. Jpn.* **1985,** *58,* 1859–1860. doi:10.1246/bcsj.58.1859
See for a report of EGAs.
50. Kawa, K.; Saitoh, T.; Kaji, E.; Nishiyama, S. *Org. Lett.* **2013,** *15,* 5484–5487. doi:10.1021/ol4026342
See for a report of EGAs.
51. Matsumoto, K.; Shimazaki, H.; Sanada, T.; Shimada, K.; Hagiwara, S.; Suga, S.; Kashimura, S.; Yoshida, J.-i. *Chem. Lett.* **2013,** *42,* 843–845. doi:10.1246/cl.130255
See for a report of EGAs.
52. Matsumoto, K.; Shimao, H.; Fujiki, Y.; Kawashita, N.; Kashimura, S. *Electrochemistry* **2020,** *88,* 262–264. doi:10.5796/electrochemistry.20-00032
See for a report of EGAs.
53. $LiBF_4$ as a fluorine source was not suitable. $LiBF_4$ in CH_2Cl_2 did not dissolve completely. It was also impossible to pass the electricity in the solution of $LiBF_4/CH_2Cl_2$.
54. The extensive and repetitive investigation for the isolation under the fourfold scale gave **2d** in 26% isolated yield as the purified compound.
55. Steckhan, E. *Angew. Chem., Int. Ed. Engl.* **1986,** *25,* 683–701. doi:10.1002/anie.198606831
See for a review of *ex-cell* electrochemical synthesis.
56. It is difficult to accurately quantify and evaluate EGA in the solution phase.
57. Cresswell, A. J.; Davies, S. G.; Roberts, P. M.; Thomson, J. E. *Chem. Rev.* **2015,** *115,* 566–611. doi:10.1021/cr5001805
See for a review of BF_4^- as the F^- source.
58. Pfeifer, L.; Gouverneur, V. *Org. Lett.* **2018,** *20,* 1576–1579. doi:10.1021/acs.orglett.8b00321
See for a recent example for the synthesis of vinyl fluoride compounds.
59. Yang, M.-H.; Matikonda, S. S.; Altman, R. A. *Org. Lett.* **2013,** *15,* 3894–3897. doi:10.1021/ol401637n
See for a recent example for the synthesis of vinyl fluoride compounds.
60. Zhao, M.; Ming, L.; Tang, J.; Zhao, X. *Org. Lett.* **2016,** *18,* 416–419. doi:10.1021/acs.orglett.5b03448
See for a recent example for the synthesis of vinyl fluoride compounds.

License and Terms

BEILSTEIN JOURNAL OF ORGANIC CHEMISTRY

Efficient one-step synthesis of diarylacetic acids by electrochemical direct carboxylation of diarylmethanol compounds in DMSO

Hisanori Senboku*[1,2] and Mizuki Hayama[2]

Full Research Paper

Open Access

Address:
[1]Division of Applied Chemistry, Faculty of Engineering, Hokkaido University, Kita 13 Nishi 8, Kita-ku, Sapporo, Hokkaido 060-8628, Japan and [2]Graduate School of Chemical Sciences and Engineering, Hokkaido University, Kita 13 Nishi 8, Kita-ku, Sapporo, Hokkaido 060-8628, Japan

Email:
Hisanori Senboku* - senboku@eng.hokudai.ac.jp

* Corresponding author

Keywords:
C(sp^3)–O bond cleavage; diarylacetic acid; diarylmethanol; electrochemical reduction; fixation of carbon dioxide

Beilstein J. Org. Chem. **2024,** *20,* 2392–2400.
https://doi.org/10.3762/bjoc.20.203

Received: 25 July 2024
Accepted: 05 September 2024
Published: 20 September 2024

This article is part of the thematic issue "Synthetic electrochemistry".

Guest Editor: K. Lam

Abstract

An efficient one-step synthesis of diarylacetic acids was successfully performed by electrochemical direct carboxylation of diarylmethanol compounds in DMSO. Constant-current electrolysis of diarylmethanol species in DMSO using a one-compartment cell equipped with a Pt cathode and a Mg anode in the presence of carbon dioxide induced reductive C(sp^3)–O bond cleavage at the benzylic position in diarylmethanol compounds and subsequent fixation of carbon dioxide to produce diarylacetic acids in good yield. This protocol provides a novel and simple approach to diarylacetic acids from diarylmethanol species and carbon dioxide without transformation of the hydroxy group into appropriate leaving groups, such as halides and esters including carbonates.

Introduction

Electrochemical reduction of benzyl alcohol derivatives can induce reductive cleavage of a C(sp^3)–O bond [1] at the benzylic position to generate the corresponding benzylic anion species. This protocol has been frequently applied to electrochemical carboxylation [2-11], yielding phenylacetic acids. For example, Troupel et al. successfully performed electrochemical reduction of benzyl ethers and several esters such as acetate, trifluoroacetate, benzoate, and dibenzyl carbonate derived from benzyl alcohols, including 1-phenylethanol compounds, in the presence of carbon dioxide to give the corresponding phenylacetic acids [12]. We found that alkyl benzyl carbonates and benzal diacetates (benzylidene diacetates) were also applicable to electrochemical carboxylation with C(sp^3)–O bond cleavage at the benzylic position, yielding phenylacetic acids [13] and mandel acetates [14], respectively. Electrolysis of styrene oxide and related 2-phenylcyclic ethers in the presence of carbon dioxide

also induced carboxylation at the benzylic position by reductive cleavage of a C(sp^3)–O bond to give the corresponding ω-hydroxy-2-phenylalkanoic acids [15,16]. In contrast, little attention has been paid to electrochemical direct carboxylation of benzyl alcohols, although it is a more straightforward and simple protocol toward phenylacetic acids. In 2015, we reported an electrochemical direct carboxylation of benzyl alcohols having an electron-withdrawing group on the phenyl ring [17]. To the best of our knowledge, this is the first report on electrochemical carboxylation of benzyl alcohols. Only benzyl alcohols having an electron-withdrawing group, such as cyano or ester in the *ortho*- or *para*-position of the phenyl ring, were efficiently carboxylated by constant-current electrolysis in DMF using an undivided cell equipped with a Pt cathode and a Mg anode in the presence of carbon dioxide. On the other hand, carboxylation scarcely took place in DMF when other benzyl alcohols were used as substrates. Lundberg and co-workers recently reported similar results showing that electrochemical carboxylation of benzyl alcohols in the presence of Bu_4NBH_4 in DMF using graphite electrodes gave the corresponding carboxylic acids only in poor yield [18]. We recently found that DMSO is a more suitable solvent for electrochemical carboxylation of benzyl alcohols. Even though there was no electron-withdrawing group on the phenyl ring in the benzyl alcohols, electrochemical carboxylation of the benzyl alcohols in DMSO provided the corresponding phenylacetic acids in moderate yield by reductive C(sp^3)–O bond cleavage followed by fixation of carbon dioxide at the benzylic position [19]. Notably, when diphenylmethanol (**1a**) was used as substrate for electrochemical carboxylation in DMSO, the carboxylation efficiently proceeded to give diphenylacetic acid (**2a**) in high yield. In this paper, we focus on electrochemical carboxylation of diarylmethanol compounds **1** in DMSO and report the efficient one-pot synthesis of diarylacetic acids **2** using this protocol (Scheme 1, bottom). Although photochemical synthesis of diarylacetic acids **2** from diarylmethanol species **1** and carbon dioxide has been reported (Scheme 1, top) [20], to the best of our knowledge, this is the first electrochemical and the second efficient example of diarylacetic acid **2** synthesis from diarylmethanol compounds **1** and carbon dioxide in one step.

Results and Discussion

Although we have previously obtained diphenylacetic acid (**2a**) in 81% yield by electrochemical carboxylation of diphenylmethanol (**1a**) [19], screening of reaction conditions for the substrate **1a** was carried out. Constant-current electrolysis of **1a** using an undivided cell in the presence of carbon dioxide at room temperature was conducted. The effects of the current density (Table 1, entries 1–3), solvent (Table 1, entries 2, 4, and 5), electrodes (Table 1, entries 2, 6, and 7), and electricity (Table 1, entries 2 and 8–10) were investigated. A current density between 10 and 30 mA/cm^2 had little effect on the yield of **2a** (Table 1, entries 1–3). Carboxylation of **1a** also took place in DMF instead of DMSO as solvent. However, the efficiency and yield were lower than those in DMSO (Table 1, entry 4). Acetonitrile seemed to be unsuitable for the reaction (Table 1, entry 5). Glassy carbon (GC) was usable as cathode material to give **2a** in 59% yield, slightly lower than when using Pt as cathode, probably due to the high hydrogen overpotential (Table 1, entry 6). In contrast, zinc was not effective as an anode material in the carboxylation, probably due to competitive electrochemical reduction of zinc ions generated by electrochemical oxidation of the zinc anode. The deposition of a black precipitate was observed visually at the cathode (Table 1, entry 7). After tuning of the electricity, electrochemical carboxylation of **1a** under the reaction conditions shown in Table 1, entry 8 gave **2a** in 79% isolated yield. In all cases, diphenylmethane, probably produced by protonation of the generated benzyl anion species, was detected as a byproduct in less than 10% yield, determined through ^{1}H NMR analysis, except for Table 1, entries 3 (13%) and 5 (25%). It should also be noted that electrolysis was carried out at room temperature, but the temperature of the reaction mixture increased to 40–50 °C at the end of the electrolysis in every case due to heat generation by electric resistance.

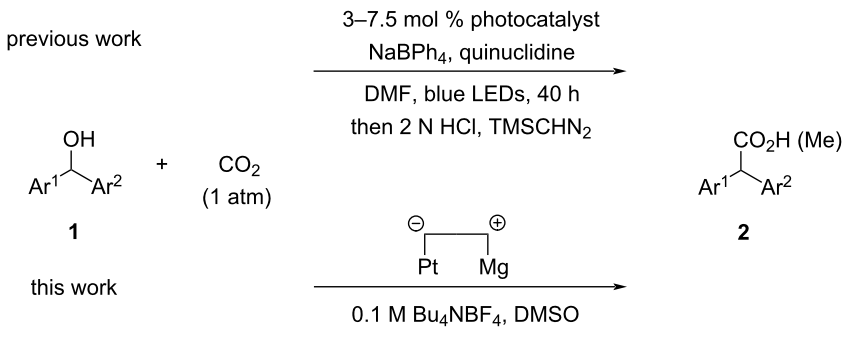

Scheme 1: Synthesis of diarylacetic acids **2** from diarylmethanol compounds **1** and carbon dioxide.

Table 1: Screening of reaction conditions in the electrochemical carboxylation of **1a**.

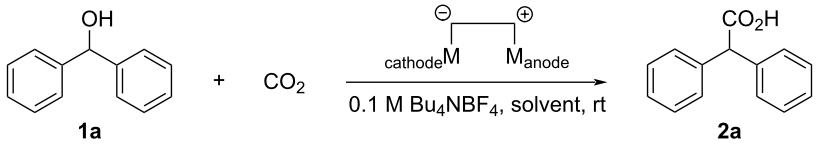

1a **2a**

entry	cathode	anode	solvent	current density, mA/cm^2	electricity, F/mol	conversion, %[a]	yield, %[b]
1	Pt	Mg	DMSO	10	6	83	69
2	Pt	Mg	DMSO	20	6	84	69
3	Pt	Mg	DMSO	30	6	76	61
4	Pt	Mg	DMF	20	6	48	39
5	Pt	Mg	CH_3CN	20	6	42	14
6	GC	Mg	DMSO	20	6	71	59
7	Pt	Zn	DMSO	20	6	38	28
8	Pt	Mg	DMSO	20	8	92	79
9	Pt	Mg	DMSO	20	10	94	80
10	Pt	Mg	DMSO	20	12	98	80

[a]Determined by ^{1}H NMR spectroscopy using 1,4-dinitrobenzene as internal standard. [b]Isolated yield.

With these results in hand, the substrate scope was investigated. First, the applicability of halogen-containing diphenylmethanol compounds **1b** and **1c** to the electrochemical carboxylation under the reaction conditions shown in Table 1, entry 8 was investigated, and the results are summarized in Scheme 2. Electrochemical carboxylation of bis(4-chlorophenyl)methanol (**1b**) unfortunately proceeded along with dehalogenation of the phenyl ring to give **2a** in 31% yield. The absence of mono- and dichlorocarboxylic acids such as **2b** in the product and the existence of dechlorinated diphenylmethanol (**1a**) in the recovered starting material were confirmed by ^{1}H NMR analysis. These results suggested that **2a** was produced from **1a**, which was generated in situ by electroreductive dechlorination of **1b**. In other words, electroreductive dechlorination of **1b**, producing **1a**, took place preferentially over electroreductive C(sp^3)–O bond cleavage of **1b**. It should also be noted that no aromatic carboxylic acids were detected by ^{1}H NMR analysis. In contrast, the electrochemical carboxylation of **1c**, containing a fluorine atom, gave a mixture of fluorine-containing carboxylic acid **2c** and defluorinated carboxylic acid **2a**. Fluorine-containing starting material **1c** and defluorinated diphenylmethanol (**1a**) were detected by ^{1}H NMR analysis. At the same time, it is

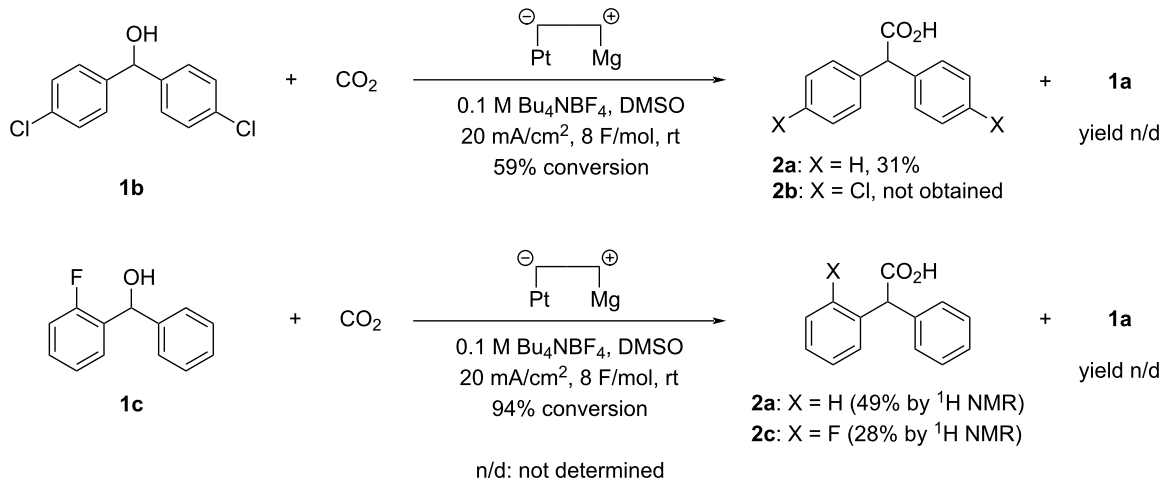

Scheme 2: Attempted electrochemical carboxylation of halogen-containing diphenylmethanol compounds **1b** and **1c**.

presently unclear whether **2a** was produced in a carboxylation–defluorination or defluorination–carboxylation sequence.

Other results of the electrochemical carboxylation are summarized in Scheme 3. Electrochemical carboxylation of diphenylmethanol species **1d** and **1e**, having a methyl or methoxy group on the phenyl ring, also proceeded to give the corresponding diphenylacetic acids **2d** and **2e** in 61% and 63% yield, respectively. In the electrocarboxylation of **1f** and **1g**, having a methyl or methoxy group on both phenyl rings, the yield of **2f** and **2g** was comparably lower, namely 32% and 21%, respectively, probably due to the electron-donating groups. When diphenylmethanol **1h**, having a hydroxy group on the phenyl ring, was used as substrate, selective C–O bond cleavage, followed by fixation of carbon dioxide, occurred at the benzylic C(sp^3)–O bond rather than the C(sp^2)–O bond on the phenyl ring to give the corresponding diphenylacetic acid **2h** in 45% yield. Not only a secondary alcohol but also a tertiary alcohol was applicable to the reaction. When 1,1-diphenylethanol (**1i**) was subjected to electrochemical carboxylation, electroreductive C(sp^3)–O bond cleavage and subsequent carboxylation also took place, similarly to that of secondary alcohols, to give 2,2-diphenylpropanoic acid (**2i**) in 57% yield. Cyclic alcohols and heteroarylmethanol were also suitable and efficient substrates. Electroreductive C(sp^3)–O bond cleavage and subsequent carboxylation proceeded efficiently when dibenzocycloheptenol (**1j**) was used as substrate to give the corresponding dibenzocycloheptenecarboxylic acid (**2j**) in 84% yield. Electrocarboxylation of xanthenol (**1k**) provided xanthene-9-carboxylic acid (**2k**) in an excellent yield of 90%. Phenyl(thiophen-2-yl)acetic acid (**2l**) could also be synthesized in an excellent yield of 92% yield by electrochemical carboxylation of phenyl(thiophen-2-yl)methanol (**1l**).

Although a wide range of substrates was shown to be applicable, a limitation of the reaction also existed. Electrochemical carboxylation of 9*H*-fluoren-9-ol (**1m**) failed, and only a complex mixture was obtained, probably due to the electrochemical reduction and/or carboxylation of the biphenyl moiety in fluorenol (**1m**, top of Scheme 4). Similarly, when triphenylmethanol (**1n**) was subjected to the electrochemical carboxylation, a small amount of carboxylic acid was obtained as a complex mixture. However, in the ^{1}H NMR spectrum of the organic component after extraction with aqueous base, we observed a singlet at δ 5.55 ppm, which could be assigned to the methine proton in triphenylmethane (**3**, Scheme 4, bottom). Further, the yield was determined to be 67% by ^{1}H NMR spectroscopy. These results indicated that the triphenylmethyl anion species generated by electroreductive C(sp^3)–O bond cleavage acted not as nucleophile toward carbon dioxide but as base, performing proton abstraction from DMSO to produce **3** as main product. It was thought that the increase of steric hindrance caused a reduction in nucleophilicity and an increase in basicity in the generated triphenylmethyl anion species, in comparison to the diphenylmethyl anion species.

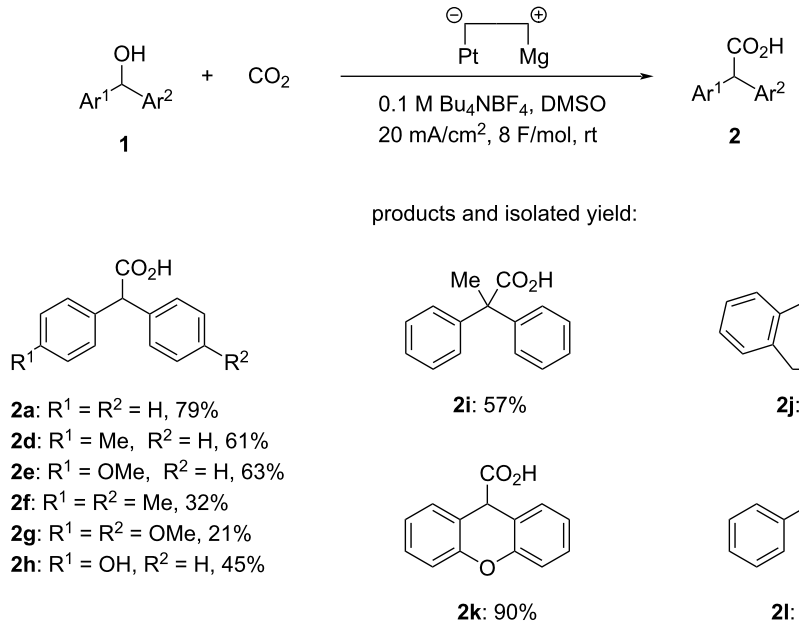

Scheme 3: Synthesis of diarylacetic acids **2** by electrochemical carboxylation of diarylmethanol species **1**.

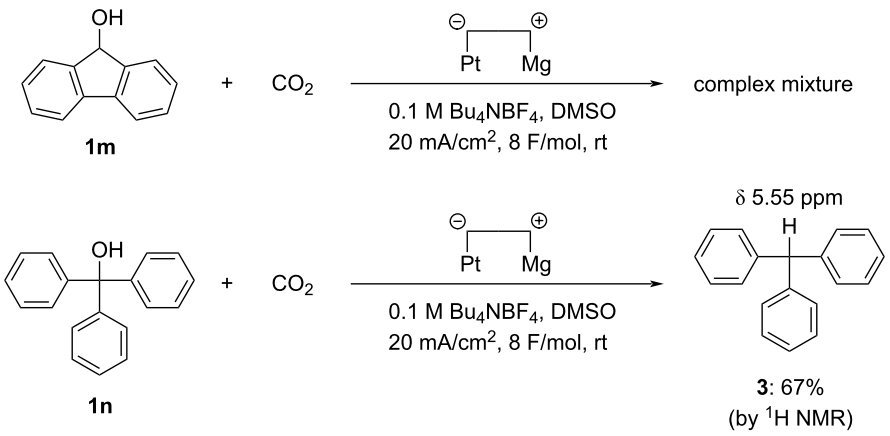

Scheme 4: Attempted electrochemical carboxylation of **1m** and **1n**.

To elucidate the mechanism of the electroreductive C(sp^3)–O bond cleavage, one additional experiment was carried out as shown in Scheme 5. Constant-current electrolysis of **1a** in DMSO with 20 mA/cm^2 of current density and 6 F/mol of electricity at room temperature under a nitrogen atmosphere instead of carbon dioxide resulted in the recovery of 98% of the starting material **1a**. This result indicated that carbon dioxide played an important role not only as a carboxy source but also in the electroreductive C(sp^3)–O bond cleavage.

From these and our previous results for the electrochemical carboxylation of benzyl carbonates [13], plausible reaction pathways are proposed as seen in Scheme 6. At the cathode, one-electron reduction of the hydroxy group in diarylmethanol **1** generates H_2 and the corresponding alkoxide ion **A**, which captures carbon dioxide to form carbonate ion **B**. Although it is currently unclear whether this proceeds in a stepwise or concerted manner, two-electron reduction of carbonate ion **B** generates the corresponding diphenylmethyl anion **C**, which reacts with carbon dioxide to produce a carbon–carbon bond that results in the formation of diphenyl acetate ion **D**. Electrochemical reduction of carbon dioxide competitively occurs at the cathode, and an excess amount of electricity should therefore be necessary to obtain acceptable results. At the anode, on the other hand, dissolution of magnesium ions by electrochemical oxidation of magnesium metal occurs, preventing electrochemical oxidation of the product and intermediates at the anode. The produced acetate ion **D** and a magnesium ion form the salt **E**, which upon acid treatment during workup gives a diphenylacetic acid **2**. The effects of DMSO as solvent are not clear at present, and one reasonable and acceptable aspect might be the solubility of the salt of intermediate **B** in DMSO solvent. Electrochemical reduction of intermediate **B** should occur in solution, and this would mean that intermediate **B** must be dissolved in the solvent used. DMSO is well known as a good solvent for dissolving organic metal salts. In this electrochemical reaction medium, a main counter cation of intermediate **B** is thought to be the magnesium ion, and the magnesium salt of **B** must be dissolved in the solvent. Although other magnesium salts, such as magnesium carbonate and magnesium oxalate, are also generated during the electrolysis, the magnesium salt of **B** would be dissolved sufficiently in DMSO for electrochemical reduction at the cathode.

Conclusion

Efficient one-pot synthesis of diarylacetic acids **2** was accomplished by electrochemical direct carboxylation of diarylmethanol species **1** in DMSO. 2,2-Diphenylpropanoic acid (**2i**) and phenyl(thiophen-2-yl)acetic acid (**2l**) could also be synthesized from 1,1-diphenylethanol (**1i**) and phenyl(thiophen-2-yl)methanol (**1l**), respectively, in one step by this electrochemical method. Notably, synthesis of xanthene-9-carboxylic acid

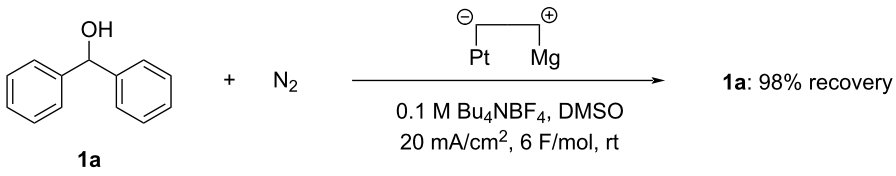

Scheme 5: Electrolysis of **1a** under a nitrogen atmosphere.

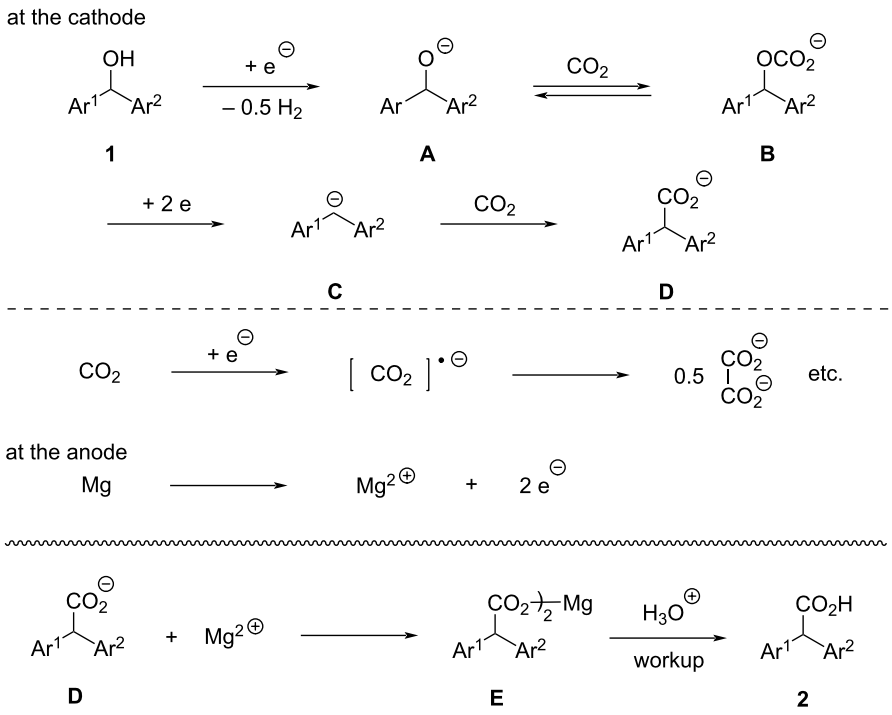

Scheme 6: Plausible reaction pathways.

(**2k**) and dibenzocycloheptene-5-carbocylic acid **2j** was conducted with excellent yield. Direct substitution of a hydroxy by a carboxy group using carbon dioxide as carboxy source is generally difficult under neutral and mild conditions without the use of metal catalysts and/or ligands. This protocol represents a novel method for synthesizing diarylacetic acids **2** from the corresponding alcohols **1** in one step by using an electrochemical method. Instead of DMF and acetonitrile, which have frequently been used for electrochemical carboxylation, DMSO was found to be effective for electrochemical carboxylation of diarylmethanol compounds **1** in order to provide diarylacetic acids **2**. The present electrochemical synthesis is promising as a novel, efficient, facile, and green organic method.

Experimental

General information

^{1}H (400 MHz) and ^{13}C (100 MHz) NMR spectra were recorded in $CDCl_3$ or DMSO-d_6 with a JEOL JNM-ECS400 FT NMR spectrometer. The chemical shifts δ are given in ppm with tetramethylsilane (δ 0 ppm) or DMSO (δ 2.50 ppm) for ^{1}H and $CDCl_3$ (δ 77.0 ppm) or DMSO-d_6 (δ 39.5 ppm) for ^{13}C as internal references. *J* values are in Hz. Peak multiplicities are given as follows: s, singlet; d, doublet; t, triplet; q, quartet; m, multiplet; br, broad. Reagents and solvents, including anhydrous DMSO, are commercially available and were used as received without further purification. Electrochemical reactions were carried out using a constant current power supply (model 5944), Metronix Corp., Tokyo.

Diphenylmethanol (**1a**) [21], bis(4-chlorophenyl)methanol (**1b**) [22], (2-fluorophenyl)phenylmethanol (**1c**) [23], (4-methylphenyl)phenylmethanol (**1d**) [21], (4-methoxyphenyl)phenylmethanol (**1e**) [21], bis(4-methylphenyl)methanol (**1f**) [24], bis(4-methoxyphenyl)methanol (**1g**) [25], (4-hydroxyphenyl)phenylmethanol (**1h**) [26], 10,11-dihydro-5*H*-dibenzo[*a*,*d*]cyclohepten-5-ol (**1j**) [27], 9*H*-xanthen-9-ol (**1k**) [28], and phenyl(thiophen-2-yl)methanol (**1l**) [21] are known compounds and were prepared from the corresponding commercially available ketones by reaction with $NaBH_4$ in EtOH or EtOH/THF 1:1. 1,1-Diphenylethanol (**1i**) is also a known compound and was prepared according to the reported procedure [29]. 9*H*-Fluoren-9-ol (**1m**) and triphenylmethanol (**1n**) are commercially available.

General procedure for electrochemical carboxylation of 1

A test-tube-like (≈25 mm ⌀) undivided cell equipped with a Pt plate cathode (2 × 2 cm^2), a Mg rod anode (6 mm ⌀, 2 cm), and a Teflon® tube (1 mm ⌀) for supplying carbon dioxide were used for the electrolysis. A solution of a diarylmethanol **1** (1 mmol) in anhydrous DMSO (10 mL) containing 0.1 M Bu_4NBF_4 (329 mg, 1 mmol) was set in the cell under a nitrogen

atmosphere. Carbon dioxide was bubbled through the solution at room temperature for 10 min, and then the solution was electrolyzed with a constant current (20 mA/cm^2) under atmospheric pressure of bubbling carbon dioxide at room temperature. The temperature of the reaction mixture increased to 40–50 °C at the end of the electrolysis in every case due to generation of heat by electric resistance during the electrolysis. After 8 F/mol of electricity had been supplied, 1 M hydrochloric acid (100 mL) was added to the electrolyzed solution, and then the mixture was extracted with ethyl acetate (30 mL × 5). The combined organic layer was washed with aqueous saturated $NaHCO_3$ (40 mL × 3), and the resulting aqueous solution was acidified with 3 M hydrochloric acid and then extracted with ethyl acetate (30 mL × 5). The combined ethyl acetate solution was washed with H_2O (100 mL × 3) and dried over $MgSO_4$. Evaporation of the solvent gave a diarylacetic acid **2**. The organic layer, extracted by aqueous saturated $NaHCO_3$, was washed with H_2O (100 mL × 3) and dried over $MgSO_4$. Evaporation of the solvent gave a residue that was analyzed by ^{1}H NMR spectroscopy, during which 1,4-dinitrobenzene was used as an internal standard for quantification of the substances.

The products diphenylacetic acid (**2a**) [30,31], (4-methylphenyl)phenylacetic acid (**2d**) [32], (4-methoxyphenyl)phenylacetic acid (**2e**) [32], bis(4-methylphenyl)acetic acid (**2f**) [30,32], bis(4-methoxyphenyl)acetic acid (**2g**) [30,33], (4-hydroxyphenyl)phenylacetic acid (**2h**) [34], 2,2-diphenylpropaoic acid (**2i**) [35], 10,11-dihydro-5*H*-dibenzo[*a*,*d*]cycloheptene-5-carboxylic acid (**2j**) [30], 9*H*-xanthene-9-carboxylic acid (**2k**) [36], and phenyl(thiophen-2-yl)acetic acid (**2l**) [30] are known compounds, and their spectral data were good agreement with previously reported values.

Spectral data of the products **2**

Diphenylacetic acid (**2a**): ^{1}H NMR (400 MHz, $CDCl_3$, δ) 5.05 (s, 1H), 7.25–7.34 (m, 10H); ^{13}C NMR (100 MHz, $CDCl_3$, δ) 56.9, 127.5, 128.7 (× 2), 137.8, 178.1.

(4-Methylphenyl)phenylacetic acid (**2d**): ^{1}H NMR (400 MHz, $CDCl_3$, δ) 2.32 (s, 3H), 5.01 (s, 1H), 7.14 (d, J = 8.2 Hz, 2H), 7.21 (d, J = 8.2 Hz, 2H), 7.25–7.29 (m, 1H), 7.31–7.32 (m, 4H); ^{13}C NMR (100 MHz, $CDCl_3$, δ) 21.0, 56.6, 127.4, 128.5, 128.59, 128.61, 129.3, 134.9, 137.2, 138.0, 178.9.

(4-Methoxyphenyl)phenylacetic acid (**2e**): ^{1}H NMR (400 MHz, $CDCl_3$, δ) 3.78 (s, 3H), 4.99 (s, 1H), 6.86 (d, J = 8.7 Hz, 2H), 7.24 (d, J = 8.7 Hz, 2H), 7.23–7.32 (m, 5H); ^{13}C NMR (100 MHz, $CDCl_3$, δ) 55.2, 56.1, 114.0, 127.4, 128.5, 128.6, 129.7, 129.9, 138.3, 159.0, 179.2.

Bis(4-methylphenyl)acetic acid (**2f**): ^{1}H NMR (400 MHz, $CDCl_3$, δ) 2.32 (s, 6H), 4.97 (s, 1H), 7.13 (d, J = 8.2 Hz, 4H), 7.20 (d, J = 8.2 Hz, 4H); ^{13}C NMR (100 MHz, $CDCl_3$, δ) 21.0, 56.2, 128.5, 129.3, 135.1, 137.1, 178.9.

Bis(4-methoxyphenyl)acetic acid (**2g**): ^{1}H NMR (400 MHz, $CDCl_3$, δ) 3.78 (s, 6H), 4.95 (s, 1H), 6.86 (d, J = 8.7 Hz, 4H), 7.23 (d, J = 8.7 Hz, 4H); ^{13}C NMR (100 MHz, $CDCl_3$, δ) 55.2 (OMe and $\underline{C}HCO_2H$), 114.0, 129.6, 130.3, 158.9, 179.2.

(4-Hydroxyphenyl)phenylacetic acid (**2h**): ^{1}H NMR (400 MHz, DMSO-d_6, δ) 4.91 (s, 1H), 6.70 (d, J = 8.7 Hz, 2H), 7.10 (d, J = 8.7 Hz, 2H), 7.20–7.36 (m, 5H), 9.35 (s, 1H); ^{13}C NMR (100 MHz, DMSO-d_6, δ) 56.0, 115.8, 127.2, 128.8, 128.9, 130.0, 130.2, 140.1, 156.8, 174.3.

2,2-Diphenylpropanoic acid (**2i**): ^{1}H NMR (400 MHz, $CDCl_3$, δ) 1.94 (s, 3H), 7.26–7.34 (m, 10H); ^{13}C NMR (100 MHz, $CDCl_3$, δ) 26.8, 56.4, 127.0, 128.06, 128.12, 143.7, 181.3.

10,11-Dihydro-5*H*-dibenzo[*a*,*d*]cycloheptene-5-carboxylic acid (**2j**): ^{1}H NMR (400 MHz, $CDCl_3$, δ) 2.85–2.93 (m, 2H), 3.31–3.39 (m, 2H), 4.81 (s, 1H), 7.14–7.24 (m, 8H); ^{13}C NMR (100 MHz, $CDCl_3$, δ) 32.4, 58.7, 126.3, 128.1, 130.4, 131.3, 135.4, 139.6, 178.2.

9*H*-Xanthene-9-carboxylic acid (**2k**): ^{1}H NMR (400 MHz, $CDCl_3$, δ) 4.97 (s, 1H), 7.06–7.10 (m, 2H), 7.12–7.15 (m, 2H), 7.28–7.32 (m, 4H); ^{13}C NMR (100 MHz, $CDCl_3$, δ) 44.9, 117.0, 117.6, 123.4, 129.1, 129.3, 151.3, 177.1.

Phenyl(thiophen-2-yl)acetic acid (**2l**): ^{1}H NMR (400 MHz, $CDCl_3$, δ) 5.24 (s, 1H), 6.95–6.97 (m, 1H), 7.01–7.02 (m, 1H), 7.24–7.25 (m, 1H), 7.29–7.37 (m, 3H), 7.39–7.42 (m, 2H); ^{13}C NMR (100 MHz, $CDCl_3$, δ) 52.1, 125.5, 126.6, 126.7, 128.0, 128.3, 128.8, 137.6, 140.0, 177.8.

Supporting Information

Supporting Information File 1

NMR spectra.
[https://www.beilstein-journals.org/bjoc/content/supplementary/1860-5397-20-203-S1.pdf]

Acknowledgements

^{1}H and ^{13}C NMR spectra were measured at Instrumental Analysis Support Office, Frontier Chemistry Center, Faculty of Engineering, Hokkaido University. The authors are grateful for the support.

Funding

This work was partly supported by Grant-in-Aid for Scientific Research(C) (JSPS KAKENHI Grant Number 22K0518202).

ORCID® iDs

Hisanori Senboku - https://orcid.org/0000-0003-2205-626X

Data Availability Statement

All data that supports the findings of this study is available in the published article and/or the supporting information to this article.

References

1. Villo, P.; Shatskiy, A.; Kärkäs, M. D.; Lundberg, H. *Angew. Chem., Int. Ed.* **2023,** *62,* e202211952. doi:10.1002/anie.202211952
2. Senboku, H. *Curr. Org. Chem.* **2024,** *28,* 76–88. doi:10.2174/1385272827666230915162055
3. Mao, J.; Wang, Y.; Zhang, B.; Lou, Y.; Pan, C.; Zhu, Y.; Zhang, Y. *Green Carbon* **2024,** *2,* 45–56. doi:10.1016/j.greenca.2024.02.001
4. Zhang, K.; Liu, X.-F.; Ren, W.-M.; Lu, X.-B.; Zhang, W.-Z. *Chem. – Eur. J.* **2023,** *29,* e202204073. doi:10.1002/chem.202204073
5. Wang, J.; Wei, Z.-F.; Luo, Y.-X.; Lu, C.-H.; Song, R.-J. *SynOpen* **2024,** *8,* 116–124. doi:10.1055/s-0043-1763748
6. Wang, Q.; Wang, Y.; Liu, M.; Chu, G.; Qiu, Y. *Chin. J. Chem.* **2024,** *42,* 2249–2266. doi:10.1002/cjoc.202400008
7. Yao, H.; Wang, M.-Y.; Yue, C.; Feng, B.; Ji, W.; Qian, C.; Wang, S.; Zhang, S.; Ma, X. *Trans. Tianjin Univ.* **2023,** *29,* 254–274. doi:10.1007/s12209-023-00361-2
8. Pradhan, S.; Das, S. *Synlett* **2023,** *34,* 1327–1342. doi:10.1055/a-2012-5317
9. Mena, S.; Peral, J.; Guirado, G. *Curr. Opin. Electrochem.* **2023,** *42,* 101392. doi:10.1016/j.coelec.2023.101392
10. Senboku, H. *Chem. Rec.* **2021,** *21,* 2354–2374. doi:10.1002/tcr.202100081
11. Senboku, H.; Katayama, A. *Curr. Opin. Green Sustainable Chem.* **2017,** *3,* 50–54. doi:10.1016/j.cogsc.2016.10.003
12. Gal, J.; Folest, J. C.; Troupel, M.; Moingeon, M. O.; Chaussard, J. *New J. Chem.* **1995,** *19,* 401–407.
13. Ohkoshi, M.; Michinishi, J.-y.; Hara, S.; Senboku, H. *Tetrahedron* **2010,** *66,* 7732–7737. doi:10.1016/j.tet.2010.07.067
14. Senboku, H.; Sakai, K.; Fukui, A.; Sato, Y.; Yamauchi, Y. *ChemElectroChem* **2019,** *6,* 4158–4164. doi:10.1002/celc.201900200
15. Zhang, K.; Ren, B.-H.; Liu, X.-F.; Wang, L.-L.; Zhang, M.; Ren, W.-M.; Lu, X.-B.; Zhang, W.-Z. *Angew. Chem., Int. Ed.* **2022,** *61,* e202207660. doi:10.1002/anie.202207660
16. Wang, Y.; Tang, S.; Yang, G.; Wang, S.; Ma, D.; Qiu, Y. *Angew. Chem., Int. Ed.* **2022,** *61,* e202207746. doi:10.1002/anie.202207746
17. Senboku, H.; Yoneda, K.; Hara, S. *Tetrahedron Lett.* **2015,** *56,* 6772–6776. doi:10.1016/j.tetlet.2015.10.068
18. Villo, P.; Lill, M.; Alsaman, Z.; Kronberg, A. S.; Chu, V.; Ahumada, G.; Agarwala, H.; Ahlquist, M.; Lundberg, H. *ChemElectroChem* **2023,** *10,* e202300420. doi:10.1002/celc.202300420
19. Hayama, M.; Senboku, H. *Electrochemistry* **2023,** *91,* 112011. doi:10.5796/electrochemistry.23-67082
20. Li, W.-D.; Wu, Y.; Li, S.-J.; Jiang, Y.-Q.; Li, Y.-L.; Lan, Y.; Xia, J.-B. *J. Am. Chem. Soc.* **2022,** *144,* 8551–8559. doi:10.1021/jacs.1c12463
21. Gaykar, R. N.; Bhunia, A.; Biju, A. T. *J. Org. Chem.* **2018,** *83,* 11333–11340. doi:10.1021/acs.joc.8b01549
22. Kamijo, S.; Tao, K.; Takao, G.; Tonoda, H.; Murafuji, T. *Org. Lett.* **2015,** *17,* 3326–3329. doi:10.1021/acs.orglett.5b01550
23. Jakhar, V. K.; Barman, M. K.; Nembenna, S. *Org. Lett.* **2016,** *18,* 4710–4713. doi:10.1021/acs.orglett.6b02310
24. Han, H. J.; Kim, H. T.; Kim, J.; Jaladi, A. K.; An, D. K. *Tetrahedron* **2023,** *142,* 133500. doi:10.1016/j.tet.2023.133500
25. Yadav, S.; Kuram, M. R. *Eur. J. Org. Chem.* **2023,** *26,* e20220134. doi:10.1002/ejoc.202201344
26. Li, C.-J.; Meng, Y. *J. Am. Chem. Soc.* **2000,** *122,* 9538–9539. doi:10.1021/ja001699b
27. Varjosaari, S. E.; Skrypai, V.; Suating, P.; Hurley, J. J. M.; Gilbert, T. M.; Adler, M. J. *Eur. J. Org. Chem.* **2017,** 229–232. doi:10.1002/ejoc.201601256
28. Wei, Z.; Li, H.; Wang, Y.; Liu, Q. *Angew. Chem., Int. Ed.* **2023,** *62,* e202301042. doi:10.1002/anie.202301042
29. Lei, C.; Yip, Y. J.; Zhou, J. S. *J. Am. Chem. Soc.* **2017,** *139,* 6086–6089. doi:10.1021/jacs.7b02742
30. Yuan, P.-F.; Yang, Z.; Zhang, S.-S.; Zhu, C.-M.; Yang, X.-L.; Meng, Q.-Y. *Angew. Chem., Int. Ed.* **2024,** *63,* e202313030. doi:10.1002/anie.202405333
31. Navale, B. S.; Laha, D.; Banerjee, S.; Vanka, K.; Bhat, R. G. *J. Org. Chem.* **2022,** *87,* 13583–13597. doi:10.1021/acs.joc.2c01185
32. Liao, L.-L.; Cao, G.-M.; Ye, J.-H.; Sun, G.-Q.; Zhou, W.-J.; Gui, Y.-Y.; Yan, S.-S.; Shen, G.; Yu, D.-G. *J. Am. Chem. Soc.* **2018,** *140,* 17338–17342. doi:10.1021/jacs.8b08792
33. Moore, D. L.; Denton, A. E.; Kohinke, R. M.; Craig, B. R.; Brenzovich, W. E., Jr. *Synth. Commun.* **2016,** *46,* 604–612. doi:10.1080/00397911.2016.1158269
34. Müller, C.; Gleixner, J.; Tahk, M.-J.; Kopanchuk, S.; Laasfeld, T.; Weinhart, M.; Schollmeyer, D.; Betschart, M. U.; Lüdeke, S.; Koch, P.; Rinken, A.; Keller, M. *J. Med. Chem.* **2022,** *65,* 4832–4853. doi:10.1021/acs.jmedchem.1c02033
35. Gaydou, M.; Moragas, T.; Juliá-Hernández, F.; Martin, R. *J. Am. Chem. Soc.* **2017,** *139,* 12161–12164. doi:10.1021/jacs.7b07637
36. Yedage, S. L.; Bhanage, B. M. *J. Org. Chem.* **2017,** *82,* 5769–5781. doi:10.1021/acs.joc.7b00570

BEILSTEIN JOURNAL OF ORGANIC CHEMISTRY

Entry to 2-aminoprolines via electrochemical decarboxylative amidation of *N*-acetylamino malonic acid monoesters

Olesja Koleda[1,2], Janis Sadauskis[1,2], Darja Antonenko[1,2], Edvards Janis Treijs[1,2], Raivis Davis Steberis[1,2] and Edgars Suna[*1,2]

Full Research Paper

Open Access

Address:
[1]Latvian Institute of Organic Synthesis, Aizkraukles 21, Riga LV-1006, Latvia and [2]Faculty of Medicine and Life Sciences, Department of Chemistry, University of Latvia, Jelgavas 1, Riga LV-1004, Latvia

Email:
Edgars Suna[*] - edgars@osi.lv

* Corresponding author

Keywords:
anodic oxidation; decarboxylation; electrosynthesis; Hofer–Moest reaction; non-proteinogenic amino acids

Beilstein J. Org. Chem. **2025,** *21,* 630–638.
https://doi.org/10.3762/bjoc.21.50

Received: 18 December 2024
Accepted: 06 March 2025
Published: 19 March 2025

This article is part of the thematic issue "Synthetic electrochemistry".

Guest Editor: K. Lam

Abstract

The electrochemical synthesis of 2-aminoprolines based on anodic decarboxylation–intramolecular amidation of readily available *N*-acetylamino malonic acid monoesters is reported. The decarboxylative amidation under Hofer–Moest reaction conditions proceeds in an undivided cell under constant current conditions in aqueous acetonitrile and provides access to *N*-sulfonyl, *N*-benzoyl, and *N*-Boc-protected 2-aminoproline derivatives.

Introduction

Non-proteinogenic cyclic amino acids are common structural motifs in the design of small-molecule drugs and peptidomimetics [1]. For example, the clinically used anesthetics carfentanil (**1**) and remifentanil (**2**), the FDA-approved antipruritic medication defelikefalin (**3**), and the arginase inhibitor **4** [2] possess cyclic α,α-disubstituted piperidine-containing amino acid subunits. Likewise, a cyano-substituted cyclic aminal is a core structural unit of the fibroblast activation protein inhibitor **5** [3] (Figure 1). The widespread use of non-proteinogenic cyclic amino acids in drug discovery justifies both the design of new analogs and the development of efficient synthetic methods to access these medicinally relevant structural motifs. Herein, we report an electrochemical synthesis of 2-aminoproline and 2-aminopipecolic acid derivatives **6** (Figure 1).

Recently, we disclosed an electrochemical approach to tetrahydrofuran and tetrahydropyran-containing amino acid derivatives via anodic decarboxylation of *N*-acetylamino malonic acid monoesters to generate a stabilized carbocation (Hofer–Moest conditions), which were then reacted with a tethered oxygen nucleophile [4]. In this follow-up study, we demonstrate that *N*-protected amines are also suitable as nucleophiles for the cyclization into 2-aminoproline and 2-aminopipecolic acid derivatives **6** (Figure 2, reaction 3). The starting disubstituted

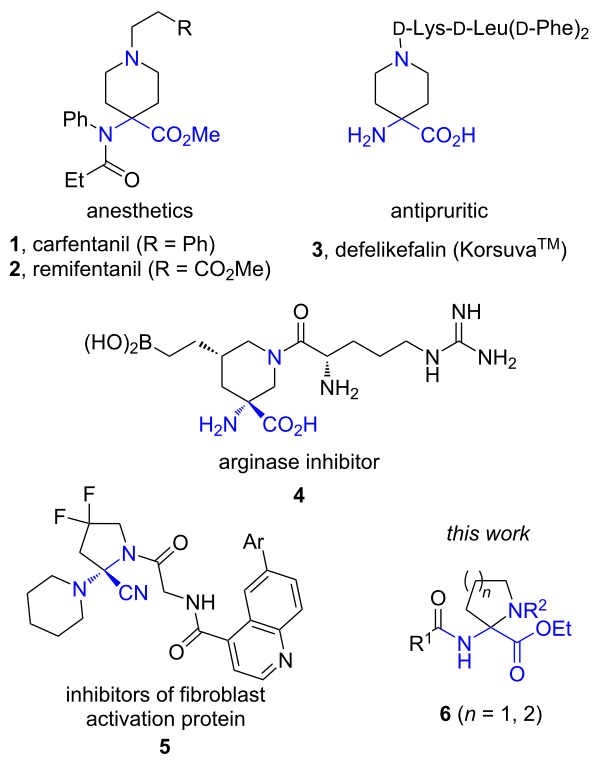

Figure 1: Selected examples of α,α-disubstituted cyclic amino acids in drug design.

malonic esters are readily available by *C*-alkylation of inexpensive and readily available diethyl acetamidomalonate, followed by monohydrolysis under basic conditions. The electrolysis proceeds in an undivided cell under galvanostatic control using low-cost graphite or stainless-steel electrodes, and the protocol was easily upscaled. Notably, an excellent diastereoselectivity (97:3 dr) could be achieved in the cyclization of a tethered chiral nitrogen nucleophile as shown below. To the best of our knowledge, the electrosynthesis of *gem*-α,α-diamino acid derivatives **6** has not been accomplished, and all published electrochemical amination examples under Hofer–Moest conditions [5] targeted either *N*-substituted heteroarenes [6] or aminals [7,8] (Figure 2, reactions 1 and 2, respectively).

Results and Discussion

N-Acetylamino malonic acid monoester **9a** possessing a tosyl-protected tethered amine was selected as a model substrate for the development of the intramolecular amidation under Hofer–Moest conditions. The acid **9a** was prepared in three steps (62% overall yield) from commercially available diethyl acetamidomalonate by an alkylation/hydrolysis/Boc-cleavage sequence (Scheme 1).

The development of decarboxylative amidation commenced by examining the published conditions for anodic decarboxylation/etherification [4]. Accordingly, the electrolysis of monoester **9a** in a 2:1 MeCN/H_2O mixture in the presence of 0.025 M $LiClO_4$ solution under constant current conditions (j = 12 mA/cm^2) with graphite both as an anode and a cathode material afforded the desired *N*-tosylpyrrolidine **6a** in 67% yield (Table 1, entry 1). The water quench of a transient *N*-acyliminium species was found to be a major side-reaction as evidenced by the formation of an open-chain hemiaminal **10a** (the hemiaminal could not be isolated due to the instability on silica gel). Screening of

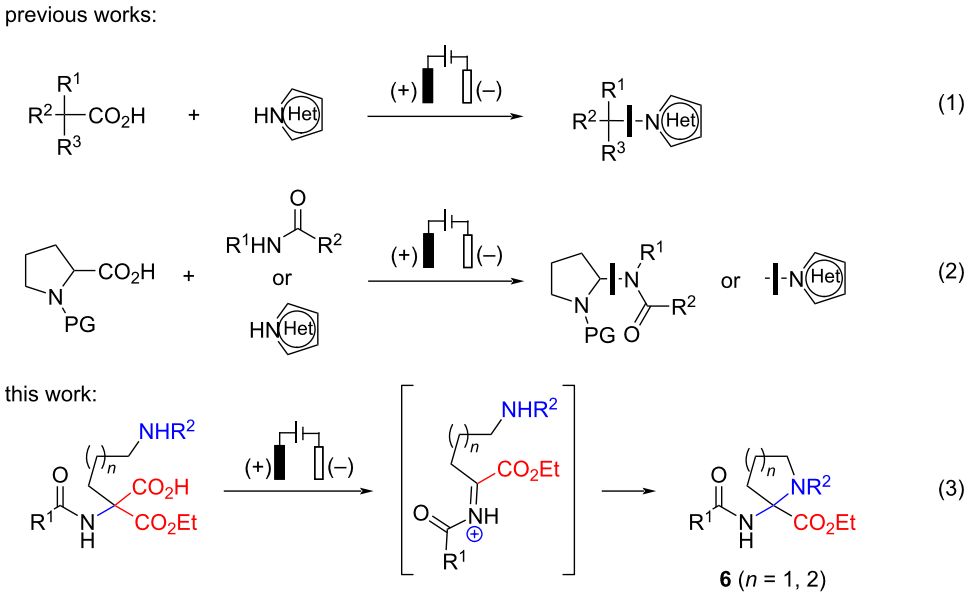

Figure 2: Electrochemical decarboxylative amination reactions.

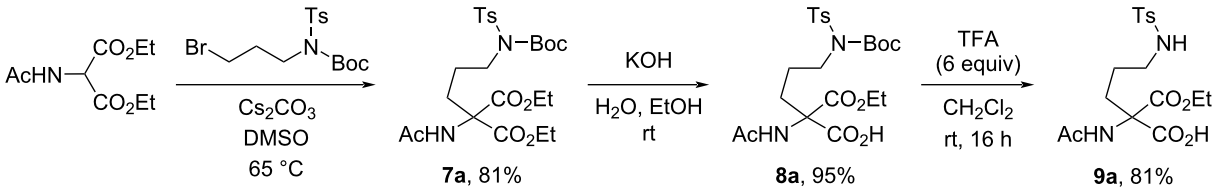

Scheme 1: Preparation of malonic acid monoester **9a**.

Table 1: Optimization of anodic decarboxylation/amidation reaction.

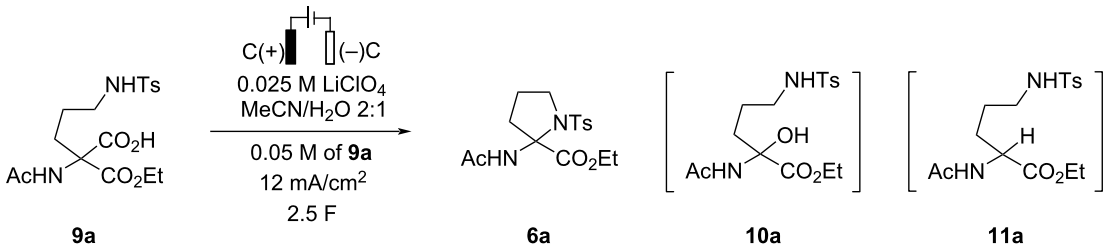

9a **6a** **10a** **11a**

Entry	Deviations from the starting conditions	Yield, %[a]	**6a**:**10a**:**11a**[b]
1	none	67	84:16:0
2	K_2CO_3, 2.0 F	54	86:3:11
3	Na_2CO_3, 2.0 F	54	86:4:10
4	NaOAc, 2.0 F	56	71:13:16
5	Bu_4N–ClO_4, 2.3 F	67	85:15:0
6	Et_4N–PF_6	66	85:15:0
7	Et_4N–BF_4	71	84:16:0
8	**Et_4N–BF_4, 5:1 MeCN/H_2O**	**72**	**86:13:1**
9	0.05 M Et_4N–BF_4, 5:1 MeCN/H_2O	67	85:13:2
10	**Et_4N–BF_4, 5:1 MeCN/H_2O, 2.0 F, SS (–)**	**70**	**87:13:0**
11	Et_4N–BF_4, 5:1 MeCN/H_2O, 2.0 F, Pt (–)	63	84:16:0
12	Et_4N–BF_4, 5:1 MeCN/H_2O, 2.8 F, BDD(–)	62	86:12:2

[a]Yields were determined by ^{1}H NMR post-electrolysis using CH_2Br_2 as an internal standard. The reactions were performed on a 0.15 mmol scale.
[b]Ratios determined by LC–MS (UV detection).

other supporting electrolytes revealed that basic salts (K_2CO_3, Na_2CO_3, NaOAc) did not improve the efficiency of the anodic decarboxylation/cyclization reaction (Table 1, entries 2–4). Even though the amount of hemiaminal **10a** was slightly reduced, the formation of amino acid ester **11a** as side product was observed in the crude reaction mixture (Table 1, entries 2–4). The latter could be suppressed completely by using non-basic anion-containing tetraalkylammonium salts as the supporting electrolytes (Table 1, entries 5–7) with Et_4N–BF_4 providing the highest yield of the desired product **6a**. The anodic decarboxylation/cyclization reaction was similarly efficient when the amount of water was reduced from 33% to 17% (Table 1, entry 8 vs entry 7), an observation that might be useful for substrates of low aqueous solubility. However, further reduction of water amount to 5 equivalents completely inhibited the anodic oxidation of **9a**, and only traces of the desired **6a** were observed (see Supporting Information File 1, page S3). Decrease in supporting electrolyte concentration led to a drop in yields (Table 1, entry 9 vs entry 8), whereas current density deviations from 12 mA/cm^2 did not affect the outcome of **6a** (see Supporting Information File 1, page S4). Interestingly, replacement of graphite with stainless steel (SS) [9] as the cathode material afforded similar yields of the desired heterocycle **6a** (72% and 70%, respectively; Table 1, entries 8 and 10), so both graphite and SS were subsequently used in the scope studies (vide infra). Other cathode materials such as Pt or BDD (boron-doped diamond) delivered **6a** in reduced yields (Table 1, entries 11 and 12). Finally, brief examination of passed charge returned 2.0 F as the optimal amount. The amount of charge could be increased to 2.5 F in case of incomplete conversion of the starting

6a, however, further rise above 2.5 F led to a drop in the pyrrolidine **6a** yield due to the formation of a new side-product.

We hypothesized that the side-product formation at increased amounts (>2.5 F) of passed charge results from undesired Shono oxidation of pyrrolidine **6a** [10,11]. Indeed, CV studies of **6a** revealed an irreversible feature at E_p = 1.78 V vs Ag/Ag^+ (100 mV/s scan rate; see Figure 3A), and the electrolysis of pyrrolidine **6a** under the optimized anodic decarboxylative cyclization conditions (entry 8, Table 1) afforded cyclic hemiaminal **12a** (33% NMR yield), whose structure was proved by NMR experiments (Figure 3B). The relatively narrow potential window of 0.22 V between the desired decarboxylation of **9a** (E_p = 1.56 V vs Ag/Ag^+) and the undesired Shono-type oxidation of the formed **6a** required careful control of the amount of passed charge to afford high yields of **6a**.

Next, the formation of decarboxylation product **11a** was addressed. Initially, we hypothesized that **11a** may form by a single-electron oxidation/decarboxylation (Kolbe reaction) of **9a** to generate carbon-centered radical, followed by hydrogen abstraction from solvent. To verify the hypothesis, an electrolysis of acid **9d** was performed under optimized conditions (entry 10, Table 1) in deuterated solvents (Scheme 2; for details, see Supporting Information File 1, page S40). Surprisingly, the electrolysis in a 5:1 mixture of MeCN-d_3 and water delivered **11d** without deuterium incorporation (Scheme 2, reaction 1). In contrast, the formation of deuterated **11d-D** was observed by LC–MS when the electrolysis was performed in 5:1 $MeCN/D_2O$ (Scheme 2, reaction 2). The considerably higher O–H bond dissociation energy (119 kcal/mol) [12] as compared to that of the C–H bond in MeCN (86 kcal/mol) [13] renders the hydrogen atom abstraction from water by a carbon-centered radical a very unlikely mechanistic scenario. In the meantime, slow formation of **11d-D** was observed upon stirring of **9d** in the 5:1 $MeCN/D_2O$ mixture even without applying electric charge (Scheme 2, reaction 3). Apparently, **11d** was formed upon spontaneous loss of CO_2 from equilibrating deuterated carboxylate **9d-D**. Furthermore, monoesters **9** are also prone to spontaneous decarboxylation upon storage. Therefore, freshly prepared material should be used in the electrolysis.

Based on experimental evidence, a working mechanism for the formation of 2-aminoproline **6a** is proposed (Figure 4). Accordingly, an initial deprotonation of carboxylic acid **9a** by cathodically generated hydroxide is followed by anodic oxidation/decarboxylation of the formed carboxylate **9a-I** to generate stabilized cation **9a-II**. The latter undergoes intramolecular cyclization with the tethered *N*-nucleophile into cyclic aminal **6a**. In a competing reaction, the cation **9a-II** reacts with water to form acyclic hemiaminal **10a**.

With the optimized conditions in hand (Table 1, entries 8 and 10) the scope of the developed decarboxylative amidation was briefly explored (Scheme 3). *N*-Acetyl, *N*-Cbz, and *N*-Bz protecting groups are compatible with the decarboxylation/cyclization conditions, and the respective 2-aminoproline derivatives **6a–c** were obtained in 49–75% yield. Redox-sensitive 4-anisoyl and 4-cyanobenzoyl groups-containing monoesters **9d**,**e** are also suitable as substrates as evidenced by the formation of **6d**,**e** in 38–63% yields. Not only *N*-tosylates undergo the decarboxylative cyclization, but also *N*-mesyl-protected monoester **9f** could be converted into 2-aminoproline derivative **6f** in 60% yield using a graphite cathode. However, the *N*-*o*-nosyl-protecting group is not compatible with the developed electrolysis conditions, likely because it undergoes an undesired cathodic reduction. Indeed, trace amounts of 2-aminoproline derivative **6g** (<4%) could be obtained by

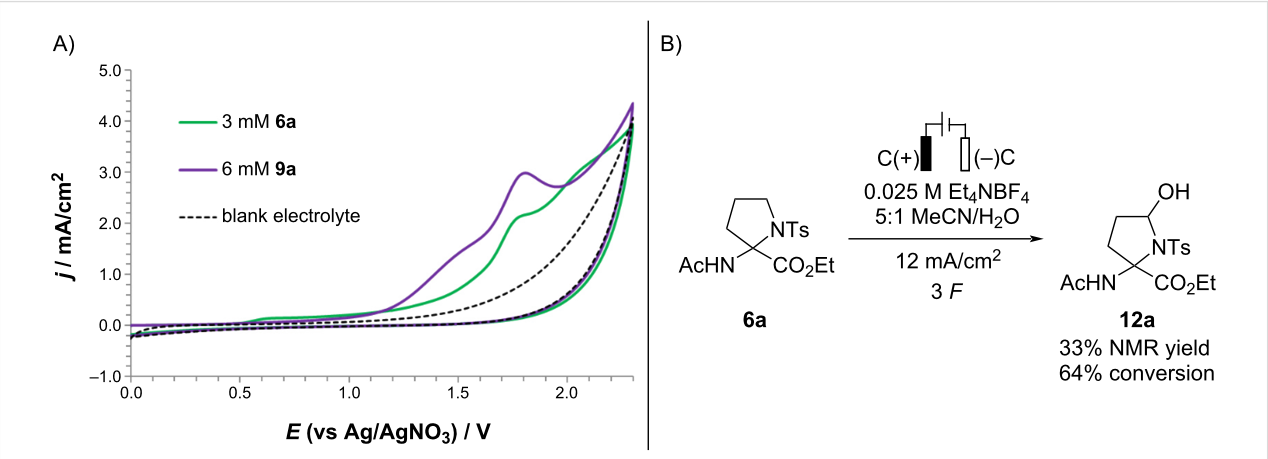

Figure 3: A) Cyclic voltammograms of **6a** and **9a** at 3 mM and 6 mM concentration, respectively, in 5:1 $MeCN/H_2O$ (0.1 M $Et_4N–BF_4$). B) Anodic oxidation of pyrrolidine **6a**.

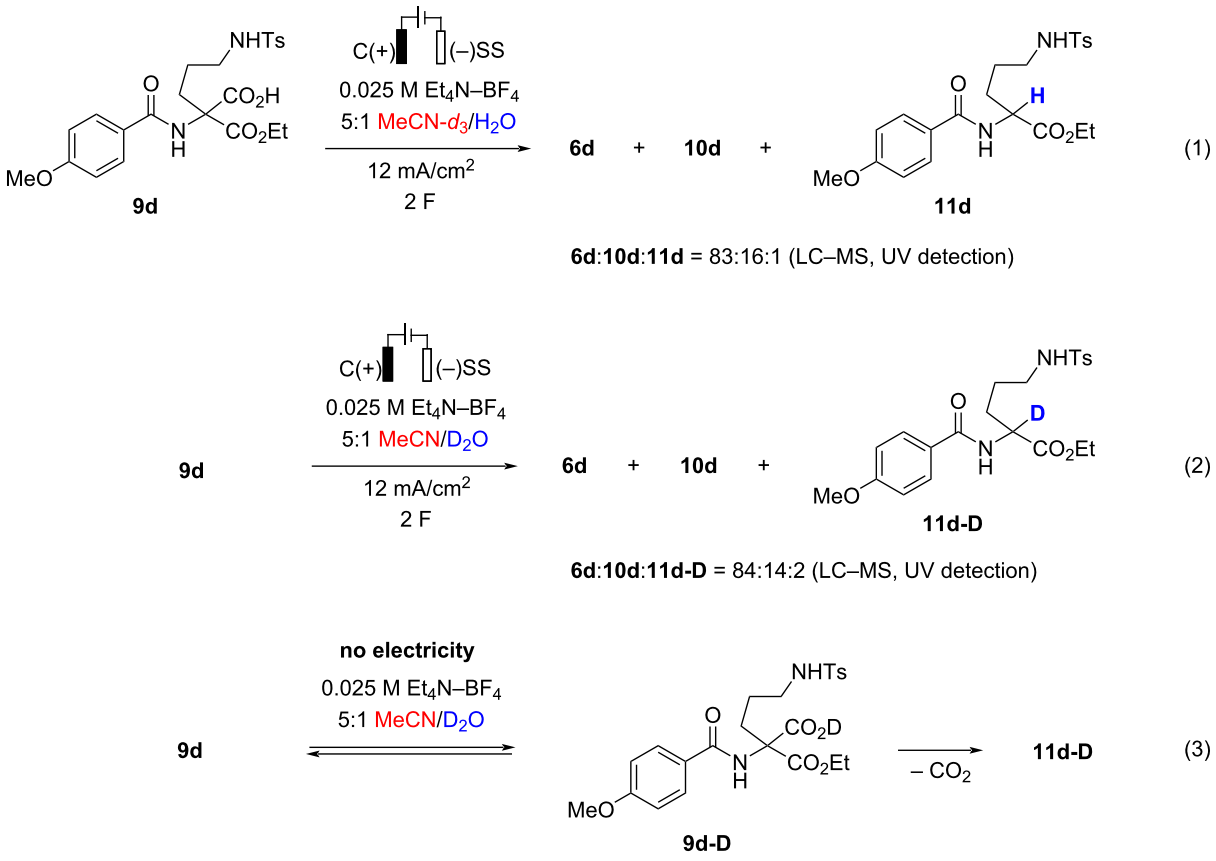

Scheme 2: Electrolysis of acid **9d** in deuterated solvents.

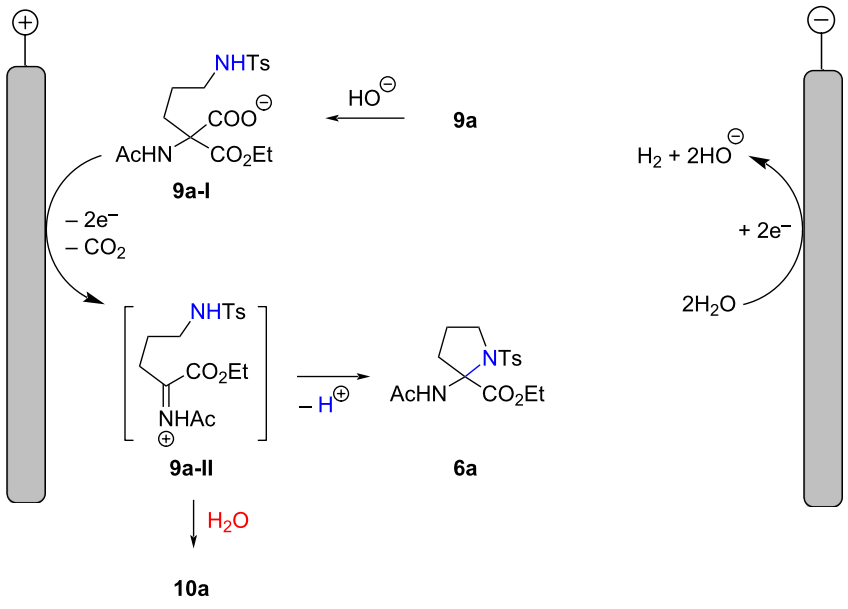

Figure 4: Plausible mechanism for formation of pyrrolidine **6a** and hemiaminal **10a**.

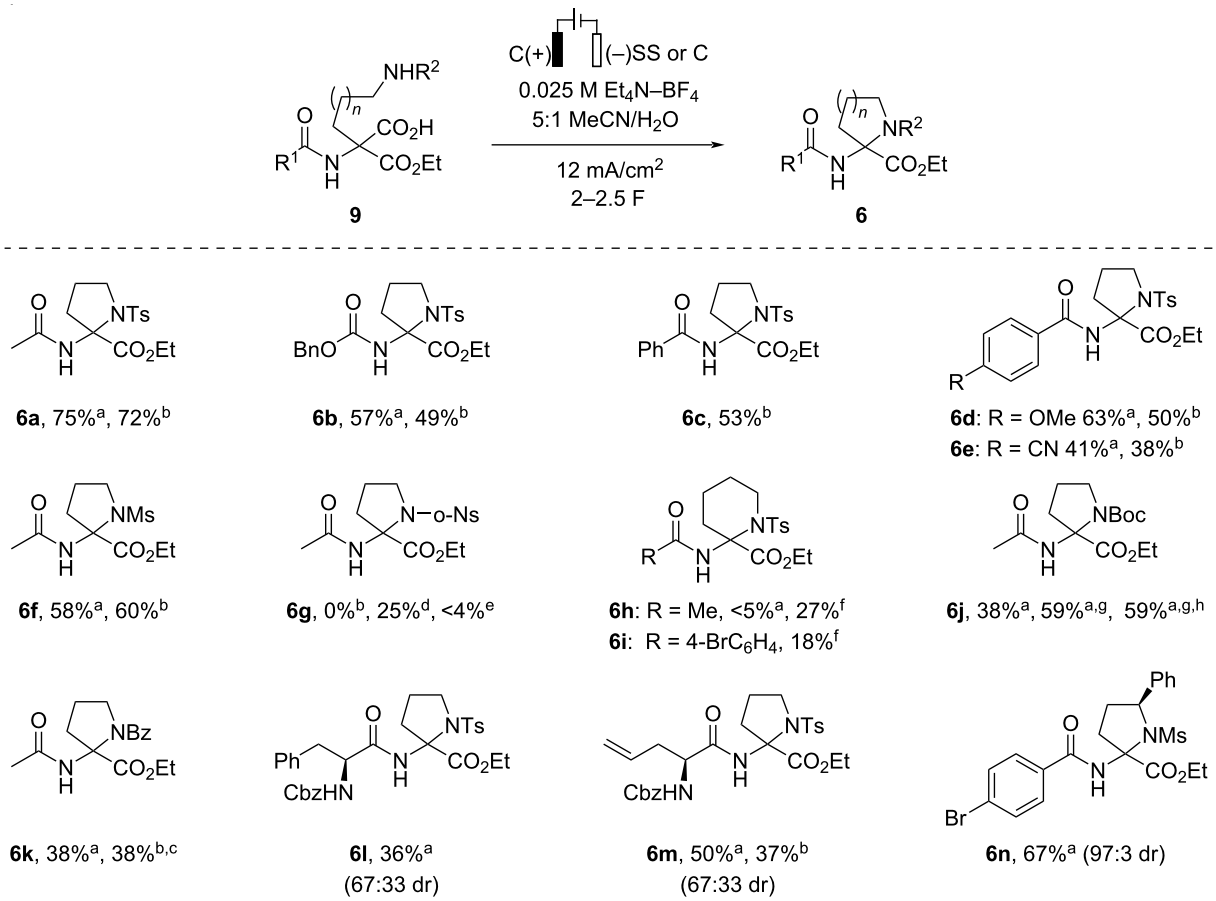

Scheme 3: Scope of the decarboxylative amidation. [a]Stainless-steel cathode; [b]graphite cathode; [c]yield determined by ^{1}H NMR using CH_2Br_2 as an internal standard; [d]electrolysis in divided cell with NaOH (1 equiv); [e]Pt cathode; [f]with KOH (1 equiv); [g]with KOH (0.5 equiv); [h]performed on 925 mg (2.7 mmol) scale.

replacing SS as the cathode material with platinum that has a low overpotential for hydrogen evolution reaction [14]. To avoid the undesired cathodic reduction of the nitro group, the electrolysis of *N*-*o*-nosyl-protected monoester **9g** was performed in a divided cell in the presence of NaOH as a base (1 equiv). Gratifyingly, by this route *N*-*o*-nosyl-protected **6g** was obtained in 25% yield.

The attempted synthesis of 2-aminopipecolic acid derivative **6h** under the developed conditions was unsuccessful, and afforded trace amounts of **6h** together with the corresponding acyclic hemiaminal **10h** as the major product. Such an outcome can be attributed to a slower formation of a 6-membered ring [15] from transient *N*-acyliminium species. Gratifyingly, the addition of KOH (1 equiv) to the electrolysis mixture facilitated the cyclization, and the 6-membered heterocycles **6h**,**i** could be obtained in 27% and 18% yield, respectively.

In addition to sulfonamides, carbamates such as *N*-Boc and benzamide are also suitable as nucleophiles for the anodic decarboxylation/cyclization reaction. However, the corresponding 2-aminoproline derivatives **6j**,**k** were obtained in considerably lower yields (38%) as compared to those of *N*-Ts analog **6a**. Surprisingly, the addition of KOH (0.5 equiv) to the electrolysis solution has helped to improve yield of *N*-Boc-protected 2-aminoproline derivative **6j** from 38% to 59%. However, the addition of KOH was not always beneficial. For instance, the anodic oxidation of benzamide **9k** in the presence of KOH afforded pyrrolidine **6k** only as a minor product and a mixture of **6k**/**10k**/**11k** in 15:32:53 ratio, respectively, was formed. Finally, the loading of **9j** was increased from 0.3 to 2.7 mmol to demonstrate the scalability of the method, and 470 mg of 2-aminoproline derivative **6j** was obtained in a single electrolysis batch.

The wide application of unnatural amino acids in the design of peptidomimetics prompted us to examine the suitability of the developed conditions for dipeptide synthesis. Gratifyingly, the cyclization of the amino acid fragment-containing monoesters **9l**,**m** afforded dipeptides **6l**,**m** in 36% and 50% yield, respec-

tively. Notably, the decarboxylative cyclization is compatible with the alkene moiety (product **6m**). Both dipeptides **6l**,**m** were obtained as a 67:33 mixture of diastereomers. In the meantime, an excellent diastereoselectivity (97:3 dr) was achieved in the decarboxylative cyclization of *N*-mesylamide **9n** possessing an *S* stereogenic center in the α-position to the nitrogen. Unfortunately, the configuration of the newly formed quaternary stereogenic center in **6n** could not be established by NMR methods, and all attempts to obtain crystals suitable for X-ray crystallographic analysis were unsuccessful.

N-Protected 2-aminoproline derivatives **6** are relatively stable under basic conditions as evidenced by successful hydrolysis of the ester moiety in **6a**,**d**,**e** using aqueous LiOH to provide acids **13a**,**d**,**e** in 71–83% yield (Scheme 4). Carboxylic acid **13a** could be reacted with glycine benzyl ester in the presence of HATU and Et_3N to form dipeptide **16** (66%). In contrast, *N*-unprotected 2-aminoprolines are unstable and could not be isolated. Thus, the cleavage of the *N*-Cbz protecting group in **6b** under Pd-catalyzed hydrogenolysis afforded diamino acid ester **14** (75% yield) that was likely formed by ring-opening of the unstable *N*-unprotected 2-aminoproline followed by the reduction of the open-chain imine tautomer. Likewise, the open-chain amino alcohol **15** was formed also upon the reduction of the ester moiety with $LiBH_4$. In the meantime, the hydrogenolysis of the benzyl ester in dipeptide **16** proceeded smoothly and afforded carboxylic acid **17** in 81% yield (Scheme 4) [16].

Conclusion

In summary, the developed electrochemical decarboxylative amidation of readily accessible malonic acid monoesters provides access to previously unreported 2-aminoproline derivatives. The decarboxylative amidation proceeds under constant current conditions in an undivided cell in aqueous acetonitrile and involves initial anodic decarboxylation followed by an intramolecular reaction of the formed stabilized cation with tethered nitrogen nucleophiles such as sulfonamides, carbamates, and benzamide. The decarboxylative cyclization of a stereogenic center-containing sulfonamide proceeds with excellent diastereoselectivity (97:3 dr). The *N*-protected 2-aminoproline derivatives can be incorporated into dipeptides by an ester hydrolysis/amide bond formation sequence, and therefore they are suitable for the design of peptidomimetics. Further work is in progress in our laboratory to expand the scope of nucleophiles in the decarboxylative functionalization of malonic acid monoesters.

Experimental

General procedure for the electrochemical synthesis of pyrrolidines **6a**–**f**,**j**–**n** from the corresponding malonic acid monoesters **9a**–**f**,**j**–**n**.

An undivided electrochemical cell (5 mL, IKA ElectraSyn 2.0) was charged with starting carboxylic acid **9a**–**f**,**j**–**n** (0.2–0.3 mmol) and Et_4N–BF_4 (0.025 M), followed by addition of MeCN (2.5 mL) and H_2O (0.5 mL). A graphite plate (8 × 52.5 × 2 mm; immersed electrode surface area A = 1.12 cm^2) was used as a working electrode and stainless steel or graphite (8 × 52.5 × 2 mm; immersed electrode surface area A = 1.12 cm^2) was used as a counter electrode. The electrolysis was carried out under galvanostatic conditions at room temperature, and 2.0 F charge (if not otherwise noticed)

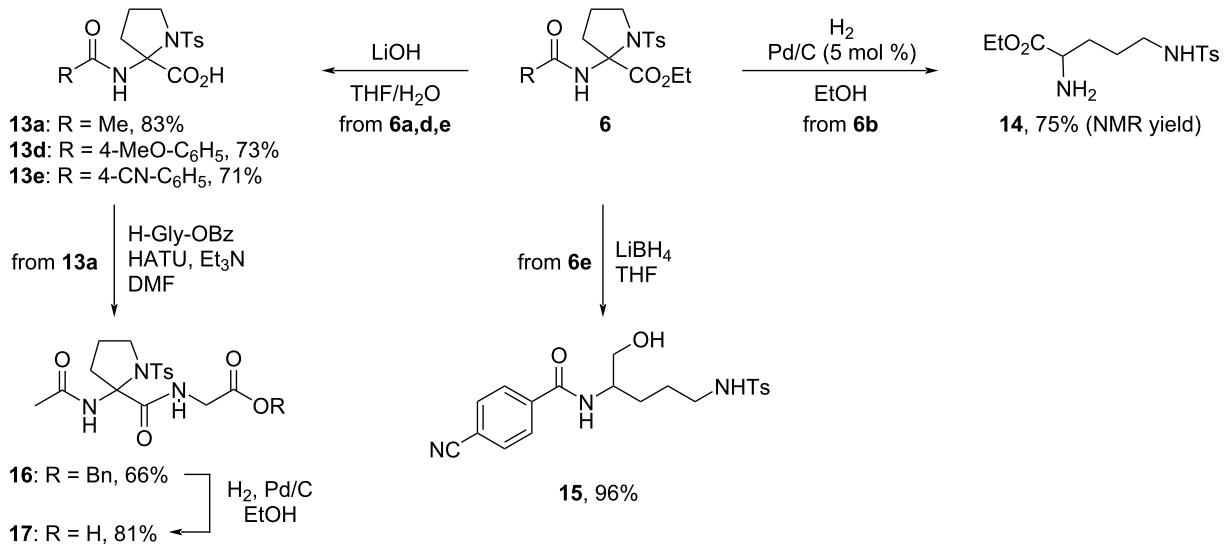

Scheme 4: Synthetic modifications of 2-aminoproline derivatives **6**.

with current density of 12 mA/cm^2 was passed through the colorless reaction solution. The resulting clear, colorless (sometimes pale yellow) solution was concentrated under reduced pressure and the crude product was purified by column chromatography.

Cyclic voltammetry studies

CV experiments were carried out in an SVC-2 (ALS, Japan) three-electrode cell using a PalmSens4 (PalmSens). A glassy carbon disk (diameter: 1.6 mm) served as the working electrode and a platinum wire as the counter electrode. The glassy carbon disk was polished using polishing alumina (0.05 µm) prior to each experiment. As a reference, an $Ag/AgNO_3$ electrode [silver wire in 0.1 M NBu_4ClO_4/MeCN solution; $c(AgNO_3)$ = 0.01 M; E_0 = −87 mV vs Fc/Fc^+ couple] [17] was used, and this compartment was separated from the rest of the cell with a Vycor frit. Et_4NBF_4 (0.1 M, electrochemical grade) was employed as the supporting electrolyte in 5:1 MeCN/H_2O solution. The electrolyte was purged with argon for at least 3 min prior to recording. Compounds **6a** and **9a** were analyzed at a concentration of 3 mM or 6 mM and at a scan rate of 100 mV s^{-1}. The peak potential E_p was not extracted from background-corrected voltammograms. All CV graphs are plotted using IUPAC polarographic convention.

Supporting Information

Supporting Information File 1

Detailed experimental procedures, analytical and spectroscopic data for the synthesized compounds, and copies of NMR spectra.
[https://www.beilstein-journals.org/bjoc/content/supplementary/1860-5397-21-50-S1.pdf]

ORCID® iDs

Olesja Koleda - https://orcid.org/0000-0002-5173-8561
Janis Sadauskis - https://orcid.org/0009-0002-6962-7621
Raivis Davis Steberis - https://orcid.org/0009-0001-2610-0208
Edgars Suna - https://orcid.org/0000-0002-3078-0576

Data Availability Statement

All data that supports the findings of this study is available in the published article and/or the supporting information of this article.

Preprint

A non-peer-reviewed version of this article has been previously published as a preprint: https://doi.org/10.3762/bxiv.2024.71.v1

References

1. Blaskovich, M. A. T. *J. Med. Chem.* **2016,** *59,* 10807–10836. doi:10.1021/acs.jmedchem.6b00319
2. Gzik, A.; Borek, B.; Chrzanowski, J.; Jedrzejczak, K.; Dziegielewski, M.; Brzezinska, J.; Nowicka, J.; Grzybowski, M. M.; Rejczak, T.; Niedzialek, D.; Wieczorek, G.; Olczak, J.; Golebiowski, A.; Zaslona, Z.; Blaszczyk, R. *Eur. J. Med. Chem.* **2024,** *264,* 116033. doi:10.1016/j.ejmech.2023.116033
3. Pujala, B.; Panpatil, D.; Bernales, S.; Belmar, S.; Ureta Díaz, G. A. Inhibitors of Fibroplast Activation Protein. WO Pat. Appl. WO2020132661A2, June 25, 2020.
4. Koleda, O.; Prane, K.; Suna, E. *Org. Lett.* **2023,** *25,* 7958–7962. doi:10.1021/acs.orglett.3c02687
5. Hawkins, B. C.; Chalker, J. M.; Coote, M. L.; Bissember, A. C. *Angew. Chem., Int. Ed.* **2024,** *63,* e202407207. doi:10.1002/anie.202407207
6. Sheng, T.; Zhang, H.-J.; Shang, M.; He, C.; Vantourout, J. C.; Baran, P. S. *Org. Lett.* **2020,** *22,* 7594–7598. doi:10.1021/acs.orglett.0c02799
7. Shao, X.; Zheng, Y.; Tian, L.; Martín-Torres, I.; Echavarren, A. M.; Wang, Y. *Org. Lett.* **2019,** *21,* 9262–9267. doi:10.1021/acs.orglett.9b03696
8. Yu, P.; Huang, X.; Wang, D.; Yi, H.; Song, C.; Li, J. *Chem. – Eur. J.* **2024,** *30,* e202402124. doi:10.1002/chem.202402124
9. Collin, D. E.; Folgueiras-Amador, A. A.; Pletcher, D.; Light, M. E.; Linclau, B.; Brown, R. C. D. *Chem. – Eur. J.* **2020,** *26,* 374–378. doi:10.1002/chem.201904479
10. Shono, T.; Matsumura, Y.; Tsubata, K.; Uchida, K.; Kanazawa, T.; Tsuda, K. *J. Org. Chem.* **1984,** *49,* 3711–3716. doi:10.1021/jo00194a008
11. Novaes, L. F. T.; Ho, J. S. K.; Mao, K.; Liu, K.; Tanwar, M.; Neurock, M.; Villemure, E.; Terrett, J. A.; Lin, S. *J. Am. Chem. Soc.* **2022,** *144,* 1187–1197. doi:10.1021/jacs.1c09412
12. Benson, S. W. *J. Chem. Educ.* **1965,** *42,* 502. doi:10.1021/ed042p502
13. Kerr, J. A. *Chem. Rev.* **1966,** *66,* 465–500. doi:10.1021/cr60243a001
14. Hickling, A.; Salt, F. W. *Trans. Faraday Soc.* **1940,** *36,* 1226–1235. doi:10.1039/tf9403601226
15. Di Martino, A.; Galli, C.; Gargano, P.; Mandolini, L. *J. Chem. Soc., Perkin Trans. 2* **1985,** 1345. doi:10.1039/p29850001345
16. Preliminary data indicate that the *N*-Ts protecting group in **6b** undergoes cleavage by magnesium in anhydrous methanol in an ultrasound bath at room temperature within one hour. Simultaneously, the transesterification of the ethyl ester into the corresponding methyl ester was observed. The authors express their gratitude to the manuscript reviewer for the valuable suggestion to investigate the cleavage of the *N*-Ts protecting group.
17. Pavlishchuk, V. V.; Addison, A. W. *Inorg. Chim. Acta* **2000,** *298,* 97–102. doi:10.1016/s0020-1693(99)00407-7

License and Terms